Humboldt-Universität zu Berlin – Geographisches Institut

# Utilizing the depth of the Landsat archive to reconstruct recent land change in the Carpathian ecoregion

## DISSERTATION

Zur Erlangung des akademischen Grades
doctor rerum naturalium
(Dr. rer. nat.)

Im Fach Geographie

eingereicht an der

Mathematisch-Naturwissenschaftlichen Fakultät II

der Humboldt-Universität zu Berlin

von

Dipl. Geogr. Patrick Griffiths

Präsident der Humboldt-Universität zu Berlin

Prof. Dr. Jan-Hendrik Olbertz

Dekan der Mathematisch-Naturwissenschaftlichen Fakultät II

Prof. Dr. Elmar Kulke

Gutachter:

Prof. Dr. Patrick Hostert

Prof. Dr. Eric Lambin

Dr. habil Daniel Müller

Eingereicht: 31. Juli 2013

Tag der Verteidigung: 27. September 2013

# Abstract

Remote sensing based monitoring of land change is a prerequisite to reduce the negative impacts of global environmental change. However, available monitoring methods suffer from spatial and/or temporal limitations. The opening of the Landsat archive, advancements in data quality, processing algorithms and capabilities, can improve pattern-process understanding if these limitations are overcome. The overall aim of this dissertation was first, to develop and apply methods that better utilize the rich Landsat record and then, to map and quantify land change in the Carpathian ecoregion since 1985. The secondary objective is to investigate how the collapse of socialism and accession to the European Union (EU) affected regional land change. First, a trajectory based change detection approach was used to investigate how increased observation frequency helps understanding how forest ownership changes affected forest disturbance dynamics. Second, compositing algorithms are developed to facilitate mapping and change detection over large areas. This allowed assessing changes in forest cover and agriculture. Results showed that overall the collapse of socialism led to drastic declines in forest disturbances and simultaneously to widespread cropland abandonment. Forest cover overall expanded but excessive harvesting prevailed in certain areas, due to combined effects of land use legacies, natural disturbances and forest management. Following the EU accession, disturbance levels increased compared to the transition years, potentially relating to a re-established forestry sector with access to EU timber markets. Abandoned cropland was recultivated throughout the Carpathians during the most recent years, likely influenced by the EU Common Agricultural Policy and increasingly by global markets. This dissertation exemplifies the value of the Landsat archive for land change research which can improve our understanding of land change globally and thus help mitigate its negative impacts.

# Zusammenfassung

Fernerkundungsbasiertes monitoring von Landnutzungswandel ist eine Grundvoraussetzung um die negativen Auswirkungen globaler Umweltveränderungen zu reduzieren. Verfügbare Methoden sind allerdings räumlichen und/oder zeitlichen Einschränkungen unterworfen. Die Öffnung des Landsat Archivs, verbesserte Datenqualität, sowie fortgeschrittene Algorithmen und Kapazitäten für die Datenprozessierung erlauben verbessertes Verständnis von Muster-Prozess Zusammenhängen, falls diese Einschränkungen überwunden werden. Das Ziel dieser Dissertation war es, Methoden zu entwickeln und anzuwenden, die eine bessere Nutzung des umfangreichen Landsat Archivs ermöglichen, um Landnutzungswandel in den Karpaten seit 1985 zu kartieren und quantifizieren. Das sekundäre Ziel war es zu untersuchen, wie der Zusammenbruch des Sozialismus und der Beitritt zur Europäischen Union den regional Landnutzungswandel beeinträchtigt hat. Dafür wurde zunächst ein zeitreihenbasiertes Verfahren genutzt, um zu untersuchen inwiefern eine verbesserte zeitliche Auflösung zu einem besseren Verständnis führt und wie sich Waldstörungsdynamiken während der Umstrukturierung von Forstbesitzverhältnissen entwickeln. Außerdem wurden Compositing Algorithmen entwickelt, um großflächige Ableitung von Landnutzung und deren Veränderungen zu ermöglichen. Diese erlaubten es, die regionalen forst- und landwirtschaftlichen Veränderungen zu quantifizieren. Die Ergebnisse zeigten, dass das Ende des Sozialismus zu einer drastischen Reduzierung der Waldstörungen geführt hat und gleichzeitig weitflächig Ackerland aufgegeben wurde. Insgesamt nahm die Waldfläche leicht zu aber übermäßige Störungen wurden in verschiedenen Gebieten beobachtet, vermutlich verursacht durch den kombinierten Effekt forstwirtschaftlicher Vermächtnisse, natürlicher Störungen sowie Waldbewirtschaftung. Nach dem EU-Beitritt nahmen Störungsdynamiken in den Karpatenwäldern im Vergleich zu den ersten Übergangsjahren wieder zu, was auf neuorganiserte Forstwirtschaft mit Zugang zu dem EU Markt hindeuten kann. Ehemals aufgegebene Ackerflächen in den gesamten Karpaten wurden in den letzten Jahren vermehrt wiederbewirtschaftet, wahrscheinlich bedingt durch die Agrarpolitik der EU sowie einen zunehmenden Einfluss globaler Märkte. Die vorliegende Dissertation veranschaulicht die Bedeutung des Landsat Archivs für die Landnutzungsforschung und verdeutlicht, wie dieses Archiv potentiell zu einem verbesserten Verständnis des globalen Umweltwandels beisteuern kann und daher hilft, dessen negative Auswirkungen abzumildern.

# Contents

**Abstract** **v**

**Zusammenfassung** **vii**

**Contents** **ix**

**List of Figures** **xiii**

**List of Tables** **xix**

**Chapter I: Introduction** **1**

1 Land use and global environmental change 2
2 Remote sensing based land change monitoring 6
3 The Carpathian ecoregion and recent socio-economic transformations 8
4 Overall aim, research questions and methodological approach 12
5 Structure of this dissertation 15

**Chapter II: Using annual time-series of Landsat images to assess the effects of forest restitution in post-socialist Romania** **17**

Abstract 18
1 Introduction 19
2 Methods 21
2.1 Study region 21
2.2 Image data and preprocessing 23
2.3 Time-series segmentation procedure 23
2.4 Forest / non-forest map 24
2.5 Forest disturbance mapping 25
2.6 Growth and recovery mapping 26
2.7 Analyzing rates and patterns of disturbance and recovery 27
2.8 Assessing the effect of ownership 27
3 Results 28
4 Discussion 37
5 Conclusions 42
Acknowledgements 42

**Chapter III: A pixel-based Landsat compositing algorithm for large area land cover mapping** **45**

Abstract 46
1 Introduction 47
2 Methodology 50
2.1 Data used and test region 50

2.2 Pre-processing 52
2.3 Image compositing 52
2.4 Evaluating annual, seasonal and radiometric consistency 56
2.5 PBC-based land cover mapping 57
3 Results 58
4 Discussion and conclusions 65
Acknowledgments 69

**Chapter IV: Forest disturbances, forest recovery, and changes in forest types across the Carpathian ecoregion from 1985 to 2010 based on Landsat image composites 71**

Abstract 72
1 Introduction 73
2 Methods 76
2.1 Study area 76
2.2 Satellite data, pre-processing and compositing 78
2.3 Forest type, disturbance and recovery mapping 80
2.4 Forest inventory data, validation strategy, and result summaries 84
3 Results 87
3.1 Image compositing 87
3.2 Forest composition and changes within forest types 87
3.3 Forest disturbances 88
3.4 Forest recovery from disturbance 93
3.5 Mapping accuracy 95
4. Discussion 97
Acknowledgements 102

**Chapter V: Agricultural land change in the Carpathian ecoregion after the breakdown of socialism and expansion of the European Union 105**

Abstract 106
1 Introduction 107
2 Methods 109
3 Results 113
4 Discussion 119
Acknowledgements 122

**Chapter VI: Synthesis 125**

1 Summary 126
2 Main conclusions 131

**References 139**

**Publikationen 162**

**Eidesstattliche Erklärung 166**

# List of Figures


Figure I-1: Maps illustrating the geographic setting of the Carpathian ecoregion in Eastern Europe: (A) Overview map showing the regional political situation during the existence of the Soviet Union; (B) Overview map showing the most recent political setting and specifically the years when different countries were accessioned to the European Union; (C) The main map shows the Carpathian ecoregion and its terrain as well as todays political borders and populated places. ..... 9

Figure II-1: The study region's terrain, populated areas and boundaries (main frame), location of the study region within the Carpathians (Carpathian Ecoregion Initiative boundaries) (top left), as well the distribution of broad forest types and private forest districts in the study region (lower left). ..... 22

Figure II-2: Three examples of trajectories and related imagery. Images show an early, intermediate and late point in time (RGB=453). Trajectory locations are indicated by the crosshair. Source value trajectories are shown in blue (gaps indicate masked no data values), fitted trajectories are shown in red. ..... 24

Figure II-3: Overview of the disturbance map and five subsets (subset scale is 1:500,000). ..... 31

Figure II-4: (A) Annually disturbed area with error bars indicating the 95% confidence intervals (dashed lines indicate the onset of the three restitution laws, dotted line points to the collapse of the Soviet Union), (B) mean disturbance per period, (C) annual number of disturbance patches, (D) patch based recovery state five years after disturbance onset, (E) annual mean patch size, (F) percentage of pixels above (grey) and below (black) three ha, (G) average patch based relative disturbance magnitude, (H) percentage of disturbance patches above (grey) and below (black) 60% relative disturbance magnitude. Notice that Y-axes for (F) and (H) are inverted. ..... 32

Figure II-5: (A) Overview and five subsets of the patch based recovery state, given as the percentage of the relative disturbance magnitude recovered after five years (subsets correspond to Fig.3, their scale is 1:500,000). (B) Map of growth areas exhibiting vegetative increase over 10-26 years (given in absolute cover increase, subset scale is 1:500,000). ..... 33

Figure II-6: Four details of the disturbance map, (B) imagery of one point in time close to the main disturbance events, (C) imagery of one point in time ca. five years later, (D) patch based percentage of recovered relative disturbance magnitude after five years (Imagery is shown as RGB=453). ..... 34

Figure II-7: (A) Relationship between the percentage of the annual allowable cut reserved for private owners of PFDs and disturbances rates within PFDs between 2006 and 2010 (note that the annual allowable cut for private and public owners of a PFD adds up to 100%). (B) Correlation between the annual disturbance rates detected in the PFDs and the percentage of coniferous species (note that the percentage of coniferous and deciduous species adds up to 100% for each PFD). Grayscale shading of points ranges from white (2006) to black (2010). ..... 35

Figure II-8: Distribution of detected disturbances within individual private forest districts per period (given in percent of total detected disturbances). ..... 36

Figure II-9: Three examples of the disturbance map (left column) and of imagery (RGB=453) for the area of private forest districts. The development of the annual disturbance rates for the three PFDs is given (forth column, dotted line indicated year of legal establishment). The examples show the PFD Papusa-Rucar (top), PFD Reghin-Gheorghieni (middle), PFD Targu–Secuiesc (bottom) [compare figure 8]. Red frames on the imagery indicate the location of two pictures taken during a field visit, exemplifying areas of excessive logging (right). ..... 37
Figure III-1: Landsat footprints from path 190 / row 25 in the northwest to path 182 / row 29 in the southeast (overlaid on Shuttle Radar Topography Mission elevation data). Sub regions for evaluation purposes are indicated by grey rectangles. ..... 51
Figure III-2: Score functions: (A) Seasonal correspondence of available images with three selected reference images (indicated by vertical dashed lines) in Landsat band 5, horizontal dashed line indicates the 0.8 $R^2$ cut-off value; (B) DOY score function with all year median DOY of 193 and all year standard deviation of 34.33, green and red dashed lines indicate the ±30 and ±45 day offset scores, respectively; (C) year score function; (D) cloud distance score function. ..... 53
Figure III-3: Output examples of the 2005 PBC: (A) best observation composite (RGB = 4,5,3); (B) year flag image; (C) relative difference to target DOY; (D) number of clear observations per pixel. ..... 59
Figure III-4: Radiometric consistency evaluation (from left to right): (column 1) aggregated PBC imagery (RGB = 4, 5, 3); (column 2) corresponding year flag images; (column 3) corresponding DOY flag images; (columns 4 – 7) band wise scatterplots for red, NIR, SWIR1 and SWIR2 bands of MODIS (Y axis) and PBC (X axis) data; (column 8) corresponding MODIS nadir BRDF-adjusted 16-day reflectance product (MCD43A4, RGB = 2, 6, 1)... 61
Figure III-5: Classification results (60x60 km) for the best observation composite only (left column) and for the best observation composite plus spectral variability measures (right column). Corresponding regions of the 2005 PBC in RGB = 4, 5, 3 (center column). ..... 65
Figure IV-1: The study region boundaries (red), the Carpathian Ecoregion (green), the national borders (black) overlaid on the best observation image composite for the target year 2005 (RGB = 4, 5, 3). A total of 1,407 scenes were provided to the compositing algorithm, which was parameterized to produce a cloud free, leaf-on seasonal state composite, considering imagery from 2003 to 2007. A series of six similar composites was made at five year intervals between 1985 and 2010. Coverage of Landsat footprints is superimposed in grey rectangles. The small inset shows the regional setting (AU = Austria, CZ = Czech Republic, HU = Hungary, PL = Poland, SK = Slovakia, RO = Romania, UA = Ukraine). ..... 77
Figure IV-2: An illustration of the recovery assessment methodology: the example shows (A) the disturbance map (the legend is provided on the lower right), and corresponding image chips for the years 1985, 1995 and 2010. For the central disturbance patch (indicated by the cross hair) the mean DI trajectory is shown (B, blue plot) as well as the resulting patch recovery metric (B, green plot). The patch mean pre-disturbance DI value is written into the first two recovery bands (1985, 1990), the disturbance magnitude is written into band three (1995) and the post-disturbance recovery status is written into bands four to six. ..... 82

Figure IV-3: Total forest area and forest type by country for the years 1985 and 2010 in square kilometers (top), changes in the proportion of forest types between 1985 and 2010 for the seven countries, expressed as the percentage of the total country forest area in the study region (bottom). ..... 88
Figure IV-4: The disturbance map showing the stable forest areas as well as the five disturbance classes, the national boundaries are overlaid in white. The extent of four details in the disturbance map is indicated by the red frames. Below we provide for each detail the disturbance map subset along with the respective composite imagery subsets for two points in time. ..... 89
Figure IV-5: Error adjusted area estimates of disturbed forest area for the five disturbance classes in square kilometers, with error bars indicating the 95% confidence interval around these estimates (top). Disturbed forest area for the five disturbance classes and the seven countries in the study area, expressed as the percentage of the 2010 country's forest cover in the study region (bottom). ..... 90
Figure IV-6: (A) Annual disturbance rates provided for the five disturbance periods and the administrative units in the study region (NUTS3 level for Austria, Hungary and Romania, district level for Czech Republic, Poland, Ukraine and Slovakia), (B) relative disturbance recovery rate, (C) relative net Change rate, (D) percent 2010 forest cover per region. ..... 91
Figure IV-7: Disturbance patch-based pre-disturbance forest type, provided for the five disturbance classes and the seven countries in the study region, expressed as the percentage of all disturbance patches of a given class in a given country. 92
Figure IV-8: The percentage of disturbance patches that had recovered by at least 70% spectral recovery magnitude in 2010, provided for the seven countries in the study region and the five disturbance classes. ..... 93
Figure IV-9: Four process examples (all provided at 1:475,000 scale): (A) areas with pronounced forest cover increase between 1985 and 2010 on former agricultural land in Hungary (forest type maps and composite subsets provided for 1985 and 2010), (B) large-scale disturbances in the Polish-Slovakian-Czech border region, (C) disturbance patterns in Czech Republic, (D) large-scale disturbances in the Romanian Eastern Carpathians (The legend for the forest type and disturbance map is provided in Fig.4). ..... 94
Figure V-1: Overview of the Carpathian study region (yellow), the ecoregion boundaries (black) and country borders (white). Additionally, the coverage of Landsat footprints is shown (magenta), which were used to produce three seasonal image composites (spring, summer and fall) for three reference years (1985, 2000 and 2010). ..... 110
Figure V-2: (Top) Error adjusted area estimates of change processes (compare table 1) for 2000 and 2010: ABD = cropland abandonment; GC = grassland conversion; RC = recultivation; FX = forest expansion on non-forest land. (Bottom) Error adjusted area estimates of change map results. Error bars indicate the 95% confidence interval around these estimates. ..... 114
Figure V-3: (Center) Change map derived from image composites and variance metrics. Classes relate to the land use / land cover during the respective reference year. Class acronyms: C = cropland, B = built up, F = forest, G = grassland, W = water. Six representative close-up frames are provided for relevant process regimes (top and bottom): (1) cropland-grassland conversion in the Czech Republic; (2) contrasting land change on the Polish-Ukrainian border; (3) cropland changes in Ukraine; (4) change dynamics in the Ukrainian-Hungarian border region; (5) widespread forest expansion in

Eastern Hungary; (6) cropland-grassland conversions and extensive recultivation in Romania. Map scale for all close-up frames is 1:750,000.115
Figure V-4: Process maps showing rates of cropland abandonment, grassland conversion, recultivation and forest expansion summarized to the level of administrative units (NUTS3 for Romania, Hungary and Austria; district level for Poland, Ukraine, Slovakia and the Czech Republic). The top row shows the rates for the transition period (1985 - 2000) the bottom row provides rates for the EU accession period (2000 – 2010). Note: different color table scaling for the two periods of cropland abandonment rates. .... 117
Figure V-5: Comparison of the average crop suitability index (Y axis) and cropland abandonment rates (X axis) aggregated to administrative units. Results are provided for the transition period (top) and the EU accession period (bottom). ..... 118
Figure V-6: Comparison of the average crop suitability index (Y axis) and recultivation rates (X axis) aggregated to administrative units. Results are provided for the transition period (top) and the EU accession period (bottom)..... 118

# List of Tables


Table II-1: Summary of results of the accuracy assessment for the disturbance map showing omission and commission errors (NF = Stable non-forest, F = stable forest, OAC = overall accuracy). ..... 29
Table II-2: Confusion matrix resulting from the validation of the disturbance map (NF = stable non-forest; F = stable forest). ..... 30
Table III-1: Landsat data used for the compositing in 2000, 2005 and 2010. ..... 51
Table III-2: Overview of different compositing outputs produced per target year result 56
Table III-3: Evaluated cases for temporal compositing of acquisition dates. The column "Priority" indicates the ranked preference of cases for compositing. ..... 57
Table III-4: Acquisition years of pixels used for compositing (Note: no input imagery existed for 1998 and 2012). ..... 58
Table III-5: Temporal composition of cases in the three best observation composites ... 58
Table III-6: Results of the evaluation of the radiometric consistency assessed for the 10 sub regions (first column), coefficients of determination ($R^2$) and root mean squared errors (RMSE) for the 6 corresponding MODIS and aggregated PBC bands. ..... 62
Table III-7: Results of the evaluation of the temporal composition of pixels according to the 9 defined cases assessed for the 10 sub regions (first column), provided for each target year composite. Additionally, the average number of available unclouded observations is provided. ..... 63
Table III-8: Result of the cross validation of the classification results for (a) only best observation bands as input, and (b) the best observation bands and the spectral variability measures (PA = Producer's accuracy, UA = user's accuracy, OAC = overall accuracy, CF = coniferous forest, MF = mixed forest, DF = deciduous forest, AG = agriculture, GL = grassland, BU = built up, WT = water). Additionally the number of samples per class for training is provided. ..... 64
Table IV-1: Total number of images used to create the series of six image composites over the 32 footprints. Moreover, the distribution of acquisition dates is provided. ..... 79
Table IV-2: Annual and seasonal composition of pixels in the six generated composite datasets. Annual composition refers to the offset in years to the respective target year, seasonal composition refers to the percentage of pixels with a relative acquisition date within 30 and 45 days from the target DOY (193 or July 12th). ..... 86
Table IV-3: Summary of forest cover changes between 1985 and 2010 for the country areas in the study region. Provided is the total forest area for 1985 and 2010 as well as the proportion of the three forest types of the total forest area and the changes in forest area and forest type proportions (CF = coniferous forest, MF = mixed forest, DF = deciduous forest). ..... 87
Table IV-4: Summary of the disturbance map validation (omission and commission errors provided). ..... 95
Table IV-5: Confusion matrix obtained from the validation of the disturbance map (CF = coniferous forest, MF = mixed forest, DF = deciduous forest, NF = non forest, DYY/YY refers to the disturbance class detected between the respective years). ..... 95

Table IV-6: Summary of the comparison of the 1985 and 2010 forest type maps with forest inventory data (omission and commission errors provided), for 2010 comparison with statistically sampled ground truth data is additionally provided (OAC = overall accuracy). ..... 96
Table V-1: Overview of the study design: The top section shows the targeted classes during change detection and mapping, which are provided with acronyms that refer to the land use / land cover during the individual reference years (top left). Class acronyms: C = Cropland, F = Forest, G = Grassland. Using black squares, sections two to four illustrate how the spatial extents of cropland, grassland and forest were derived for the three reference years. Definitions of the class constituents are provided on the far right. Finally, sections five to eight illustrate (using colored squares) how the targeted land change processes were derived. For example “Abandonment 2000” was derived by summing up "C-F-F", "C-G-C", "C-G-F" and "C-G-G". The abandonment rate for the socialist period was then derived as the percentage of the total “Cropland 1985” against “Abandonment 2000” (accordingly, “Grassland conversion 2000” and “Recultivation 2000” rates were derived relative to the “Grassland 1985”, while the “Recultivation 2010” rate was calculated relative to “Abandonment 2000”). ..... 112
Table V-2: Change processes summarized for the countries in the Carpathian study region as total area [km²] and as percentage. Country acronyms are: AU = Austria, CZ = Czech Republic, HU = Hungary, PL = Poland, RO = Romania, SK = Slovakia, UA = Ukraine. Percentages relate to the total country cropland area in 1985 for the abandonment rates and to the 1985 grassland area for the grassland conversion rates. Note that the rate for “Recultivation 2010” is relative to the “Abandonment 2000” areas, while the rate for “Recultivation 2000” is calculated relative to the 1985 grassland areas. Forest expansion rates are calculated relative to the 1985 forest area in a given country. We used results from a Landsat based forest disturbance mapping to make sure that forest expansion does not include forest areas that are regenerating after disturbances (similarly grassland conversions exclude regenerating forest disturbances). ..... 116
Table V-3: Validation results providing the confusion matrix as well as overall, user’s and producer’s accuracy for the change map derived from the analysis of the 9 seasonal composites and spectral variance metrics (Note: the producer’s accuracy was obtained from the area adjusted error assessment). ..... 119

# Chapter I:
# Introduction

## 1 Land use and global environmental change

The use of land and the utilization of natural resources are essential elements of human existence (Vitousek 1997; DeFries et al. 2004; MEA 2005). With the onset of agriculture humans began using land to cultivate plants, graze domesticated animals, and eventually started to trade after achieving production surpluses. Since the industrial revolution, the scope of human activities has been amplified through the exploitation of fossil energy sources, and the rampant increase of the world population, enabled mainly through innovations that allowed for global transport and trade as well as the mechanization of agriculture and production systems but also better nutrition and medical advancements (Steffen et al. 2007). The continuous population growth over the past century and the accompanied increasing demand for food has generally been met, partly thanks to the 'Green revolution', i.e., the production and application of industrial fertilizers and pesticides, new crop varieties, and use of irrigation systems (Tilman et al. 2011). These achievements allowed for an unprecedented portion of the world population to prosper and become increasingly affluent, but this also amplified the demand for natural resources especially food, fiber, fuel and fresh water (Godfray et al. 2010). As a result, the scope of human activities on Earth has started jeopardizing the functioning of central components of the Earth System (Lenton et al. 2008; Rockstrom et al. 2009), ultimately threatening human well-being (GLP 2005; MEA 2005).

The appropriation of nature by humans and the conversion of natural ecosystems to provide specific human requirements are global in scale (Vitousek 1997; Kareiva et al. 2007). About half of the terrestrial land surface is currently used as cropland or pastures (Kareiva et al. 2007). The list of negative environmental impacts caused by the increasing influence of human activities on Earth is extensive. Most prominent and overarching, the accumulation of greenhouse gases in the atmosphere can be linked to human activities and is accelerating global climate change which in turn affects ecosystems and their functioning (IPCC 2000; Houghton 2003; GLP 2005; IPCC 2007). Agricultural land use accounts for the greatest consumption of freshwater and simultaneously degrades the quality of surface and ground waters (Bennett et al. 2001). The natural geochemical cycles of Nitrogen and Phosphorous have been drastically altered, and the riverine transport of agricultural fertilizer runoff has led to extensive 'dead zones' near many marine estuaries (Diaz and Rosenberg 2008). Land changes (i.e., changes in land use and/or land cover) also

alter the radiative properties of land surfaces and thus affect water and energy balances, and aggregated to larger scales these changes affect regional climates (IPCC 2000; Foley et al. 2003; Bonan 2008). Current rates of species extinctions are unprecedented in Earth's recent past and are mainly driven by habitat destruction and are amplified by climate change (Vitousek 1997; Sala et al. 2000; Bellard et al. 2012). More than half of the world's forests have been cleared with direct consequences for the climate system mainly through alterations of the global carbon cycle (FAO 2010; Pan et al. 2011). Forest plantations are increasingly replacing natural forests but often only provide a fraction of the environmental benefits that are provided by natural forests (Chazdon 2008; Paquette and Messier 2010). The transformation of natural ecosystems thus has far reaching consequences, and land change has become a principal driver of global environmental change (Foley et al. 2005).

These transformations of natural ecosystems are of concern though due to the dependence of humanity on the goods and services that those ecosystems provide (Daily et al. 2000; MEA 2005; Turner et al. 2007). Such ecosystem services include water purification, pollination, climate regulation, and these services enable and support life on Earth. When humans convert ecosystems to a specific type of land use (e.g. agriculture or urban areas), existing ecosystem services are diminished in favor of the targeted service, for example food or timber production (DeFries et al. 2004; Foley et al. 2005). In order to mitigate the negative consequences of future land use on ecosystem functioning (Nagendra et al. 2013), it is important to understand where and why land change occurs. Unfortunately though, we are far from thoroughly understanding the drivers of land change globally or where these changes occur (DeFries et al. 2004; Foley et al. 2005; Lambin and Meyfroidt 2010). This dissertation makes a contribution towards filling these knowledge gaps.

Generally speaking, land change is driven by a variety of influences operating at different temporal and spatial scales and which are often interlinked (Lambin and Geist 2006b). These drivers include direct or proximate causes (e.g., fuel wood extraction or cropland expansion driving deforestation locally), as well as root or underlying causes (e.g., migration dynamics or subsidy policies). While proximate causes of land change are predominantly linked to the local scale, underlying causes can also operate from the regional, national and even global scales and modulate the intensity of proximate causes. Understanding the influence of proximate causes on land change processes can be achieved through spatial analytical methods, such as provided through GIS and spatial statistics, but identifying the underlying causes of land change is more difficult, partly because data on land change is commonly not available over large spatial scales or for longer time periods.

Conceptual models can help to improve our understanding of land change (DeFries et al. 2004; Rudel et al. 2005; Lambin and Meyfroidt 2010). Land use transition theory, for example, assumes that land systems (i.e. the amalgamation of land use and land cover within a country or region) undergo different stages of varying land use intensity depending on their level of socio-economic development. Land systems in an early stage of their developments (e.g. agricultural frontiers) are dominated by natural ecosystems with an increasing share of clearings to establish settlements and subsistence agriculture. As economic and societal development progresses, natural and subsistence landscapes are progressively replaced by more intensive agricultural production systems and urban areas, until ultimately the only larger tracts of remaining natural ecosystems are protected areas. Forest transition theory illustrates how land systems can undergo non-linear land use trends (Mather et al. 1999; Rudel et al. 2005; Rudel et al. 2010). In many countries, forest cover first declines with increasing population and socio-economic development. After reaching a low point, however, net forest cover increases again. Different causal mechanisms have been proposed to explain this transition (Rudel et al. 2005; Lambin and Meyfroidt 2010). According to one school of thought, scarcity of forest resources leads to ecosystem degradation, increasing environmental problems (e.g. floods, landslides, soil erosion), which in turn create greater societal awareness regarding the importance of forest resources. This awareness then triggers policy interventions that increase national forest cover. Other explanations suggest that increasing economic development and innovation are the main causes of the forest transition, since they lead to more employment in the service sector as well as to the intensification and spatial concentration of agriculture on more fertile lands and thus eventually to the abandonment and subsequent reforestation of marginal lands.

Land systems are generally assumed to gradually transition through different developmental stages, but key events can cause land systems to rapidly shift between different stages or even overleap stages entirely (DeFries et al. 2004). Such drastic, non-linear shifts in land use systems can be triggered by profound changes in socio-economic and institutional conditions (Hostert et al. 2011a). For example, wars or revolutions can lead to migration of large population segments and thus decrease the degree of land use in a given area (Dudley et al. 2002; Machlis and Hanson 2008). Conversely, technological innovation can suddenly lead to increased profitability of agricultural commodities thereby accelerating deforestation driven by cropland expansion (Zak et al. 2008). Similar to natural ecosystems, such drastic events can shift land systems onto new long-term land use

trajectories (Scheffer et al. 2001; Dearing et al. 2010). Studying land change under rapidly changing socio-economic conditions might reveal insights regarding the role of broad scale underlying drivers of change. Such a better understanding of such drastic changes is needed to better forecast land change globally and thus mitigate the negative impacts of global environmental change (Steffen et al. 2004). The collapse of the Soviet Union and of the socialist regimes in Eastern Europe represents a unique opportunity to study land change during drastic socio-economic transformations.

Other factors currently challenging our understanding of land change relate to the increasing interconnectedness of the world and especially the globalized trade and production systems, which make the underlying drivers for land change increasingly important (Meyfroidt et al. 2013). Distant markets increasingly influence local or regional land use decisions (Barona et al. 2010), globalized consumption and production systems demand more natural resources from distant countries and thereby externalize their land use requirements (Meyfroidt et al. 2010; Weinzettel et al. 2013). Countries with scarce arable lands are increasingly involved in large scale land acquisitions and investments in agro-enterprises abroad (Rulli et al. 2013).

In summary, land use is a central component of global environmental change and a better understanding of where and when land change occurs is a prerequisite for creating more sustainable land systems. Additionally, a better understanding of what drives land change globally is needed in order to anticipate future developments and mitigate ecosystem degradation. The general pattern of land change globally is that land conversions (i.e., categorical change of land use or cover types) predominantly occur in developing countries, while industrialized nations increasingly experience land use modifications (i.e. changes within a land use / land cover category), especially the intensification of land use on productive land and the abandonment of marginal lands. Yet, drastic socio-economic perturbations can cause severe and non-linear land change responses. Moreover, distant global forces increasingly drive land change locally and an escalating scarcity of arable lands increases competition over land resources globally. A key piece of refining land change theories is the improvement of land change monitoring. This involves reconstructing past land change as well as setting up operational monitoring systems to track present and future land change, and to develop new remote sensing approaches to monitor not only land conversions, but also land use modifications.

## 2 Remote sensing based land change monitoring

Since the advent of modern earth observation in the 1970s, remote sensing has greatly advanced in terms of the variety of available sensors, the derived products, and the diverse fields of its application (Lillesand and Kiefer 2000; Xie et al. 2008). First and foremost, remote sensing observations are temporally and spatially explicit, they are synoptic in that they capture large areas irrespective of political or ecological boundaries, and they are repeatable and often have been acquired over long time periods and therefore allow for assessing changes over time (Lu et al. 2004; Richards 2005; Richards and Jia 2005). It is due to these characteristics that remote sensing has become the most important tool to map and monitor land change.

Today, a multitude of sensors operationally acquire data at different spatial scales, with different temporal and spectral characteristics. Among these, Landsat satellites are unique in several aspects (Goward and Masek 2001; Loveland and Dwyer 2012). Landsat imagery covers the most important spectral regions needed for terrestrial applications. The spatial resolution of the more recent sensors provides a good compromise between the area coverage of an image (roughly 185 x 185 km) and the spatial resolution (30 x 30 m), which is well suited to monitor changes in natural and man-made environments (Cohen and Goward 2004; Wulder and Masek 2012). Landsat data provide the longest, continuous record of earth observation imagery and the global Landsat archive currently contains more than 4 million scenes. Imagery has been continuously acquired since 1972 in the case of the Multispectral Scanner system, and since 1982 with the Thematic Mapper instruments, and this long-term data record allows for retrospective land change assessments over several decades (Williams et al. 2006). Additionally, persistent research and engineering efforts have focused on maximizing spatial and radiometric consistency across sensors and platforms, further contributing to the exceptional suitability of Landsat data for land monitoring applications (Markham et al. 2004; Chander et al. 2009).

Analytical methods for performing change detection and mapping of land change with Landsat imagery have progressed greatly since the beginning of the Landsat program (Singh 1989; Coppin et al. 2004). The fundamental basis of most of these change detection approaches are sets of multi-temporal imagery that are compared in different ways in order to extract spectral differences that are associated with changes in land cover (Lu et al. 2004). The majority of established change detection approaches focus on one or several pairs of images (Coppin et al. 2004; Kennedy et al. 2007). Such approaches have several shortcomings because detailed spatial and temporal aspects of these changes remain

unknown. Moreover, while land conversions are well captured with such approaches, because there is sufficient spectral change, subtle processes such as land cover modifications or long-term trends such as forest degradation, are difficult to map using pairs of multi-temporal imagery. In recognition of these shortcomings, first Landsat time series approaches compiled longer sequences of imagery and aimed at quantifying long term and often subtle trends in the data, commonly utilizing regression approaches (Hostert et al. 2003; Roder et al. 2008b).

Another common drawback of many change detection approaches is that they analyze one footprint at a time, and heavily rely on the availability of could-free imagery. In many regions, such imagery is difficult to obtain. On the one hand due to persistent cloud coverage and on the other, because Landsat satellites have a repeat cycle of 16 days (NASA 2009), and thus the actual number of images may be lower than potentially achievable, according to the long term acquisition plan and especially for areas outside the United States (Ju and Roy 2008). Finally, until recently Landsat data were expensive to obtain which additionally limited the applicability of approaches that utilized larger collections of imagery (Hansen et al. 2008).

Many of the limitations outlined above disappeared when the United States Geological Survey (USGS) provided Landsat data for free, starting in 2008 (Woodcock et al. 2008). Besides access to formerly expensive data at no cost, imagery now was provided with unprecedented absolute and relative geometric accuracy (Wulder et al. 2012). Additionally, new highly automated preprocessing algorithms for atmospheric correction, radiometric normalization and cloud/shadow masking were developed (Masek et al. 2006; Zhu and Woodcock 2012). These developments were accompanied by considerable increases in computational performance and data storage capacity. These factors jointly opened many new opportunities for the use of Landsat data for land change studies. For example, analyses algorithms can now incorporate and consider individual pixels rather than using entire scenes, thus making partially clouded images potentially useful for analyses. In addition, much greater volumes of imagery could now be automatically converted into physically comparable absolute units, which improved the ability to spatially and temporally integrate large collections of images.

The significance of the Landsat archive for land change research increased considerably as a consequence of these developments (Wulder et al. 2012). Furthermore, with most international ground station holdings now being consolidated into the USGS archive

(Loveland and Dwyer 2012), the new Landsat 8 satellite operationally acquiring imagery since May 2013 (Irons et al. 2012), and the upcoming European Sentinel-2 satellite which was developed to provide continuity to Landsat observations (Drusch et al. 2012), the importance of the Landsat archive for Earth sciences will only increase. This makes it both exciting and important to refine methods for both, temporally dense time series analyses for limited spatial extents, and change detection and mapping at full 30-m Landsat resolution at regional to continental scales. Developing such methods is far from trivial though, and some of the remaining technical challenges include implementing efficient mass data processing workflows, as well as integration of data from multiple sensors and spatial scales. Moreover, while many analytical methods are developed for cover types with predictable phenology (i.e., temperate forests), agricultural land change requires more sophisticated methodological approaches, especially in drylands, mountain areas, and the tropics. Finally, the intensification of land use is expected to become more prevalent in the near future, and remote sensing methods are much better at detecting land cover conversions rather than intensification (Kuemmerle et al. 2013). However, if these challenges are met, then the Landsat record will allow for a detailed reconstruction of past land change. The ability of generating consistent maps of land change processes at 30-m resolution and over large areas will advance our understanding of the causes of land change and improve the forecasting of future change and the mitigation of its negative consequences.

## 3 The Carpathian ecoregion and recent socio-economic transformations

The Carpathians are Europe's largest continuous mountain range, extending in an arc shape over approximately 1,500 km in Central Eastern Europe (CEE), and covering parts of Austria, the Czech Republic, Slovakia, Poland, Hungary, Ukraine, Romania and Serbia (Figure I-1). The Carpathians feature a temperate-continental climate and overall lower elevations than the Alps. Within Europe the Carpathians hold special ecological significance. For example they are an important source of freshwater to a region considerably larger than the mountain range (Turnock 2002). Despite a long land use history, human impact is not as pervasive as in other European mountain regions (Anfodillo et al. 2008). They also represent Europe's largest continuous temperate forest ecosystem, and contain some of the largest tracts of remaining unmanaged old growth forest, as well as a generally rich floristic diversity with high levels of endemic species

(UNEP 2007; Veen et al. 2010). Biodiversity is also very rich, and in terms of its fauna, includes several carnivore flagship species such as Lynx (*Lynx lynx*), Wolf (*Canis lupus*) and the largest population of Brown Bears (*Ursus arctos*) in Europe (Rozylowicz et al. 2011). The Carpathians also have a rich cultural history featuring traditional low-intensity farming landscapes that provide habitat to a large variety of plants and mammals (Spulerova et al. 2011; Fischer et al. 2012). Moreover, the national economies of the Carpathian countries profit from agricultural and forestry land use, mining and increasingly from tourism (Björnsen Gurung et al. 2009). Approximately 16% of the Carpathians today are under some form of nature protection and different initiatives promote interdisciplinary research efforts to aid sustainable land use development in the Carpathian ecoregion(CERI2001).

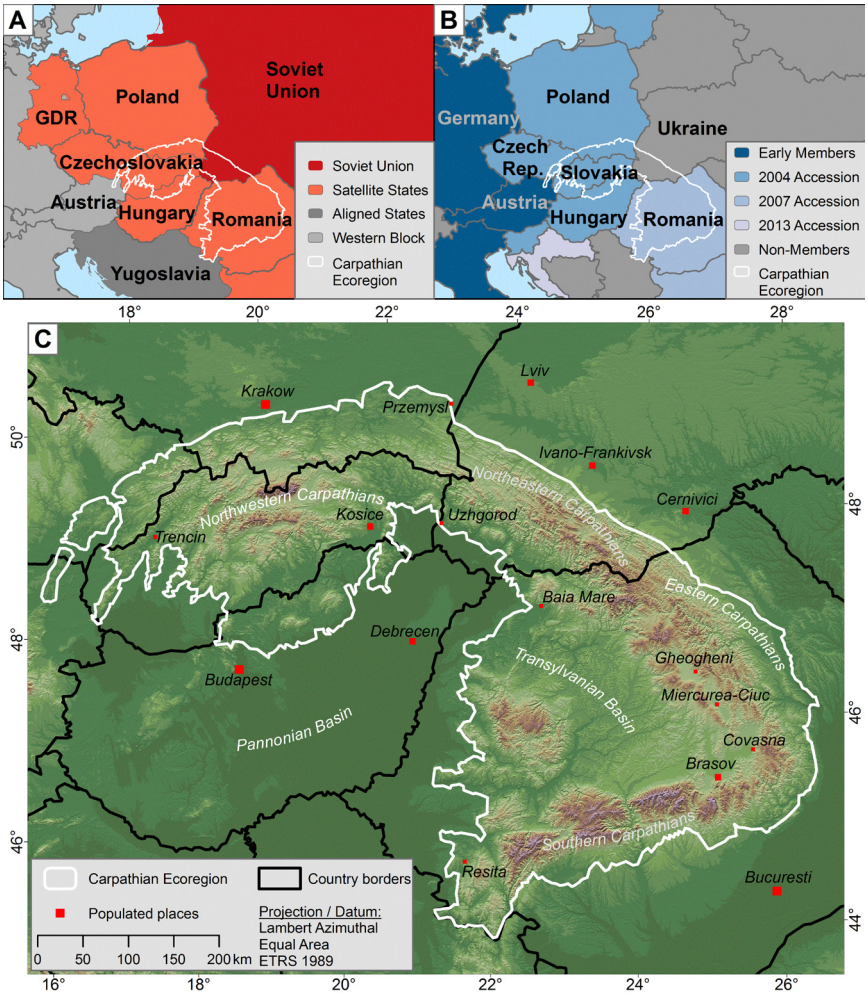


Figure I-1: Maps illustrating the geographic setting of the Carpathian ecoregion in Eastern Europe: (A) Overview map showing the regional political situation during the existence of the Soviet Union; (B) Overview map showing the most recent political setting and specifically the years when different countries were accessioned to the European Union; (C) The main map shows the Carpathian ecoregion and its terrain as well as todays political borders and populated places.

With regard to its socio-economic conditions, the Carpathian region experienced a turbulent history over the past century. Until World War I, most of the region belonged to the Austro-Hungarian Empire which led to a homogenization of land management and land use traditions (Munteanu et al. Submitted). Several independent states emerged during the inter-war period and land use trajectories generally diversified thereafter (Turnock 2002). Following the end of World War II (WWII), most Carpathian countries became either part of the Soviet Union (Ukraine), or satellite states with their own socialist governments, with the exception of Austria (Figure I-1(A)). More recently though, two episodes of major socio-economic transformations occurred in CEE, that deeply affected governance, institutions, policies and demography and had strong implications for the entire land systems in the Carpathians: First the collapse of socialism in 1991, and second the accession to the European Union after 2004. Both individual events differed in quality and magnitude, yet as both led to profound changes in political, societal and economic systems, I refer here to both as socio-economic shocks or disturbances (Hostert et al. 2011a).

The first socio-economic shock occurred with the collapse of the Soviet Union in 1991 after which the socialist regimes of the Eastern Block and CEE embarked on a series of institutional, economic and political transformations (Turnock 2002).These transformations included the establishment of political independence, transitioning from a state-led to a market driven economy, reforming collectivized production systems and creating a land tenure system. As such, these transformations affected land management and ownership and impacted the land system and affected the regional agricultural and forestry sectors in particular.

The socialist collapse triggered what has been called ‘the most drastic period of land change in the 20th century’ (Henebry 2009). Land reforms were a central aspect of post-socialist transformation with profound implications for land use. Following the end of WWII, forest land was largely collectivized under most communist regimes in the Carpathian countries (however, to a lesser extent in Poland). In terms of agricultural land, non-governmental ownership (e.g. private ownership or property of churches) persisted through the socialist period, yet to varying degrees in the individual countries. Irrespective of ownership, virtually all land was managed by the socialist regimes during the communist era, either through large collective farms or through state-led forest management enterprises.

After the collapse, individual countries followed different strategies to redistribute collectivized land, including distribution, market driven auctioning, and the legal land restitution processes (Lerman 2001; Weiss et al. 2012). As a consequence, forest and agricultural land ownership is today highly fragmented in many parts of the Carpathians. The forestry sector also faced many other challenging reforms during the transition. The entire forest management and timber processing industry was restructured and the logging industry in CEE declined considerably (Csóka 2005). However, due to weak governance and economic hardship during the transition period, illegal timber exploitation was widespread (Brandlmaier and Hirschberger 2005).

Changes in the agricultural sector were as profound as in the forestry sector. The socialist agricultural production was based on large scale, collective farms mostly managing vast areas and utilized an essentially exhaustless workforce (Lerman 2004). Agricultural production relied heavily on subsidies, virtually all land was farmed including marginal areas, and Soviet outlet markets for agricultural commodities were guaranteed and provided stable input and output prices (Csaki 1990; Lerman et al. 2002). Following the collapse of the Soviet Union, all of these supporting components of the socialist agricultural production system vanished. The market and price liberations that were part of the transition to market economies made agricultural production no longer economically viable. Moreover, large population segments, especially young people, migrated to urban centers or abroad (Müller and Munroe 2008). As a consequence agricultural production decreased throughout CEE during the transition period.

The second socio-economic shock that strongly affected the land systems in the Carpathians was triggered by the accession to the EU. Most Carpathian countries (except Ukraine and Serbia) became members of the EU in 2004 (Romania was accessioned in 2007 and Austria had been a member since 1995, compare Figure I-1(B)). Forestry and agricultural sectors of the accession countries now benefited from being part of the European market. However, forest management and the timber industries now had to comply with European forest legislations including the guiding principles of sustainable forestry in Europe with regard to biodiversity and other ecosystem services, such as carbon sequestration (UNECE and FAO 2011).

With the EU accession, the agricultural sectors of most Carpathian countries were covered by the EU's Common Agricultural Policy (CAP) under which farmers receive subsidies for the land they manage for agricultural production. On the other hand, the EU environmental

directives and the CAP provided incentives to control pests, curb the use of pesticides, preserve soil quality and improve water management in the accession states (World Bank 2007). The most recent reform of the CAP links payments to environmental conditions and sustainable production, which will again affect agricultural production in the accession states. Finally, the Natura2000 habitat directive requires the designation of special protection areas in order to preserve rare and threatened habitats within European landscapes and the new member states were obliged to propose such candidate areas which have direct effects on land use (Stancioiu et al. 2010).

In summary, the Carpathians are of unique ecological value within Europe, harboring high levels of biodiversity and providing a wide array of ecosystem services to an area much larger than the actual mountain range. While the region has a long land use history, which is likely to still affect the land systems today, the post-socialist transformation processes and the subsequent accession to the EU had profound impacts on land use and especially on the agricultural and forestry sectors. While it is commonly understood that the collapse of socialism resulted in drastic declines in both sectors, the rates and spatial patterns of land change remain largely unclear. The main consequences of the EU accession on agriculture and forestry are even less understood. Studying land change in the Carpathians thus may provide insights into the effects of socio-economic perturbations on land systems. While several case studies have addressed land changes for smaller areas, land change research across the Carpathians as a whole is still missing (Björnsen Gurung et al. 2009; Kozak et al. 2011). This is unfortunate, because the ecoregion spans several political borders, and that studying land change across administrative boundaries potentially allows for insights regarding the role of underlying drivers of land change (Kuemmerle et al. 2008).

## 4 Overall aim, research questions and methodological approach

The primary objective of this dissertation was to develop and apply new remote sensing based methods for land change monitoring that make better use of the rich Landsat archive and specifically improve the temporal detail and spatial coverage of these methods. The secondary objective was to map and analyze rates and spatial patterns of land change in the Carpathians since 1985 and to interpret these changes against the background of recent socio-economic transformations, namely the post-socialist transition and the EU accession.

The Carpathians offer unique research opportunities and the effects and outcomes of the most recent transformation processes on the regional land system are not well understood. This is unfortunate as such understanding might reveale insights regarding the role of underlying drivers of land change. Remote sensing is the key technology for land change monitoring and the Landsat archive offers new analyses approaches. Alternative data sources are not readily available, often not spatially explicit, and commonly not comparable among countries or time periods. Yet, the required methodological toolset to map and quantify land change over the Carpathians with Landsat data is not readily available, as existing methodologies are commonly impeded by temporal and/or spatial constraints. Thus, in order to better understand rates and spatial patterns of land change in the Carpathians, the temporal interval of observation needs to be improved and the spatial coverage of the analyses has to be extended to ideally enclose the entire Carpathian ecoregion. Chapter II of my dissertation targets these temporal aspects by addressing:

*Research Question I (Dissertation chapter II)*: How can refined image analysis approaches better utilize the temporal depth of the Landsat archive in order to improve our understanding of how rates and patterns of forest disturbance changed during massive ownership changes?

I answer this question by employing a trajectory-based change detection approach with near-annual resolution to assess how three successive stages of the forest restitution in central Romania affected the utilization of forest resources. I specifically investigate how forest disturbance rates and patterns changed after the collapse of socialism and how three individual forest restitution phases affected disturbance rates and patterns. Finally, I examined differences in the frequency and extent of forest disturbances among state, community, and privately owned forest lands. Subsequently, I addressed:

*Research Question II (Dissertation chapter III)*: How can image datasets of regional extent be derived from the Landsat archive and how can these datasets be used for broad-scale land cover mapping and change detection?

Extending land monitoring and change mapping capabilities beyond the scale of single Landsat footprints requires new methodological developments. Besides prohibitive data costs and insufficient processing capabilities, other factors that constrained Landsat analyses in the past were the seasonal timing of the imagery and differences in atmospheric conditions among image acquisition dates. This is a problem because using imagery from different seasons (e.g., mid summer and late autumn) in classic change detection is likely

going to result in false positive errors due to differences in vegetation phenology. With the availability of fully automated atmospheric correction and cloud masking algorithms, Landsat observations can now for the first time expediently be considered on the per-pixel basis. Consequently, I extended processing approaches that were initially developed for high temporal frequency sensors in order to derive new, regional data sets from the Landsat archive, and described this new approach in my Chapter III.

The algorithmic toolset developed in Chapter III is then put into value in two subsequent chapters that target the analysis of land change across the entire Carpathian ecoregion, specifically the mapping and analysis of regional forest dynamics as well as agricultural land change processes. First, my Chapter IV addresses regional forest cover dynamics:

*Research Question III (Dissertation chapter IV)*: What were the rates and spatial patterns of forest cover changes in the Carpathians since 1985?

Forest and agricultural changes are to a certain extent complementary to each other and therefore need to both be assessed in order to fully understand land change dynamics in the Carpathians since the mid1980s. Yet, both processes are very different in terms of their spectral-temporal characteristics and therefore require specifically tailored analysis approaches. Therefore, Chapter V investigates:

*Research Question IV (Dissertation chapter V)*: What were the rates and spatial patterns of agricultural land change in the Carpathians since 1985?

In Chapter IV I specifically assessed changes in the distribution of broad forest types as well as the rates and patterns of forest disturbances and subsequent forest recovery are addressed. The research study presented in Chapter V of my dissertation investigates the main changes in agricultural land use over the Carpathian ecoregion. Several land cover/land use trajectories were aggregated to broader process classes and these were then compared against the environmental and agro-ecological characteristics of the localities where they occurred.

## 5 Structure of this dissertation

This dissertation consists of six chapters. This introduction is followed by four core research chapters (Chapters II-V) that have been outlined in the previous section. Chapter VI provides a synthesis of the entire thesis, summarizing the main outcomes of the individual research chapters and providing answers to the research questions. Finally the main conclusions are drawn.

The core research chapters (Chapters II – V) were prepared for publication within international peer reviewed research journals, two of them have been published already, a third is accepted, and the last in review:

Chapter II: Griffiths, P., Kuemmerle, T., Kennedy, R.E., Abrudan, I.V., Knorn, J., & Hostert, P. (2012). Using annual time-series of Landsat images to assess the effects of forest restitution in post-socialist Romania. *Remote Sensing of Environment*, 118, 199-214.

Chapter III: Griffiths, P., van der Linden, S., Kuemmerle, T., & Hostert, P. (2013). A Pixel-Based Landsat Compositing Algorithm for Large Area Land Cover Mapping. *IEEE Journal of Selected Topics in Applied Earth Observations and Remote Sensing*, PP, 1-14.

Chapter IV: Griffiths, P., Kuemmerle, T., Baumann, M., Radeloff, V. C., Abrudan, I.V., Lieskovský, J., Muntenau, C., Ostapowicz, K., & Hostert, P. (accepted). Forest disturbances, forest recovery, and changes in forest types across the Carpathian ecoregion from 1985 to 2010 based on Landsat image composites. *Remote Sensing of Environment*.

Chapter V: Griffiths, P., Mueller, D., Kuemmerle, T., & Hostert, P. (in review). Agricultural land change in the Carpathian ecoregion after the breakdown of socialism and expansion of the European Union. *Environmental Research Letters*.

# Chapter II:
# Using annual time-series of Landsat images to assess the effects of forest restitution in post-socialist Romania

*Remote Sensing of Environment 118 (2012) 199-214*

Patrick Griffiths, Tobias Kuemmerle, Robert E. Kennedy,
Ioan V. Abrudan, Jan Knorn and Patrick Hostert


*doi: 10.1016/j.rse.2011.11.006*
*Received 09 August 2011; revised 08 November 2011;*
*accepted 18 November 2011.*

**Abstract**

The increasing availability of the Landsat image archive and the development of approaches to make full use of these data provide novel insights into the drivers and dynamics of land use systems change. Focusing on Romania, we asked how the drastic institutional and socio-economic transformation after the collapse of socialism in Eastern Europe affected forestry. We used an annual time series of Landsat images to investigate how three phases of forest restitution affected forest disturbances (due to both, natural events and forest management). We employed the LandTrendr (Landsat-based detection of trends in disturbance and recovery) set of change detection algorithms to perform temporal segmentation and fitting of the Landsat time series, and derived annual disturbance maps (95.72% overall accuracy) along with recovery dynamics. Our change map suggested that forest disturbances increased substantially since the collapse of socialism in 1989, with 75,000 ha of disturbed forest land (4.5% of the total studied forest area). Whereas the late socialist years were characterized by relatively low disturbance levels (12% of all detected disturbances), disturbances increased especially after each of the restitution laws were passed in 1991, 2000, and 2005 (34%, 21% and 32% respectively). Non-state ownership regimes (i.e. private owners vs. public property of local communities) and species composition of restituted forests were two important factors determining disturbance levels. The widespread disturbances we found also raise concerns about timber overexploitation in many areas of the Romanian Carpathians. Our study demonstrates the value of the temporal depth of the Landsat archive and highlights that trajectory-based change detection approaches can be highly beneficial for gaining insights on the effect of institutional shocks on land use patterns.

# 1 Introduction

Land use change is among the primary drivers of global environmental change, affecting ecosystem services and biodiversity, and thus ultimately human well-being (Foley et al. 2005; MEA 2005). Until recently, land use changes were assumed to occur gradually, with land use systems transitioning from one state to another, often following similar intensification pathways as economic development progresses (DeFries et al. 2004). New paradigms for land use change are now evolving, recognizing that land use transitions (i.e., fundamental shifts in land use systems) can also occur very rapidly, sometimes following long periods of relative stability (DeFries et al. 2004; Lambin and Meyfroidt 2010).

Sudden changes in land systems are particularly frequent in the case of drastic institutional or socio-economic transformations, for example, in the case of revolutions (Kuemmerle et al. 2007; Mueller et al. 2009), economic shocks (Sunderlin et al. 2001), failing states (Irland 2008), technological breakthroughs (Zak et al. 2008) and warfare (Dudley et al. 2002; Machlis and Hanson 2008). Although remote sensing has been instrumental for understanding patterns of land use and land cover change, most change detection approaches (Coppin and Bauer 1996; Coppin et al. 2004) are not well-suited to detect such sudden changes or tipping points as they focus on the comparison of two points in time. Separating gradual changes from sudden ones, however, is challenging using such bi-temporal approaches, and this represents a major obstacle for determining how and why land systems change (Dearing et al. 2010).

The recent opening of much of the global Landsat archive by the United States Geological Survey (USGS) provides new opportunities to advance land use science and has sparked the development of new methodological approaches. For example, change detection methods based on annual Landsat time series (i.e. trajectory-based change detection methods) such as the Landsat-based detection of Trends in Disturbance and Recovery (LandTrendr) and the Vegetation Change Tracker (VCT) (Huang et al. 2010b; Kennedy et al. 2010) make better use of the temporal depth of the Landsat archive to reconstruct forest disturbance histories with annual resolution and to map trends, such as forest regeneration and succession. Likewise, annual time series of Landsat images can help to separate sudden from gradual vegetation change in rangelands (e.g., fires vs. grazing pressure - (Hostert et al. 2003; Roder et al. 2008a; Sonnenschein et al. 2011). New change detection approaches based on time series of Landsat images offer several methodological

advantages, including robustness against spectral variations arising from topography and phenology. Data availability issues are alleviated by choosing the best suited pixel from potentially many cloud-obscured images. Overall, trajectory-based methods should thus also provide opportunities to assess the effects of socio-economic disturbances, such as rapid political and institutional changes, on land use systems, but to our knowledge no study has used annual stacks of Landsat images for this purpose.

The changes initiated by the collapse of socialism led to fundamental restructuring of the political-, social and economical systems in Central and Eastern European countries (Swinnen 1999; Lerman et al. 2002). This triggered widespread transformations in the countries land use systems, resulting for example in agricultural abandonment and extensification, rural depopulation and increased illegal logging of forests (Henebry 2009; Kuemmerle et al. 2009a). The question of land ownership and the re-privatization of formerly collectivized agricultural and forest land was among the key issues during the post-socialist phase and countries followed different strategies. Regarding forest ownership, Romania opted for restitution to historically entitled owners or their heirs.

Prior to 1948, forests belonged to the state (28%), were in private possession (23%) or were owned by local communities, religious or educational institutions or by forms of communal ownership (about 50%, so called public property) (Ioras and Abrudan 2006). During socialism (1948 - 1989), Romania's forests were almost entirely owned by the state (here and in the following, 'state' refers to the federal/central government). Restitution was implemented in three distinct laws: law 18/1991 returned up to one ha to historically entitled private individuals (350,000 ha in total), irrespective of historic location or extend (Vasile 2009). The second law was passed in 2005 and favored public owners while constraining the restituted forest area for individuals (10 ha), churches (30 ha), and community members (20 ha). Since 2005 the third law aims at returning all remaining pre-World War II not state-owned forest property. Once complete, up to 70% of Romanian forests will have been restituted, increasing the number of non state forest owners to 800,000 (Lawrence 2005; Ioras and Abrudan 2006; Lawrence 2009). However, it remains unclear how the end of socialism and the restitution process have affected rates and spatial patterns of forest cover change.

Realization of the restitution proved to be complex, often leading to confusion and frustration among prospective owners (Abrudan 2005; Vasile 2009) and concern has been expressed about forest utilization through new non state owners (e.g. immediate felling).

Today, forests can either be (1) state property, (2) public property owned by local communities, (3) private property of local communities or (4) private property of individuals or legal entities (associations, schools, churches) (Stancioiu et al. 2010). All forests are grouped into two functional categories: (1) protection forests and (2) protection and production forests (Anfodillo et al. 2008; Stancioiu et al. 2010). Protection forests serve important ecological functions (e.g. along water bodies) and limit economic benefits for owners. New forms of forest management include private forest districts (PFDs). These are associations of non-state forest owners providing coordinated management across larger areas of at least 3,000 ha. Currently, 126 of such associations exist.

Our main goal was to use a trajectory-based change detection approach (LandTrendr) in order to assess the effects of the collapse of socialism and the Romanian forest restitution on forest disturbances. Disturbances here refer to intermediate to high intensity canopy disturbances caused by either natural events (e.g. wind throws, fire or spruce dieback) or forest management (e.g. clear cut harvesting, sanitary logging). Temporal segmentation and fitting of annual Landsat time series (LTS), the core features of the LandTrendr approach, provide great opportunities to better understand forest dynamics in Romania during recent decades, and thus will help researchers better understand how land systems respond to drastic institutional changes. Specifically, we ask the following research questions:

- How have forest disturbance rates and patterns changed after the collapse of socialism?
- How have the three individual forest restitution phases affected disturbance patterns?
- Are there differences in forest disturbance rates and patterns between state, community, and privately owned forest land?

## 2 Methods

### 2.1 Study region

Our study region comprises one Landsat footprint (path/row 183/028) in central-eastern Romania including large parts of the Transylvanian basin (Fig.1). Elevations extend up to 2,545 m in the Fagaras Mountains in the southern Carpathians and up to 1,700 m in the Eastern Carpathian Mountains, whereas the Transylvanian basin has hilly terrain with elevations between 500 and 800 m. The bedrock comprises crystalline schist, sedimentary

rocks and some volcanic strata. The region is characterized by temperate continental climate. Average temperature is about 8°C and annual precipitation is about 650 mm but can be as high as 2,000 mm in the alpine zone. The majority of the study region's land cover comprises forests and forestry has traditionally been an important component of the regional economy and a major source of rural income (Ioras and Abrudan 2006). Forests can be stratified by elevation into an alpine zone (>2,200 m) dominated by mountain meadows, a subalpine zone (1,800 – 2,200 m) with mostly dwarf pine (*Pinus mugo*) and juniper (*Juniperus nana*), a coniferous zone (1,300 – 1,800 m) and a deciduous and mixed forest zone below 1,300 m (Mihai et al. 2007). Coniferous forests are dominated by Norway spruce (*Picea abies*) and silver fir (*Abies alba*), whereas deciduous forests consist mostly of European beech (*Fagus silvatica*) with some birch (*Betula pendula*), hornbeam (*Carpinus betulus*) and Pedunculate oak (*Quercus robur*).

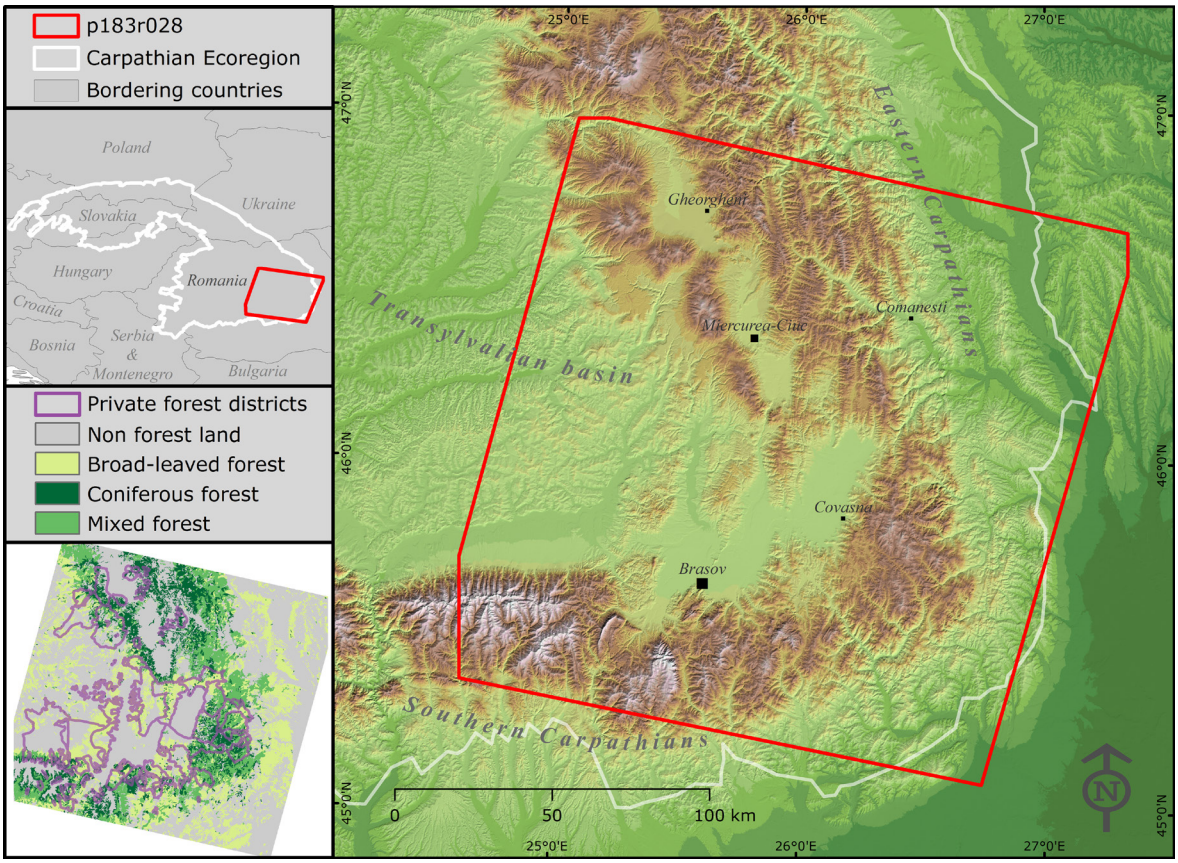


Figure II-1: The study region's terrain, populated areas and boundaries (main frame), location of the study region within the Carpathians (Carpathian Ecoregion Initiative boundaries) (top left), as well the distribution of broad forest types and private forest districts in the study region (lower left).

## 2.2 Image data and preprocessing

We acquired a near-annual time series of Landsat TM/ETM+ images for the period 1984 - 2010. We selected only images from the peak growing season (early June - mid September) and acquired multiple images from the same year if a cloud-free image was not available. Clouds and cloud shadows were masked from all images in the time series based on image differencing with a cloud-free reference image (Kennedy et al. 2010). For some years, (e.g. 1984 - 1991) cloud cover was extensive and we therefore also incorporated some spring/autumn images and used images from adjacent footprints (184/028 and 182/028, 35% across-track overlap). We also included Landsat 7 SLC-off images for years after 2003, omitting scan line observations with missing values.

Most images had already been orthorectified (L1T) by the USGS. For the period 1996 - 1999, only one suitable L1T image was available. We therefore acquired three additional images from the European Landsat archive and co-registered them to the L1T images. This was done using ~1500 tie points located via automated point matching and considering both Landsat acquisition geometry and relief displacement (Aschbacher and Milagro-Perez 2012). Co-registration resulted in an overall positional error <0.5 pixels. Our entire time series consisted of 52 images that were acquired at a median Julian day of 223 (August 11th) with a standard deviation of 33 days. The earliest acquisition date was May 31st and the latest October 14th. Suitable images were unavailable for four years in the Landsat time series (1985, 1990, 1992 and 1997).

We atmospherically corrected the image from August 27th 1998 using the COST method (Chavez 1996). Subsequently, all other images were radiometrically normalized to this reference based on the Multivariate Alteration Detection algorithm (Canty and Nielsen 2008). After radiometric normalization, all images were transformed into Tasseled Cap (TC) space (Crist and Cicone 1984). Initial tests showed that full-canopy disturbances had highest contrast to undisturbed forests when using Tasseled Cap Wetness ($TC_W$) (Cohen and Goward 2004) and only $TC_W$ worked equally well for very dark coniferous and bright deciduous forest canopies, both of which are common in our study area.

## 2.3 Time-series segmentation procedure

The preprocessed time series was then used as input to the temporal segmentation and fitting algorithms, which form the core of the LandTrendr approach and are described in detail in Kennedy et al. (2010). In sum, these procedures identify those sections of a pixel's temporal profile, that feature a consistent spectral development (hereafter: segments) and

then fit a spectral trajectory that minimizes residual variation related to differences in illumination or phenology to that segment. Input for the segmentation and fitting algorithms is a best observation composite generated from the normalized $TC_W$ values (hereafter: source stack). This is done by selecting the one unmasked pixel value per year (from potentially many images) that was acquired closest to the median Julian day of the LTS. If no cloud-free observation for a given year was available, a no-data value was written into the source stack. Subsequently, the fitting algorithms were applied to the source stack and derived a simplified spectral description of the source stack trajectory (Fig.2) by using both, regression methods and point-to-point fitting (Kennedy et al. 2010). This resulted in a stack of annual fitted $TC_W$ images (hereafter: fitted stack), representing the basis for all further analyses.

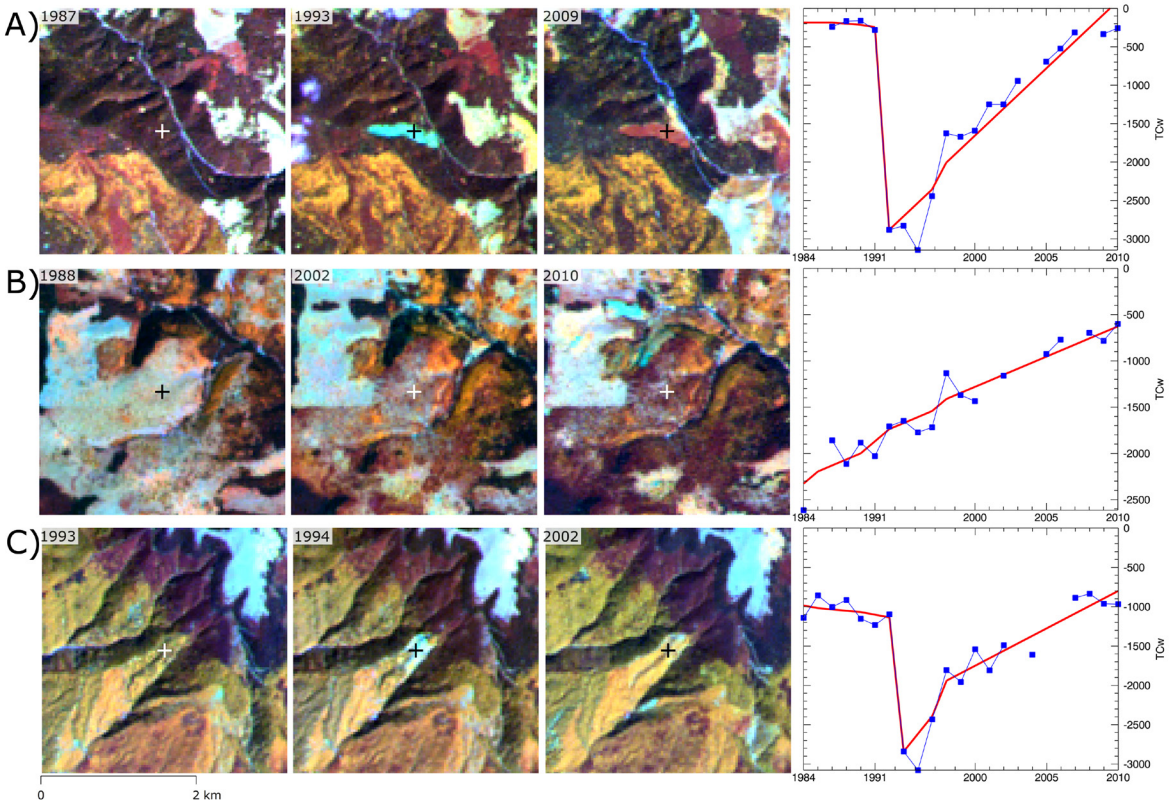


Figure II-2: Three examples of trajectories and related imagery. Images show an early, intermediate and late point in time (RGB=453). Trajectory locations are indicated by the crosshair. Source value trajectories are shown in blue (gaps indicate masked no data values), fitted trajectories are shown in red.

## 2.4 Forest / non-forest map

Analyzing the outputs of the LandTrendr segmentation and fitting procedures to map forest disturbances first requires separating forest (including disturbed and recovering forest) from permanent non-forest land. To do so, we derived Tasseled Cap greenness ($TC_G$) and brightness ($TC_B$) stacks using the fitted $TC_W$ values and the TC coefficients. For each

segment of a given pixel in the LTS, we calculated the Tasseled Cap angle index (Powell et al. 2010) as arctan($TC_G/TC_B$). This index ranges from zero to 45 degrees as vegetative cover increases, taking advantage of the long-recognized distinctive shape of the Kauth-Thomas brightness-greenness spectral space (Atzberger and Richter 2012; Malenovský et al. 2012). In order to exclude areas with high spectral variability over time (e.g. agricultural lands), we calculated the average and variability of each of the three TC components for a given pixel's segment featuring the greatest angle index. Based on these six indices, we classified forest and non-forest land using Support Vector Machines (Pal and Mather 2005) and a total of 431 training samples. We excluded orchards and vineyards based on the CORINE land cover map (www.eea.europa.eu), as those caused false disturbance detections later on. Finally, we removed isolated forest patches of less than two ha (23 pixels), because such areas are functionally not forest (e.g. hedgerows, tree groups) and applied a minimum mapping unit of approximately one ha (11 pixels).

### 2.5 Forest disturbance mapping

The detection of forest disturbances was constrained according to the disturbance magnitude. To provide an approximation of vegetative cover, we transformed $TC_W$ values into percent vegetative cover estimates by linearly scaling the $TC_W$ values of bare ground pixels representing 0% cover with the $TC_W$ values of closed canopies (100% cover):

$$PercentCover = \left( \frac{TC_w - lowVal}{highVal - lowVal} \right) * 100 \quad (1)$$

The upper and lower ends of the range (i.e. *highVal* and *lowVal*) are scene based and were empirically determined based on image interpretation and field visits. We were primarily interested in stand-replacing disturbances, and therefore extracted the largest disturbance segment from the fitted stack for each pixel in our forest mask. We mapped disturbances only if the relative disturbance magnitude exceeded 30% over one year and 5% over a 20 year duration using a sliding scale for years in between. Relative disturbance magnitude was defined as:

$$Magnitude_{rel.} = \frac{100 * (PercentCover_{preDist.} - PercentCover_{postDist.})}{PercentCover_{preDist.}} \quad (2)$$

Additionally the pre-disturbance vegetation cover had to be at least 10%. A total of 22 disturbance classes were mapped (1986 - 2010, no image data for four years). For each disturbance we derived the year of onset, relative disturbance magnitude, and the duration

of the disturbance event. For the disturbance map, we used a minimum mapping unit of 0.63 ha (7 pixels), which is roughly the smallest forest management unit in Romania (0.5 ha).

We combined the results of both analyses (separation of forest from non-forest areas, and disturbance detection) into a single map and carried out an accuracy assessment. To do so, we selected a stratified random sample of 30 points per disturbance class (i.e. disturbance year) and 300 points each for undisturbed forest areas and permanent non-forest land. For each disturbance class sample, we recorded the year of disturbance onset (or the absence of disturbances) based on the full Landsat time series visualized in TimeSync (Cohen et al. 2010) and complemented through high-resolution imagery available in Google Earth. In cases where clouds or cloud shadows masked disturbances, disturbance onset was labeled as the first year when a disturbance could be detected by LandTrendr. Remaining points were interpreted as permanent non-forest if the sample location did not once represent forest throughout the LTS. Points were labeled as forest if they represented undisturbed forest cover. We calculated an error matrix and derived overall accuracies as well as omission and commission errors taking into account the area proportions of the classes to calculate area-adjusted accuracy measures (Card 1982). We calculated true area-estimates for all classes as well as the 95% confidence around these estimates (Cochran 1977).

### 2.6 Growth and recovery mapping

From the fitted stack we extracted all segments of vegetative increase where the change in cover was at least 15% and that occurred over a three to 26 year period (increase below three years was considered irrelevant, 26 years is the entire time span of the LTS). Based on these segments, we mapped areas of long forest growth (hereafter: growth areas) as well as areas recovering from a previous disturbances (hereafter: recovery). Note that our estimates of percent cover technically apply to all vegetation types, not strictly forest cover, and thus do not imply that forest had recovered to its pre-disturbance state, but that vegetative cover had reestablished.

Disturbance recovery was assessed on the basis of individual disturbance patches. Here we assessed the five year post disturbance recovery state in order to understand how far annual disturbance patches had regenerated. This was done by averaging the percent cover value of all pixels in an individual disturbance patch after five years after disturbance onset. We produced maps showing how much percent of the disturbance magnitude had recovered within individual disturbance patches after five years.

In order to quantify growth areas, pixels with trajectories increasing over at least 10 years or at least 20 years were summarized separately. These areas were not affected by any disturbances and we categorized two groups based on their absolute cover increase: (1) cover increase between 20% and 50%, and (2) cover increase between 50% and 100%.

### 2.7 Analyzing rates and patterns of disturbance and recovery

To summarize disturbance rates and patterns, we calculated the total disturbed area per year in our time series. Four years in our LTS lacked imagery and in order to avoid overestimating the amount of disturbances detected in years following such missing years, we split up disturbances equally among years when disturbances were detected and preceding no-data years (e.g., we distributed the total disturbed area mapped in 1986 equally among 1985 and 1986, because no image was available in 1985). We calculated average disturbance areas for four periods: (a) late socialist period (1984 - 1989), (b) first restitution period (1991 – 1999), (c) second restitution period (2000 – 2004) and (d) third restitution period (2005 – 2010).

We also calculated the number of disturbance patches, average patch recovery after five years, and mean patch size for each year by aggregating disturbed pixels using a clumping algorithm based on a four pixel neighborhood. We assessed the annual fraction of disturbance patches exceeding the three ha maximum allowed harvesting size (Brandlmaier and Hirschberger 2005) for each disturbance class. We assessed mean disturbance magnitude on a patch basis. Finally, we derived the percentage of annual patches exhibiting disturbance magnitudes above the all year mean magnitude value.

### 2.8 Assessing the effect of ownership

To compare forest disturbance patterns among forest ownership regimes, we acquired harvesting and ownership statistics which were available from the Romanian National Institute of Statistics for the 27 private forest districts (PFDs) in our study region. For each of these districts, administrative boundaries were available along with attributes such as the functional distribution of forests within (e.g. percentage of protection or production forest), species composition (from which we derived the ratio of deciduous and coniferous species), and the annual allowable cut for the year 2006 (i.e. the amount of timber permitted to be harvested with in PFD in a certain year) given separately for public and private PFD owners. For all years after 2006, we assumed that the area of a given PFD as

well as the above described attributes remained stable. Using our disturbance maps, we derived annual disturbance rates (DR) for the PFDs according to:

$$DR_{PFD(i)} = \left( \frac{D_{PFD(i)}}{F_{PFD} - D_{PFD(<i)}} \right) * 100 \quad (3)$$

Where $D_{PFD(i)}$ denotes the disturbed area in year $i$, $F_{PFD}$ denotes the forest area in a PFD as indicated by our forest mask and $D_{PFD(<i)}$ indicates the accumulated disturbed forest area until time $i$. We also related annual disturbance rates within PFDs to the species composition ratio of deciduous and coniferous trees to assess if forest composition influenced disturbance regimes. To explore whether disturbance levels changed within individual PFDs over time, we derived the percentage of disturbances occurring for the four time periods.

## 3 Results

The available imagery provided more than 21 cloud-free observations for >50% of pixels and at least 19 cloud-free observations for >80% of the study region. Only <0.2% of all pixels in the study region were covered by 10 or fewer cloud-free observations. Despite incorporating multiple images for most years, on average 13% of the study region was masked annually in the source stack due to prevalent cloud cover (often related to topography). Nevertheless, only 7% of the study region was masked in the source stack for 10 out of 23 years (2004 was most severe with 67% of masked area).

Our forest / non-forest analysis determined 1.66 million ha of the study region as forested (50% of the study region). The forest area comprised disturbed areas, as well as unforested areas that recovered to a forested condition only in the late years of the LTS. Approximately 1.4 million ha (88% of the delineated forest area) were permanent forests, i.e. neither mapped as disturbed nor as growth areas.

The results of the segmentation and fitting algorithms suggest that both long-term forest cover trends (e.g. growth and recovery) as well as forest disturbances were successfully captured by LandTrendr (Fig.2). Segments depicted both, the timing of intermediate to high intensity disturbances as well as that of recovery trajectories well (Fig.2a & Fig. 2c). Likewise, long-term forest cover trends in undisturbed areas were captured well, often despite noisy source value trajectories or data gaps (blue lines in the plots of Fig. 2).

Table II-1: Summary of results of the accuracy assessment for the disturbance map showing omission and commission errors (NF = Stable non-forest, F = stable forest, OAC = overall accuracy).

| Year | Omission | Commission |
|---|---|---|
| 1986 | 0% | 25.81% |
| 1987 | 12.15% | 16.13% |
| 1988 | 39.53% | 16.67% |
| 1989 | 5.32% | 0.00% |
| 1991 | 0% | 13.33% |
| 1993 | 11.45% | 10.00% |
| 1994 | 0% | 22.58% |
| 1995 | 6.17% | 22.58% |
| 1996 | 7.88% | 3.33% |
| 1998 | 9.83% | 9.68% |
| 1999 | 1.87% | 12.90% |
| 2000 | 21.39% | 10.00% |
| 2001 | 2.58% | 32.26% |
| 2002 | 4.75% | 10.00% |
| 2003 | 4.39% | 3.33% |
| 2004 | 8.37% | 3.23% |
| 2005 | 0% | 6.45% |
| 2006 | 6.10% | 6.25% |
| 2007 | 0% | 6.67% |
| 2008 | 5.86% | 0.00% |
| 2009 | 0% | 12.90% |
| 2010 | 2.21% | 12.12% |
| NF | 4.73% | 3.39% |
| F | 3.73% | 4.83% |
| OAC = | | 95.72% |

LandTrendr yielded a highly reliable disturbance map with an overall accuracy of 95.72% (Table 1). The stable forest and non-forest classes showed both omission and commission errors below 5%. Commission errors for the individual disturbance classes were generally low (mean = 11.6%, standard deviation = 0.08) with lowest errors for 1989 and 2008, and highest errors for 2001 and 1986. Similarly, omission errors were low (mean = 6.8%, standard deviation = 0.09) with greatest errors in 1988 and 2000 (Tables 1 and 2). The disturbance classes to the end of the LTS generally exhibited lower commission and omission errors.

Our disturbance map (Fig.3) revealed that a total of 75,000 ha of forest was disturbed between 1986 and 2010, corresponding to 4.5% of the studied forest area. Overall, disturbances predominantly occurred in forests of the Eastern Carpathian Mountains and were spatially highly clustered around Covasna, Miercurea-Ciuc, Gheorgheni and Comanesti (subsets 4, 3, 1 and 2 in Figure 3 respectively). Additional disturbance hotspots appeared during more recent years in the Southern Carpathian Mountains (southwest of

Brasov, subset 5 in Figure 3). Disturbances were generally not very prevalent in the east of the study region.

Table II-2: Confusion matrix resulting from the validation of the disturbance map (NF = stable non-forest; F = stable forest).

| | | Reference | | | | | | | | | | | | | | | | | | | | | | | | |
|---|---|---|---|---|---|---|---|---|---|---|---|---|---|---|---|---|---|---|---|---|---|---|---|---|---|---|
| | | 1986 | 1987 | 1988 | 1989 | 1991 | 1993 | 1994 | 1995 | 1996 | 1998 | 1999 | 2000 | 2001 | 2002 | 2003 | 2004 | 2005 | 2006 | 2007 | 2008 | 2009 | 2010 | NF | F | Total |
| Disturbance Map | 1986 | 23 | 2 | - | - | - | - | - | - | - | - | - | - | - | - | - | - | - | - | - | - | - | - | 2 | 4 | 31 |
| | 1987 | - | 26 | 4 | - | - | - | - | - | - | - | - | - | - | - | - | - | - | - | - | - | - | - | - | 1 | 31 |
| | 1988 | - | 4 | 25 | 1 | - | - | - | - | - | - | - | - | - | - | - | - | - | - | - | - | - | - | - | - | 30 |
| | 1989 | - | - | - | 30 | - | - | - | - | - | - | - | - | - | - | - | - | - | - | - | - | - | - | - | - | 30 |
| | 1991 | - | - | - | - | 26 | 3 | - | - | - | - | - | - | - | - | - | - | - | - | - | - | - | - | 1 | - | 30 |
| | 1993 | - | 1 | - | - | - | 27 | - | 1 | - | - | - | - | - | - | - | - | - | - | - | - | - | - | 1 | - | 30 |
| | 1994 | - | - | - | - | - | 2 | 24 | 2 | - | - | - | - | - | - | - | - | - | - | - | - | - | - | 2 | 1 | 31 |
| | 1995 | - | - | - | - | - | - | - | 24 | 2 | - | - | - | - | - | - | - | - | - | - | - | - | - | - | 5 | 31 |
| | 1996 | - | - | - | - | - | - | - | - | 29 | 1 | - | - | - | - | - | - | - | - | - | - | - | - | - | - | 30 |
| | 1998 | - | - | - | - | - | - | - | - | 1 | 28 | - | 1 | - | - | - | - | - | - | - | - | - | - | 1 | - | 31 |
| | 1999 | - | - | - | - | - | - | - | - | 1 | - | 27 | - | - | - | - | - | - | - | - | - | - | - | - | 3 | 31 |
| | 2000 | - | - | - | - | - | - | - | - | - | 1 | 1 | 27 | 1 | - | - | - | - | - | - | - | - | - | - | - | 30 |
| | 2001 | - | - | - | - | - | - | - | - | - | - | - | 2 | 21 | 1 | - | - | - | - | - | - | - | - | 1 | 6 | 31 |
| | 2002 | - | - | - | - | - | - | - | - | - | - | - | - | - | 27 | 2 | 1 | - | - | - | - | - | - | - | - | 30 |
| | 2003 | - | - | - | - | - | - | - | - | - | - | - | - | - | - | 29 | 1 | - | - | - | - | - | - | - | - | 30 |
| | 2004 | - | - | - | - | - | - | - | - | - | - | - | 1 | - | - | - | 30 | - | - | - | - | - | - | - | - | 31 |
| | 2005 | - | - | - | - | - | - | - | - | - | - | - | - | - | - | - | - | 29 | - | - | - | - | - | - | 2 | 31 |
| | 2006 | - | - | - | - | - | - | - | - | - | - | - | - | - | - | - | 1 | - | 30 | - | - | - | - | - | 1 | 32 |
| | 2007 | - | - | - | - | - | - | - | - | - | - | - | - | - | - | - | - | - | 1 | 28 | 1 | - | - | - | - | 30 |
| | 2008 | - | - | - | - | - | - | - | - | - | - | - | - | - | - | - | - | - | - | - | 30 | - | - | - | - | 30 |
| | 2009 | - | - | - | - | - | - | - | - | - | - | - | - | - | - | - | - | - | - | - | 1 | 27 | 1 | - | 2 | 31 |
| | 2010 | - | - | - | - | - | - | - | 1 | - | - | - | - | - | - | - | - | - | 1 | - | - | - | 29 | - | 2 | 33 |
| | NF | - | - | - | - | - | - | - | - | - | - | - | - | - | - | - | - | - | - | - | - | - | - | -285 | 10 | 295 |
| | F | - | - | - | - | - | - | - | - | - | - | - | - | - | - | - | - | - | - | - | - | - | - | - | 14276 | 290 |
| | Total | 23 | 33 | 29 | 31 | 26 | 32 | 24 | 28 | 33 | 30 | 28 | 31 | 22 | 28 | 31 | 33 | 29 | 32 | 28 | 32 | 27 | 30 | 307 | 313 | 1260 |

The mean annually disturbed area is 3,191 ha, which relates to 0.20% of the forest area analyzed. The disturbed area for the four periods showed a steady increase in annual disturbance rates over time. Annual disturbances increased from about 1,900 ha (late socialist period) to about 2,500 ha during the first restitution period (Fig.4b). A further increase to more than 3,200 ha yearly during the second restitution period was followed by almost 4,000 ha during the third restitution period. More than 60% of all disturbances occurred during the second and third forest restitution period. Annual disturbance rates amounted to 0.11%, 0.15% and 0.19% for the late socialist, first and second restitution period, respectively, and to 0.24% for the third restitution period. Recent disturbance rates are thus more than twice as high as during the late socialist period.

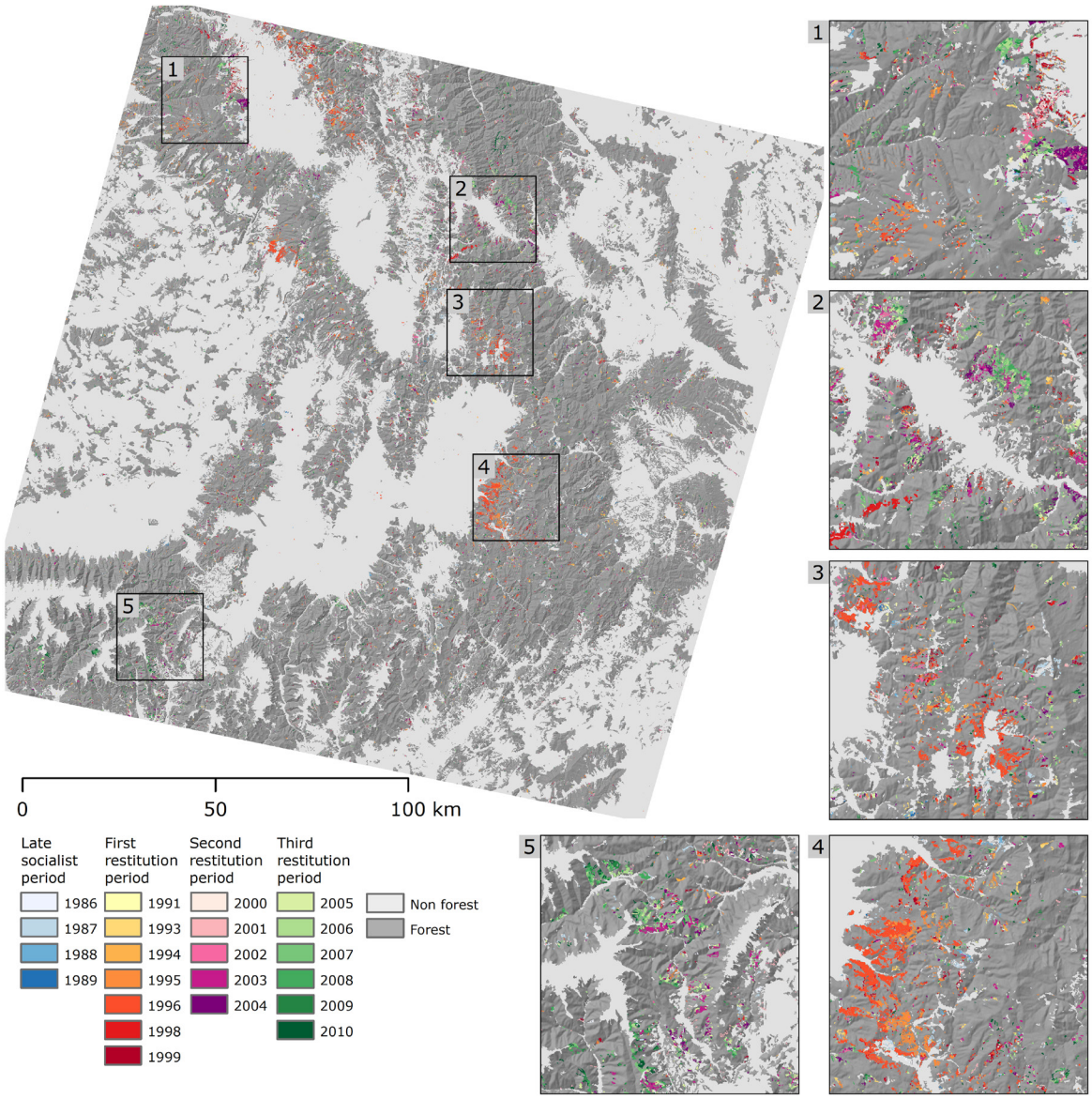


Figure II-3: Overview of the disturbance map and five subsets (subset scale is 1:500,000).

The area of forest disturbances per year ranged between 302 ha in 1991 and 8,596 ha in 1996 (Fig.4a). Yearly disturbance rates declined towards the end of the socialist period compared to the very early years in the LTS (i.e. 1986/1987). Following the first restitution law in 1991, annual disturbance rates were relatively low at first, but then increased markedly until 1995 and 1996, with more than 5,500 ha and 8,500 ha of disturbed forest area, respectively. Disturbance rates were also relatively low during the first years of the second restitution period, but spiked again by the end of that period (Fig. 4a). The years following the third restitution law in 2005 all featured annual disturbance rates of more than 4,000 ha, with the exception of 2005 and 2009 (3,135 ha and 2,424 ha, respectively). After 2007, annual disturbances declined with the exception of 2010 which featured a slight increase.

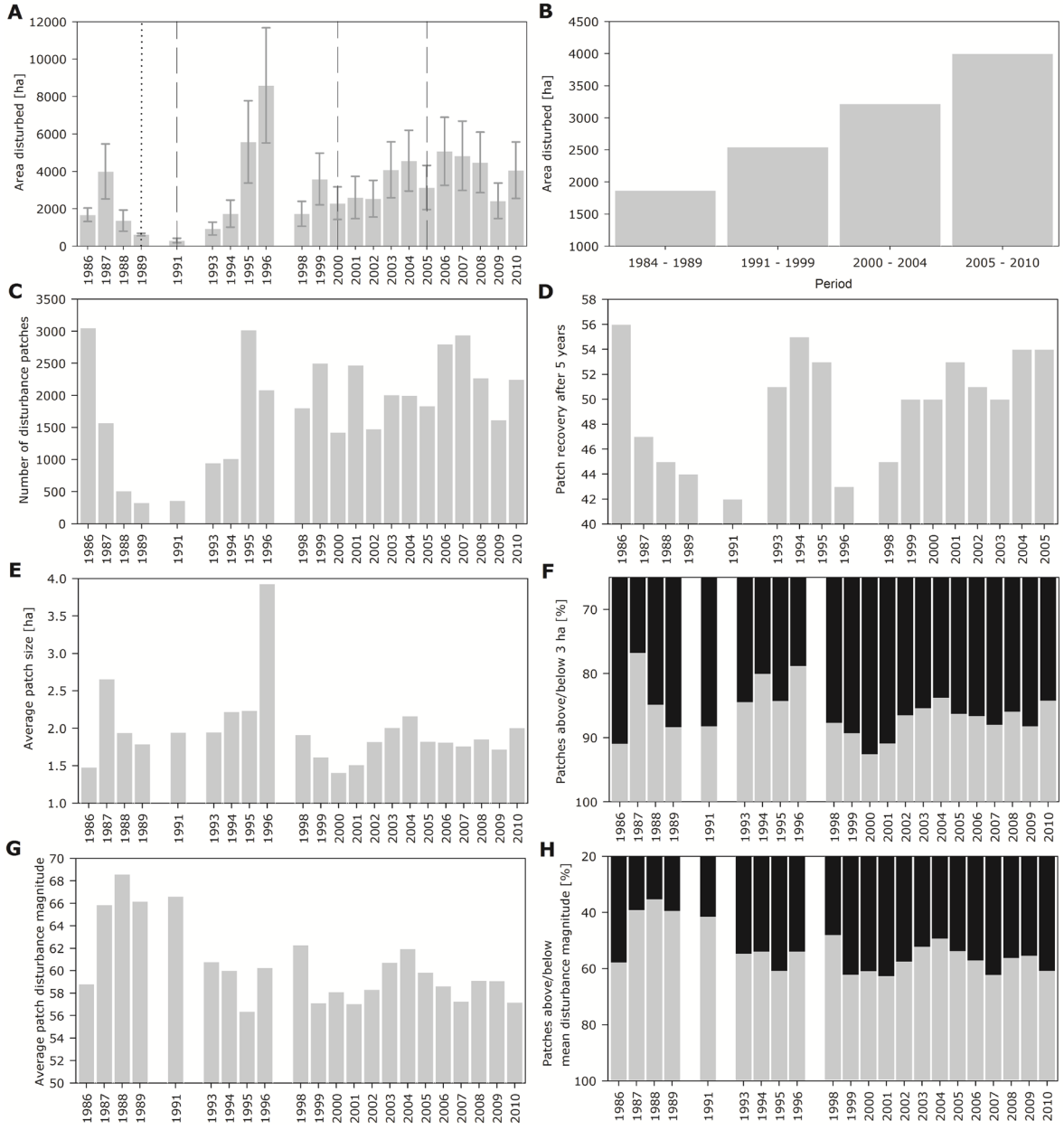


Figure II-4: (A) Annually disturbed area with error bars indicating the 95% confidence intervals (dashed lines indicate the onset of the three restitution laws, dotted line points to the collapse of the Soviet Union), (B) mean disturbance per period, (C) annual number of disturbance patches, (D) patch based recovery state five years after disturbance onset, (E) annual mean patch size, (F) percentage of pixels above (grey) and below (black) three ha, (G) average patch based relative disturbance magnitude, (H) percentage of disturbance patches above (grey) and below (black) 60% relative disturbance magnitude. Notice that Y-axes for (F) and (H) are inverted.

The number of disturbance patches followed relatively closely the trends in total disturbance area over time (Fig.4c), with comparatively higher patch numbers in 1986 and 1995, and a lower number of patches in 1996. Disturbances tended to occur in larger patches during the late socialist period and following the first restitution law. Average disturbance patch size was 1.98 ha, ranging from 1.41 ha in 2000 to 3.93 ha in 1996 (Fig.4e). The proportion of disturbance patches exceeding the legal three ha harvesting size

limit was 14% across the entire time series, but substantially higher for individual years (e.g., 23%, 21% and 19% for 1987, 1996 and 1995, respectively, Fig.4f). The fraction of disturbance patches above three ha increased until the late 1990s, decreased between 1998 and 2000, and increased again markedly between 2001 and 2005 (Fig.4f). Summarizing patch size for the four time periods showed that the proportion of disturbance patches above three ha was overall relatively similar, with the highest fraction during the first restitution period (15.3%) and the lowest during the second restitution period (12.1%).

The average patch disturbance magnitude across all years was 60% (Fig.4g), but average annual disturbance magnitude varied noticeably between years and time periods. For example, disturbances had highest magnitudes during the late socialist period and the first restitution period (65% and 60%, respectively), and were consistently lower during the second- and third restitution period (<60%). The fraction of disturbance patches above the all-year mean magnitude value of 60% was higher for the years until 1991, then relatively low until 1999, increasing again from 1999 to 2004, and then again declining towards 2007 (Fig.4h).

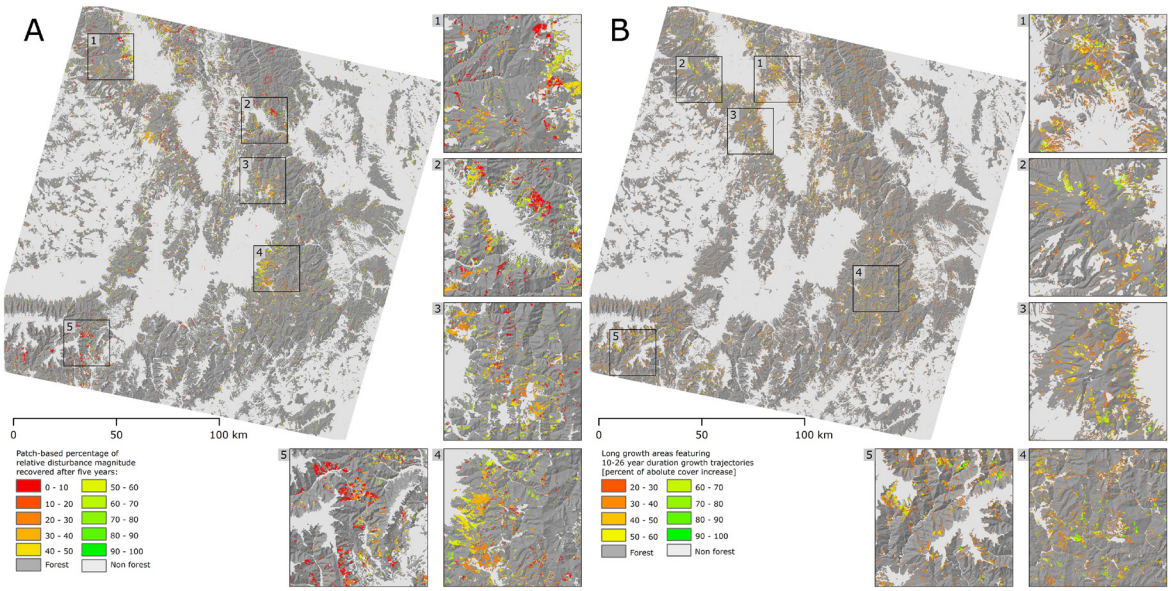


Figure II-5: (A) Overview and five subsets of the patch based recovery state, given as the percentage of the relative disturbance magnitude recovered after five years (subsets correspond to Fig.3, their scale is 1:500,000). (B) Map of growth areas exhibiting vegetative increase over 10-26 years (given in absolute cover increase, subset scale is 1:500,000).

Forest recovery following disturbances proved to be highly variable within the time period. Accordingly, on average over all years disturbances had regenerated 50% of the relative disturbance magnitude after five years (Fig.4d). Comparing five year recovery rates over time showed that recovery rates were not uniform (Fig.5a), with exceptionally high rates

for 1986 and 1994 (recovery rates of 56% and 55%, respectively), and relatively low recovery rates for other years (e.g., 43% in 1996, Fig.4d). Figure 6 illustrates how different disturbance patches had regenerated after five years in detail and provides examples from the imagery.

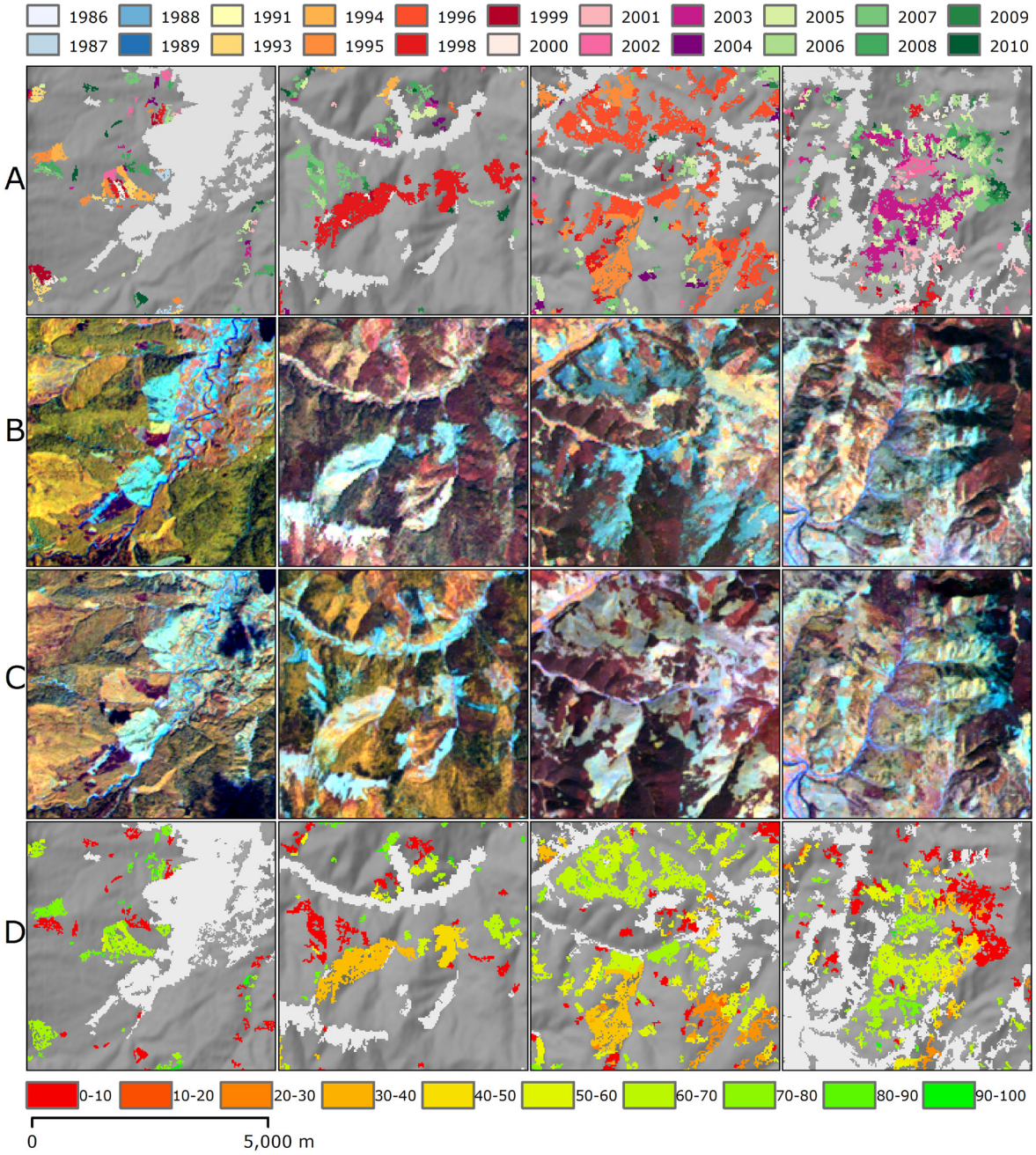


Figure II-6: Four details of the disturbance map, (B) imagery of one point in time close to the main disturbance events, (C) imagery of one point in time ca. five years later, (D) patch based percentage of recovered relative disturbance magnitude after five years (Imagery is shown as RGB=453).

Regarding the summary of growth areas (Fig. 5b), more than 52,000 ha (3.2% of all forested pixels) increased between 20% and 50% cover over 20 or more years and almost 13,000 ha (0.8%) increased between 50% and 100% cover the same time span. More than

39,000 ha (2.4%) increased by between 20% and 50% cover over a period of only 10 to 20 years. Approximately 4500 ha (0.3%) increased between 50% and 100% over the same time period. In total, more than 6.6% (110,000 ha) of all pixels inside the forest mask showed a substantial (20 - 100%) increase in forest cover over 10 and more years (Fig.5b).

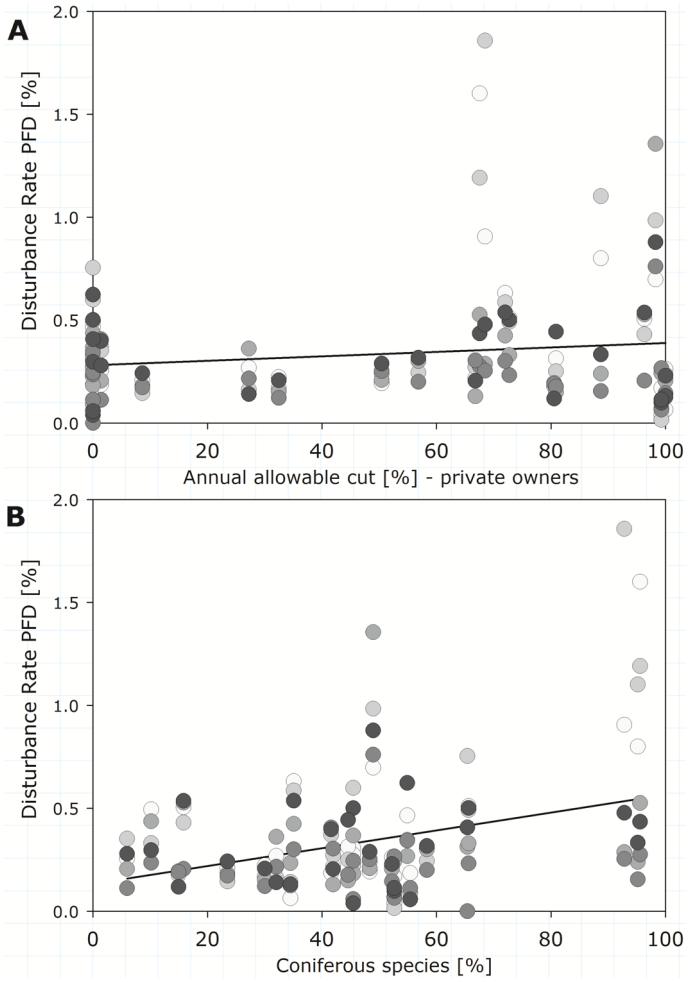


Figure II-7: (A) Relationship between the percentage of the annual allowable cut reserved for private owners of PFDs and disturbances rates within PFDs between 2006 and 2010 (note that the annual allowable cut for private and public owners of a PFD adds up to 100%). (B) Correlation between the annual disturbance rates detected in the PFDs and the percentage of coniferous species (note that the percentage of coniferous and deciduous species adds up to 100% for each PFD). Grayscale shading of points ranges from white (2006) to black (2010).

The 27 private forest districts (PFDs), all of which were established between 2003 and 2006, covered about 22% of our study region and about 27% of the forested land. The observed disturbance rates with the PFDs indicate a connection between ownership regime and the annual allowable cut (Fig.7a). In cases where the majority of the allowable cut was assigned to private forest owners, disturbance rates tended to be higher. In districts where the allowed cut was mostly harvested through local communities disturbance rates tended to be lower. Forest cover types (coniferous vs. deciduous) within the PFD also indicated a correlation with disturbance levels (Fig.7b): a higher share of coniferous species was

associated with higher disturbance rates whereas PFDs with a high portion of deciduous species had lower disturbance rates. For the majority of the restituted forests within the later established PFD areas, disturbance rates were also much lower during the late socialist period (<20% of all disturbances detected, Fig.8) than during the years following the first restitution law (e.g., 22 PFDs experienced more than 20% of all disturbances during these 9 years). Likewise, almost half of the PFDs experienced more than 30% of all detected disturbances during the third restitution period and much less during the second restitution period.

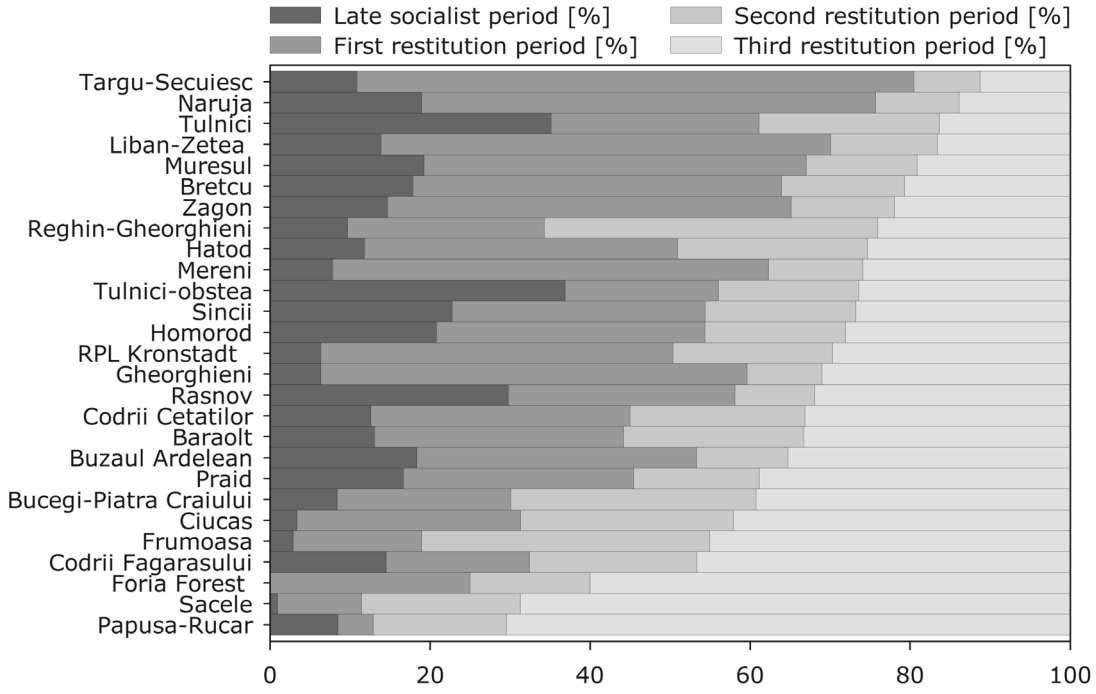


Figure II-8: Distribution of detected disturbances within individual private forest districts per period (given in percent of total detected disturbances).

Focusing on a few individual PFDs illustrates that connections exist between detected disturbance patterns and the restitution phases (Fig. 9). PFDs often showed low disturbance levels during the late socialist and the first and second restitution phases (e.g. Fig.9, top). In two PFDs, more than 70% of the disturbances detected occurred after the third restitution law was put in place in 2005. A common pattern was also that many PFDs exhibited markedly higher disturbance rates immediately before the legal establishment of the private forest districts themselves (Fig. 9, middle). Some PFDs showed low disturbance levels throughout the assessed time period. Finally, high disturbance rates were in a few cases attributable to major wind throw events that occurred in some PFDs in 1995 (Fig. 9, bottom).

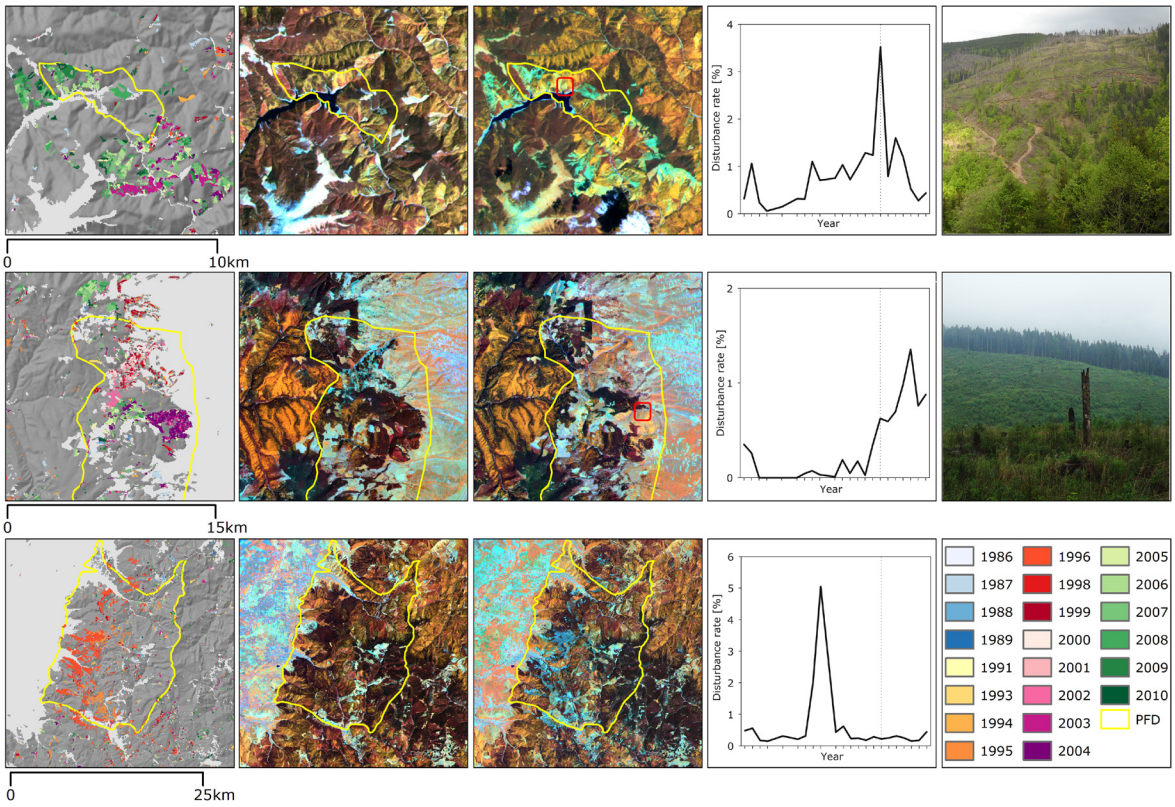


Figure II-9: Three examples of the disturbance map (left column) and of imagery (RGB=453) for the area of private forest districts. The development of the annual disturbance rates for the three PFDs is given (forth column, dotted line indicated year of legal establishment). The examples show the PFD Papusa-Rucar (top), PFD Reghin-Gheorghieni (middle), PFD Targu–Secuiesc (bottom) [compare figure 8]. Red frames on the imagery indicate the location of two pictures taken during a field visit, exemplifying areas of excessive logging (right).

## 4 Discussion

Applying the LandTrendr temporal segmentation and fitting routines to a near-annual time series of Landsat images of central Romania revealed widespread forest disturbances between 1984 and 2010. Forest disturbance levels increased since the collapse of socialism, with considerably elevated levels after 1991, when many state forests were transferred into non-state ownership. All three restitution laws led to markedly increased annual disturbances, whereas annual disturbance levels decreased slightly after Romania's accession to the EU. We also found pronounced differences in disturbance rates among different non-state ownership regimes, with local communities generally being associated with lower disturbance rates compared to restituted forests in individual private ownership. Our study thus highlights the effect that drastic institutional changes, such as the restitution of more than 60% of Romania's forests, can have on land use systems, and emphasizes the

value of the temporal depth of the Landsat archive to isolate and better understand rapid land use and land cover change.

Our disturbance map had a high overall accuracy (95.72%), as did most of our disturbance classes. Our disturbance area estimates also exhibited relatively narrow confidence intervals (note that the width of the confidence interval also depends on the number of validation points, and an even larger sample would have further narrowed the confidence intervals around our area estimates). Some disturbance classes had slightly higher commission errors (1986, 1994, 1995 and 2001) than others. For 1986, these misclassifications are likely caused by the higher susceptibility of the fitting algorithm to outliers during the first years in the time series. For 2001 and 1995, the acquisition dates of some images (mid-October and late-May) explain lower accuracies due to strong phenology and illumination differences.

Despite low error estimates, a few sources of uncertainty remain. First, setting a relatively high magnitude for threshold-based filtering reduced false detections (as has been shown via parameter evaluation tests in (Kennedy et al. 2010) as have our spatial filtering procedures, however possibly excluding a range of smaller and lower intensity disturbances. Second, dividing disturbances for years that followed years lacking data may have caused an underestimation of the disturbance rates for one of these years, if disturbance rates were unequal. None of these potential uncertainties, however, affect the general temporal trends that we observed and thus our conclusions.

Our study clearly highlights the considerable advantages that the annual temporal resolution of the LTS holds over bi- or multi-temporal change detection approaches. For example, a change map at five or 10-year interval would not have been able to distinguish a large disturbance occurring in a single year from individual patches clustering to a large area over time (important for monitoring both annual harvesting limits and maximum harvesting patch size). Likewise, assessing the effect of institutional shocks and socio-economic disturbances on land use, such as the passing of restitution laws or the establishment of PFDs, would not be possible without an annual time series of disturbance maps such as those provided by LandTrendr.

Forest cover in central Romania changed extensively throughout the 27-year time period we assessed, with about 110,000 ha exhibiting long-term forest cover increase, often recovering from pre-1984 disturbances, and a total of 75,000 ha of forests experiencing major disturbances. Above all, field visits, expert opinions and local case studies suggest

that harvesting accounts for the majority of disturbances we detected. Reliably separating natural disturbances from harvesting is not easy based on remote sensing alone. Generally, natural disturbances do occur in Romania but large-scale forest fires are very rare as are insect pests (Anfodillo et al. 2008). The main cause of natural disturbances in the Romanian Carpathians are wind throws (Anfodillo et al. 2008). Yet, the vast majority of wind throws cause small-scale disturbances and extreme wind throw events only occur every 10-15 years (Popa 2008). Moreover, catastrophic wind throw events almost exclusively affect spruce monocultures but not natural forests (Kozak et al. 2011). Extensive salvage logging always follows large-scale wind throws and forest management may in some cases even have been carried out in ways to make stands purposefully vulnerable to wind throws in order to enable salvage harvesting (Woodcock et al. 2008; Schmidt et al. 2012). Our results show the effect of the most severe wind throw during our study period, which occurred in November 1995 and blew down 140,000 ha of spruce and fir forest (Mihalciuc et al. 1999). This event is evident in the 1996 disturbance peak, the largest annual disturbance patch size, less disturbance patches and lower recovery rates after five years compared to other years (Fig.4). Together, this suggests that natural disturbances are scarce. Generally, although not very abundant, natural disturbances certainly contributed to the disturbances we mapped. However, it is at least questionable whether large-scale wind throws should be considered natural disturbances and there is no reason to assume that natural disturbances followed any trend.

Instead, we suggest that the trends in disturbance rates relate to the major institutional and socio-economic changes, in particular the drastic reorganization of forest ownership following the end of socialism in Romania. We caution that we cannot prove a causal connection as long as spatially explicit ownership data is unavailable. Nevertheless, the temporal trends we observe strongly suggest that forest ownership changes are the main drivers behind these trends. Specifically, the step-wise implementation of forest restitution over a 20-year period is likely to have resulted in widespread immediate capitalization of forest resources by new owners (Irimie and Essmann 2009; Vasile 2009). Four factors explain why new forest owners favor instant economic returns over more long-term forest resource utilization. First, uncertainty about the legal persistency of the restitution process encouraged many new owners to immediately convert forests into economic benefits (Csóka 2005). Second, descendants or heirs of historic forest owners often lacked knowledge of sustainable forest management practices that would be needed to avoid long-term depletion of forest resources and many new owners considered forest property solely

as an additional source of funds (Vasile 2009). Third, economic hardship during the transition period forced new owners to draw economic benefits from their new forests. Finally, frustration among restitution beneficiaries due to area restrictions, difficulties in physical allocation of forests, or even multiple claims for the same forest plot, may have further encouraged excessive felling (Abrudan et al. 2009; Vasile 2009).

Our study shows, that the analysis of an annual Landsat time series with trajectory-based change detection methods (such as LandTrendr) can provide deep insight into the effects of the institutional and socioeconomic changes on Romania's forests. Annual resolution is important in that respect. For example, continuously decreasing disturbance levels between 1986 and 1991 possibly relate to Romania's economic decline after 1989, when decreasing demands for timber and diminishing of socialist subsidies for the wood products industry resulted in plummeting harvesting rates (Csóka 2005; World Bank 2005; Ioras and Abrudan 2006). After 1991, more than 400,000 small-scale private forest owners emerged as forest management actors and forest fragmentation increased accordingly (Abrudan et al. 2009), mirrored in our results as increased disturbance rates and a higher number of annual disturbance patches (Fig.4 a & c). Also, the restitution under the 1991 law is known to have been very slow (Cartwright 2000), and the majority of forest restituted under law 18/1991 was returned only around 1994 (Abrudan et al. 2009), likely explaining the high disturbance rates in 1995.

Above all, the consistent and objective nature of remote sensing measurements allows unbiased comparison, for example, of forest disturbance across ownership types. This is of great value especially when disturbance levels vary with ownership regime. As no spatially explicit and up-to-date database of forest ownership in Romania is publically available at the moment, we used PFD boundaries and harvesting statistics as a proxy to investigate on the influence of non-state ownership types. Our results generally support assumptions of higher exploitation of restituted forests by private owners compared to local communities (Fig.7a). Although the second restitution law (i.e. law 1/2000) was intended to return forests primarily to public, non-state forest owners, the major increase in disturbances on restituted forests did not occur during this period but rather during the first and third restitution period (Fig.8). Partly this might be caused by increased timber harvests through private owners following the 1991 law. Also, PFDs were established between 2003 and 2005 and often small-scale owners within these districts only considered harvesting after management plans had been established under the PFD management (Stancioiu et al. 2010). Restituted forests with higher levels of economically valuable coniferous stands

were increasingly exploited (Fig.7b). It should be noted, that we assumed PFD attributes and boundaries to remain constant after 2006, and although interviews with forestry officials do not suggest these have changed substantially since, our results may involve some uncertainty.

In addition to forest restitution, unauthorized timber exploitation due to weakened institutions, emerging shadow markets, and decreased law enforcement, provide additional explanations for increased forest harvesting in the transition period (Bouriaud 2005; Abrudan et al. 2009; Irimie and Essmann 2009). For example, deliberate underestimations of stand age/volume, false registration of functional forest categories, of sanitation or conservation cutting became widespread after 1989 in Romania (Brandlmaier and Hirschberger 2005), similar to other regions in the Carpathians (Turnock 2002; Irland 2008; Kuemmerle et al. 2009a). Since 1989, transparency in the National Forest Administration has decreased and excessive or unauthorized logging has been tolerated or even promoted (Banaduc 2002). Some PFDs exhibited increased disturbance rates immediately prior to the PFD's legal establishment (e.g. Fig.9, middle). One explanation for this is that in some cases economically valuable mature stands were harvested through the state forest management before the districts came under new non-state management (Banaduc 2002). Moreover, excessive clear cutting by private owners sometimes exceeded PFD boundaries and frequently disregards forest management laws (e.g. harvesting of forests with watershed protection function, Fig.9, top). Our results show that while disturbances levels increased in 2005 - 2006, they declined again after Romania's accession to the EU in 2007. Although we cannot isolate the effect of the EU accession from the ongoing third restitution period, the deep reforms in Romanian legislation and economy that occurred since 2007 likely affected forest harvesting patterns as well (World Bank 2005).

Besides providing detailed forest disturbance histories, an asset of trajectory approaches is their ability to simultaneously detect gradual forest cover trends. Despite increasing annual disturbance rates and widespread logging, our results also show large areas of forest cover increase (Fig.5b) and disturbance recovery (Fig.5a and Fig.6), overall suggesting relatively fast recovery rates of the highly productive forests in the Carpathians (Abrudan 2005; Toader and Dumitru 2005). Concerning some ecosystem services, for instance carbon storage, this may partly compensate disturbance related carbon releases, even though such releases especially from old growth stands are not easily compensated (Berger and Aschbacher 2012). However, we caution that our study only tracks the recovery of

vegetative cover, whereas monitoring other aspects of forest ecosystem condition, such as changes in biodiversity, would require more detailed ground assessments. In some cases the spectral recovery we found does not necessarily relate to a restoring forest canopy (Fig.6). Generally, despite relatively strong recovery, the high harvesting rates that we detected point to an ongoing loss of older forests, and these forests likely are important for ecosystem service flows and are often of high conservation value, and do not regenerate quickly (Drusch et al. 2012).

## 5 Conclusions

Romania experienced drastic institutional- and socio-economic changes during the last three decades. Here we showed that annual Landsat time series and trajectory-based change detection methods such as the LandTrendr can provide deep insights as to the effects of rapid institutional change. While natural disturbances contributed to the disturbances we mapped, they cannot explain the annual trends we observed. Whereas the collapse of socialism resulted in lower harvesting rates in the early transition years, three phases of forest restitution each resulted in increased forest harvesting right after restitution laws were implemented, likely due to a combination of economic hardships, tenure insecurity, and weak law enforcement. Private ownership and presence of economically valuable timber were both associated with increased disturbance rates. Thus, our results raise substantial concerns regarding the sustainability of the logging practices in the Romanian Carpathians. Moreover, our study highlights the value of the temporal depth of the Landsat archive, which can help to reconstruct detailed histories of land use/cover change. This provides new insights into the dynamics of land systems, and can help us better understand the effects of rapid and transient changes in the drivers of land use decisions.

**Acknowledgements**

This research was funded by the Belgian Science Policy, Research Program for Earth Observation Stereo II, contract SR/00/133, as part of the FOMO project (Remote sensing of the forest transition and its ecosystem impacts in mountain environments). Support is gratefully acknowledged by the Alexander von Humboldt Foundation, the European Union (VOLANTE, FP7-ENV-2010-265104) and the Land Cover/Land-Use Change Program of

the National Aeronautics and Space Administration (grant number NNX09AK88G). We thank William S. Keeton for providing insightful and constructive comments. We also thank three anonymous reviewers who further improved this manuscript.

# Chapter III:
# A pixel-based Landsat compositing algorithm for large area land cover mapping

*IEEE Journal of Selected Topics in Applied Earth Observations and Remote Sensing PP (2013) 1-14*

Patrick Griffiths, Sebastian van der Linden,
Tobias Kuemmerle and Patrick Hostert


*doi: 10.1109/jstars.2012.2228167*
*Received 11 August 2012; revised 12 October 2012;*
*accepted 23 October 2012.*

**Abstract**

Information on the changing land surface is required at high resolutions as many processes cannot be resolved using coarse resolution data. Deriving such information over large areas for Landsat data, however, still faces numerous challenges. Image compositing offers great potential to circumvent such shortcomings. We here present a compositing algorithm that facilitates creating cloud free, seasonally and radiometrically consistent datasets from the Landsat archive. A parametric weighting scheme allows for flexibly utilizing different pixel characteristics for optimized compositing. We describe in detail the development of three parameter decision functions: acquisition year, day of year and distance to clouds. Our test site covers 42 Landsat footprints in Eastern Europe and we produced three annual composites. We evaluated seasonal and annual consistency and compared our composites to BRDF normalized MODIS reflectance products. Finally, we also evaluated how well the composites work for land cover mapping. Results prove that our algorithm allows for creating seasonally consistent large area composites. Radiometric correspondence to MODIS was high (up to $R^2 > 0.8$), but varied with land cover configuration and selected image acquisition dates. Land cover mapping yielded promising results (overall accuracy 72%). Class delineations were regionally consistent with minimal effort for training data. Class specific accuracies increased considerably (~10%) when spectral metrics were incorporated. Our study highlights the value of compositing in general and for Landsat data in particular, allowing for regional to global LULCC mapping at high spatial resolutions.

## 1 Introduction

Remote sensing based information on land use and land cover change (LULCC) is required at spatial resolutions higher than those currently available from existing global land cover products (Pekkarinen et al. 2009; Fritz et al. 2011). This is because many LULCC processes, such as logging, deforestation, land abandonment or urban sprawl, represent critical drivers of global environmental change, but occur at spatial scales that cannot be resolved with coarse resolution data in many areas of the world. This is specifically true for many regions in Africa or South-East Asia, where fine scale processes and patterns prevail. The global Landsat archive allows for reconstructing LULCC back to the 1970s and therefore has become an integral component of global LULCC research (Cohen and Goward 2004; Loveland and Dwyer 2012).

Despite large amounts of Earth Observation (EO) data available at spatial resolutions of 20 to 50m (in the following referred to as high spatial resolution), land cover and LULCC products with such spatial detail are commonly not available across large areas (Fritz et al. 2011). The reason for this is that mapping and monitoring of land cover across large regions at high spatial resolutions still poses unique challenges (Pax-Lenney et al. 2001). These challenges partly relate to the spatial detail of Landsat, which comes at the cost of a relatively small swath. A great number of Landsat footprints are therefore often needed for a full regional coverage. Additionally, phenologically and radiometrically consistent datasets are required when analyzing LULCC and complex changes in vegetation cover in particular (Masek et al. 2006). This is not easily feasible, considering that Landsat has a repeat frequency of 16-days and thus might only provide few or not even a single unclouded scene per growing season in many areas (Ju and Roy 2008). Data availability is further aggravated by discontinuities in image archives, as well as data or sensor related errors (e.g. the scan line correction (SLC) failure of Landsat 7 after May 2003 Arvidson et al. (2006)). Thus, conceptually more advanced approaches have to be developed to allow for robust mapping and monitoring at high spatial resolution over large areas.

In many studies where land cover has been mapped at high resolution over large areas, unsupervised and/or supervised classification methods are used, requiring considerable user interaction and thus limiting the potential for automation (Homer et al. 2007; Olthof et al. 2009). Land cover products at Landsat resolution also are available for Europe (CORINE land cover, Heymann et al. 1994). However, CORINE data are derived through

interpretation and digitization of Landsat data, have very high production costs and are limited to a minimum mapping unit of 25ha (Feranec et al. 2007). A number of operational land cover monitoring approaches using Landsat data over regional to continental scales have been developed in Australia prior to the opening of the USGS Landsat archive (Caccetta et al. 2007; Furby et al. 2008a; Furby et al. 2008b). Some studies have investigated the potential of transferring classification models across space or generating training data for an unclassified image from the overlap with an existing classification (Woodcock et al. 2001; Olthof et al. 2005; Knorn et al. 2009). More recently, different groups have investigated the potential of exploiting annual time series of Landsat data for enhanced process understanding in forest ecosystems (Huang et al. 2010a; Kennedy et al. 2010). However, existing approaches for large area mapping with Landsat data have only limited potential for automation, work only for simple class separation problems or are thematically restricted to certain environments. Therefore, further improvements in large area mapping methods are required (Cihlar 2000).

Image compositing offers opportunities to overcome restrictions in data availability and to improve large area mapping and monitoring at the same time. Compositing was originally developed for wide-swath sensors that frequently provide global coverage. New image datasets are created by selecting one specific observation from numerous acquisitions or averaging spectral values. For coarse resolution sensors, such as AVHRR, the main purpose was to reduce the influence of clouds on the signal. Most commonly, simple decision rules were applied, such as the maximum/minimum band value or NDVI (Choudhury et al. 1994; Cihlar 2000). More advanced compositing approaches additionally take a pixel's view angle into account (Wolfe et al. 1998; Tan et al. 2006). However, compositing was not often considered when working with high resolution data, mostly due to high data costs and processing constraints. Recent developments therefore encourage image compositing for Landsat data. These include a changed data policy (i.e. free data access - Loveland and Dwyer (2012)), enhanced preprocessing algorithms leading to improved standard image product quality (Chander et al. 2010; Wulder et al. 2012) and advances in storage and computational resources (Richards 2005; Plaza et al. 2011). These developments will also affect future satellite missions beyond Landsat-8, such as Sentinel-2, which will most likely adapt to these standards (Drusch et al. 2012).

Pixel-based compositing (PBC) of high-resolution optical imagery, as opposed to scene-based compositing or mosaicking, offers advantages for large area LULCC analysis. Global analysis models can be based on a single, homogeneous and cloud free dataset that

ideally provides a consistent radiometric response across large areas (Hansen and Loveland 2012). As all unclouded observations per pixel are extracted from the Landsat archive, different image metrics can be generated as valuable byproducts of the compositing process. Such metrics can for example be produced to capture relevant phenologic states in the seasonal cycle of vegetation or can correspond to descriptive statistics that provide a measure of average spectral response or spectral variability (Hansen et al. 2002). Above all, the change from a scene based- to a pixel-based perspective yields several improvements:

- analyses are no longer restricted to a few "best" images, where low cloud cover often had to be favored over seasonally suited acquisitions
- the artificial partitioning into footprints can be overcome
- the entire image archive can be exploited and partially useful image areas (e.g. in SCL-off data) can easily be included
- observation frequency is increased as pixels unaffected by clouds can be incorporated from cloud contaminated images
- observation frequency is additionally increased by across track overlap exploitation

Taking these considerations into account, PBC emerges as a valuable tool for large area applications using high resolution optical data. First examples of Landsat large area image composites have recently been produced to map boreal forest change in Russia or to monitor deforestation in tropical Africa (Potapov et al. 2011; Potapov et al. 2012). For the area of the United States, composited ETM+ top-of-atmosphere imagery has recently been made available via a web interface (Roy et al. 2010). Existing approaches, however, either rely on evaluating a single, often spectral criterion, do not utilize surface reflectances or do not retain all spectral bands at the original 30m resolution of Landsat data. In this paper we present a compositing algorithm that takes advantage of state-of-the-art Landsat pre-processing and that can be flexibly parameterized to user-specific needs. Most importantly, we may optimize a compositing product for specific process and change regimes, varying applications and different geographic regions. Accordingly, our objectives were to:

(1) Develop an algorithm that generates cloud free, radiometrically and phenologically consistent Landsat composites, based on flexible rule sets for pixel selection

(2) Evaluate the radiometric consistency of the output composites with respect to MODIS BRDF normalized reflectance products

(3) Assess the suitability of the composites and the surplus value of spectral variability byproducts from compositing for regional land cover mapping

## 2 Methodology

### 2.1 Data used and test region

We developed our algorithm and evaluated the outputs over a region in Eastern Europe covered by 42 Landsat World-Reference-System-2 footprints (Fig. 1). The test region (~850,000 km²) features mountainous terrain with elevations of up to 2,600m in the Carpathian Mountains, as well as the lowlands of the Pannonian Basin, extending towards the South and the Adriatic Sea. For the detailed assessment of radiometric consistency, 10 sub regions of 60x60 km were selected. These sub regions were purposefully located in the central part of the study region and within scene overlaps. They were chosen to represent a broad variety of land cover configurations (Fig. 1). The region features a temperate-continental climate with increasing maritime influences towards the southwest. The forests in the region comprise coniferous mixed and deciduous forests. Coniferous forests are mostly dominated by Norway spruce (*Picea abies*) and silver fir (*Abies alba*) and deciduous forests feature European beech (*Fagus sylvatica*), pedunculate oak (*Quercus robur*), hornbeam (*Carpinus betulus*) and lime (*Tilia cordata*). The regional growing season begins in April and ends in October, but varies over elevation ranges and in response to annual rainfall variability (Rotzer and Chmielewski 2001).

We here aimed at producing image composites for three years, i.e. 2000, 2005 and 2010. Such even spaced, nominal dates are commonly used for quantifying LULCC (Lambin and Geist 2006a). Available imagery in the Landsat archive was not sufficient to achieve a full coverage from yearly data for each of these years. We therefore considered imagery acquired within ± two years of the respective year for compositing. To differentiate between the five year interval composites and the actual acquisition date of the respective data set used in the compositing, we hereafter refer to 2000, 2005 and 2010 as “target years”. We used all available precision terrain corrected (L1T) Landsat TM and ETM+ imagery with less than 70% cloud cover from the USGS Landsat archive (Table 1). Images acquired between mid-November and mid-February were excluded to avoid the prevalent snow coverage, low sun elevation angles and shadowing, and consequently poor signal-to-noise-ratio.

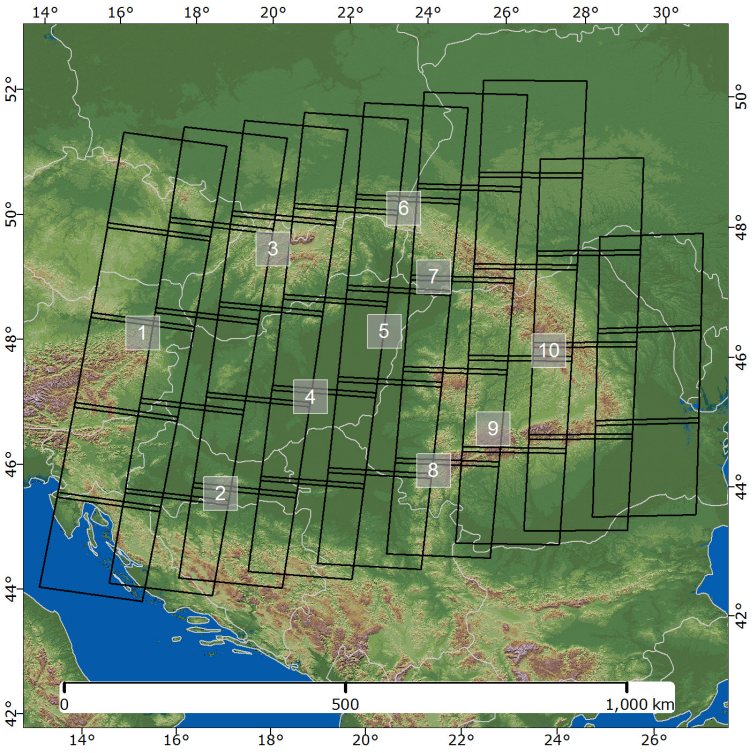


Figure III-1: Landsat footprints from path 190 / row 25 in the northwest to path 182 / row 29 in the southeast (overlaid on Shuttle Radar Topography Mission elevation data). Sub regions for evaluation purposes are indicated by grey rectangles.

Table III-1: Landsat data used for the compositing in 2000, 2005 and 2010.

| | 2000 | 2005 | 2010 |
|---|---|---|---|
| Total number of images | 890 | 1478 | 1590 |
| Total data volume [TByte] | 0.80 | 1.82 | 1.51 |
| Target year images [%] | 29.1 | 15.3 | 34.7 |
| Median day of year | 181 | 203 | 198 |
| Average cloud cover [%] | 38.1 | 38.6 | 40.4 |

We additionally acquired MODIS reflectance data to assess the consistency of spectral responses in Landsat composites. We considered MODIS surface reflectance to be a state of the art, large area image product that provides consistent spectral reference across space. We used the BRDF-adjusted, 16-day surface reflectance product (MCD43A4) with 500m spatial resolution for 6 spectral bands to assess the radiometric response of our results. For this product, spectral responses are normalized to nadir viewing geometry, thus view-angle related effects are minimized (Lucht et al. 2000). Despite varying spatial resolutions, MODIS and Landsat data are well suited to be compared spectrally, as their equatorial overpass times are similar (Hwang et al. 2011), both sensors have comparable spectral bands with corresponding center wavelengths (Chander et al. 2010). Furthermore, the

atmospheric correction algorithm applied to MODIS data is similar to the correction method applied to the Landsat data in this study (Masek et al. 2006).

### 2.2 Pre-processing

We atmospherically corrected all input images, converting digital numbers into surface reflectance to assure comparability of results across different Landsat sensors, footprints and acquisition dates. We used the Landsat Ecosystem Disturbance Adaptive Processing System (LEDAPS) algorithm to perform the correction (Masek et al. 2006). The algorithm uses the Second Simulation of the Satellite Signal in the Solar Spectrum (6S, Vermote et al. 1997) radiative transfer model in a similar manner as used to correct MODIS imagery. Surface reflectance bands 1-5 and 7 were used for further analysis at the original 30m spatial resolution. Cloud masks were subsequently developed for all images using the FMASK algorithm (Zhu and Woodcock 2012). The FMASK approach is an extended and improved rule-based method of the automated cloud cover assessment system (ACCA, Irish et al. 2006). Parameters such as cloud probability thresholds were set to conservative values to capture as many clouds and cloud shadows as possible. Additionally, we developed distance images providing the distance of each pixel to the next cloud or cloud shadow. All data was subsequently re-projected to Lambert Azimuthal Equal Area (LAEA) with a European Terrestrial Reference System 89 (ETRS89) datum so that imagery from different UTM zones can be composited into one single output dataset.

### 2.3 Image compositing

As image frames of individual footprints are always shifted against each other, the greatest possible spatial extent of all inputs was determined and tile-wise parallel processing subsequently used. All data that spatially overlapped was extracted based on a tile-wise bounding-box test and the potentially unclouded observations according to the cloud masks were extracted.

During compositing, all available observations of a given pixel are assessed regarding their suitability for the composite. This assessment can be based on different parameters, for which a score is calculated for each available observation. The weighting of these parameter scores is obtained regarding the respective objectives pursued, e.g. with a high scoring weight on the day-of-year in the leaf-on season in case of temperate forests analysis. Subsequently, scores are summed up, and the spectral values of the observation with the highest score are written into the composite. All other available observations are

used to produce spectral variability metrics. In the following section we describe the development of the parameter score functions.

We implemented a parametric weighting scheme to assess the suitability of observations, based on score functions for three parameters: (1) acquisition year (i.e. annual suitability), (2) acquisition day of year (DOY – seasonal suitability), as well as (3) the distance of a given pixel to the next cloud (risk of remnants of atmospheric disturbances). Compositing images from different dates and years requires considering the trade-offs between inter- and intra-annually matching acquisition dates, i.e. potential land cover changes and phenologic effects. As we focused on generic land use and land cover mapping, we aimed at producing composite datasets representing the seasonal period of main photosynthetic activity (i.e. a leaf-on state) and therefore first needed to assess the favored seasonal window.

We did this by first extracting all imagery from 1999 to 2011 available for selected areas with high data availability. From these, we selected three largely cloud free reference images for the target years (dashed vertical lines in Fig. 2(a)), and as close as possible to the middle of the year (DOY 183), which is an approximation of the peak photosynthetic activity in our study region.

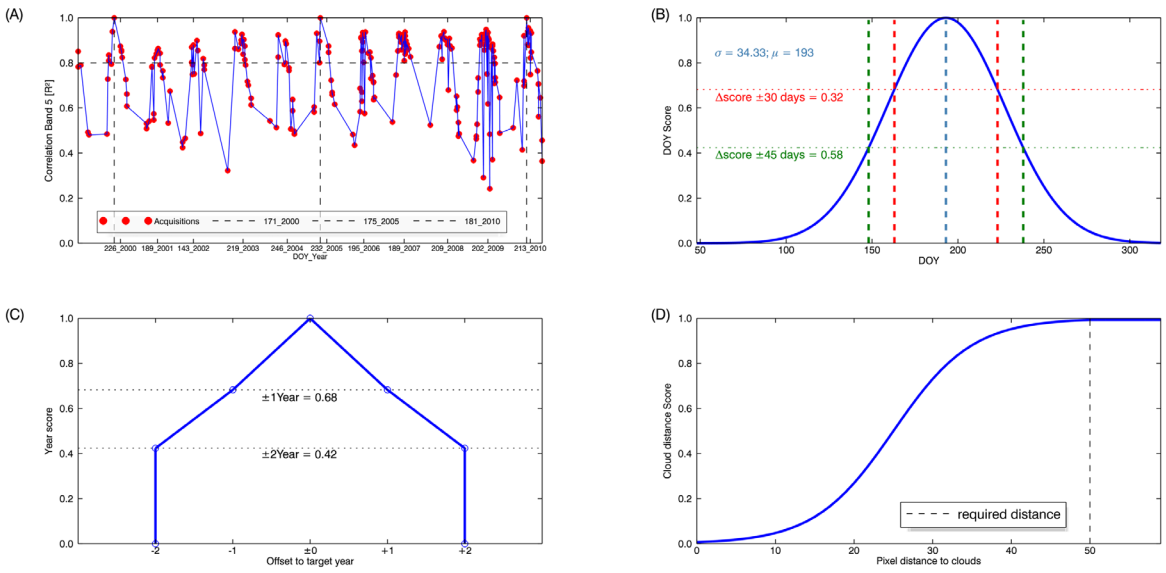


Figure III-2: Score functions: (A) Seasonal correspondence of available images with three selected reference images (indicated by vertical dashed lines) in Landsat band 5, horizontal dashed line indicates the 0.8 $R^2$ cut-off value; (B) DOY score function with all year median DOY of 193 and all year standard deviation of 34.33, green and red dashed lines indicate the ±30 and ±45 day offset scores, respectively; (C) year score function; (D) cloud distance score function.

We then assessed how well all other images spectrally corresponded to these reference images. This assessment was based on stable broadleaf or mixed forest areas (i.e. areas

with climate-dependent phenology). We then correlated shortwave infrared (SWIR - band five) reflectances of these areas for unclouded pixels in each image with reflectances in the respective reference image (target year +/- two years). We based this assessment on SWIR reflectance, which has been shown to be temporally more stable than near infrared (NIR), e.g. against understory or other background signal (Cohen and Goward 2004). Fig. 2(a) shows the temporal variation of the correlation coefficient over time with a seasonal pattern becoming apparent for individual years.

We finally used an $R^2$ of 0.8 as a cut-off criterion to provide seasonally comparable observations and derived the median and standard deviation of these images. The resulting all year median DOY (193 or July 12th) was employed to anchor a Gaussian scoring function (Fig. 2(b)) with the resulting standard deviation for all images with an $R^2$ higher than 0.8 (34 days). We used this function to evaluate the seasonal suitability (i.e. DOY) of all images for all years according to (1):

$$Score_{DOY} = \frac{1}{\sigma\sqrt{2\pi}} e^{\frac{1}{2}(\frac{\chi_i - \mu}{\sigma})^2} \quad (1)$$

where $\sigma$ denoted the all year DOY standard deviation, $\mu$ is the all year median DOY and $X_i$ is the DOY for a given acquisition.

Next, we defined a preferred seasonal window to ensure favoring a certain range of DOYs within the target year over a more central DOY of previous or subsequent years. On the one hand, favoring an optimum DOY over choosing a pixel from the central target year is reasonable, as yearly phenological cycles largely drive image statistics in a central European setting. This implies that the DOY criterion is more important than the year itself. On the other hand, extending the number of years considered during compositing increases the likelihood of including land cover changes in the output datasets. Intra-annual NDVI profiles from MODIS data and field experience proved that images acquired within 30 days from the median DOY always related to phenological states of photosynthetic peak activity for forest areas. The peak of intra-annual NDVI profiles examined for deciduous and mixed forests always occurred within this seasonal window. During the selection of acquisition dates, a ±30 day offset to the median DOY was therefore always favored over images acquired later or earlier than the target year. About ±15 days around this central window of peak phenology, some of the regions' forest stands appeared to be in a slightly pre-peak phenologic state or already showed first signs of senescence. Therefore, we estimated a DOY offset of ±45 days to be a suitable threshold to delineate the secondary

period of main photosynthetic activity for temperate forests encountered in our test region. To balance the risk of including non-peak phenology (larger DOY offset) against the risk of including potential land cover changes (increasing with increasing temporal offset from the target year), acquisitions from within 45 days of the target DOY (i.e. May 28th and August 26th) should always be favored over images acquired two years from the target year. We therefore assessed the difference in the DOY score for 30 and 45 days (Fig. 2(b)) and constructed a piecewise linear year scoring function (Fig. 2(c)).

We scored a pixel's distance to clouds or cloud shadows based on a sigmoidal function in conjunction with a user defined value defining the minimum required distance to clouds/shadows. Examination of Landsat images with different atmospheric conditions indicated that many pixels directly adjacent to clouds are not always identified as such during cloud masking, but may still be strongly affected by neighboring clouds. While this influence can be assumed to decrease exponentially with increasing distance from clouds, the minimum required distance is not easily derivable from the input imagery alone. Therefore, this value needs to be defined depending on the abundance of imagery, providing more conservative (i.e. higher) values if lots of imagery is available and to lower values in cases where imagery is relatively scarce. For this study we defined a minimum required distance of 50 pixels (dashed line in Fig. 2(d)), as a compromise between falsely excluded clear pixels and including undesired observations (e.g. affected by water vapor or haze). All pixels that were located closer to clouds than 50 pixels obtained a score according to (2):

$$Score_{CloudDist.} = \frac{1}{1 + e^{\left(-0.2 \cdot \min\{D_i, D_{req}\} - \left(\frac{D_{req} - D_{\min}}{2}\right)\right)}} \quad (2)$$

Where $D_i$ indicates a given pixels distance to clouds, $D_{req}$ is the defined minimum required distance, $D_{min}$ is the minimum distance of the given pixel observations. As the data still contained some cloud remnants, a threshold based cloud-remnant removal was performed. Thresholds were based on the visible wavelengths' reflectance and the relation between visible, NIR and SWIR bands, yielding the final unclouded observations (hereafter: clear observations).

The provided scores are subsequently summed up with the cloud distance score weighted half of the scores for DOY and year, respectively. Finally all 6 spectral band values of the observation with the highest final score are written into the best observation composite. Should there be several observations with identical final scores, the one closest to the target

year is selected. The observation featuring the lower reflectance in the blue band is selected if no winner could be determined during the previous steps, to additionally minimize atmospheric effects.

After the clear observations have been determined, additional datasets and metrics were assembled. Besides the best observation composites, we produced image variability measures and flag images. Spectral variability measures take advantage of all extracted clear observations. Thus they contain implicit information on land cover phenology and spectral-temporal stability. Here, we produced mean, standard deviation and range images for each spectral band. Additionally, we created a band providing the sum of SWIR/NIR bands normalized over the number of clear observations. The flag bands provide information on acquisition date (year and DOY), the number of clear observations, the selected image footprint, the score determined for the best observation as well as winner acquisition sun zenith angle. Table 2 summarizes the individual outputs produced during compositing and Fig. (3) provides examples of compositing outputs for the target year 2005.

Table III-2: Overview of different compositing outputs produced per target year result

| Output type | Description |
|---|---|
| Best observation composite | Pixels with highest score for evaluated parameters |
| Spectral variance metrics | Mean, standard deviation and range images for spectral bands 1-5 and 7. Sum of reflectance in nIR and swIR bands normalized by number of observations |
| Flag metrics | Path/row, Acquisition year/month/day, Acquisition DOY, Number of clear observations, determined decision score value, sun zenith during acquisition |

### 2.4 Evaluating annual, seasonal and radiometric consistency

We evaluated the best observation composites for the three target years in terms of annual and seasonal consistency. This evaluation was based on the respective flag images for different cases relating to the decision for a certain acquisition date: The ideal case-1 has a pixel selected from the target year and a DOY within 30 days from the target DOY. The least desirable case would represent a two year offset from the target year and a DOY offset that is greater than 45 days (case-9). Table 3 provides an overview of the investigated temporal compositing cases.

The evaluation of radiometric consistency was based on the comparison with MODIS reflectance data. We acquired the temporally closest MODIS 16-day composite to the target DOY and year. We then adjusted our best observation composites to 500m resolution using simple pixel aggregation. To assess how well our PBC outputs corresponded to the

MODIS products, we derived band wise Pearson correlation coefficients ($R^2$) and RMSE for the 10 sub regions and the three PBC outputs. We additionally assessed the temporal composition of selected pixels within the sub regions according to the 9 defined cases. We also provided the average number of available clear observations for each subset and PBC output.

Table III-3: Evaluated cases for temporal compositing of acquisition dates. The column "Priority" indicates the ranked preference of cases for compositing.

| Case # | Offset to target year | Offset to target DOY | Priority |
|---|---|---|---|
| Case 1 | 0 years | ± 30 days | 1 |
| Case 2 | 0 years | > 30 days - ≤ 45 days | 4 |
| Case 3 | 0 years | > 45 days | 7 |
| Case 4 | ± 1 year | ± 30 days | 2 |
| Case 5 | ± 1 year | > 30 days - ≤ 45 days | 5 |
| Case 6 | ± 1 year | > 45 days | 8 |
| Case 7 | ± 2 years | ± 30 days | 3 |
| Case 8 | ± 2 years | > 30 days - ≤ 45 days | 6 |
| Case 9 | ± 2 years | > 45 days | 9 |

### 2.5 PBC-based land cover mapping

Finally, we evaluated the performance of our composited image products for land cover classification. Land cover mapping performance was assessed using a random forest (RF) classifier (Waske et al. 2012) and a sample of interpreted randomly sampled points. We sampled a total of 2,000 points randomly with a minimum distance of 1 km to minimize spatial autocorrelation. The samples were then interpreted using VHR imagery along with the original Landsat imagery and ground truth data. We only retained samples if their interpreted land use / land cover did not change between 2003 and 2007, yielding a total sample size of 1623 points. We aimed at achieving a thematic depth comparable to that of common global land cover products (Bartholome and Belward 2005; Arino et al. 2008; Friedl et al. 2010). We consequently targeted at separating coniferous forest, mixed forest, deciduous forest, agriculture, grassland, built-up and water. We used a single RF model over the entire test region to assess if the composited input data allows for homogeneous classification results based on one global classification model. We then trained different RF classification models for the entire test region for the 2005 PBC using different input feature stacks: (a) only the best observation composite, and (b) the best observation composite together with the spectral variability metrics. The RF models were trained using 500 individual trees and the number of features at each split was set to the square root of the number of input features (Waske et al. 2010). Validation was based on 10-fold cross

validation of the interpreted samples, with 10% of the samples left out for the validation of each resulting model that was trained with the remaining 90% of samples (Kohavi 1995). We derived overall accuracies, producer's and user's accuracy as well as kappa statistics.

## 3 Results

The resulting composites were free of clouds and homogeneous in appearance even though data from different years and different seasons was broadly mixed (Fig. 3(a), (b), (c)). Between 91% (2010) and 66% (2000) of all pixels consisted of observations acquired within the respective target year (Table 4). No more than 3.5% of all pixels selected during compositing were acquired two years earlier or later than any of the target years. Even though the seasonal range spanned spring to autumn in all three composites, the majority of selected observations captured peak phenology of green vegetation.

Table III-4: Acquisition years of pixels used for compositing (Note: no input imagery existed for 1998 and 2012).

| Target Year | -2 | -1 | 0 | +1 | +2 |
|---|---|---|---|---|---|
| 2000 [%] | --- | 9.52 | 65.91 | 21.30 | 3.27 |
| 2005 [%] | 0.43 | 2.40 | 67.91 | 26.26 | 3.01 |
| 2010 [%] | 0.13 | 8.06 | 91.24 | 0.57 | --- |

Accordingly, between 52% (2000) and 88% (2010) of selected pixels were case 1 pixels, i.e. acquired within the target year and within 30 days of the target DOY (Table 5). For target year 2000, about 14% of pixels were acquired within 45 days of the target DOY (case 2), while the share of case 2 pixels was considerably lower for the other years (< 3%). The distribution of case 4 pixels was relatively even for the 2000 and 2005 result (30% and 29%, respectively) and considerable lower for the 2010 result (8.5%). Thus, seasonal consistency was highest within the 2010 outputs, with more than 96% of pixels acquired within the preferred seasonal window (cases 1, 3, 7).

Table III-5: Temporal composition of cases in the three best observation composites

| | Case-1 | Case-2 | Case-3 | Case-4 | Case-5 | Case-6 | Case-7 | Case-8 | Case-9 |
|---|---|---|---|---|---|---|---|---|---|
| 2000 [%] | 51.65 | 13.60 | 0.66 | 30.21 | 0.49 | 0.12 | 3.02 | 0.04 | 0.21 |
| 2005 [%] | 66.51 | 1.21 | 0.19 | 28.50 | 0.06 | 0.09 | 2.74 | 0.15 | 0.55 |
| 2010 [%] | 88.18 | 2.83 | 0.23 | 8.51 | 0.06 | 0.06 | 0.05 | 0.04 | 0.04 |

The share of pixels with an unfavorable seasonal state (i.e. DOY offset to target DOY > 45 days) was below 1% for all PBC outputs. The number of extracted cloud free observations per pixel ranged from one to 114 for the 2005 composite. On average, between 21 (2000) and 39 (2005) unclouded observations were available for each pixel. The number of clear

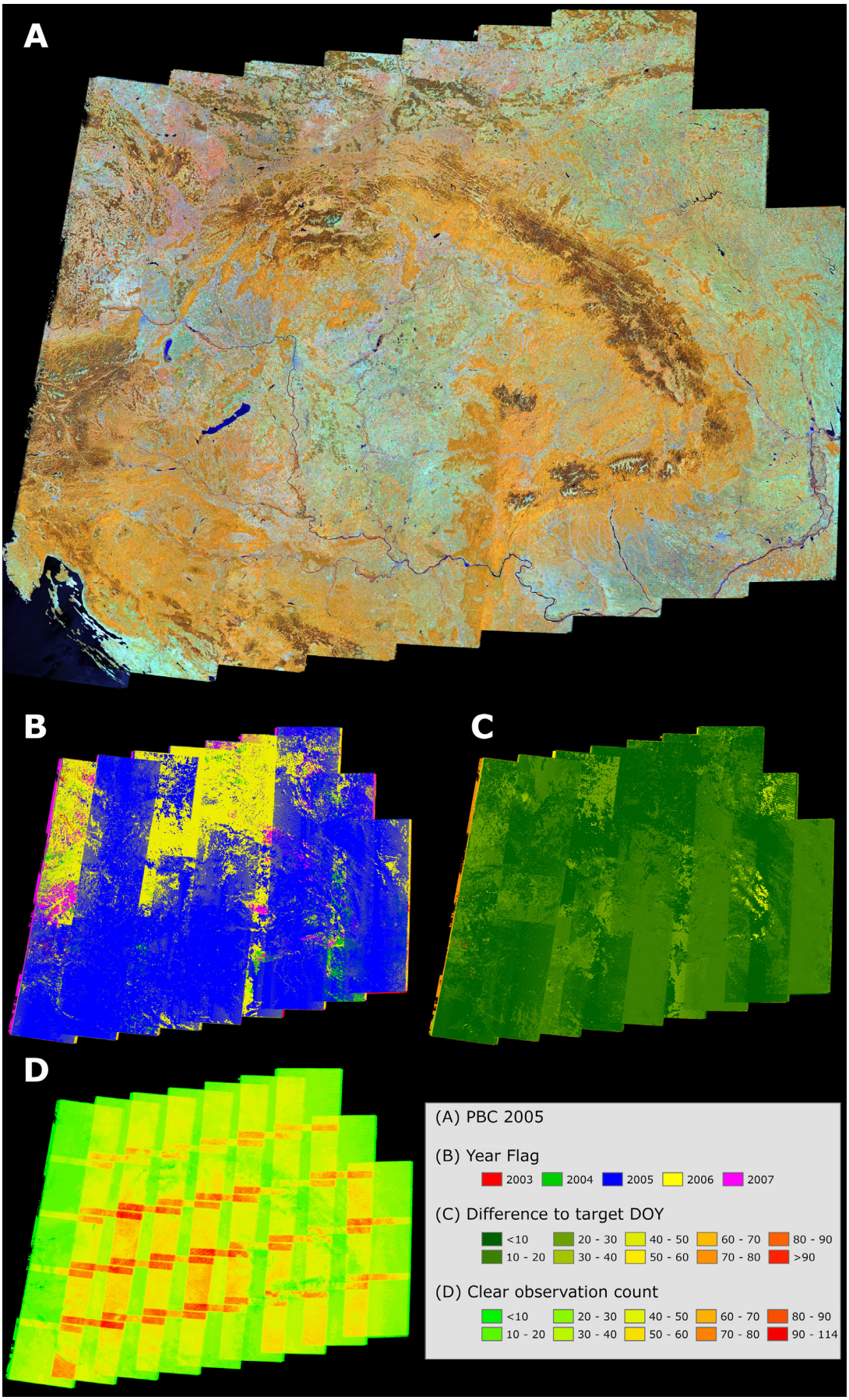


Figure III-3: Output examples of the 2005 PBC: (A) best observation composite (RGB = 4,5,3); (B) year flag image; (C) relative difference to target DOY; (D) number of clear observations per pixel.

observations was especially increased within the across track overlap areas (Fig. 3(d)). For mountainous areas, the number of available unclouded observations was considerably lower (Fig. 3(d)). These areas also exhibited higher year and DOY offsets (Fig. 3 (b), (d)).

The PBC resembled spectral and radiometric characteristics of the MODIS 16-day reflectance composites well (Fig. 4). However, the land cover composition in the sub regions influenced the level of agreement. Forests generally lead to high correlations while spectrally dynamic land cover types, such as agriculture or grasslands, suffered from spectral variation or land cover changes. Second, the visible bands generally exhibited lower correspondence between MODIS and PBC reflectances, presumably due to atmospheric effects. In many cases, this effect seemed to be related to considerable spectral scatter in the MODIS visible bands (e.g. Fig. 4(d), (j)).

Sub region 1 was strongly dominated by broadleaved and coniferous forests within mountainous terrain (Fig. 4(a), (b)). The 2005 and 2010 results achieved $R^2$ values higher than 0.8 in five bands (Table 6). The 2010 result resulted in correlations of 0.9 in the blue and red spectral bands. The temporal composition of pixels was very different between the 2005 and 2010 results (Table 7). More than 80% of the 2005 result consisted of pixels acquired with at least one year offset. In the case of the 2010 result, 83% of pixels related to case 1. The temporal composition in the 2000 case was more variable with 3% of case 2 and case 3 pixels. The average number of extracted clear observations was relatively low (15) and the corresponding MODIS image lacked more than 50% of observations (Fig. 4(a)).

Forest dominated sub region 3 is located in mountainous terrain at higher elevations where cloud coverage is frequent (Fig.4 (c), (d)). Here the year 2000 result had the lowest average number of clear observation available (13), about 48% of pixels were case-2 observations. The corresponding MODIS data for this period lacked more than 90% of observations. The composition of acquisition dates for the 2000 result covered a wider range of cases and correlations to MODIS bands were comparatively low. The 2005 result (~74% case 4) achieved higher $R^2$ values in five out of 6 bands (Fig. 4(d)), even though the 2010 output consisted to over 98% out of case-1 pixels.

Sub region 5 featured mostly agricultural land and grassland and was located at lower elevations (Fig. 4(e)). Here the 2000 result performed worst in four out of 6 bands, relating to a 41% of case-4 pixels and 12% of case-7 pixels. The corresponding MODIS product featured approximately 10% of no data pixels and the number of observations was as low

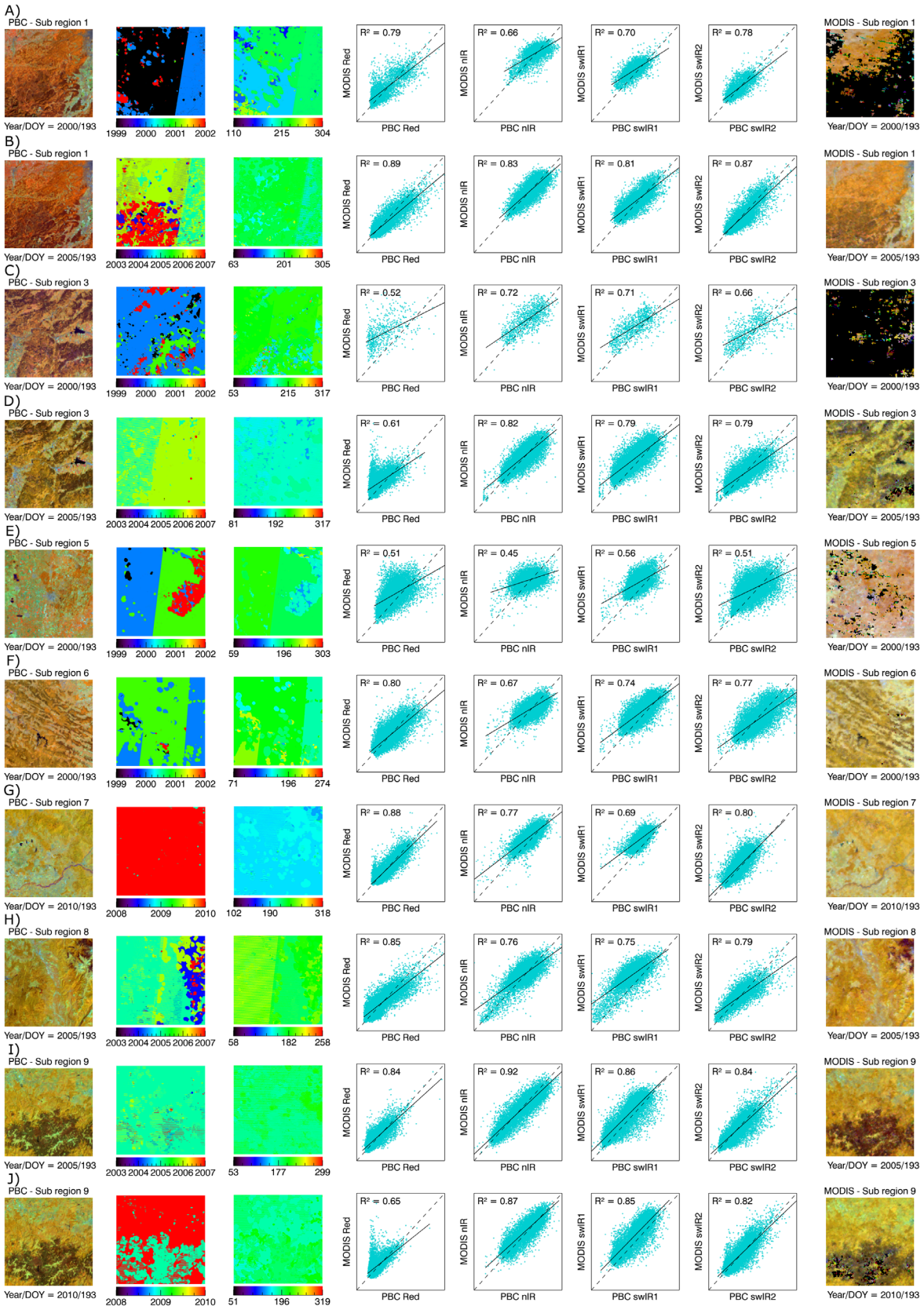


Figure III-4: Radiometric consistency evaluation (from left to right): (column 1) aggregated PBC imagery (RGB = 4, 5, 3); (column 2) corresponding year flag images; (column 3) corresponding DOY flag images; (columns 4 – 7) band wise scatterplots for red, NIR, SWIR1 and SWIR2 bands of MODIS (Y axis) and PBC (X axis) data; (column 8) corresponding MODIS nadir BRDF-adjusted 16-day reflectance product (MCD43A4, RGB = 2, 6, 1).

Table III-6: Results of the evaluation of the radiometric consistency assessed for the 10 sub regions (first column), coefficients of determination ($R^2$) and root mean squared errors (RMSE) for the 6 corresponding MODIS and aggregated PBC bands.

| | | Radiometric consistency: PBC vs. MODIS ($R^2$ / RMSE) | | | | | |
|---|---|---|---|---|---|---|---|
| | | TM 1 vs. MOD 3 | TM 2 vs. MOD 4 | TM 3 vs. MOD 1 | TM 4 vs. MOD 2 | TM 5 vs. MOD 6 | TM 7 vs. MOD 7 |
| Sub region 1 | 2000 | 0.35 / 195.59 | 0.7 / 168.1 | 0.79 / 173.4 | 0.66 / 396.24 | 0.7 / 334.17 | 0.78 / 207.68 |
| | 2005 | 0.77 / 133.78 | 0.88 / 96.93 | 0.89 / 125.73 | 0.83 / 331.04 | 0.81 / 275.93 | 0.87 / 175.09 |
| | 2010 | 0.81 / 124.25 | 0.9 / 100.67 | 0.91 / 121.81 | 0.82 / 308.56 | 0.85 / 337.87 | 0.88 / 180.75 |
| Sub region 2 | 2000 | 0.85 / 86.71 | 0.86 / 131.1 | 0.87 / 130.46 | 0.76 / 491.67 | 0.76 / 436.25 | 0.83 / 195.08 |
| | 2005 | 0.75 / 87.2 | 0.85 / 107.66 | 0.85 / 102.1 | 0.74 / 371.07 | 0.68 / 424.3 | 0.79 / 157.82 |
| | 2010 | 0.77 / 95.59 | 0.88 / 98.77 | 0.88 / 108.85 | 0.79 / 289.42 | 0.79 / 402.81 | 0.85 / 169.67 |
| Sub region 3 | 2000 | 0.11 / 542.31 | 0.5 / 436.72 | 0.52 / 374.51 | 0.72 / 593.87 | 0.71 / 488.62 | 0.66 / 276.88 |
| | 2005 | 0.1 / 232.82 | 0.62 / 223.65 | 0.61 / 185.9 | 0.82 / 472.36 | 0.79 / 356.3 | 0.79 / 168.38 |
| | 2010 | -0.04 / 273.7 | 0.51 / 217.42 | 0.57 / 195.98 | 0.8 / 436.19 | 0.8 / 358.94 | 0.79 / 190.44 |
| Sub region 4 | 2000 | 0.48 / 168.23 | 0.56 / 156.07 | 0.58 / 218.5 | 0.48 / 397.8 | 0.6 / 477.01 | 0.62 / 380.35 |
| | 2005 | 0.79 / 162.31 | 0.81 / 79.74 | 0.81 / 119.01 | 0.73 / 288.33 | 0.73 / 333.02 | 0.77 / 261.31 |
| | 2010 | 0.42 / 114.96 | 0.66 / 121.81 | 0.68 / 142.27 | 0.73 / 370.34 | 0.66 / 443.23 | 0.67 / 303.31 |
| Sub region 5 | 2000 | 0.31 / 134.78 | 0.51 / 166.53 | 0.51 / 209.91 | 0.45 / 483.42 | 0.56 / 490.78 | 0.51 / 374.38 |
| | 2005 | 0.42 / 130.15 | 0.64 / 99.31 | 0.56 / 166.74 | 0.48 / 557.04 | 0.5 / 318.36 | 0.48 / 388.15 |
| | 2010 | 0.63 / 140.23 | 0.75 / 83.04 | 0.77 / 126.9 | 0.75 / 354.93 | 0.67 / 337.17 | 0.69 / 250.56 |
| Sub region 6 | 2000 | 0.52 / 143.5 | 0.82 / 92.04 | 0.8 / 86.86 | 0.67 / 390.69 | 0.74 / 293.05 | 0.77 / 144.44 |
| | 2005 | 0.08 / 243.88 | 0.53 / 246.88 | 0.48 / 207.4 | 0.67 / 477.81 | 0.63 / 361.75 | 0.64 / 167.69 |
| | 2010 | 0.1 / 146.07 | 0.61 / 159.65 | 0.55 / 138.57 | 0.67 / 462.88 | 0.65 / 391.88 | 0.64 / 157.7 |
| Sub region 7 | 2000 | 0.69 / 152.95 | 0.77 / 149.84 | 0.72 / 235.84 | 0.7 / 428.37 | 0.61 / 383.6 | 0.66 / 352.63 |
| | 2005 | 0.31 / 144.94 | 0.75 / 139.49 | 0.8 / 146.53 | 0.74 / 343.01 | 0.59 / 299.43 | 0.75 / 184.4 |
| | 2010 | 0.67 / 114.32 | 0.85 / 94.51 | 0.88 / 91.11 | 0.77 / 335.81 | 0.69 / 386.71 | 0.8 / 143.04 |
| Sub region 8 | 2000 | 0.76 / 85.19 | 0.81 / 157.34 | 0.76 / 198.61 | 0.43 / 582.38 | 0.7 / 562.07 | 0.68 / 311.28 |
| | 2005 | 0.57 / 113.38 | 0.84 / 89.71 | 0.85 / 81.64 | 0.76 / 374.26 | 0.75 / 365.26 | 0.79 / 124.11 |
| | 2010 | -0.1 / 235.41 | 0.4 / 192.15 | 0.42 / 165.45 | 0.74 / 355.06 | 0.73 / 324.72 | 0.73 / 120.13 |
| Sub region 9 | 2000 | 0.86 / 84.24 | 0.86 / 121.46 | 0.86 / 158.29 | 0.84 / 442.9 | 0.87 / 377.5 | 0.87 / 227.75 |
| | 2005 | 0.53 / 107.88 | 0.84 / 99.92 | 0.84 / 102.28 | 0.92 / 343.05 | 0.86 / 310.78 | 0.84 / 151.11 |
| | 2010 | 0.02 / 206.79 | 0.55 / 179.75 | 0.65 / 161.17 | 0.87 / 399.34 | 0.85 / 370.79 | 0.82 / 166.82 |
| Sub region 10 | 2000 | 0.69 / 106.84 | 0.83 / 107.15 | 0.81 / 118.25 | 0.84 / 430.16 | 0.86 / 356.22 | 0.82 / 194.65 |
| | 2005 | 0.27 / 116.39 | 0.74 / 140.13 | 0.7 / 125.58 | 0.89 / 383.13 | 0.83 / 356.38 | 0.82 / 130.09 |
| | 2010 | -0.09 / 188.15 | 0.55 / 161.04 | 0.47 / 140.84 | 0.83 / 441.1 | 0.81 / 338.59 | 0.77 / 131.69 |

as 19. With more than 99% of case-1 acquisitions, the 2010 result achieved the highest correlations to the MODIS bands.

Sub region 6 exhibits a mosaic of grassland and agriculture dominated valleys and forested slopes and ridges over medium elevation terrain (Fig. 4(f)). For the 2000 result, relatively few acquisitions were available (21) and consequently only 24% of pixels corresponded to case-1, while the majority (68%) were case-4 pixels. About 7% of pixels were acquired within the extended seasonal window. The achieved $R^2$ values were the highest in all bands. The 2010 result contained 21% of case-2 pixels but the 2005 output, with 53% case-4 acquisitions, mostly achieved lower $R^2$ values.

Table III-7: Results of the evaluation of the temporal composition of pixels according to the 9 defined cases assessed for the 10 sub regions (first column), provided for each target year composite. Additionally, the average number of available unclouded observations is provided.

| | | Radiometric consistency: Temporal composition of pixels | | | | | | | | | Clear |
|---|---|---|---|---|---|---|---|---|---|---|---|
| | | Case 1 | Case 2 | Case 3 | Case 4 | Case 5 | Case 6 | Case 7 | Case 8 | Case 9 | observations |
| Sub region 1 | 2000 | 25.19 | 3.06 | 3.14 | 64.83 | 0.21 | 0.01 | 3.56 | 0.00 | 0.00 | 15 |
| | 2005 | 17.90 | 0.08 | 0.31 | 59.61 | 0.00 | 0.00 | 22.09 | 0.00 | 0.01 | 32 |
| | 2010 | 82.71 | 0.15 | 0.18 | 16.93 | 0.00 | 0.00 | 0.01 | 0.00 | 0.02 | 26 |
| Sub region 2 | 2000 | 77.03 | 21.66 | 0.00 | 1.29 | 0.00 | 0.00 | 0.02 | 0.00 | 0.00 | 38 |
| | 2005 | 96.30 | 0.00 | 0.00 | 3.66 | 0.00 | 0.00 | 0.03 | 0.00 | 0.00 | 66 |
| | 2010 | 99.66 | 0.01 | 0.00 | 0.33 | 0.00 | 0.00 | 0.00 | 0.00 | 0.00 | 67 |
| Sub region 3 | 2000 | 26.54 | 47.66 | 0.92 | 17.07 | 0.00 | 0.51 | 7.08 | 0.20 | 0.01 | 13 |
| | 2005 | 26.13 | 0.01 | 0.03 | 73.61 | 0.00 | 0.00 | 0.21 | 0.00 | 0.00 | 30 |
| | 2010 | 98.34 | 0.66 | 0.00 | 0.97 | 0.00 | 0.02 | 0.01 | 0.00 | 0.00 | 15 |
| Sub region 4 | 2000 | 78.11 | 7.95 | 0.10 | 11.88 | 0.00 | 0.00 | 1.96 | 0.00 | 0.00 | 27 |
| | 2005 | 94.09 | 0.00 | 0.00 | 5.89 | 0.00 | 0.00 | 0.01 | 0.00 | 0.00 | 57 |
| | 2010 | 99.67 | 0.00 | 0.00 | 0.32 | 0.00 | 0.00 | 0.00 | 0.00 | 0.00 | 41 |
| Sub region 5 | 2000 | 44.20 | 0.19 | 2.78 | 40.64 | 0.00 | 0.00 | 12.19 | 0.00 | 0.00 | 19 |
| | 2005 | 77.31 | 0.00 | 0.00 | 22.67 | 0.00 | 0.00 | 0.02 | 0.00 | 0.00 | 41 |
| | 2010 | 99.12 | 0.01 | 0.00 | 0.87 | 0.00 | 0.00 | 0.00 | 0.00 | 0.00 | 23 |
| Sub region 6 | 2000 | 23.58 | 7.01 | 0.27 | 68.45 | 0.01 | 0.15 | 0.52 | 0.00 | 0.00 | 21 |
| | 2005 | 46.17 | 0.15 | 0.00 | 53.42 | 0.00 | 0.00 | 0.26 | 0.00 | 0.00 | 39 |
| | 2010 | 70.68 | 20.45 | 0.01 | 8.61 | 0.18 | 0.00 | 0.07 | 0.00 | 0.00 | 29 |
| Sub region 7 | 2000 | 62.98 | 2.07 | 0.00 | 34.94 | 0.00 | 0.00 | 0.00 | 0.00 | 0.00 | 36 |
| | 2005 | 46.17 | 0.15 | 0.00 | 53.42 | 0.00 | 0.00 | 0.26 | 0.00 | 0.00 | 61 |
| | 2010 | 99.54 | 0.00 | 0.00 | 0.46 | 0.00 | 0.00 | 0.00 | 0.00 | 0.00 | 53 |
| Sub region 8 | 2000 | 20.90 | 36.98 | 0.00 | 42.11 | 0.00 | 0.00 | 0.00 | 0.00 | 0.00 | 20 |
| | 2005 | 65.83 | 0.00 | 0.00 | 31.41 | 0.11 | 0.01 | 2.64 | 0.00 | 0.00 | 39 |
| | 2010 | 91.65 | 0.67 | 0.00 | 7.67 | 0.00 | 0.00 | 0.00 | 0.01 | 0.00 | 38 |
| Sub region 9 | 2000 | 99.14 | 0.42 | 0.00 | 0.43 | 0.00 | 0.00 | 0.00 | 0.00 | 0.00 | 19 |
| | 2005 | 92.05 | 0.00 | 0.00 | 6.30 | 0.00 | 0.00 | 1.64 | 0.00 | 0.00 | 38 |
| | 2010 | 68.63 | 0.44 | 0.00 | 30.91 | 0.00 | 0.00 | 0.02 | 0.00 | 0.00 | 29 |
| Sub region 10 | 2000 | 73.61 | 1.91 | 0.00 | 24.46 | 0.00 | 0.00 | 0.02 | 0.00 | 0.00 | 26 |
| | 2005 | 80.71 | 7.75 | 0.00 | 8.85 | 0.00 | 0.00 | 2.68 | 0.00 | 0.00 | 44 |
| | 2010 | 65.99 | 0.33 | 0.00 | 33.68 | 0.00 | 0.00 | 0.00 | 0.00 | 0.00 | 36 |

Sub region 8 featured a variety of land cover types over a range of elevations. The highest correlations were achieved in the 2005 result (in 5 out of 6 bands) even though one third of pixels were acquired with one year offset to the target year. Most of these pixels were located over forested slopes in the eastern part of the sub region (Fig. 4(h)). The 2010 result did not achieve high correlations despite of featuring more than 90% of case-1 pixels. Sub region 9 again was strongly dominated by coniferous forests (Fig. 4(i), (j)). Here the highest overall correspondence to MODIS reflectances was achieved in the NIR bands for the 2005 result (0.92). The 2000 and 2005 results both achieved similarly high correlations and both were composed of more than 90% of case-1 pixels. The NIR and SWIR bands for the 2010 result resulted in comparably high correlations and 1/3 of pixels were case 4 observations.

Table III-8: Result of the cross validation of the classification results for (a) only best observation bands as input, and (b) the best observation bands and the spectral variability measures (PA = Producer's accuracy, UA = user's accuracy, OAC = overall accuracy, CF = coniferous forest, MF = mixed forest, DF = deciduous forest, AG = agriculture, GL = grassland, BU = built up, WT = water). Additionally the number of samples per class for training is provided.

| | RF classification model | | | | |
|---|---|---|---|---|---|
| | (a) only PBC | | (b) PBC + Stats | | |
| Class | PA [%] | UA [%] | PA [%] | UA [%] | # samples |
| CF | 53.75% | 83.98% | 59.60% | 92.19% | 256 |
| MF | 36.19% | 16.03% | 50.41% | 26.16% | 237 |
| DF | 62.11% | 69.82% | 69.70% | 74.85% | 338 |
| AG | 76.71% | 85.62% | 81.50% | 93.93% | 577 |
| GL | 50.00% | 13.73% | 75.00% | 8.82% | 102 |
| BU | 72.22% | 32.50% | 87.50% | 43.75% | 80 |
| WT | 90.00% | 81.82% | 95.83% | 69.70% | 33 |
| OAC | 64.70% | | 71.47% | | |
| Kappa | 0.54 | | 0.62 | | |

Results from the land cover classification underlined the radiometric consistency of the results. The composited imagery is radiometrically stable enough to train and apply a single classification model over the entire region. The achieved overall accuracies (Table 8) were 65% for the classifications using only the best observation composite (run (a)), and 72% for the run using the variability measures as additional input features (run (b)). There were considerable differences among both classification runs. Overall, the grassland class (training sample size 102) achieved the lowest accuracies with user's accuracies of 14% and 9% for run (a) and run (b) respectively. Forest classes achieved better results. For example the coniferous forest class was validated with a user's accuracy of 54% and 60%, and even higher user's accuracies of 84% and 92% for classification runs (a) and (b), respectively. The mixed forest class showed the weakest performance among the three forest classes with relatively high omission and commission errors. We found considerable improvements in classification accuracies when the spectral variability measures were included as input features. The agriculture, built up and water classes achieved high accuracies in both classification runs and were validated with even higher accuracies when the variability metrics were additionally used. User's accuracies improved by about 10% during classification run (b) for the deciduous and mixed forest and built up classes. Similarly, producer's accuracies improved considerable for mixed forest, grassland and built up classes. It is interesting to note that compositing artifacts related to SLC-off scan line errors were visible in some areas of the land cover map when using only the PBC. However, these artifacts were not visible in the map resulting from the PBC plus the variability measures as inputs. Moreover, the result obtained from only using the PBC as input features appeared to be stronger affected by salt-and-pepper like speckle in the

classified image. Also the delineation of built-up areas was spatially more consistent using the PBC and variability measures for the classification (Fig.5 top).

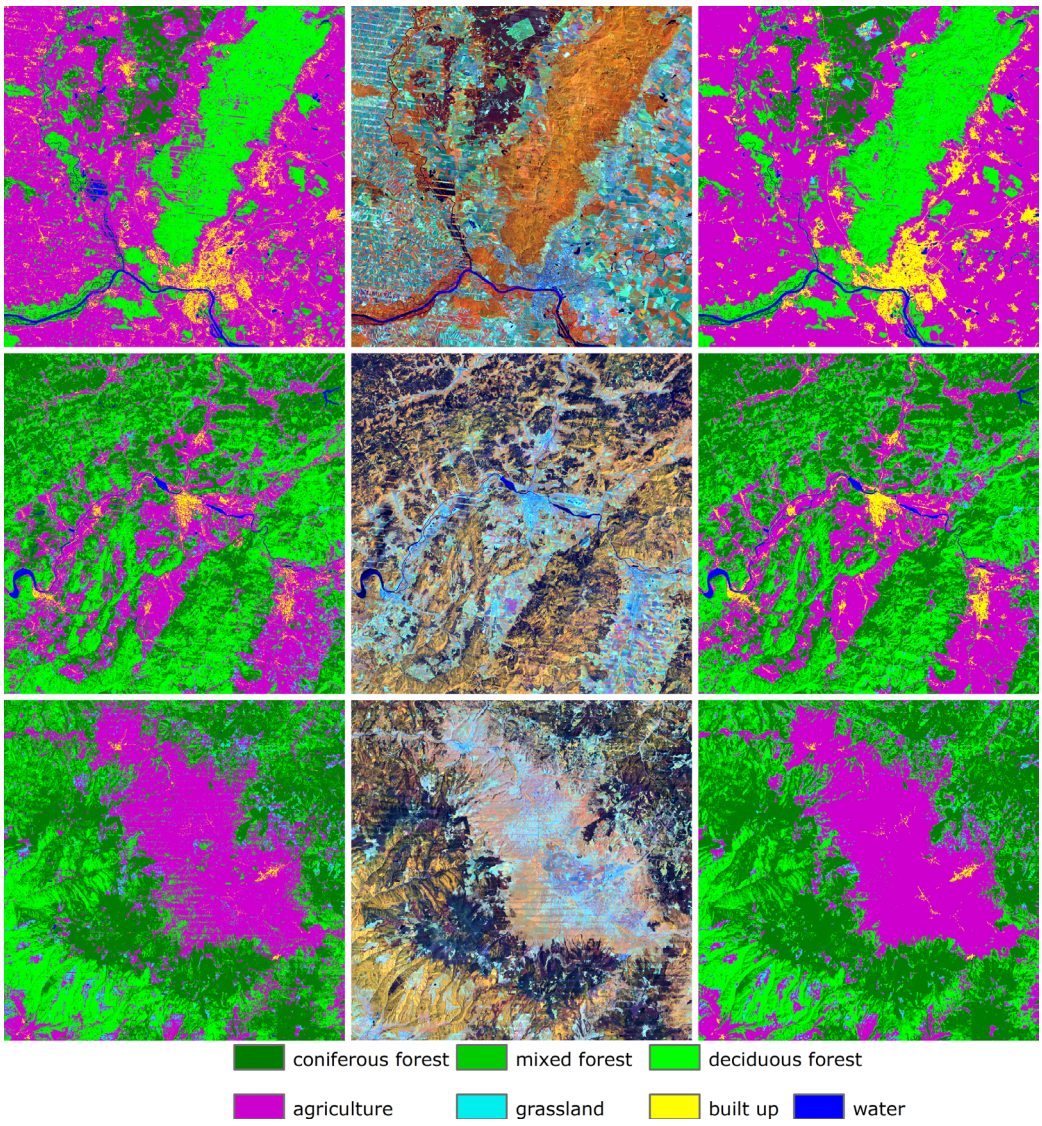


Figure III-5: Classification results (60x60 km) for the best observation composite only (left column) and for the best observation composite plus spectral variability measures (right column). Corresponding regions of the 2005 PBC in RGB = 4, 5, 3 (center column).

## 4 Discussion and conclusions

In this paper we describe a new algorithm for pixel based compositing of Landsat data. Our approach takes advantage of automated pre-processing approaches and facilitates generating regional image data sets from the Landsat archive. For selecting the most suitable from all available observations, we implemented a parametric weighting scheme. We described the development of score functions that facilitate homogeneous surface reflectance composites at 30m resolution. Seasonal and annual consistency was satisfying

and complete coverage was achieved even over mountainous terrain with frequent cloud cover.

We further achieved high radiometric correspondence to MODIS reflectance products. The level of correlation varied according to land cover composition. Our results underpin that optimizing phenologic consistency is more relevant to achieve radiometrically consistent composites than using data from the target year itself – at least in a temperate setting. We successfully utilized PBC to map land cover using a relatively small training set. Overall and class specific accuracies improved considerably when spectral variability metrics were additionally provided to the classifier.

With regard to the opening of the Landsat archive and considerable advancements of pre-processing methods, compositing is a logical consequence of these recent developments. Our approach takes advantage of automated procedures for cloud masking (Zhu and Woodcock 2012) and atmospheric correction (Masek et al. 2006). These methods allow for full automatization and processing of large volumes of data. Using atmospherically corrected surface reflectance data is a great asset, as relative radiometric normalization is not easily feasible with thousands of input scenes from different years and seasons. Our implementation of the here presented compositing methodology builds on parallel processing capacities and was run on a relatively modest multi-core server. However, the composites were produced within a time window comparable to time invested 10 years ago into manual cloud masking for single scene classifications. The potential to increase the performance using more advanced high performance computing environments (e.g. graphics processing units, cloud computing) thus is considerable (Lee et al. 2011).

We base the decision for image selection during compositing on a flexible parametric weighting scheme that evaluates available observations for their suitability. While this decision system can be easily extended to include additional parameters (e.g. local solar incidence angle, off-nadir pixel position, etc.), we here focused on three important parameters that are essential for achieving homogeneous composites. Designing the scoring functions for the selection of annual and seasonal acquisition dates appeared most important. We developed these scoring functions empirically based on the available data and knowledge of the regional seasonality. We used intra-annual vegetation profiles from MODIS for validation purposes only. This approach allows to parameterize the temporal score functions independent of the availability of MODIS data and thus also retrospectively for data since the beginning of the Landsat archive. However, the potential

of integrating MODIS-scale data for seasonal fine-tuning during compositing or to account for annual variation in phenology is considerable and should be subject of future research. While the performance of the scoring functions in other regions still needs to be evaluated the parameterization can be derived in a similar manner elsewhere. If annual consistency is focal e.g., when analyzing deforestation in quickly regrowing tropical forest regions, the annual weight has to be increased relative to the seasonal weight (Broich et al. 2011). Moreover, the weighting scheme can be parameterized to produce datasets tailored for specific mapping applications. For example, a leaf-on vegetation state could potentially be supplemented by a senescent seasonal state to improve the differentiation of forests types (Baumann et al. 2012). However, as Landsat data is predominantly acquired during the growing season in the temperate zone, the annual window for compositing would have to be increased considerably in order to achieve full coverage when compositing spring or autumn observations.

The results were annually and seasonally overall consistent for all three output composites. The annual consistency was slightly higher for the 2005 and 2010 result. The reason for this is that more images were available during the corresponding time periods, as the long term data acquisition plan was adjusted to compensate for the SLC failure after 2003 (Ju and Roy 2008). The ability to produce PBCs from the Landsat archive for large areas with surface reflectance at 30m spatial resolution is a great asset for many applications (Townshend et al. 2012). Within our results we achieved full regional coverage also for areas with persistent cloud cover. In such cases, the seasonal and annual offset of selected pixels was relatively high to enable a complete coverage (i.e. up to two years offset to the target and possibly DOY offsets greater than 45 days). The corresponding MODIS 16-day products often also lacked many observations within these areas (e.g. Fig. 4(a), (c)).

Our results showed that PBCs can achieve high radiometric consistency across space and time. In many cases, our results strongly correlated with the MODIS reflectance product even when imagery from different years was used for compositing. Larger shares of pixels with a greater seasonal offset (i.e. greater than 30 days) increased variance in the correspondences between MODIS and aggregated PBC bands. Multi annual imagery was increasingly incorporated into the PBC for mountainous areas with frequent cloud cover where MODIS data did not provide sufficient observations for a given 16-day period (e.g. Fig. 4(a), (c)). Land cover composition had a marked effect on the correlation between Landsat PBC and MODIS data. We showed that for areas exhibiting a natural phenology (especially forests), seasonal consistency over multiple years is more important than annual

consistency (i.e. cases 1, 4 and 7 are more crucial than cases 2, 5 and 8). Areas with spectrally variable and spatially heterogeneous land cover configurations, such as agricultural areas, only achieved high correlations with MODIS data when annual and seasonal acquisition dates were very similar. For these areas, land cover changes (i.e. cropped vs. barren fields) that occurred during the multi-year compositing period considerably decreased spectral correspondence to the MODIS data. Specifically in the case of fine-textured land cover configurations introducing MODIS point spread functions during aggregation might have influenced our analysis. However, the averaging effect related to introducing the PSF would not have altered the overall results (Huang et al. 2002).

As an example for an application using PBCs, we performed a set of land cover classifications. Results showed that the PBCs proved suitable for consistent and easy to implement land cover mapping over large areas. We used a relatively small set of randomly selected and visually labeled samples for training and a generic training strategy of the classification models. Regardless of this simple and straightforward approach, class delineations were consistent across the entire region. Several classes achieved consistently high accuracies over a heterogenous region covered by 42 Landsat footprints. Our training sample was too small to fully characterize all spectral varieties of some heterogeneous classes (e.g. grassland, compare table 9). Nevertheless, results demonstrated what can be achieved with only one iteration of training, based solely on temporarily stable and randomly selected training samples. In the future, training data automation will certainly further improve the classification accuracies (Huang et al. 2008; Townshend et al. 2012) , but was beyond the scope of this paper. As class boundaries are not always easily separable using a single “best” observation, we incorporated spectral variability measures that can be effortlessly derived from the best pixel assessment. Incorporating spectral variability measures led to considerable improvements in mapping accuracies for all classes. Moreover, compositing artifacts resulting from incorporated SLC-off imagery and salt-and-pepper effects are effectively eliminated when including variability metrics in the classification process, as these artifacts do not translate into averaged spectral measurements (Fig. 5 top). Many classes were delineated with much greater consistency and omission errors were minimized when we provided these additional input features (e.g. built up or mixed forest classes).

Compositing Landsat surface reflectance data provides stable radiometrically consistent data sets across large areas. In the future, such products will allow for integrated change

classification approaches based on multiple composites, targeted at capturing different points in time. Such a methodology is commonly assumed to outperform other LULCC analysis methods, such as post classification comparison (Coppin et al. 2004). So far, our methodology exploits the temporal information only partially using the spectral variability measures. More explicit utilization of the temporal context (e.g. seasonally weighted variability measures) from all available unclouded observations per pixel will further enhance information extraction. Future versions of our PBC algorithm will therefore address the potential of different phenology measures and draw on exploiting the feature space available from multiple composites.

Our approach will profit from data continuity through forthcoming satellite missions such as the Landsat Data Continuity Mission and the Sentinel-2 constellation (Drusch et al. 2012; Irons et al. 2012). Increased image acquisition capabilities and temporal repeat frequencies will provide unique opportunities for cross-sensor compositing and improved process understanding from such integrated data analyses.

**Acknowledgments**

This research was funded by the Belgian Science Policy, Research Program for Earth Observation Stereo II, contract SR/00/133, as part of the FOMO project (Remote sensing of the forest transition and its ecosystem impacts in mountain environments) and the European Union (VOLANTE, FP7-ENV-2010-265104). We would like to thank M. Baumann, B. Jakimow, A. Rabe, D. Pflugmacher and V. C. Radeloff for insightful discussions. We also thank G. Aronson for support with the data pre-processing.

# Chapter IV:
# Forest disturbances, forest recovery, and changes in forest types across the Carpathian ecoregion from 1985 to 2010 based on Landsat image composites

*Remote Sensing of Environment ForestSAT Special Issue (Accepted)*

Patrick Griffiths, Tobias Kuemmerle, Matthias Baumann,
Volker C. Radeloff, Ioan V. Abrudan, Juraj Lieskovsky,
Catalina Munteanu, Katarzyna Ostapowicz and Patrick Hostert


*Received 19 December 2012; revised 23 April 2013;
accepted 07 May 2013.*

**Abstract**

Detailed knowledge of forest cover dynamics is crucial for many applications from resource management to ecosystem service assessments. Landsat data provides the necessary spatial, temporal and spectral detail to map and analyze forest cover and forest change processes. With the opening of the Landsat archive, new opportunities arise to monitor forest dynamics on regional to continental scales. In this study we analyzed changes in forest types, forest disturbances, and forest recovery for the Carpathian ecoregion in Eastern Europe. We generated a series of image composites at five year intervals between 1985 and 2010 and utilized a hybrid analysis strategy consisting of radiometric change classification, post-classification comparison and continuous index- and segment-based post-disturbance recovery assessment. For validation of the disturbance map we used a point-based accuracy assessment, and assessed the accuracy of our forest type maps using forest inventory data and statistically sampled ground truth data for 2010. Our Carpathian-wide disturbance map achieved an overall accuracy of 86% and the forest type maps up to 73% accuracy. While our results suggested a small net forest increase in the Carpathians, almost 20% of the forests experienced stand-replacing disturbances over the past 25 years. Forest recovery seemed to only partly counterbalance the widespread natural disturbances and clear-cutting activities. Disturbances were most widespread during the late 1980s and early 1990s, but some areas also exhibited extensive forest disturbances after 2000, especially in the Polish, Czech and Romanian Carpathians. Considerable shifts in forest composition occurred in the Carpathians, with disturbances increasingly affecting coniferous forests, and a relative decrease in coniferous and mixed forests. Both aspects are likely connected to an increased vulnerability of spruce plantations to pests and pathogens in the Carpathians. Overall, our results exemplify the highly dynamic nature of forest cover during times of socio-economic and institutional change, and highlight the value of the Landsat archive for monitoring these dynamics.

## 1 Introduction

Globally, forests provide important resources and ecosystem services that are essential for human well-being, including timber and non-timber forest product provision, watershed protection, habitat for biodiversity, and recreational amenities (GLP 2005; MEA 2005). Similarly, the role of forests for climate regulation, carbon sequestration, and surface radiation modulation is of global importance (IPCC 2000). However, forest resources and related ecosystem services depend on forest type and composition as well as on forest condition and management (e.g. rotation interval, mechanization, fertilizer use, plantation schemes), making it paramount to monitor forests repeatedly and consistently across larger areas and with high spatial detail.

Remote sensing has long been instrumental for mapping and monitoring forest cover changes and it was satellite imagery that highlighted widespread deforestation in the World's tropical regions (Skole and Tucker 1993; Pfaff 1999). In contrast though, forest area is increasing in many developed nations due to combined effects of advances in agricultural productivity and increasing awareness regarding the environmental importance of forests (Lambin and Meyfroidt 2010; Meyfroidt and Lambin 2011). However, information on forests and forest cover changes are not always publicly accessible and we still lack comprehensive knowledge of spatio-temporally explicit forest cover dynamics, especially across large areas and with sufficient spatial detail to resolve the full range of forest change processes.

Knowing forest area alone does not suffice. In many regions, natural primary forest is or has been converted to plantations and secondary forests. While the total forest area may remain stable or even increase, such forest types often do not provide the ecological services provided by natural forests (FAO 2005). Last but not least, the disturbance regime is crucial for ecological functioning, with related spatial disturbance patterns and frequencies being equally important to understand if natural disturbance regimes persist or have been replaced by forest harvesting.

Remote sensing has established itself as the key technology for forest mapping and monitoring at different spatial and temporal scales. Sensor systems such as the Moderate Resolution Imaging Spectrometer (MODIS) enable global forest monitoring and can be used to map broad-scale changes in temperate forests (Potapov et al. 2009), but are limited in their ability to provide detailed information on forest composition changes or fine-scale

forest change processes. Data from the Landsat sensors, on the other hand, provide spatial and spectral detail that allows capturing forest attributes at adequate scales, while featuring archived data back to the early 1970s. When working over larger geographical extents (i.e., ecoregions, biomes or continents) at 30m spatial resolution, however, Landsat data analysis poses numerous challenges. The sensor-specific field-of-view and the resulting scene coverage, coupled with frequent cloud cover and phenological effects due to the timing of image acquisitions, require specific conceptual frameworks to allow for adequate mapping and monitoring over larger areas. The opening of the USGS Landsat archive in 2008 sparked many new algorithms in this respect. Continental or even global Landsat data analyses are now feasible as advanced and automated preprocessing methods as well as improved processing and data storage capabilities allow for mass processing of imagery (Townshend et al. 2012; Wulder et al. 2012).

One approach to better exploit the wealth of Landsat images with partial cloud cover are pixel-based compositing methods, which combine several images into one cloud-free composite (Roy et al. 2010; Potapov et al. 2011). Compositing algorithms were initially developed for wide-swath sensor data, where observations are very frequent, but no image is ever completely cloud-free, and reducing cloud contamination and other atmospheric effects is therefore essential (Holben 1986; Cihlar et al. 1994). For Landsat data, compositing offers comparable advantages, though. By selecting the best observation on a per-pixel basis, cloudy imagery (typically discarded within scene-based approaches) can be exploited for high quality observations and the 16-day repeat cycle can be overcome through utilization of the across track overlap between adjacent image acquisition paths, which is considerable at higher latitudes. A single, “global” classification/regression model can be trained and applied if composites have sufficient seasonal and radiometric consistency, making large area mapping and monitoring approaches with Landsat more practicable.

Initial attempts to composite Landsat data were made during the generation of the Global Land Survey 2005 dataset (Gutman et al. 2008). Compositing was then used to fill data gaps in ETM+ imagery due to the failure of the scan line corrector since May 2003 (Arvidson et al. 2006). Compositing has also been implemented to allow broad-scale deforestation mapping. Hansen et al. (2008), for example, produced two regional Landsat composites for change detection in the Congo basin and incorporated the MODIS Vegetation Continuous Field product (Hansen et al. 2003) for training of the classifiers. Potapov et al. (2011) studied boreal forest changes between 2000 and 2005 in European

Russia using composited Landsat data and achieved high agreement with independently derived samples of forest change. Both studies demonstrated the ability of Landsat imagery for wall-to-wall mapping and regional monitoring of forest cover changes. Thus, Landsat image compositing has so far greatly advanced regional forest mapping and monitoring with a focus on reporting changes in forest extents. It is therefore desirable to advance remote sensing based methods towards analyzing spatio-temporal patterns of forest types, disturbance and recovery regimes across large areas. Also, more applications in diverse forested regions of the world are necessary to advance compositing and related algorithms, and to better assess their potential and limitations.

In this study, we utilize a series of large-area composites to map forest disturbances, forest recovery, and changes in forest types in a temperate forest region, the Carpathian ecoregion in Eastern Europe. The forests in the Carpathian Mountains represent Europe's largest temperate forest ecosystem and are of exceptional ecological value, providing resources and ecological services to a region much larger than the Carpathians themselves. Carpathian forests have been exploited and managed for centuries, leading to the widespread conversion of natural forests (i.e., beech–dominated, deciduous and mixed forests) to monoculture plantations of Norway spruce (UNEP 2007; Keeton and Crow 2009). These spruce plantations are highly susceptible to pest outbreaks and storm damages, and during the last decades forest managers are increasingly converting them to more natural forest types (Keeton and Crow 2009). The remaining semi-natural and old-growth forests, on the other hand, are threatened by the major socio-economic restructuring processes that occurred with the transition from state-led to market-oriented economy after the collapse of Eastern European socialism (Kuemmerle et al. 2009a; Kuemmerle et al. 2009b; Hostert et al. 2011b; Knorn et al. 2012a). This highlights the importance to analyze forest dynamics across the entire Carpathians.

Accordingly, our goal here was to map forest disturbances and change in forest types across the Carpathian region from 1985 to 2010 using Landsat satellite images, applying automated image pre-processing and compositing as well as a hybrid change detection approach. Our specific research questions were:

- How were broad forest types distributed in the Carpathians at the end of the socialist period and how did this distribution change over time?
- What were the rates and spatial and temporal patterns of forest disturbances since 1985?

- What were the spatio-temporal patterns of post-disturbance forest recovery?

*The results of this study are publicly available (see http://www.hu-geomatics.de).*

## 2 Methods

### 2.1 Study area

We studied the Carpathian mountain range in Central Eastern Europe. The study region boundaries were based on the Carpathian Ecoregion Initiative (CERI) boundaries (CERI 2001) and were extended to include adjacent administrative units in their entirety (Nomenclature of Territorial Units for Statistics (NUTS) level three, and oblasts in the case of Ukraine). The study region covered 390,000 km² including parts of the Czech Republic, Austria, Poland, Hungary, Ukraine, Romania and all of Slovakia (Fig.1). The total population of the Carpathian ecoregion is around 17 million (CERI 2001). The Carpathians extend in a curve shaped arc over a length of about 1,500 km at a maximal width of 350 km. Elevations reach 2,600 m in the Tatra Mountains in Poland and Slovakia, and 2,500 m in the Făgăraș Mountains in Romania. The region is characterized by a temperate continental climate. Precipitation ranges from 400 mm in the southeastern parts to over 2000 mm at the highest elevations (Ptacek et al. 2009). Annual average temperatures vary with elevation and are about 2°C around mid-elevations (UNEP 2007).

Forests cover between 50% and 60% of the Carpathian Ecoregion and approximately 30% of the region is used for agriculture (Ruffini et al. 2008). The most common tree species are European beech (*Fagus sylvatica*), Norway spruce (*Picea abies*) and silver fir (*Abies alba*). Natural forest types follow a vertical stratification. Broadleaved forests (mostly beech mixed with pedunculate oak (*Quercus robur*), sycamore maple (*Acer pseudoplantanus*) and ash (*Fraxinus excelsior*)) and mixed forests (beech mixed with silver fir and Norway spruce) dominate the lowlands and the lower mountain forest zone, while spruce-fir forests dominate at higher elevations. The treeline is located at around 1,500 m in the Tatra Mountains (Svajda et al. 2011). Despite centuries of human use, the Carpathians harbor the largest remains of semi-natural and virgin forests in Europe (Veen et al. 2010), provide habitat for Europe's largest populations of wolves, lynx, brown bear (Salvatori et al. 2002) as well as European Bison, and feature about one third of all plant species in Europe, including many endemics (UNEP 2007).

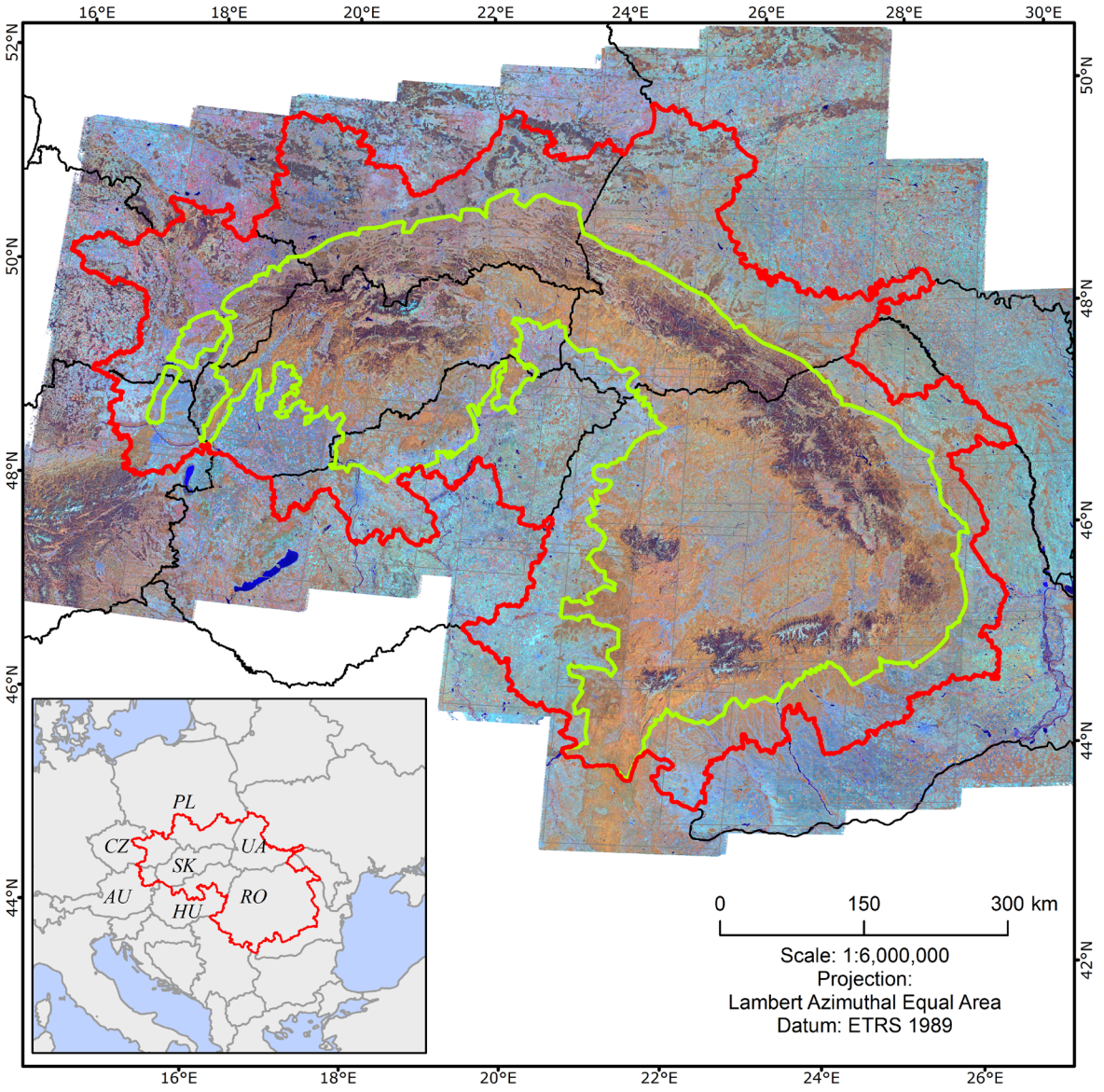


Figure IV-1: The study region boundaries (red), the Carpathian Ecoregion (green), the national borders (black) overlaid on the best observation image composite for the target year 2005 (RGB = 4, 5, 3). A total of 1,407 scenes were provided to the compositing algorithm, which was parameterized to produce a cloud free, leaf-on seasonal state composite, considering imagery from 2003 to 2007. A series of six similar composites was made at five year intervals between 1985 and 2010. Coverage of Landsat footprints is superimposed in grey rectangles. The small inset shows the regional setting (AU = Austria, CZ = Czech Republic, HU = Hungary, PL = Poland, SK = Slovakia, RO = Romania, UA = Ukraine).

The Carpathian region underwent several major political and socio-economic changes in the 19th and 20th centuries. Since the 19th century, clear-cuts in former broadleaved or mixed forests were commonly replanted with non-native spruce species altering regional forest composition (Keeton and Crow 2009). Widespread forest decline occurred during the mid-1980s partly because of severe industrial pollution and acid rain, commonly followed by fungi and other pest outbreaks (Oszlanyi 1997; Csóka 2005) and coniferous stands generally declined more severely than deciduous stands (Badea et al. 2004). Natural disturbance regimes are dominated by wind falls and to lesser degrees by snow damages

and insect infestations, and forest fires are rare (Schelhaas et al. 2003). High intensity wind throws recently increased, especially in spruce plantations (Popa 2008).

After 1989, collectively owned state forests were returned to the pre-1948 owners through restitution, distribution or auctioning in most of the Carpathians countries. Ukraine and Poland made exceptions, where most forests remained state property (Nijnik 2004; Kozak 2010). In Slovakia and Romania between 50% and 60% of the forests are now under some form of non-state ownership (Abrudan et al. 2009; Weiss et al. 2012). Carpathian forests were heavily exploited during the socialist period (e.g. payments of war debts, developing industrial capabilities) and constituted a major source of state revenues (Nijnik and van Kooten 2000; Cioroianu 2007). Harvesting rates after the regime collapse, however, are not well known. Official statistics indicate declining harvesting activities (UNEP 2007), but in the Ukrainian Carpathians satellite data revealed increased forest disturbances before and after the system collapse (Kuemmerle et al. 2009a; Kuemmerle et al. 2009b). In Romania, higher forest harvesting due to uncertainty in tenure rights after restitution emerged only after 2000 (Griffiths et al. 2012; Knorn et al. 2012a). Today, all countries with the exception of Ukraine are in the European Union and the national forest legislations follow EU guidelines (Weiss et al. 2012). Altogether, this highlights the need to monitor forest changes in the region repeatedly and over longer time periods.

### 2.2 Satellite data, pre-processing and compositing

We utilize a compositing algorithm that combines tools to mask clouds and convert images to surface reflectance with a methodology to produce seasonally and radiometrically consistent image composites from the Landsat archive (Griffiths et al. 2013). Here, we compiled regional composites of Landsat data for six five-year time steps from 1985 to 2010, and employed a hybrid analysis strategy consisting of radiometric change classification and post-classification map comparison to derive changes in forest area, forest disturbances, and forest types. In addition, we developed a method to quantify post-disturbance forest recovery from the composited data using the disturbance index (Healey et al. 2005) and image segmentation.

For the 32 footprints covering the study region (Fig.1), we obtained all precision terrain corrected Landsat imagery (L1T) from the USGS archive that were acquired between mid-February and mid-November and that had metadata based cloud cover estimates of less than or equal to 70% (Table 1). To ensure radiometric consistency, we employed the Landsat Ecosystem Adaptive Processing System (LEDAPS, Masek et al. 2006), which

converts raw Landsat data to surface reflectance. Subsequently, we generated clouds/shadows masks for each image using the Fmask algorithm (Zhu and Woodcock 2012). All masks were produced using conservative thresholds on cloud/shadow probabilities and the dilation parameter to capture as much clouds/shadows as possible. All imagery and masks were reprojected from the original UTM coordinate system to the Lambert Azimuthal Equal Area projection as our study region extended over three UTM zones. The total number of images available for compositing ranged between 323 for the 1990 and 1,407 for the 2005 composite (Table 1).

Table IV-1: Total number of images used to create the series of six image composites over the 32 footprints. Moreover, the distribution of acquisition dates is provided.

| | | Number of Images with offset to target year | | | | | |
|---|---|---|---|---|---|---|---|
| Composite | # images | -2 | -1 | 0 | +1 | +2 | median DOY |
| 1985 | 547 | 0 | 65 | 24 | 251 | 207 | 210 |
| 1990 | 323 | 94 | 43 | 29 | 92 | 65 | 204 |
| 1995 | 397 | 112 | 257 | 16 | 4 | 8 | 205 |
| 2000 | 647 | 0 | 75 | 192 | 169 | 211 | 185 |
| 2005 | 1407 | 254 | 183 | 216 | 372 | 382 | 204 |
| 2010 | 1370 | 249 | 420 | 392 | 305 | 4 | 198 |

The objective during image compositing was to produce six regional image datasets at five-year intervals from 1985 to 2010 (hereafter: target years). For each composite we considered imagery from +/- two years around the target year (in the following referred to as “ca.1990 composite” for the composite with the target year 1990, etc.). The compositing algorithm was parameterized to produce cloud-free, best-observation composites of leaf-on phenology, while prioritizing acquisitions closest to the respective target year. The best observation was selected from all cloud-free acquisitions for a given pixel via a parametric decision function. The parameters were (1) the acquisition year, (2) the acquisition day-of-year (which control annual and seasonal consistency, respectively), and (3) a pixel’s distance to the next cloud/shadow (greater distances are prioritized). For each unique acquisition, scores across the parameters were summed up and for a given pixel all spectral band values of the acquisition with the highest total score were written into the final best observation composite.

The parameterization of the day-of-year (DOY) score was based on the analysis of data from areas with high data availability over a 10-year period. We assessed how well selected unchanged areas with a natural, climate driven phenology (i.e. natural grasslands and forests) spectrally corresponded to selected reference images, which were cloud-free and acquired as close as possible to the central day of a given year (July 2$^{nd}$ or DOY 183).

We used DOY 183 to approximate leaf-on peak photosynthetic activity and assessed correlations of all available imagery to the selected reference images using coefficients of determination of band five values. This allows to parameterize a Gaussian DOY score function (the resulting target DOY was 193 or July 12$^{th}$ with a standard deviation of 33 days). We then calculated the DOY score offset values for +/-30 and +/-45 days and used these offsets to construct a piecewise linear year score function. This results, for example, in favoring acquisitions acquired within 30 days of the target DOY but with a one year offset to the target year, over images acquired within 45 days of the target DOY within the actual target year. Overall, developing the two temporal score functions interdependently, ensured that seasonal consistency was generally favored over annual consistency (Griffiths et al. 2013).

In addition to the best observation composites, we calculated temporal-spectral variability measures and datasets providing meta-information on a per-pixel basis (hereafter: flag images) for each composite. The former utilize all available cloud free acquisitions for a given pixel to calculate the band-wise spectral mean bands and variability (standard deviation & range) bands. The flag images provide information on, for example, the year and day of year of the image acquisition, and the sun zenith angle during the acquisition. Both types of additional outputs provide valuable features for subsequent analyses. Further details on the compositing methodology are provided in Griffiths et al. (2013).

### 2.3 Forest type, disturbance and recovery mapping

In order to gain better understanding of the distribution of forest types across the Carpathians, as well as of how disturbances were distributed across forest types, we produced two forest type maps, one for 1985 and one for 2010, and classified deciduous, coniferous and mixed forests. The latter was defined as having neither a dominance (i.e. more than 70%) of deciduous nor coniferous trees (Herold et al. 2009). For each classification, we stacked the best-observation composite (6 bands), the spectral variability layers (19 bands) and selected flag images (year, DOY, decision score, and acquisition sun zenith angle), yielding 29 bands.

Training data were selected independently for both classifications based on the interpretation of the original Landsat input data. We used spring and autumn acquisitions together with the summer leaf-on imagery to improve the delineation of our training data for conifer, deciduous and mixed forests. Areas where the forest type was clearly discernible were digitized on screen for both time steps simultaneously to ensure

comparability of both training datasets. Additional ancillary data for image interpretation and training data generation included high-resolution imagery in GoogleEarth, CORINE land-cover data and data from several field trips conducted in the Carpathians between 2006 and 2011. The digitized training areas were spatially relatively evenly distributed over the study region and the total number of polygons was between 60 and 80 for the three forest classes combined, for both 1985 and 2010. We drew a stratified random sample of pixels from all training polygons to select the final training dataset, yielding approximately 4,500 pixels for the non-forest class and between 2,000 and 3,000 samples for each of the forest types.

We used a Random Forests classifier for all classifications (Breiman 2001). Random Forests belong to the realm of machine learning classifiers and represent an ensemble of simple decision trees, each trained on a randomly selected feature subset. The final decision is made using a majority vote across all trees. Key advantages of Random Forests are that they can deal with all types of differently scaled data and that they can analyze large datasets very efficiently. Random Forests classifiers achieve comparable or better results than other classifiers, including other machine learning algorithms, with relatively small training data sets (Waske et al. 2010). We trained the Random Forests models based on 300 individual decision trees using the square root of the number of input bands as the number of random features considered at each decision tree split (Held et al. 2012).

For the forest disturbance mapping, we assembled an image stack consisting of the six composites for the years 1985 through 2010 plus the spectral variability bands and selected flag images, yielding a total of 174 bands. We then digitized training data for the disturbance classes on screen based on composite datasets in conjunction with few original (i.e. not composited) Landsat scenes. We here defined forest disturbances as full canopy removal due to natural and/or anthropogenic processes. We also derived training data for stable forest areas, where the forest class (i.e., deciduous, mixed or coniferous forest) was clearly discernible and did not appear to change over time. The training dataset also featured a generic non-forest class, which included, for example, urban and agricultural land. We then performed a stratified-random sampling within the digitized areas, yielding approximately 2000 pixels for each of the five disturbance classes, ~3000 pixels for each of the forest classes and ~4500 pixels for the non-forest class. The stable forest type training areas identified here were also used for the forest type classifications. The radiometric change classification for the disturbance map was carried out with the Random Forests classifier in a similar fashion as for the forest type mapping.

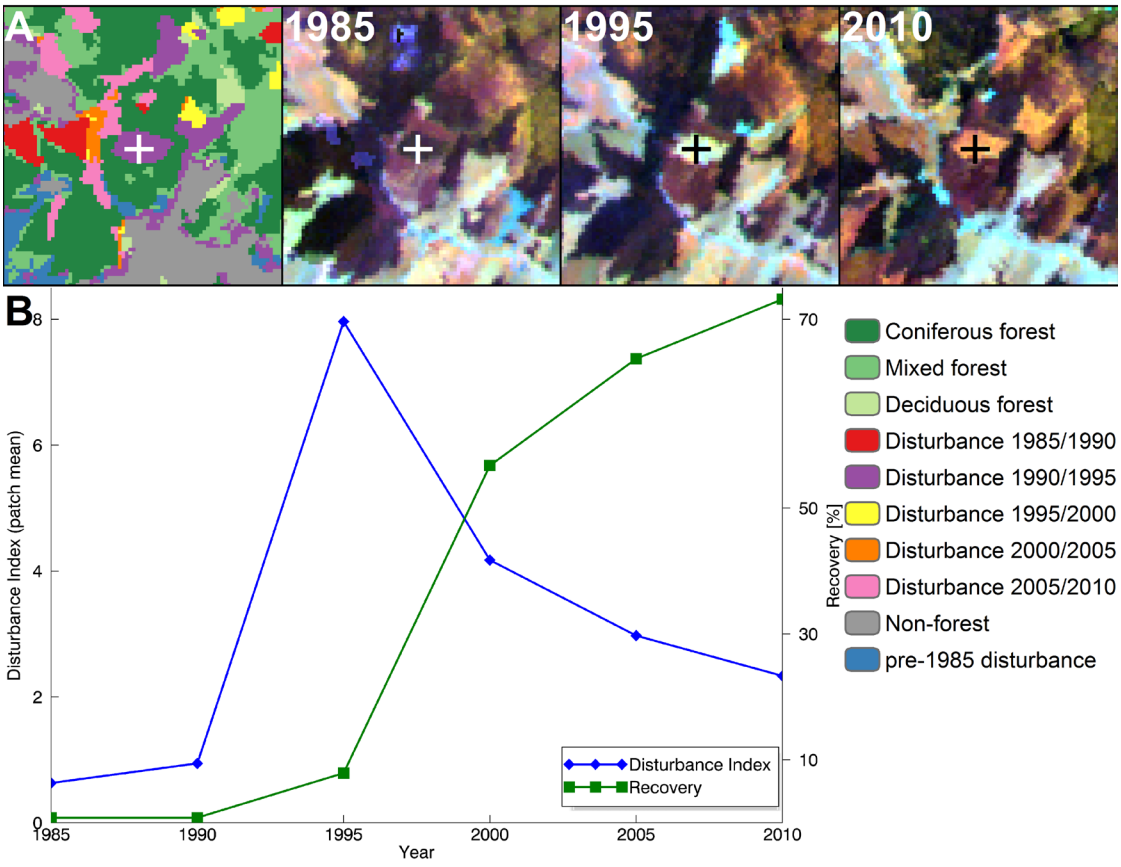


Figure IV-2: An illustration of the recovery assessment methodology: the example shows (A) the disturbance map (the legend is provided on the lower right), and corresponding image chips for the years 1985, 1995 and 2010. For the central disturbance patch (indicated by the cross hair) the mean DI trajectory is shown (B, blue plot) as well as the resulting patch recovery metric (B, green plot). The patch mean pre-disturbance DI value is written into the first two recovery bands (1985, 1990), the disturbance magnitude is written into band three (1995) and the post-disturbance recovery status is written into bands four to six.

We developed a continuous proxy for vegetation recovery for disturbance patches utilizing the disturbance index (DI, Healey et al. 2005)to evaluate post-disturbance recovery dynamics. As our recovery proxy approach quantifies spectral recovery only, it is not a direct measure of recovery in an ecological sense. Field visits and the substantial regional knowledge of the author team suggest that our recovery indicator is plausible. Still, as a validation of the recovery assessment would require extensive reference data or systematic field surveys on biomass recovery (both of which are not available), we caution that these results are experimental. We base our approach on the *DI*, which is a linear combination of the components of the Tasseled Cap transformation (Crist and Cicone 1984), which are normalized over the reflectance properties of the forest population in a Landsat image. We used those pixels identified as forest in both forest type maps as a "global" study area wide norming population to re-scale the Tasseled Cap components derived from the composites. While scene-specific normalizing might be desirable, our approach prevents the use of unrepresentative normalization statistics caused by, for example, scene statistics from very

cloudy images, which ultimately may cause unnecessary "patchiness" in the output layers. For each of the six target years, the *DI* was subsequently derived according to:

$$DI=Bn-(Gn+Wn) \quad (1)$$

where *Bn*, *Gn* and *Wn* were the normalized brightness, greenness and wetness components, respectively. We delineated disturbance patches based on an eight-pixel neighborhood and the disturbance map, and assessed the mean *DI* values for each disturbance patch.

We derived six features that we used to assess post-disturbance recovery dynamics: patch-level mean pre-disturbance *DI* value, the *DI* disturbance magnitude, and the post-disturbance recovery status (Fig.2). The mean pre-disturbance *DI* value was obtained by simply averaging the patch *DI* values of the years preceding a disturbance event. The spectral disturbance magnitude was derived according to:

$$Mag_{Dist}=\left|mean(DI_{preDistYears})-DI_{DistYear}\right| \quad (2)$$

where $DI_{preDistYears}$ is the patch-based *DI* value in the years preceding the disturbance event, and $DI_{DistYear}$ is the patch-mean *DI* value in the year of disturbance detection. The post-disturbance recovery status was derived as the percentage of recovery in a year following a disturbance relative to the disturbance magnitude (Fig.2):

$$\mathrm{Recovery}_{postDistYear}=\left(\frac{DI_{postDistYear}-mean(DI_{preDistYears})}{Mag_{Dist}}\right) \quad (3)$$

For disturbance patches where the pre-disturbance *DI* value was higher than the post disturbance *DI* value, the spectral magnitude was set to zero. This allowed for eliminating such patches during post-processing, as these cases likely represent false positive detections. We applied a minimum mapping unit of 3 pixels (i.e., 0.27 ha) using an 8-pixel neighborhood to the resulting forest type and the disturbance maps, recoding patches smaller than this threshold to the surrounding class.

The initial disturbance classification yielded high levels of false positives for the 1985/1990 and the 1995/2000 disturbance classes, due to falsely detected disturbance events on non-forest land which might relate to erroneous training pixels and likely the generally poorer data coverage for the first three target year composites (Table 1). To correct for this, a patch mapped as disturbance 1985/1990 or 1995/2000 was recoded to non-forest if the disturbance magnitude was zero. To further reduce false positives, patches classified as disturbed between 1985/1990 were recoded to non-forest if less than 50% of its pixels were mapped as non-forest in the 1985 forest type map. Second, for the

1985/1990 class, if the patch-mean 1985 *DI* value was high and the disturbance magnitude was low, this patch was recoded to the non-forest class. After carefully investigating such cases we used 3 and 0.7 as the respective thresholds. Finally, if the pre-disturbance *DI* value was higher than all subsequent patch-based *DI* values, the patch was recoded to a new class: "recovery from pre 1985 disturbance", as these cases mostly related to forest stands recovering from disturbances that occurred before 1985.

**2.4 Forest inventory data, validation strategy, and result summaries**

For the validation of the forest disturbance map, we gathered a stratified random sample of 700 points for all stable forests, 600 for the non-forest class, and a total of 650 points for the five disturbance classes. All samples were visually interpreted by independent analysts using original Landsat images and the composite imagery, as well as high resolution imagery in GoogleEarth (Cohen et al. 2010) and labeled each sample according to the interpreted class membership. As some samples could not be labeled due to data gaps, the final number of interpreted samples was 1,873. We accounted for the stratified sampling design by correcting the resulting confusion matrix by the area proportions of each class (Foody 2002). We corrected our accuracy estimates for potential sampling bias, calculated true area estimates for all disturbance classes and assessed the 95% confidence intervals around these estimates (Card 1982; Olofsson et al. 2013). Finally, we used those samples that were either interpreted as permanent forest or non-forest to validate the forest area delineation in the forest type maps for 1985 and 2010. This yielded error adjusted area estimates and the 95% confidence interval around them.

The validation of the forest type maps was more demanding, because determining the true composition of a forest on the ground reliably based on the Landsat data alone is not feasible. First, we compared our map with forest inventory data for Slovakia, Romania and Poland. All forest inventory data was generated after the year 2000 and provided varying levels of detail and spatial extent. For example, the Slovakian forest inventory data covered the entire country at the individual stand level and provided estimates of the proportion of five dominant species at 1% intervals. For Poland and Romania, the species composition was provided in 10% intervals. We categorized individual forest management stands into deciduous, mixed or coniferous forest based on these species compositions by aggregating our remote sensing based forest type classification to the same stand polygon boundaries and applying the 70% species composition threshold. We selected all units of 1 ha (11 pixels) and above to validate the 2010 forest type map. We thereby reduced

uncertainties from geometric inconsistencies between field and satellite data. Units where our disturbance map indicated disturbances between 2005/2010 were excluded. Using a total of over 300,000 units, we created confusion matrices and assessed commission and omission errors for Slovakia, Poland and Romania. We used the Land use/Cover Area frame statistical Survey (LUCAS, Palmieri et al. 2011) from 2009 as an additional data source for validating the 2010 forest type map. The LUCAS data are based on a systematic sampling design and field visits and provide information on land cover and land use across Europe, but do not include Romania and Ukraine. The forest classes in the LUCAS legend use a 75% composition threshold which is close to our 70% value. After discarding forest samples with unsuited land use categories (e.g. fisheries), we extracted a total sample of 2,965 points for the three forest classes.

In order to validate the 1985 forest type map, we created sub selections of the inventory data, including all units that had an estimated stand age of at least 30 years and that were at least 1 ha in size. The former step ensured that the forest composition in these units had not changed between 1985 and 2010 while the latter reduced uncertainties due to geometric alignment of inventory and composite data. For the Romanian inventory data we only selected units with at least 60% estimated stand closure in 2010 in order to further reduce units that had changed since 1985. For Poland, only about 40 out of 11,000 forest management units remained for the validation of the deciduous forest class and we therefore did not use the Polish inventory data to validate the 1985 forest type map. The total sample size for the validation of the 1985 forest type map was 216,000 units.

To summarize our classifications, we calculated the total forest area and the distribution of the three forest types for 1985 and 2010 for the 7 countries in our study region. We assumed that changes in forest types in the Carpathians can only happen if a pixel experienced disturbance. We calculated forest disturbances for the different points in time and the individual countries. We also calculated pre-disturbance forest cover for each disturbance patch for the different countries and the post-disturbance recovery dynamics for the five disturbance classes. For the former, we segmented all disturbance patches and categorized each patch as coniferous, mixed or deciduous if the percentage of pixels from the respective class was >70%. In order to be able to categorize inventory units where none of the forest types had a sufficient forest type share, the percentage of mixed forest pixels was evenly distributed between deciduous and coniferous forest. If then neither deciduous nor coniferous achieved more than 70%, the patch was categorized as mixed forest. Disturbance patches with less than 50% of forest pixels were categorized as non-forest.

We also derived the net change rate and summarized annual disturbance rates (Kuemmerle et al. 2009a) on the basis of administrative units (NUTS3 for Romania, Hungary and Austria, district-level for Czech Republic, Poland, Slovakia and Ukraine) according to:

$$NCR = \left( \frac{FC_{2010}}{(FC_{1985}) - 1} \right) * 100 \quad (4)$$

$$DR_j = (\frac{D_j}{FC_j}) * \frac{100}{a} \quad (5)$$

where *NCR* is the net change rate with $FC_{1985}$ denoting forest cover in the 1985 map, *DR* is the annual disturbance rate for the administrative unit at time period *j*, *D* are the disturbances at time period *j*, *FC* is the forest cover at time period *j* and *a* is the number of years between image acquisitions. Here we used the 1985 forest cover, but subtracted the disturbed forest area since 1985 and added formerly disturbed pixels if they had recovered, i.e. the post disturbance recovery rate was at least 70%. As the composites contained pixels from different years, we assessed the average time difference between two points in time (term *a* in equation (5)). Finally, we derived a relative disturbance recovery rate $RR_j$ for the years 1995 (i.e. the first year that recovery from disturbance could have occurred in our analysis) through 2010 as:

$$RR_j = \left( \frac{cum\,\mathrm{Re}\,c_{1995:j}}{cumD1985:j} \right) * 100 \quad (6)$$

Where *cumRec* is the cumulated recovery from disturbances through the years 1995 to *j* (using the 70% recovery threshold), *cumD* is the cumulated disturbances for the years 1985 to *j*.

Table IV-2: Annual and seasonal composition of pixels in the six generated composite datasets. Annual composition refers to the offset in years to the respective target year, seasonal composition refers to the percentage of pixels with a relative acquisition date within 30 and 45 days from the target DOY (193 or July 12th).

| | Annual composition [%] | | | | | | Seasonal composition [%] | |
|---|---|---|---|---|---|---|---|---|
| Year | -2 | -1 | 0 | +1 | +2 | NoData | ± 30 days | ± 45 days |
| 1985 | --- | 5.42 | 38.07 | 41.71 | 14.81 | 0.01 | 82.81 | 98.74 |
| 1990 | 6.04 | 21.86 | 29.44 | 25.02 | 17.08 | 0.56 | 95.88 | 98.36 |
| 1995 | 4.25 | 82.05 | 13.60 | 0.02 | 0.01 | 0.08 | 97.65 | 99.51 |
| 2000 | --- | 4.57 | 68.08 | 25.98 | 1.36 | 0.00 | 85.01 | 99.71 |
| 2005 | 0.08 | 2.48 | 61.64 | 34.03 | 1.78 | 0.00 | 98.76 | 99.96 |
| 2010 | 0.04 | 7.64 | 90.75 | 1.58 | 0.00 | 0.00 | 97.70 | 99.98 |

# 3 Results

## 3.1 Image compositing

Using the 4,691 preprocessed Landsat images, we generated six cloud-free, best-observation composites that provided observations for almost all pixels in the study region (the ca.1990 composite lacked observations for 0.6% of pixels). The overall annual consistency (i.e. offset to target year) was high: more than 98% of pixels had been acquired within one year of the respective target year for the ca.2000, 2005 and 2010 composites (Table 2). Similarly, high overall seasonal consistency (i.e. relative offset to the target DOY) was achieved, with four out of six composites containing 95% of observations from within 30 days of the target DOY.

## 3.2 Forest composition and changes within forest types

Our error adjusted area estimates suggest that the total forest area in the study region increased slightly from 39.4% in 1985 (153,000 km² ±6,764 km²) to 40.3% in 2010 (157,000 km² ±6,086 km²). The overall composition of forest types in the study region changed markedly: Coniferous forests made up 30% of the forest area in 1985 but only 23% in 2010. The share of mixed forests decreased by 2.3% between 1985 and 2010 while the percentage of deciduous forests increased by 9%.

Table IV-3: Summary of forest cover changes between 1985 and 2010 for the country areas in the study region. Provided is the total forest area for 1985 and 2010 as well as the proportion of the three forest types of the total forest area and the changes in forest area and forest type proportions (CF = coniferous forest, MF = mixed forest, DF = deciduous forest).

| | 1985 [km²] | | | 1985 [%] | | | 2010 [km²] | | | 2010 [%] | | | Changes 2010 - 1985 | | | | |
|---|---|---|---|---|---|---|---|---|---|---|---|---|---|---|---|---|---|
| | CF | MF | DF | Forest | CF | MF | DF | CF | MF | DF | Forest | CF | MF | DF | Forest [km²] | Forest [%] | CF [%] | MF [%] | DF [%] |
| Austria | 213 | 211 | 1205 | 22.4 | 13.1 | 13.1 | 74 | 192 | 196 | 1317 | 23.4 | 11.2 | 11.4 | 77.3 | 75 | 1.0 | -1.8 | -1.5 | 3.3 |
| Czech Rep. | 4157 | 2362 | 2967 | 36.1 | 43.8 | 24.9 | 31.3 | 3819 | 2148 | 3744 | 36.9 | 39 | 22.1 | 38.6 | 224 | 0.9 | -4.5 | -2.8 | 7.3 |
| Hungary | 410 | 602 | 5070 | 17.5 | 6.8 | 9.9 | 83.4 | 444 | 565 | 6943 | 22.9 | 5.6 | 7.1 | 87.3 | 1871 | 5.4 | -1.2 | -2.8 | 3.9 |
| Poland | 7307 | 5462 | 3918 | 36.7 | 43.8 | 32.7 | 23.5 | 7466 | 5441 | 5558 | 40.6 | 40.4 | 29.4 | 30.1 | 1778 | 3.9 | -3.4 | -3.3 | 6.7 |
| Romania | 16354 | 2047 | 3234 | 47 | 35.5 | 27.1 | 33.9 | 18143 | 2228 | 0634 | 397 | 42.2 | 20.1 | 31.8 | 64.1 | 11311 | 6.7 | -7.0 | -2.1 | 9.2 |
| Slovakia | 4925 | 5820 | 1812 | | 46 | 21.8 | 25.8 | 52.4 | 4082 | 5702 | 1337 | 0 | 47.2 | 17.6 | 24.6 | 57.7 | 597 | 1.2 | -4.2 | -1.2 | 5.4 |
| Ukraine | 7493 | 6481 | 7747 | 38.4 | 34.5 | 29.8 | 35.6 | 6491 | 6620 | 1172 | 6 | 43.9 | 26.1 | 26.6 | 47.2 | 3116 | 5.5 | -8.4 | -3.2 | 11.6 | |

On the per country level, forests covered between 47% in the Slovakian and 23% in the Hungarian parts of the study region in 2010. An increase in the countries forest area was found in all countries, but was most pronounced in Romania, Ukraine and Hungary (Table 3, Fig. 3). The composition of the countries forest area in the Carpathians differed considerably. For example, the 2010 forest area in Hungary featured 87% of deciduous forests while these only accounted for 30% of the forest area in Poland. Forests in the

Polish and the Czech parts of the study region were clearly dominated by coniferous forests (both 44% in 1985). The largest changes in forest composition occurred in Romania and Ukraine: coniferous forests decreased by 8.4% and 7%, while deciduous forests increased 12% and 9%, respectively, between 1985 and 2010. Several countries featured decreasing proportions of mixed forest, most notably Poland, Hungary and Czech Republic (Table 3, Fig. 3).

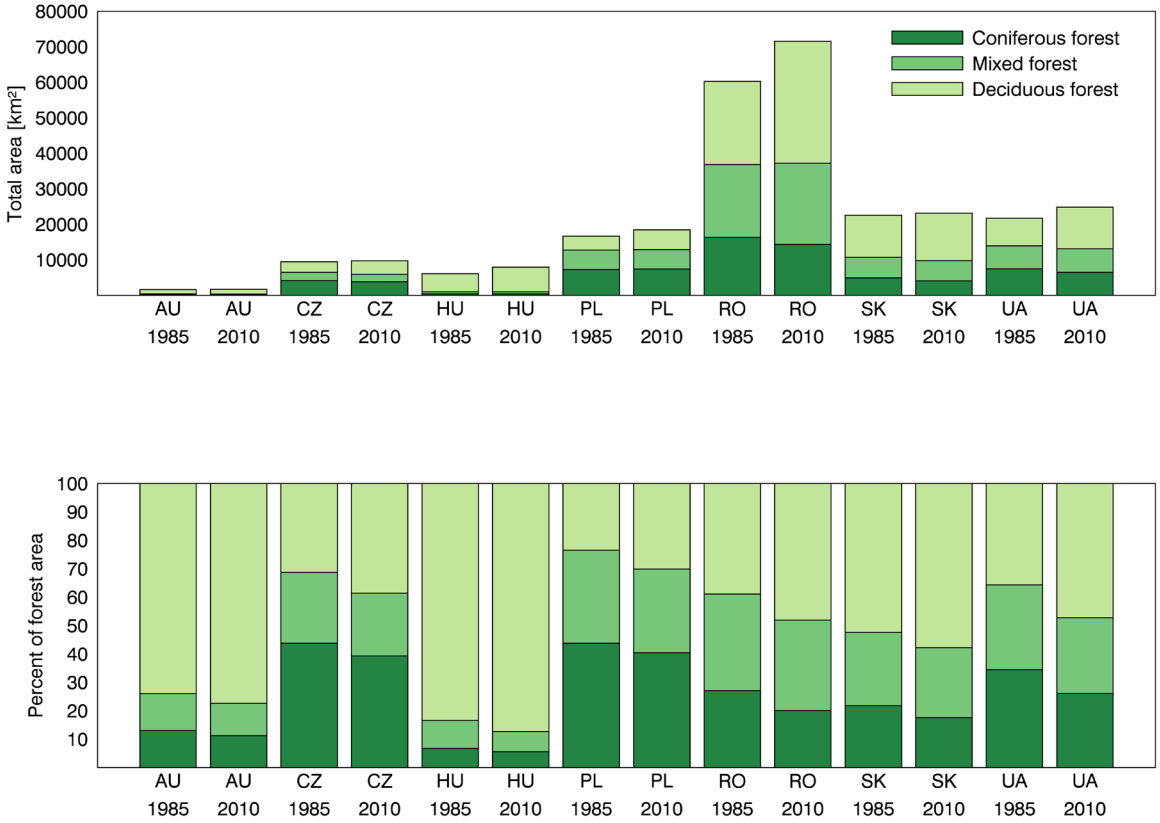


Figure IV-3: Total forest area and forest type by country for the years 1985 and 2010 in square kilometers (top), changes in the proportion of forest types between 1985 and 2010 for the seven countries, expressed as the percentage of the total country forest area in the study region (bottom).

### 3.3 Forest disturbances

Forest disturbances were infrequent and spatially dispersed in the Austrian part of the study region but were very abundant and occurred highly clustered in the Ukrainian and Romanian parts of the study region (Fig.4). We also observed strong differences within countries, for example disturbances were rather scarce in the eastern parts of the Polish Carpathians but were highly abundant and formed distinct hotspots in the western and southwestern Polish Carpathians.

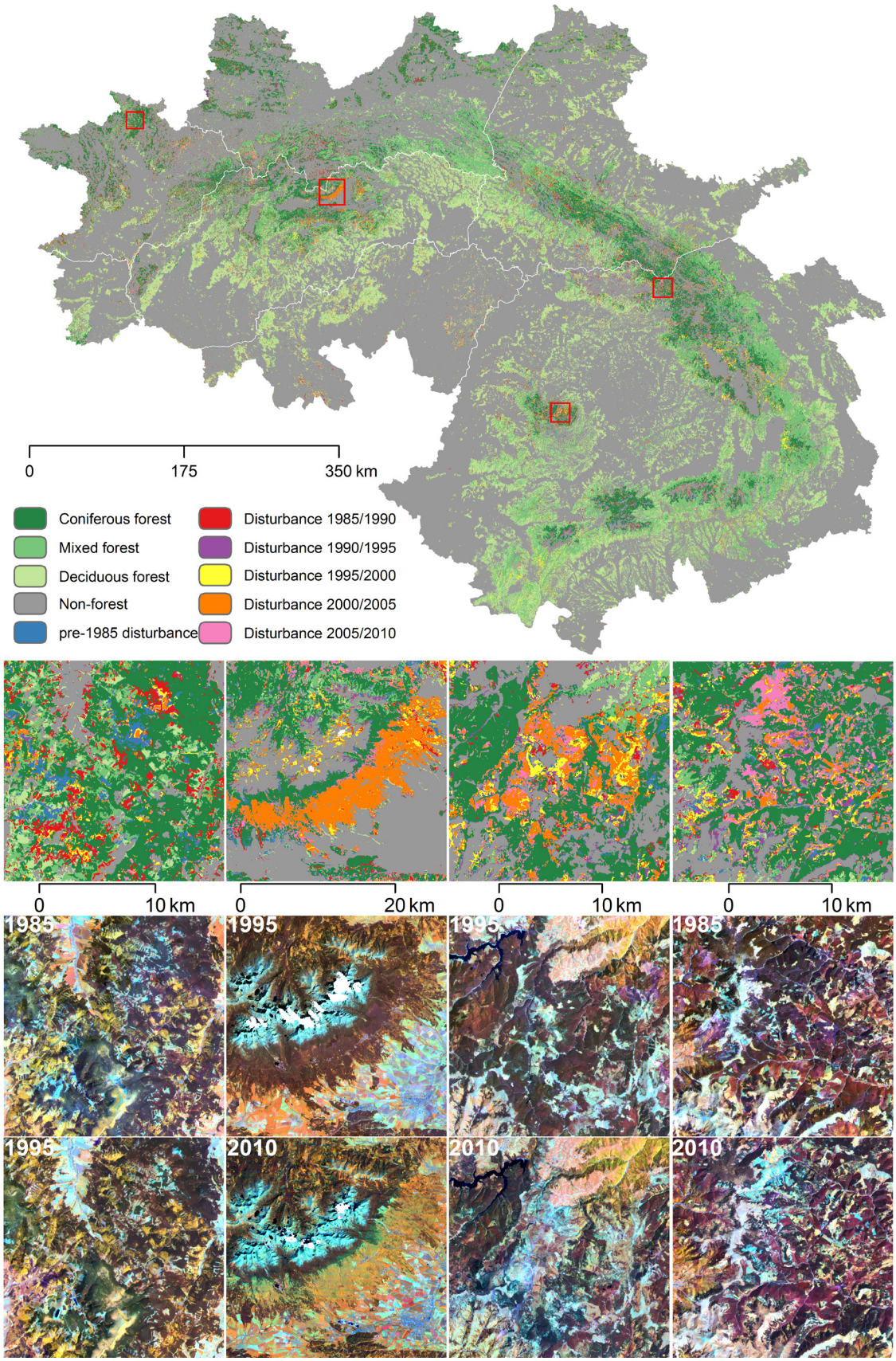


Figure IV-4: The disturbance map showing the stable forest areas as well as the five disturbance classes, the national boundaries are overlaid in white. The extent of four details in the disturbance map is indicated by the red frames. Below we provide for each detail the disturbance map subset along with the respective composite imagery subsets for two points in time.

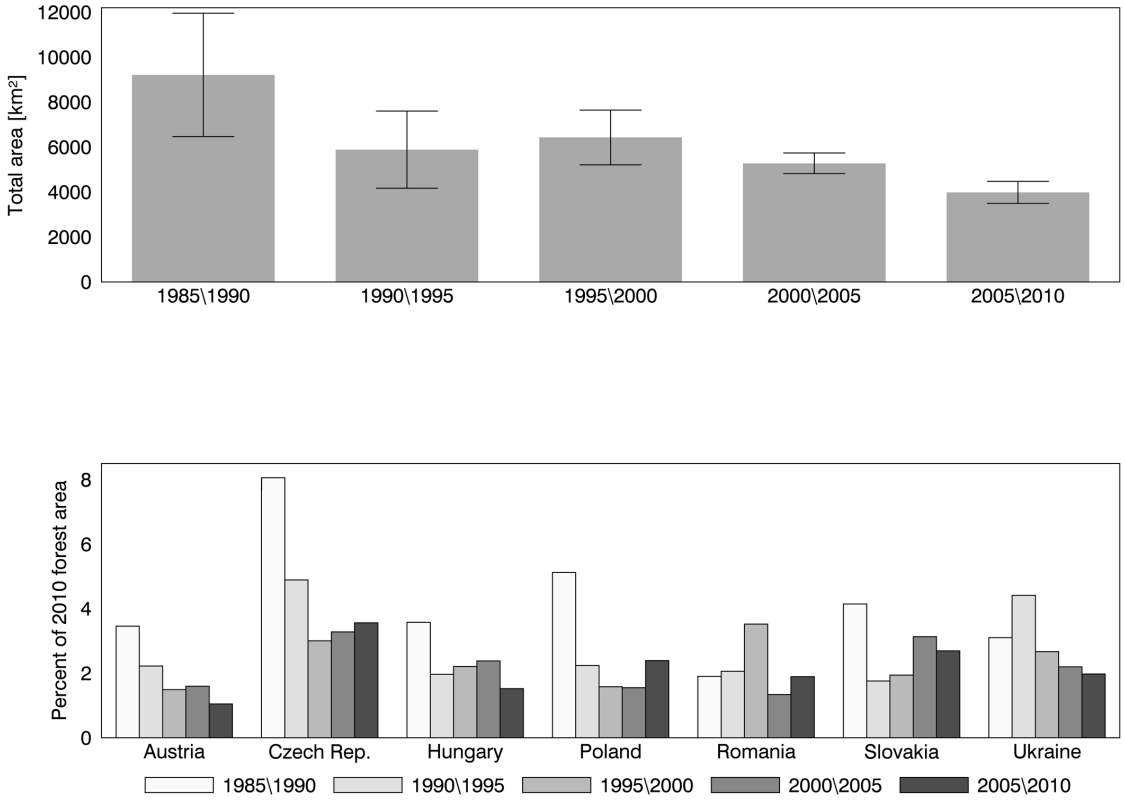


Figure IV-5: Error adjusted area estimates of disturbed forest area for the five disturbance classes in square kilometers, with error bars indicating the 95% confidence interval around these estimates (top). Disturbed forest area for the five disturbance classes and the seven countries in the study area, expressed as the percentage of the 2010 country's forest cover in the study region (bottom).

According to our error adjusted area estimates, the total area of forest disturbances detected between 1985 and 2010 amounted to 30,800 km² (±6,629 km²), which related to 19.4% of the 2010 forest area (Fig.5). Overall, most disturbances occurred between 1985/1990 (~30%) while the least disturbances took place between 2005/2010 (13%).

On the per-country basis, the greatest total forest area mapped as disturbed occurred in Romania between 1995/2000 with more than 2,500 km² (3,5% of the 2010 forest area in Romania, Fig.5). In most countries, disturbances were mainly detected between 1985/1990, with the exception of Romania and Ukraine. The Romanian Carpathians exhibited continuously increasing levels of disturbance until 2000/2005 when disturbances decreased substantially. Disturbances in the Ukrainian Carpathians peaked during 1990/1995 and then decreased continuously thereafter. Comparable temporal patterns, albeit of differing magnitude, were observed for the Czech, Polish and Slovakian Carpathians: sharp drops in disturbance levels after 1985/1990, and increasing levels of disturbance in the more recent years of the analysis.

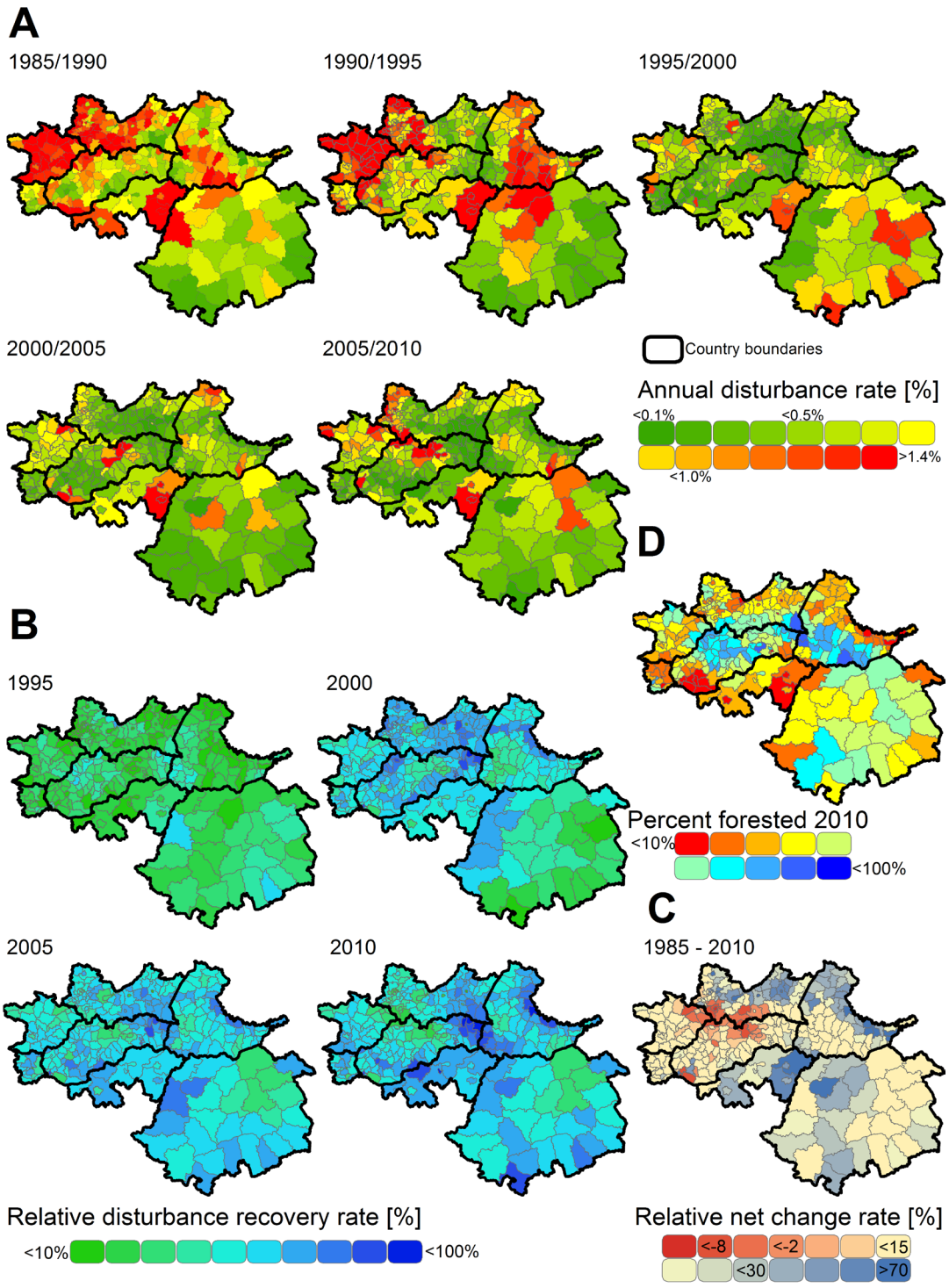


Figure IV-6: (A) Annual disturbance rates provided for the five disturbance periods and the administrative units in the study region (NUTS3 level for Austria, Hungary and Romania, district level for Czech Republic, Poland, Ukraine and Slovakia), (B) relative disturbance recovery rate, (C) relative net Change rate, (D) percent 2010 forest cover per region.

With regard to the disturbances aggregated to the level of administrative units, the mean annual disturbance rates decreased from 0.9% and 1% between 1985/1990 and 1990/1995, to no higher than 0.5% during subsequent years. The highest disturbance rates during the early periods (i.e. between 1985 and 1995) concentrated on the Czech and Polish

Carpathians as well as on the Ukrainian and Romanian boarder region (Fig.6A). This overall pattern changed considerably starting from 1995/2000: annual disturbance rates decreased markedly in all formerly mentioned regions and the highest disturbance rates were now detected within Romania (especially Covasna and Harghita regions). During 2005/2010 the Polish, Slovak and Czech boarder region emerged as a distinct disturbance hotspot.

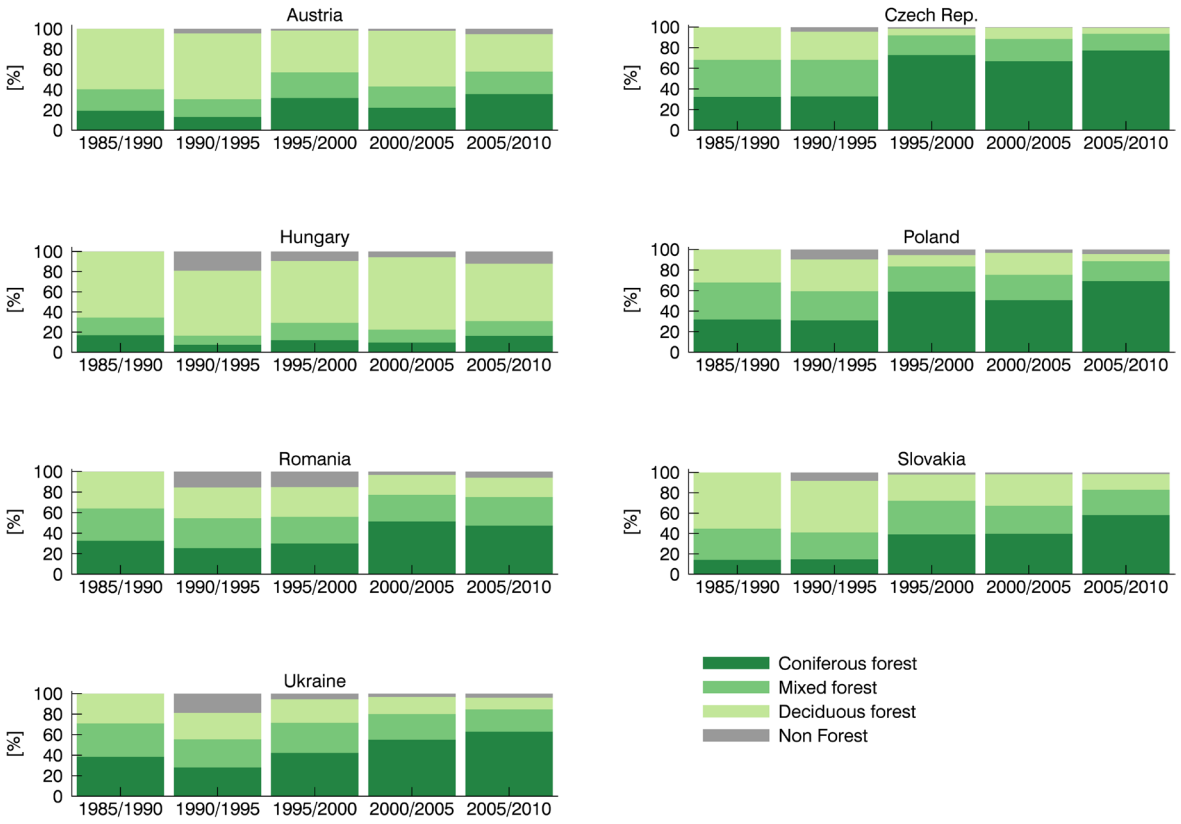


Figure IV-7: Disturbance patch-based pre-disturbance forest type, provided for the five disturbance classes and the seven countries in the study region, expressed as the percentage of all disturbance patches of a given class in a given country.

The examination of the pre-disturbance forest types clearly suggests that disturbance increasingly occurred within coniferous forests (Fig.7). This was especially true for the Polish, Czech, and Slovakian parts of the study region: the percentage of disturbances in coniferous forests more than doubled in Poland and Czech Republic between 1985 and 2010 and more than quadrupled in the Slovakian Carpathians between the same years. A similar increase was also observed in Romania and Ukraine, however to a slightly lesser degree. In Hungary, the percentage of disturbances occurring in coniferous and mixed forests remained relatively stable, and most disturbances were detected in deciduous forests.

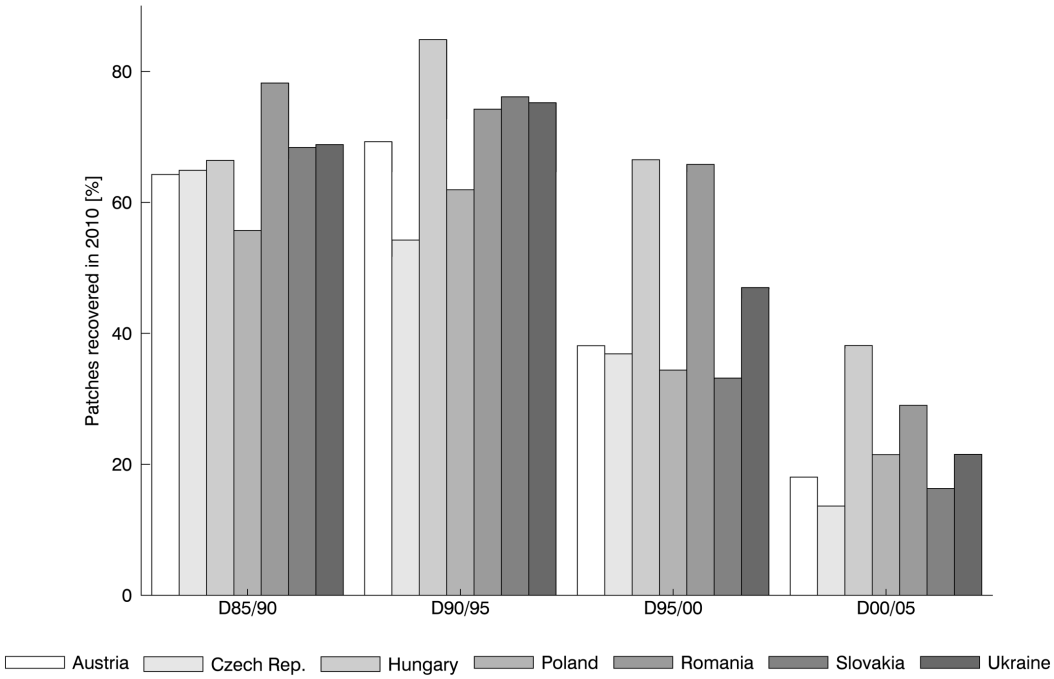


Figure IV-8: The percentage of disturbance patches that had recovered by at least 70% spectral recovery magnitude in 2010, provided for the seven countries in the study region and the five disturbance classes.

### 3.4 Forest recovery from disturbance

Post-disturbance recovery assessed in 2010 was most pronounced in the Hungarian, Romanian and Ukrainian Carpathians and much weaker in the Czech, Polish and Slovakian parts of the study region (Fig.8). Recovery from disturbance in Slovakia was strong during 1985/1990 and 1990/1995, but much weaker during the later periods. On the contrary, recovering patches disturbed between 1985/1990 in the Hungarian Carpathians did not show exceptional recovery tendencies when compared to other regions, but Hungary showed the strongest recovery dynamics among the Carpathian countries for all subsequent disturbance classes. In all countries (except Romania and Czech Republic) more disturbances patches had recovered from 1990/1995 disturbance events compared to those detected between 1985/1990.

The recovery rate (RRj) at the level of administrative units revealed lower recovery dynamics during 2000 in the eastern and southern Carpathians of Romania, but higher recovery rates in western Romania (Fig.6B). The northeastern Romanian Carpathians continued to exhibit lower recovery dynamics through 2005 and 2010 compared to other regions in the Romanian Carpathians. The relative recovery rate in the Slovakian, Polish and Czech boarder region decreased noticeably in 2010, which is related to the increasing prevalence of large-scale disturbances that occurred between 2000 and 2010 and counterbalanced the recovery.

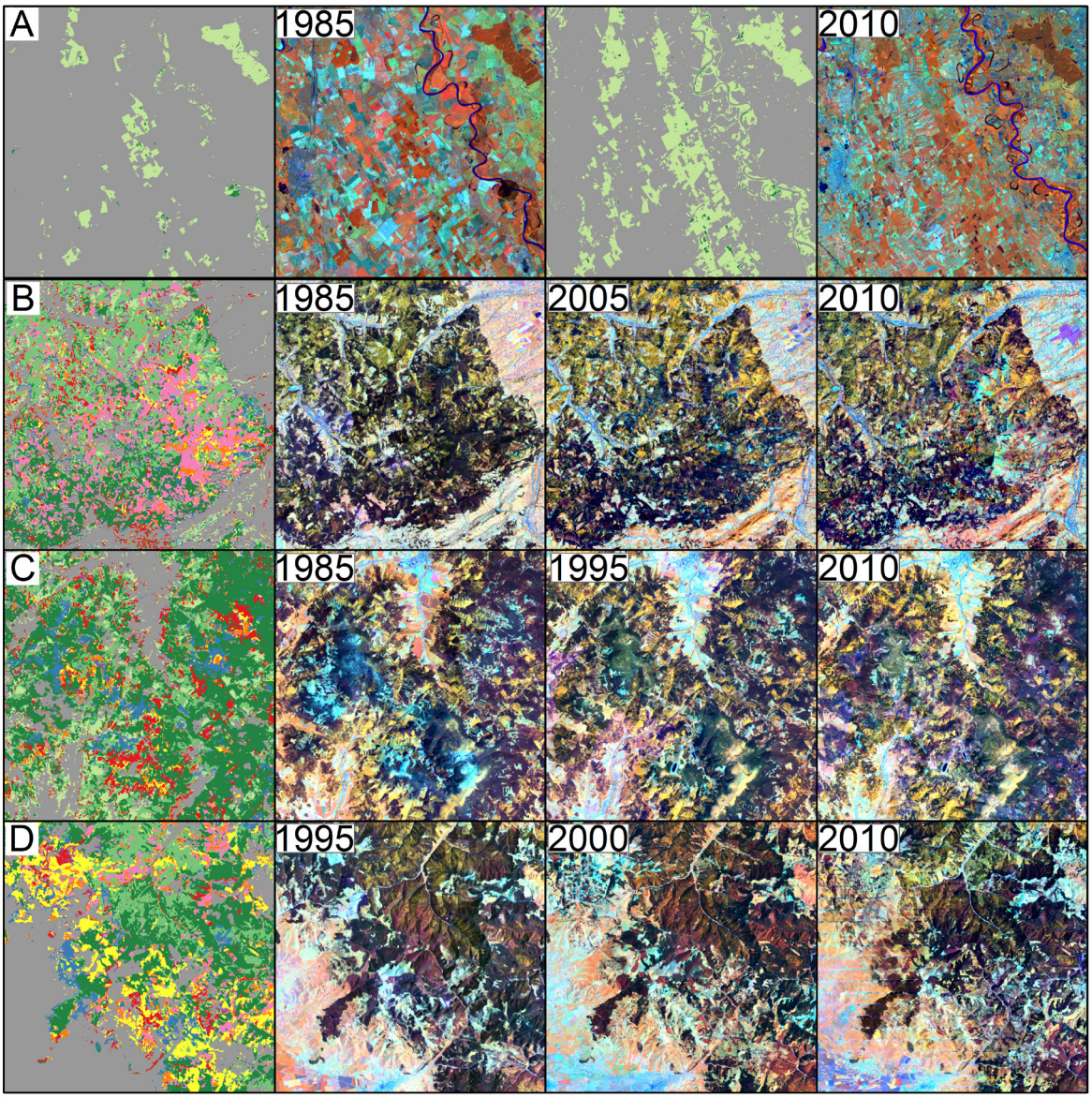


Figure IV-9: Four process examples (all provided at 1:475,000 scale): (A) areas with pronounced forest cover increase between 1985 and 2010 on former agricultural land in Hungary (forest type maps and composite subsets provided for 1985 and 2010), (B) large-scale disturbances in the Polish-Slovakian-Czech border region, (C) disturbance patterns in Czech Republic, (D) large-scale disturbances in the Romanian Eastern Carpathians (The legend for the forest type and disturbance map is provided in Fig.4).

When we assessed the relative net change in forest cover aggregated to administrative units, the overall pattern revealed a cluster of districts with strong negative balance in the Western Carpathians (Czech, Polish and Slovakian border region, Fig.6C). The strongest net increase in forest cover was observed in the foothills and forelands of the Polish and Ukrainian Carpathians, but also several areas in north eastern Hungary and western Romania showed overall positive balances.

### 3.5 Mapping accuracy

After accounting for the potential bias due to the stratified sampling design (Olofsson et al. 2013), our disturbance map achieved an overall accuracy of 85.8%. The stable deciduous and coniferous forest classes achieved relatively high user's and producer's accuracies, while the mixed forest class resulted in lower accuracies predominantly related to confusion with the other forest classes (Tables 4 & 5).

Table IV-4: Summary of the disturbance map validation (omission and commission errors provided).

| Disturbance map class | Omission | Commission |
|---|---|---|
| Coniferous forest | 38.03% | 12.58% |
| Mixed forest | 36.03% | 47.12% |
| Deciduous forest | 21.63% | 23.87% |
| Disturbance 1985/1990 | 61.51% | 31.37% |
| Disturbance 1990/1995 | 54.15% | 33.56% |
| Disturbance 1995/2000 | 43.52% | 17.86% |
| Disturbance 2000/2005 | 55.56% | 23.20% |
| Disturbance 2005/2010 | 31.27% | 19.35% |
| Non forest | 1.31% | 6.19% |

All disturbance classes contained higher omission than commission errors, with the highest commission errors assessed for the 1985/1990 disturbance class, partly owed to falsely detected disturbances on non-forest areas. Omission errors were considerably higher for the earlier disturbance classes, and commission errors were lower for the more recent disturbance classes (no more than 23%, Table 4). Errors within the disturbance classes were predominantly related to the timing, with the exception of the 2005/2010 disturbance class (Table 5).

Table IV-5: Confusion matrix obtained from the validation of the disturbance map (CF = coniferous forest, MF = mixed forest, DF = deciduous forest, NF = non forest, DYY/YY refers to the disturbance class detected between the respective years).

| | | Reference | | | | | | | | | |
|---|---|---|---|---|---|---|---|---|---|---|---|
| | Class | CF | MF | DF | D85/90 | D90/95 | D95/00 | D00/05 | D05/10 | NF | Sum |
| Classification | CF | 139 | 10 | 1 | - | 2 | 1 | 2 | 2 | 2 | 159 |
| | MF | 48 | 110 | 32 | 3 | 2 | 4 | 7 | 1 | 1 | 208 |
| | DF | 8 | 30 | 185 | 1 | 2 | 3 | 4 | 3 | 7 | 243 |
| | D85/90 | 4 | 9 | 6 | 70 | 4 | - | - | - | 9 | 102 |
| | D90/95 | 11 | 11 | 6 | 4 | 97 | 8 | - | 1 | 8 | 146 |
| | D95/00 | 5 | 3 | 5 | 4 | 3 | 138 | 5 | - | 5 | 168 |
| | D00/05 | 8 | 5 | - | 2 | 4 | 5 | 96 | 1 | 4 | 125 |
| | D05/10 | 5 | 2 | 3 | 1 | - | 1 | 10 | 100 | 2 | 124 |
| | NF | 3 | 4 | 13 | 11 | 4 | 2 | - | - | 561 | 598 |
| | Sum | 231 | 184 | 251 | 96 | 118 | 162 | 124 | 108 | 599 | 1873 |

Using the interpreted sample of permanent forest and non-forest validation points, the forest area delineation achieved overall accuracies of 95% for the 1985 and 98% for the 2010 forest type maps. The comparison of our forest type maps with the forest inventory data resulted in overall accuracies ranging from 73% in Slovakia for 1985 to 57% in Poland for the 2010 map (Table 6).

Table IV-6: Summary of the comparison of the 1985 and 2010 forest type maps with forest inventory data (omission and commission errors provided), for 2010 comparison with statistically sampled ground truth data is additionally provided (OAC = overall accuracy).

| | Omission | Commission |
|---|---|---|
| 2010 Combined | OAC = 68.24% | |
| Coniferous | 44.31% | 9.32% |
| Mixed | 55.77% | 73.34% |
| Deciduous | 15.82% | 21.25% |
| 2010 Romania | OAC = 59.65% | |
| Coniferous | 41.00% | 2.29% |
| Mixed | 33.81% | 80.15% |
| Deciduous | 41.59% | 30.92% |
| 2010 Poland | OAC = 57.35% | |
| Coniferous | 22.70% | 29.58% |
| Mixed | 62.44% | 58.41% |
| Deciduous | 61.45% | 57.54% |
| 2010 Slovakia | OAC = 69.12% | |
| Coniferous | 46.02% | 7.31% |
| Mixed | 55.90% | 73.65% |
| Deciduous | 14.39% | 20.55% |
| 2010 LUCAS | OAC = 63.43% | |
| Coniferous | 33.08% | 44.32% |
| Mixed | 62.00% | 58.19% |
| Deciduous | 24.46% | 21.08% |
| 1985 Combined | OAC = 71.19% | |
| Coniferous | 40.95% | 7.52% |
| Mixed | 45.89% | 74.07% |
| Deciduous | 16.13% | 15.44% |
| 1985 Romania | OAC = 65.86% | |
| Coniferous | 22.25% | 7.10% |
| Mixed | 38.84% | 79.51% |
| Deciduous | 51.14% | 23.78% |
| 1985 Slovakia | OAC = 72.81% | |
| Coniferous | 40.70% | 4.97% |
| Mixed | 48.43% | 74.90% |
| Deciduous | 13.77% | 15.30% |

The overall agreement with the inventory data across countries was 68% for 2010 and 71% for 1985. Mixed forests had the highest omission and commission errors, while deciduous and coniferous forest errors were lower. The coniferous forest class had the lowest errors of commission in Romania and Slovakia (all below 10%), but omission errors were higher

(up to 41%). The deciduous forest class was validated with omission and commission errors of no more than 15% in Slovakia in 1985, but errors were considerably higher in the Polish Carpathians. The validation of the 2010 forest type map based on LUCAS data resulted in an overall accuracy of 63%. The deciduous forest classes had omission and commission errors of no more than 25% and the coniferous class had only slightly higher uncertainty. The mixed forest class also had high uncertainties using the LUCAS data for validation (Table 6).

## 4. Discussion

Understanding changes in forest cover is crucial in order to address many environmental and resource related questions and results are most valuable, when major forest types and their changes are captured. Wall-to-wall analyses for large regions help avoiding extrapolations from case studies to larger regions, thereby potentially reducing uncertainties. We utilized the full Landsat archive as well as the automated image pre-processing and compositing algorithms to analyze changes in forest composition, forest disturbances and recovery from disturbance for the Carpathian ecoregion since the mid-1980s. Forests in the Carpathians have changed considerably over the past 25 years. Our results suggest a slight net increase in forest cover. Forest composition in the Carpathians changed markedly over the past 25 years. The share of mixed and especially coniferous forest decreased, while deciduous forest increased. While forest cover has likely increased locally due to abandoned agriculture or afforestation policies (Mueller et al. 2009; Kozak 2010; Baumann et al. 2011), our results indicate that almost 20% of the forests in the study area experienced disturbances, which can take a long time to regrow to forests again without targeted reforestation measures. Changes in forest composition, on the other hand, may reflect a shift towards sustainable forest management principles and a deemphasizing of timber production, but could also be the result of insect and pollution damages that mainly affect coniferous forests and especially plantations. Forest disturbances have overall decreased since the mid-1980s, most likely due to diminishing activities in the forestry sectors since the system change and a decreasing emphasis on economic returns. Forest recovery from disturbance showed regional variation and was overall most pronounced in Romania and Hungary and much weaker in Czech Republic and Poland.

A net forest cover increase has been reported for individual regions in the Carpathians (e.g. Kozak et al. 2007 for the Northern Carpathians) and on the national level in official forest

statistics (FAO 2010; Feranec et al. 2010). In accordance with those findings, our results also show a slight increase in net forest cover, which is however related to some uncertainty as the net forest cover increase was well within the confidence interval of the forest area estimates for 1985 and 2010. Agricultural land abandonment on former collectively managed land and decreasing grazing pressure at the timber line (Mihai et al. 2006) have resulted in increased forest cover locally, partly due to natural forest expansion and partly due to forest planting (Fig.9A, Oszlanyi 1997; Nijnik and van Kooten 2000; Abrudan et al. 2003; Kozak 2010). Land abandonment was most widespread in Ukraine (Baumann et al. 2011; Kuemmerle et al. 2011) and in Romania (Kuemmerle et al. 2009c; Mueller et al. 2009) but also occurred in Poland (Kozak et al. 2004). In 2010, i.e. about 20 years after the collapse of socialism, these areas have often matured from shrubland and early successional forests to young forest stands that can potentially be detected in Landsat data. Nevertheless, with almost 20% of Carpathian forests experiencing stand-replacing disturbances over the same time period, the net effect of these processes is overall small and is counterbalanced by the relatively slow recovery of forests, as forest planting is often not carried out and natural regeneration takes longer.

The overall composition of forests in the Carpathians underwent profound changes, and we found increasing dominance of broadleaved forests. Coniferous monocultures were originally economically motivated, but forest managers increasingly recognize and value ecological and social forest functions (UNEP 2007; Keeton and Crow 2009). The decrease in coniferous forests was largest in Romania and Ukraine. We observed large-scale disturbance patterns in both countries for the periods 1995/2000 and 2000/2005 which are untypical for harvesting activities (e.g. Fig.9D). Field evidence suggests that most of those disturbances can be attributed to large-scale wind throw or snow break events. This is not surprising, however, as both countries' forestry sectors focused on widespread establishment of spruce plantations in earlier decades. These spruce plantations are vulnerable to storm or snow damages and also often suffer from pest outbreaks (Oszlanyi 1997; Badea et al. 2004; Csóka 2005). In accordance with a change in management practices towards multifunctional forestry, those plantations are today often converted into stands dominated by deciduous species after harvesting (Keeton and Crow 2009).

Similarly, spruce forests experienced widespread pest outbreaks, dieback and large scale wind damages in the Czech and Polish Carpathians (Main-Knorn et al. 2009). In most Carpathian countries, disturbances were increasingly encountered in former coniferous forests (Fig.7). Maturing coniferous stands and especially spruce plantations are

increasingly vulnerable to wind damages and pest outbreaks (Nijnik 2004; Csóka 2005; Keeton and Crow 2009). Infested or degraded stands are subsequently subject to sanitary logging activities. Thus, forest managers are likely to harvest maturing spruce stands before the actual rotation age is reached to avoid suffering economic losses.

Forest disturbances were overall most abundant during the early periods of our analysis, especially 1985/1990 (Fig.5). Disturbances generally decreased thereafter, but several areas also exhibited extensive disturbances in later years. For example the Czech, Slovakian and Polish border region featured high disturbance rates between 2005/2010 (Fig.6A & 9B), while during the same period high disturbance rates occurred in northeastern Romania (Fig.6A). Natural disturbances in the Carpathians are mostly caused by wind and snow but often affect forests weakened by pests, insects or industrial pollution (Oszlanyi 1997). Forest fires are rare, especially large fires occur infrequently (Anfodillo et al. 2008). While wind damages are often below our minimum mapping unit (Popa 2008), large scale disturbances in recent decades increased in frequency and have occurred, for example in the Romanian Eastern Carpathians (Fig.9D) in 1994 (Mihalciuc et al. 1999) and in Slovakian Tatra Mountains (Fig.4) in 2004 (Soltes et al. 2010). All natural disturbances are typically followed by salvage logging which commonly account for a considerable proportion of the total annual cut, for example between 40% and 60% in the case of Slovakia since 1985 (Oszlanyi 1997). Following the 2004 wind throw in the Tatra Mountains which blew down 12,000 ha of forests (Fig.4, example 2), the regional timber market was saturated for years as a result of extensive salvage logging which again led to decreased timber harvesting (Suchomel et al. 2011).

However, the majority of detected disturbances are likely related to logging that occurred independent of prior natural disturbance events. Reasons for the elevated disturbance levels in 1985/1990 and 1990/1995 most likely relate to the fact that the timber industry was a major source of revenues and ensured large guaranteed outlet markets during socialist time. Especially in Ukraine, foresters continued to manage forest logging based on large scale clear cuts and timber remained a central source of economic revenues long after the collapse of socialism (Turnock 2002; UNEP 2007). Our results show that disturbance levels dropped after 1995 in many regions (Fig.6A). With the collapse of socialism in Eastern Europe, the timber products industry collapsed as well and subsequently had to be restructured, resulting in less logging (Csóka 2005). Moreover, as a result of excessive timber exploitation in the Ukrainian Carpathians under communism, most mature stands have been harvested, age structure of remaining stands has shifted to younger ages and

consequently timber harvesting decreased, which is also reflected in our results (Nijnik and van Kooten 2000). Official round wood extraction statistics support our findings for Slovakia and Hungary, but differ for Ukraine and Czech Republic where national statistics show increasing levels of timber extraction since 1990 (FAO 2010). Partly, this might relate to increased commercial thinning rather than clear-cutting that has been reported in Ukraine for recent years, due to a lack of mature stands (Nijnik and van Kooten 2000; Nijnik 2004). As thinning activities are mostly not captured in our mapping approach, this aspect might have influenced decreasing disturbance levels in our results. In Poland and the Czech Republic, disturbances decreased considerably after 1995, but increased again in 2005/2010 likely due to widespread spruce decline and subsequent salvage logging in the Polish-Czech-Slovakian border region (Main-Knorn et al. 2009).

In addition to changes in forest management objectives and natural forest disturbances, forest ownership changes also most likely affected the observed disturbance rates. While in Ukraine and Poland most forests remained property of the federal state, in other countries forest ownership has changed substantially. For example in the case of Romania, forests were largely restituted based on three forest restitution laws since 1991 (Abrudan et al. 2009). With poor management regulations for privately owned forest in the first years of the restitution process as well as uncertainties regarding the permanence of obtained tenure rights, many new forest owners opted for immediate economic benefits rather than sustainable forestry leading to increased logging, especially after 2000 (Irimie and Essmann 2009; Vasile 2009). As a consequence, increased foreign investment in the Romanian forestry sector has been documented since 2000 (Ioras and Abrudan 2006) and could represent a potential driver of increasing disturbance levels observed between 2005/2010. In Slovakia, restitution of forests continues and more than 50% of forests are non-state owned (Weiss et al. 2012). However, many restituted forest areas are now within protected areas or under other forms of conservation which represents a major source of conflicts in both, Romania (Knorn et al. 2012b) and Slovakia (Kovalčík et al. 2012; Sarvasova et al. 2012).

Our results show that post-disturbance forest recovery differed considerably among the countries in the Carpathians (Fig.8). Especially in recent years, forest disturbances in Hungary, Romania and Ukraine showed markedly stronger recovery than in the Czech, Polish or Slovakian Carpathians. Natural recovery after harvests is favored over replanting throughout the Carpathians, the latter being predominantly utilized for stand conversion and restoration forestry (UNEP 2007; Keeton and Crow 2009). However, natural recovery

is generally slow and can take several decades depending on the forest type, topography, soil quality, and forest management history. Overall natural regeneration has likely not counterbalanced the widespread disturbances that amounted to 20% of the Carpathian forests over the study period.

Our approach highlighted that detailed mapping of forest types, forest disturbances and forest recovery is possible using large-area composites of Landsat data. The overall spatial and temporal patterns of detected disturbances in the Ukrainian Carpathians agree well with results of previous studies, e.g., by Kuemmerle et al. (2009a). Even though the temporal intervals of the incorporated imagery are not directly comparable, we identified approximately 2.6% more disturbances in western Ukraine than Kuemmerle et al (2009a). With respect to the extent of the study area and the complexity of the target classes the achieved accuracies indicated overall reliable results, but few sources of uncertainty deserve particular mention. While composited surface reflectance data allow for extrapolating training data across large areas, the generation of representative training data over large areas with high spatial detail is not a trivial task. It is challenging to account for the total spectral variability of target classes across space and time and thus approaches for automated training data generation hold great potential and should be further pursued (Huang et al. 2008). We detected fewer disturbances during the later years and these also related to much smaller levels of uncertainty. Overall, the individual disturbance class accuracies showed higher levels of omission than commission errors (Table 4), which suggest that the total extent of disturbances in our results is rather conservative. The forest type maps achieved high accuracies for the deciduous and coniferous forests classes while the mixed forest class related to considerable uncertainties. Due to its mixed nature, the mixed forest class is intrinsically challenging to map and the comparison of rather subjectively gathered training data with objectively measured inventory data is problematic. Moreover, while absolute and relative geometric accuracy of L1T imagery is unprecedented, some images especially for the years between 1985 and 1995, exhibited some spatial inaccuracies and automated geometric quality assessments should be incorporated into future compositing approaches (Gao et al. 2009).

Overall, temporal compositing of Landsat imagery holds great potential for land cover mapping and change detection on regional to continental scales. Data availability for the 1980s and 1990s was generally lower (Table 1), but compositing still allowed for assembling of regional, cloud-free datasets. Consistent surface reflectance measurements for historic acquisitions are a great asset, and allow for radiometric change classification in

multi-temporal stacks of large-area datasets. Alternative large-area approaches using scene-based classifications are limited with respect to the number and complexity of the classes of interest (Olthof et al. 2005; Knorn et al. 2009). Scene-based change detection approaches that focus on variations of spectral indices and annual time-series trajectory approaches generally depend on the availability of cloud-free anniversary acquisitions which might not be available for many areas around the globe (Masek et al. 2008; Huang et al. 2010b; Kennedy et al. 2010). Compositing of Landsat data therefore is a valuable alternative for large-area change detection.

In this study, we successfully analyzed a series of large-area composites yielding forest type maps as well as forest disturbances and recovery dynamics. To our best knowledge, this is the first study to utilize a series of six large-area image composites in an integrated approach to analyze forest disturbances and recovery in relation to three broad forest types. Our results provided valuable insights into spatial and temporal patterns of forest changes in the Carpathians and may serve as a framework for similar studies to be conducted elsewhere. The resulting maps are foreseen to provide indispensable inputs to ecological, social and economic studies of land-change in the Carpathian ecoregion. Increased geometric and radiometric standard image quality, improved preprocessing algorithms and free-of-cost data has enabled Landsat data analyses to advance considerably in recent years. Moreover, this study again highlights the value of the open Landsat archive for retrospective land change analysis and the need for data continuity. With the upcoming Landsat-8 (Irons et al. 2012) as well as the European Sentinel-2 missions (Drusch et al. 2012), new opportunities arise for land change monitoring through combined use of both data sources featuring enhanced spectral and temporal data characteristics. Compositing will be one powerful aspect for monitoring approaches combining these new sensor systems and thus greatly enhance capabilities for global mapping and monitoring at landscape scales.

**Acknowledgements**

This research was funded by the Belgian Science Policy Research Program for Earth Observation STEREO II, contract SR/00/133, as part of the FOMO project (Remote sensing of the forest transition and its ecosystem impacts in mountain environments). PH's contribution to this research is part of his activities in the Global Land Project and the Landsat Science Team. TK acknowledges support through the Einstein foundation and the

European Union (VOLANTE, FP7-ENV-2010-265104), KO acknowledges support through the Fulbright Scholar Program. We would like to thank Oleh Chaskovskyy, Geza Kiraly, Mihai Nita and Martin Hais for valuable comments and help with the forest inventory data. We also thank the Polish State Forests National Forest Holding for free access to the state inventory data used in this study.

# Chapter V:
# Agricultural land change in the Carpathian ecoregion after the breakdown of socialism and expansion of the European Union

*Environmental Research Letters (in review)*

Patrick Griffiths, Daniel Mueller,
Tobias Kuemmerle and Patrick Hostert



*Received 15 May 2013.*

**Abstract**

Widespread changes of agricultural land use occurred in Eastern Europe since the collapse of socialism and the European Union's eastward expansion, but the rates and patterns of recent land changes remain unclear. Here we assess agricultural land change for the entire Carpathian ecoregion in Eastern Europe at 30m spatial resolution with Landsat data and for two change periods, between 1985-2000 and 2000-2010. The early period is characterized by post-socialist transition processes, the late period by an increasing influence of EU politics in the region. For mapping and change detection, we use a machine learning approach (random forests) on image composites and variance metrics which were derived from the full decadal archive of Landsat imagery. Our results suggest that cropland abandonment was the most prevalent change process, but we also detected considerable areas of grassland conversion and forest expansion on non-forest land. Cropland abandonment was most extensive during the transition period and predominantly occurred in marginal areas with low suitability for agriculture. Conversely, we observed substantial recultivation of formerly abandoned cropland in high-value agricultural areas since 2000. Hence, market forces increasingly adjust socialist legacies of land expansive production and agricultural land use clusters in favorable areas while marginal lands revert to forest.

## 1 Introduction

Humanity derives essential goods and services from land use, but simultaneously land use changes have become a primary driver of global environmental change and caused significant biodiversity loss as well as the deterioration of ecosystem services (Tilman et al. 2002; Foley et al. 2005). Changes in agricultural land use were particularly widespread, with ample consequences for humans and nature. One major environmental concern is the rapid expansion of croplands and pastures at the expense of tropical and subtropical forests, and the various adverse consequences for biodiversity and carbon budgets (Sala et al. 2000; van der Werf et al. 2009). But while agricultural land use continues to expand in many tropical regions, areas used for agricultural tend to decrease in the temperate zone. A large body of research has been devoted to understanding agricultural expansion in tropical settings, but the patterns and processes of the decrease of agricultural land are less well understood (Kuemmerle et al. 2009c; Ramankutty et al. 2010; Hostert et al. 2011a). This is unfortunate, because abandonment of agricultural land has strong implication for agricultural production and affects carbon pools (Vuichard et al. 2008), biodiversity (MacDonald et al. 2000) and food security (Schierhorn et al. 2012). A better understanding of the rates and spatial patterns of agricultural land abandonment is therefore crucial.

One of the most drastic recent episodes of land change that resulted in massive rates of agricultural abandonment occurred after the collapse of socialism in the countries of the former Soviet Union and Central and Eastern Europe (CEEC) (Henebry 2009). The socialist agricultural system was strongly subsidized in these countries with guaranteed output and input prices and high land and labor inputs, often with the aim to increase self-sufficiency in agricultural production (Csaki 1990; Lerman et al. 2002). State support largely disappeared following the collapse of socialism and agricultural production was economically no longer viable in many areas due to price liberalizations, dilapidated infrastructure and increasing competition with other economic opportunities, leading to production decreases and rural emigration (Rozelle and Swinnen 2004; Müller and Munroe 2008; Mueller et al. 2009). Consequently, vast areas of agricultural land were abandoned. Abandoned lands subsequently experienced natural succession and many areas have now retrieved back to young forests, contributing to the forest transition in Eastern Europe (Taff et al. 2010). However, most evidence regarding the extent of agricultural abandonment to

date relies on case studies, while the spatial and temporal patterns for large, contiguous areas are not well understood.

Agricultural abandonment tends to cluster in areas with comparatively low suitability, such as mountain areas, while fertile lands often continue to be cultivated (MacDonald et al. 2000; Ioffe et al. 2012; Prishchepov et al. 2013). However, today's agricultural production in Russia and the CEEC is often below the potential yields under the given environmental conditions and therefore these lands represent interesting options for increasing food production (Foley et al. 2011; Schierhorn et al. 2012). Given the recent rises in global agricultural commodity prices, abandoned agricultural land in post-socialist countries today represents an attractive source of income and increasingly becomes a target for investors (Deininger 2011; Visser and Spoor 2011). In the face of the recent increase in agricultural commodity prices, quantifying recultivation of abandonment lands can shed light on the effects of growing profit opportunities in agriculture on agricultural land use.

The eastward expansion of the European Union may also have contributed to recultivation of abandoned lands. New member states in 2004 included, among others, the Czech Republic, Hungary, Poland and Slovakia and in 2007 Romania became part of the EU. New member states became subject to the influence of the European Union Common Agricultural Policy (EU CAP), which grants direct subsidy payments in support of agricultural production and rural development. However, little is known about how the EU accession has affected agricultural land change in CEEC.

The focus of this study is to map and analyze agricultural land change across the Carpathian ecoregion in Eastern Europe since before the collapse of socialism until 2010 at high spatial resolution. The Carpathians are Europe's largest mountain region and extend over seven countries (Austria, Czech Republic, Slovakia, Poland, Hungary, Ukraine and Romania). All countries except Austria were under socialist governance between 1945 and 1991 and all countries except Ukraine are now members of the EU. The Carpathians are a highly diverse ecoregion, which historically translated into a large variety of land use structures (Turnock 2002) that may have been affected differently by the contrasting post-socialist reform policies and economic development trajectories. However, no consistent and spatially explicit dataset on recent land change exists for the Carpathians as a whole.

We utilized Landsat satellite imagery to fill this gap. Landsat imagery is a great data source for retrospective land change assessments, as it provides a continuous record of synoptic observations since decades with relatively high spatial and spectral detail. Recent changes

in data policy as well as advancements in data quality, preprocessing and analysis algorithms have greatly improved the potential of Landsat data to quantify agricultural land change for large areas (Wulder et al. 2012). Taking advantage of these developments, our objectives were to (a) quantify the spatial and temporal patterns of agricultural land change in the Carpathians between 1985 and 2000 as well as between 2000 and 2010, and to (b) assess and compare environmental and agro-ecological characteristics of areas where agricultural land change occurred.

## 2 Methods

Our study region is the Carpathian ecoregion (CERI 2001) including intersecting administrative units (Nomenclature of Territorial Units for Statistics, Level 3 - NUTS3), resulting in an area of approximately 380,000 km² (figure 1). Elevation in the study region ranges from 400 m in the plains to 2,500 m in the Southern and Western Carpathians. A wide range of agricultural land use types exists, ranging from large scale, intensively managed cropland to subsistence agriculture and kitchen gardens. Cropland in the region is predominantly used for cereals (wheat, corn, barley, rye, oat) and legumes (potatoes, sugar beets, peas), but also to grow energy crops (e.g., rapeseed). Perennial crops exist in form of fruit tree orchards, vineyards or hop fields. Grassland is utilized as pastures or hay fields and higher elevated meadows for seasonal sheep grazing. The majority of agricultural land in the Carpathian countries was under collective or state farm management during socialism, except in the Polish Carpathians where private farms persisted (Lerman 1999; Kozak 2010). After 1989, private property was reintroduced and collectivized lands were restituted, auctioned or distributed to farmers, historical owners or their heirs, which led to considerable structural change in agriculture including the emergence of many small fragmented farms alongside large private cooperatives (Sarris et al. 1999). The Carpathian ecoregion hence offers a diverse, and from a remote sensing point-of-view challenging region to study, due to the prevailing heterogeneous landscapes and mountainous terrain. This makes it an ideal test bed for an improved understanding of the complex land change trajectories that occurred during the recent turbulent decades of change and for elaborating how remote sensing can contribute to disentangling these complex spatio-temporal patterns.

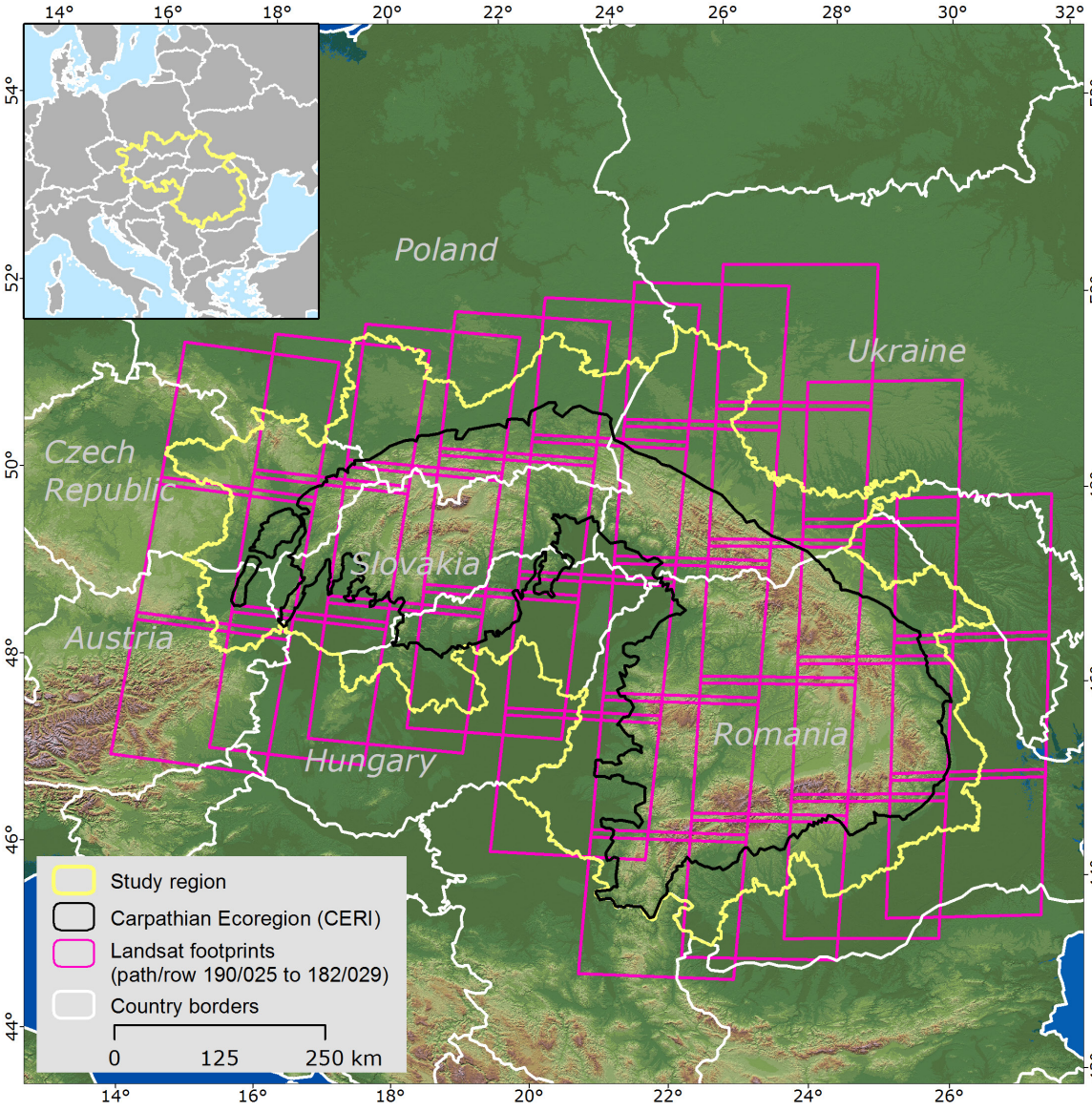


Figure V-1: Overview of the Carpathian study region (yellow), the ecoregion boundaries (black) and country borders (white). Additionally, the coverage of Landsat footprints is shown (magenta), which were used to produce three seasonal image composites (spring, summer and fall) for three reference years (1985, 2000 and 2010).

Multi-temporal Landsat imagery has recently been used to map agricultural abandonment in CEEC and it has been shown that including imagery acquired at key stages of crop development (i.e. leaf emergence, ploughing) can considerably improve the differentiation of cropland, grassland and fallow land (Baumann et al. 2011; Prishchepov et al. 2012b). However, the 16-day repeat cycle of Landsat satellites coupled with frequent cloud coverage in mountainous regions constrains the availability of such imagery. While such sets of multi-temporal imagery might be available for individual footprints, acquiring such specific datasets over larger regions is hardly feasible. Consequently, most studies that mapped agricultural abandonment only compared two reference periods, and used only one

or two observations from different seasons for each considered period. This increases the risk of false interpretations, e.g. assessing an area as being abandoned even though it was only imaged during a fallow stage within a crop rotation cycle. To circumvent these limitations, our approach incorporates all available, useful observations, i.e., thousands of images from the Landsat archive and utilizes automated data preprocessing and image compositing algorithms. Such an approach enables generating regional, cloud free datasets that are radiometrically and seasonally consistent (Griffiths et al. 2013; Griffiths et al. accepted).

For this study, we generated three image composites that approximate specific seasonal states (spring, summer and fall) centered around three reference years that capture the situation (i) during socialism (centered around 1985), (ii) after 10 years of post-socialist transition (centered around 2000), and (iii) after the EU accession (centered around 2010). These temporal image composites represent "extended snapshots" that maximize spectral and temporal separability of agricultural land use classes and changes. The seasonal composites (18 bands for each reference period = 56 spectral bands) were supplemented with 27 bands of statistical metrics that capture the spectral-temporal variability of a given pixel for each season (e.g., variation and mean of the normalized difference vegetation index (NDVI) for spring observations). We further added layers containing specific metadata information per pixel, e.g. the image acquisition day-of-year (yielding a total number of 100 bands). We focused our analysis on four main land change categories that relate directly or indirectly to changes in agricultural land use: abandonment (conversion of cropland to other uses), grassland conversion (conversion of grassland to other use), recultivation (conversion of abandoned cropland and 1985 grassland to cropland) and forest expansion (forests establishing on non-forest lands). We assessed the rates of these processes for two change periods: the transition period (1985 to 2000) and the EU accession period (2000 to 2010). In order to differentiate forest expansion occurring on non-forest land from forest areas that are regrowing after forest disturbance, we overlayed our change map with a recent forest disturbance map (Griffiths et al. accepted). We included the conversion of grassland to cropland as recultivation because we assume that the majority of these areas were once covered by forests but cleared for cropland use and later (prior to the 1985) were converted to grassland. Table 1 provides descriptions of classes targeted for change detection as well as class summaries that were used to quantify the rates and patterns of land change.

Table V-1: Overview of the study design: The top section shows the targeted classes during change detection and mapping, which are provided with acronyms that refer to the land use / land cover during the individual reference years (top left). Class acronyms: C = Cropland, F = Forest, G = Grassland. Using black squares, sections two to four illustrate how the spatial extents of cropland, grassland and forest were derived for the three reference years. Definitions of the class constituents are provided on the far right. Finally, sections five to eight illustrate (using colored squares) how the targeted land change processes were derived. For example "Abandonment 2000" was derived by summing up "C-F-F", "C-G-C", "C-G-F" and "C-G-G". The abandonment rate for the socialist period was then derived as the percentage of the total "Cropland 1985" against "Abandonment 2000" (accordingly, "Grassland conversion 2000" and "Recultivation 2000" rates were derived relative to the "Grassland 1985", while the "Recultivation 2010" rate was calculated relative to "Abandonment 2000").

| | [1]Mapped classes | | | | | | | | | | | | | Definitions |
|---|---|---|---|---|---|---|---|---|---|---|---|---|---|---|
| Socialism | C | C | C | C | C | C | C | G | G | G | G | G | F | |
| Transition | C | C | C | F | G | G | G | G | C | F | G | G | F | |
| EU accession | C | F | G | F | C | F | G | G | C | F | C | F | F | |
| Cropland 1985 | ■ | ■ | ■ | ■ | ■ | ■ | ■ | | | | | | | All farmed agricultural and cropland for cereals, root and energy crops, vegetables and others |
| Cropland 2000 | ■ | ■ | ■ | | | | | | ■ | | | | | |
| Cropland 2010 | ■ | | | | ■ | | | | ■ | | ■ | | | |
| [2]Grassland 1985 | | | | | | | | ■ | ■ | ■ | ■ | ■ | | Pastures, hayfields, meadows, natural grasslands, small scale subsistence agriculture, permanent fallow land, shrub land, orchards |
| Grassland 2000 | | | | | ■ | ■ | ■ | ■ | | | ■ | ■ | | |
| Grassland 2010 | | | ■ | | | | ■ | ■ | | | | | | |
| Forest 1985 | | | | | | | | | | | | | ■ | All deciduous, mixed and coniferous forests |
| Forest 2000 | | | | ■ | | | | | | ■ | | | ■ | |
| Forest 2010 | | ■ | | ■ | | ■ | | | | ■ | | ■ | ■ | |
| Abandonment 2000 | | | | ■ | ■ | ■ | ■ | | | | | | | All 1985/2000 cropland areas that were converted to other uses in 2000/2010 |
| Abandonment 2010 | | ■ | ■ | | | | | | | | | | | |
| [3]Grassland conversion 2000 | | | | | | | | | ■ | ■ | | | | All 1985/2000 grassland areas that were converted to other uses in 2000/2010 |
| Grassland conversion 2010 | | | | | ■ | ■ | | | | | ■ | ■ | | |
| [4]Recultivation 2000 | | | | | | | | | ■ | | | | | Grassland-cropland conversions and recultivation of formerly abandoned cropland |
| Recultivation 2010 | | | | | ■ | | | | | | ■ | | | |
| [5]Forest expansion 2000 | | | | ■ | | | | | | ■ | | | | Forest expansion on non-forest lands |
| Forest expansion 2010 | | ■ | | | | ■ | | | | | | ■ | | |

[1]We additionally mapped a permanent built-up (B-B-B) and water class (W-W-W) but as these were not within the focus of the change analysis we did not include them in this summary table

[2]As the separation of different grass-dominated land-use classes such as hayfields, pastures or natural grasslands is challenging with Landsat data, we focus on one broad grassland class. Depending on the level of management, perennial crops (vineyards, orchards, etc.) are regarded as belonging to the grassland class under low management conditions, and belonging to the cropland class under more intense management. This class also includes grass-dominated wetland areas.

[3]To prevent an overestimation of grassland conversions through inclusion of logged or harvested forest areas that are regrowing, we used a disturbance map from an earlier study to extract only those grassland conversions that are not related to regrowing forests. However, this might include forest areas recovering from logging/disturbances that occured prior to 1985.

[4]The assessment of recultivation for the transition period mostly comprises grassland to cropland conversions. Here we assume that all grassland areas were historically forest areas that were converted to cropland converted to grassland.

[5]We used results from an earlier study to extract only those forest expansion areas that were not related to logging or other forest disturbances. However, this forest expansion also entails areas that were logged prior to the mid-1980s.

For mapping and change detection, the 100 features were combined into one stacked dataset and a Random Forests (RF) classifier was parameterized to map the 15 classes of interest (Waske et al. 2012; Griffiths et al. accepted). Training areas were digitized on-screen on the original Landsat imagery using the following reference data sources to aid interpretation: high resolution imagery available in GoogleEarth, high temporal frequency satellite time series, Street View data (Google 2013) and the full temporal record of the original Landsat imagery. One global RF model was trained for the analysis. Due to imbalanced training data sizes, we sampled the same number of pixels from all classes (~1,300 each). We then parameterized a RF model consisting of 2,000 trees which considered 15 features at each tree split. For validation of the resulting change map we generated a stratified random sample of 50 points per class. Samples were carefully interpreted using all above mentioned reference data. Key feature for identifying croplands was the presence or absence of ploughed signals interchanging with vegetation in the Landsat imagery. Validation results were finally adjusted for potential sampling bias and then used to derive error adjusted area estimates and the 95% confidence intervals around these estimates (Card 1982; Olofsson et al. 2013). After applying a minimum mapping unit of five pixels (4,500 m²), we aggregated the final change map to relevant process categories (table 1) and summarized change classes per country and time period.

In order to better understand the environmental characteristics of areas where agricultural land change occurred, we acquired data from the Global Agro-Ecological Zones database (IIASA and FAO 2012). Specifically, we used the crop suitability index (CSI) for rain-fed wheat production at intermediate fertilizer input levels available at one arc second spatial resolution. The CSI combines information on climate, soils and topography into a single proxy of overall agro-ecological condition. We then aggregated the CSI data and change maps to the level of administrative units and produced maps showing change rates at district/county level as well as scatter plots comparing the CSI with change rates for the 1985-2000 and 2000-2010 periods.

## 3 Results

Our results showed that extensive land changes occurred in the Carpathians since the mid-1980s. Compared to 1985, cropland had decreased by approximately 9% in 2010 (then accounting for 88,000 km², equivalent to 23% of the study region). Forests covered 40% of the study region in 1985 and increased by 3% until 2010. The share of grassland increased

from 26% in the mid-1980s to roughly 31% in 2010. Agricultural abandonment was the most prevalent change process (figure 2). According to our error adjusted area estimates, 24% (30,000 km²) of the 1985 cropland was abandoned until 2000 and 11% (14,000 km²) until 2010. Cropland-grassland conversions contributed most to abandonment, affecting approximately 24% of the total 1985 cropland until 2000 and another 9% until 2010. Recultivation was not widespread until 2000 (4% of the 1985 grassland area) but between 2000 and 2010 about 18% of the cropland that was abandoned until 2000 was brought back into production. The total forest expansion on non-forest land summed up to 3.4% during the transition period and 2.3% during the EU accession period.

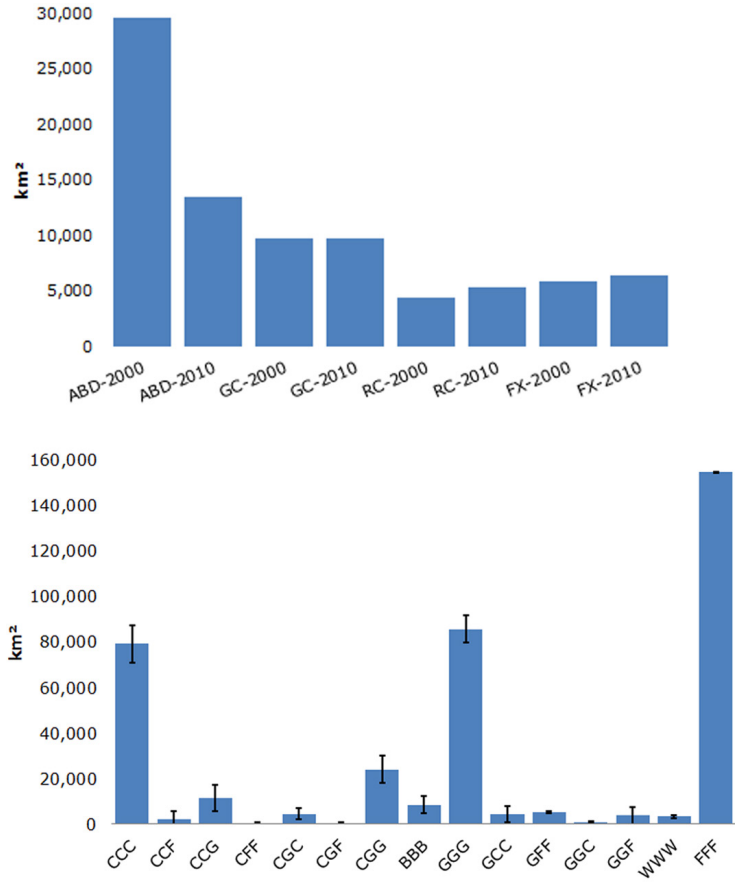


Figure V-2: (Top) Error adjusted area estimates of change processes (compare table 1) for 2000 and 2010: ABD = cropland abandonment; GC = grassland conversion; RC = recultivation; FX = forest expansion on non-forest land. (Bottom) Error adjusted area estimates of change map results. Error bars indicate the 95% confidence interval around these estimates.

Land changes showed strong regional differences. Overall, comparatively low rates of change occurred in the Austrian part of the study region while the most extensive changes were detected in the Ukrainian Carpathians (up to 25% of the included country area). Some change processes were almost entirely limited to certain countries. For example, more than 67% of all cropland-grassland-cropland conversion was mapped in Romania, almost 95%

of cropland-forest conversions between 2000 and 2010 occurred in Hungary, and cropland-grassland-forest conversions were most common in Poland (figure 3).

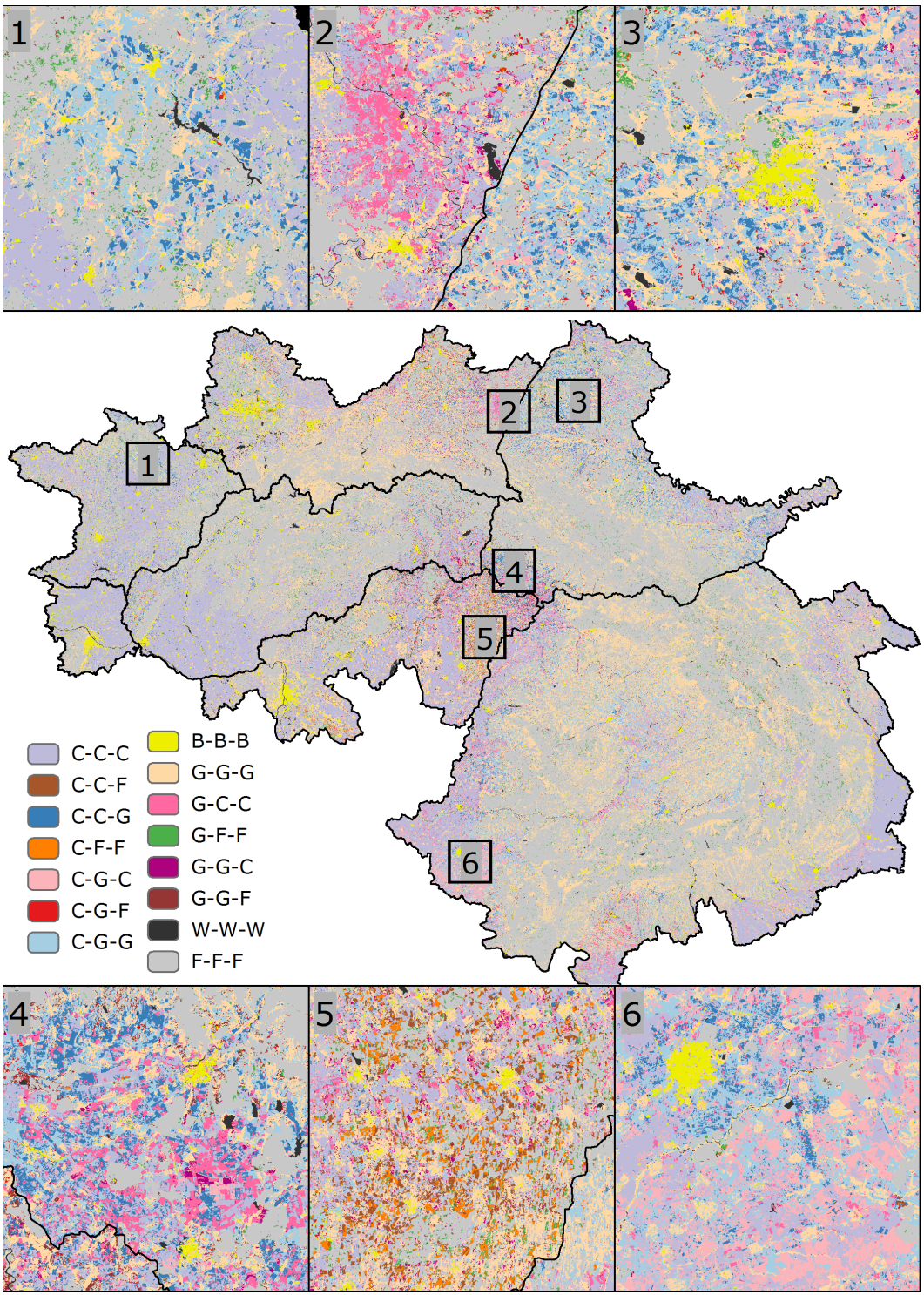


Figure V-3: (Center) Change map derived from image composites and variance metrics. Classes relate to the land use / land cover during the respective reference year. Class acronyms: C = cropland, B = built up, F = forest, G = grassland, W = water. Six representative close-up frames are provided for relevant process regimes (top and bottom): (1) cropland-grassland conversion in the Czech Republic; (2) contrasting land change on the Polish-Ukrainian border; (3) cropland changes in Ukraine; (4) change dynamics in the Ukrainian-Hungarian border region; (5) widespread forest expansion in Eastern Hungary; (6) cropland-grassland conversions and extensive recultivation in Romania. Map scale for all close-up frames is 1:750,000.

During the transition period, rates of cropland abandonment were highest in the Ukrainian Carpathians with 59%, followed by the Romanian (46%) and Polish Carpathians (27%). In the Czech, Hungarian and Slovakian parts of the study region we found abandonment rates between 20% and 30% (table 2). Abandonment rates for the EU accession period dropped drastically in all countries but were still highest in Ukraine (12%), followed by the Hungarian and Polish Carpathians (between 6 and 7%). The highest rates of grassland conversion occurred in the Ukrainian and Romanian parts of the study region and were considerably larger than during the transition period from socialist to post-socialist regimes. High grassland conversion rates were also found in the Hungarian Carpathians during the transition and EU accession periods (>13%). In the Czech part of the study region grassland conversion dropped considerably during the EU accession period compared to the transition period. The extent of areas undergoing recultivation during the EU accession period was substantially higher than during the transition period in most countries apart from Hungary (690 km² vs. 980 km², respectively). The most extensive recultivation during the EU accession period occurred in Romania and Ukraine with 28% and 19% of formerly abandoned cropland, respectively (table 2). The overall highest forest expansion rates occurred in the Hungarian Carpathians. During the transition period, forest expansion on non-forest land was most extensive Hungary and Romania and also abundant in the Czech, Polish and Ukrainian Carpathians. During the EU accession period, most countries (except Hungary and Poland) had considerably lower forest expansion rates, especially in Romania and the Czech Republic.

Table V-2: Change processes summarized for the countries in the Carpathian study region as total area [km²] and as percentage. Country acronyms are: AU = Austria, CZ = Czech Republic, HU = Hungary, PL = Poland, RO = Romania, SK = Slovakia, UA = Ukraine. Percentages relate to the total country cropland area in 1985 for the abandonment rates and to the 1985 grassland area for the grassland conversion rates. Note that the rate for "Recultivation 2010" is relative to the "Abandonment 2000" areas, while the rate for "Recultivation 2000" is calculated relative to the 1985 grassland areas. Forest expansion rates are calculated relative to the 1985 forest area in a given country. We used results from a Landsat based forest disturbance mapping to make sure that forest expansion does not include forest areas that are regenerating after disturbances (similarly grassland conversions exclude regenerating forest disturbances).

| | AU | | CZ | | HU | | PL | | RO | | SK | | UA | |
|---|---|---|---|---|---|---|---|---|---|---|---|---|---|---|
| | km² | % | km² | % | km² | % | km² | % | km² | % | km² | % | km² | % |
| Abandonment 2000 | 243 | 5.7 | 1606 | 13.7 | 2170 | 13.3 | 3044 | 27.3 | 22605 | 45.8 | 2132 | 13.1 | 10599 | 58.9 |
| Abandonment 2010 | 60 | 1.4 | 662 | 5.6 | 1104 | 6.8 | 727 | 6.5 | 1603 | 3.2 | 894 | 5.5 | 2089 | 11.6 |
| Grassland conversion 2000 | 26 | 3.9 | 393 | 10.5 | 1365 | 13.8 | 845 | 6.1 | 4460 | 9.4 | 895 | 10.8 | 1256 | 9.7 |
| Grassland conversion 2010 | 49 | 7.3 | 158 | 4.2 | 1334 | 13.5 | 1375 | 9.9 | 6984 | 14.7 | 804 | 9.7 | 2433 | 18.8 |
| Recultivation 2000 | 2 | 0.3 | 87 | 2.3 | 977 | 9.9 | 475 | 3.4 | 2169 | 4.6 | 407 | 4.9 | 571 | 4.4 |
| Recultivation 2010 | 37 | 15.0 | 92 | 5.7 | 692 | 31.9 | 607 | 19.9 | 6209 | 27.5 | 412 | 19.3 | 1984 | 18.7 |
| Forest expansion 2000 | 29 | 1.6 | 318 | 3.3 | 804 | 11.5 | 461 | 2.5 | 2369 | 3.4 | 508 | 2.2 | 767 | 3.1 |
| Forest expansion 2010 | 13 | 0.7 | 71 | 0.7 | 1014 | 14.5 | 774 | 4.1 | 784 | 1.1 | 393 | 1.7 | 452 | 1.8 |

Aggregating land change for administrative units revealed distinct spatial patterns (figure 4). The highest rates of abandonment (~90%) were found in the mountain areas in Ukraine during the transition period. Comparably high abandonment rates were only found in parts of the Polish Carpathians. In Romania, abandonment rates between 70% and 80% occurred in several counties during the transition period. During the EU accession period the highest abandonment rates clustered in the border region between Ukraine and Hungary as well as in northernmost part of the Ukrainian Carpathian foreland, but rates were drastically lower than during the transition period. The highest grassland conversion rates occurred during the transition period, but grassland conversion increased during the EU accession period in several areas, especially in Western Ukraine and Western Romania. High recultivation rates during the EU accession period concentrated on the Romanian Carpathian forelands, Western Hungary and in the North of the Polish and Ukrainian parts of the study region. Finally, areas where forests expanded on non-forest land were abundant throughout the study region during the transition period and the highest rates were found in North Eastern Hungary during the EU accession period (62% of the 1985 forest area).

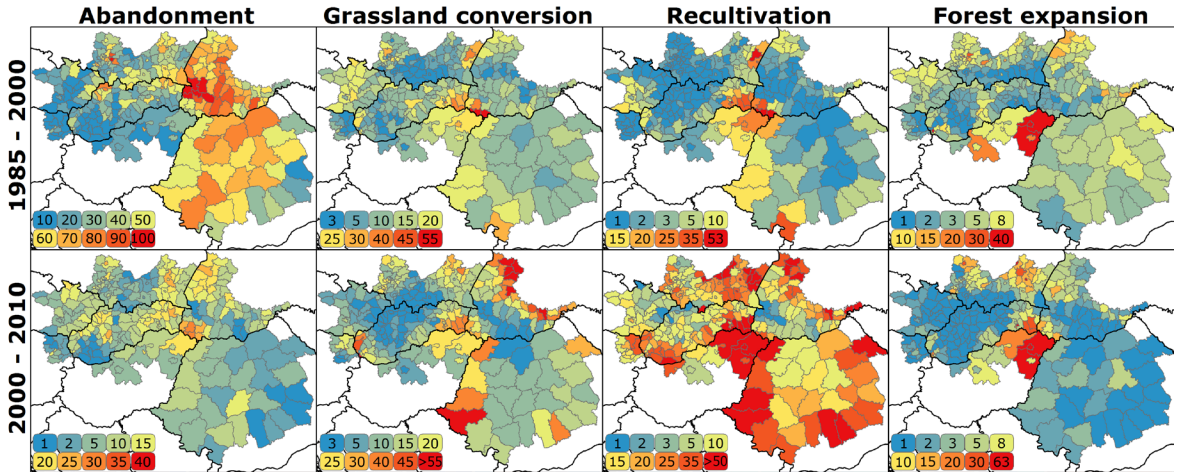


Figure V-4: Process maps showing rates of cropland abandonment, grassland conversion, recultivation and forest expansion summarized to the level of administrative units (NUTS3 for Romania, Hungary and Austria; district level for Poland, Ukraine, Slovakia and the Czech Republic). The top row shows the rates for the transition period (1985 - 2000) the bottom row provides rates for the EU accession period (2000 – 2010). Note: different color table scaling for the two periods of cropland abandonment rates.

The comparison of abandonment rates at administrative levels with agro-environmental suitability revealed predominantly negative correlations, i.e., higher suitability is associated with lower abandonment rates (figure 5). This was most pronounced during the transition period, for example, in the Czech part of the study region ($R^2$ of -0.68 in 2010) but still substantial in Austria, Romania, Slovakia and Ukraine (each around -0.53).

Abandonment rates during the EU accession period were considerably lower than during the earlier period and the correlations were consistently smaller. In Ukraine, abandonment rates tended to be higher in areas with greater crop suitability. As expected, recultivation predominantly occurred in more suitable areas in all countries and both periods (except in Ukraine with R2=0 in the transition period), and this association was considerably stronger in most countries in the EU accession period (figure 6).

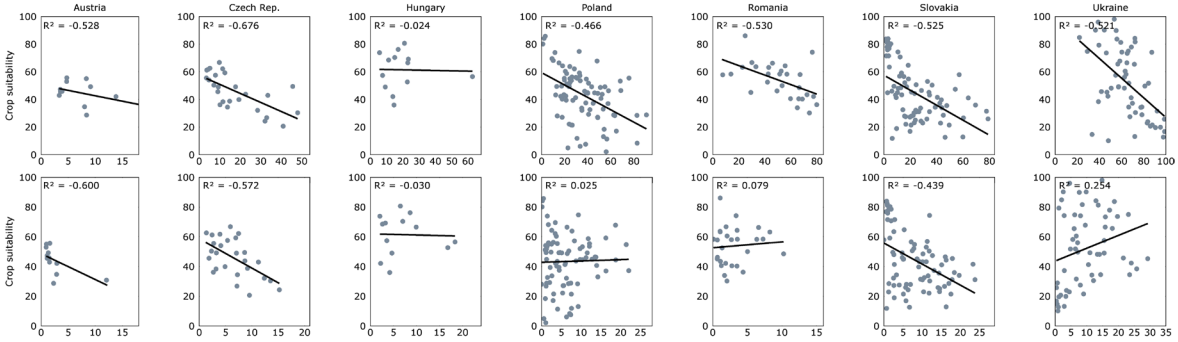


Figure V-5: Comparison of the average crop suitability index (Y axis) and cropland abandonment rates (X axis) aggregated to administrative units. Results are provided for the transition period (top) and the EU accession period (bottom).

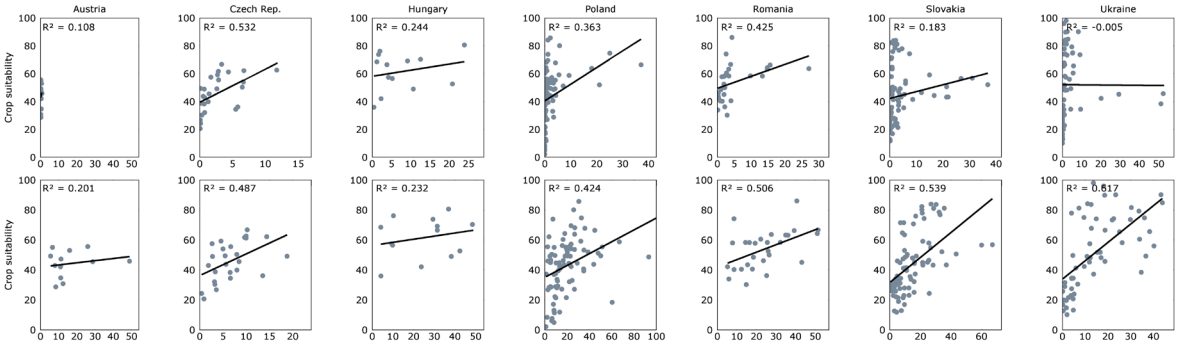


Figure V-6: Comparison of the average crop suitability index (Y axis) and recultivation rates (X axis) aggregated to administrative units. Results are provided for the transition period (top) and the EU accession period (bottom).

After adjusting our error estimates for class proportions, the validation suggested an overall high reliability with 90% overall accuracy despite the challenging class catalogue (table 3). Most stable classes were mapped with user's and producer's accuracies of >80%. The best performing change class was grassland-forest conversions (G-F-F). Cropland-grassland conversion classes achieved high accuracies and conversion detected during the transition period achieved 86% producer's accuracy but a lower user's accuracy (65%).

Table V-3: Validation results providing the confusion matrix as well as overall, user's and producer's accuracy for the change map derived from the analysis of the 9 seasonal composites and spectral variance metrics (Note: the producer's accuracy was obtained from the area adjusted error assessment).

| | Overall accuracy: | Reference | | | | | | | | | | | | | | | |
|---|---|---|---|---|---|---|---|---|---|---|---|---|---|---|---|---|---|
| | 90.29% | CCC | CCF | CCG | CFF | CGC | CGF | CGG | BBB | GGG | GCC | GFF | GGC | GGF | WWW | FFF | User's accuracy: |
| Classification | CCC | 39 | 1 | 2 | - | - | - | - | 1 | - | 1 | - | - | - | - | - | 88.6% |
| | CCF | 3 | 20 | - | 4 | - | 4 | 2 | - | - | - | 1 | - | 3 | - | - | 54.1% |
| | CCG | 7 | - | 26 | - | - | - | 5 | - | 3 | 1 | - | - | - | - | - | 61.9% |
| | CFF | - | - | - | 23 | - | 2 | 2 | - | 3 | - | 12 | - | 3 | 1 | - | 50.0% |
| | CGC | 19 | - | - | - | 13 | - | 1 | - | 3 | - | - | 1 | - | 1 | - | 34.2% |
| | CGF | - | 2 | - | 2 | - | 16 | 2 | - | 4 | - | 3 | - | 7 | - | - | 44.4% |
| | CGG | 5 | - | 5 | - | 2 | - | 30 | - | 4 | - | - | - | - | - | - | 65.2% |
| | BBB | - | - | - | - | - | - | 1 | 41 | 3 | - | - | - | - | 2 | - | 87.2% |
| | GGG | - | - | - | - | - | - | 1 | - | 43 | - | - | - | 1 | - | - | 95.6% |
| | GCC | 11 | - | 2 | - | - | - | 2 | 1 | 3 | 20 | - | 1 | - | - | - | 50.0% |
| | GFF | - | - | - | - | - | - | - | - | - | - | 48 | - | 1 | - | 1 | 96.0% |
| | GGC | 3 | - | - | - | - | - | - | - | 14 | 2 | - | 20 | - | - | - | 51.3% |
| | GGF | - | - | 1 | - | - | - | 1 | - | 2 | - | 8 | - | 32 | - | - | 72.7% |
| | WWW | - | - | - | - | - | - | - | - | - | - | - | - | - | 46 | - | 100.0% |
| | FFF | - | - | - | - | - | - | - | - | - | - | - | - | - | - | 49 | 100.0% |
| | Sum | 87 | 23 | 36 | 29 | 15 | 22 | 47 | 43 | 82 | 24 | 72 | 22 | 47 | 50 | 50 | |
| | Producer's accuracy: | 86.8% | 10.5% | 36.6% | 78.0% | 69.6% | 86.2% | 85.6% | 77.9% | 93.8% | 54.3% | 87.5% | 55.7% | 41.3% | 82.6% | 99.9% | |

## 4 Discussion

We provide the first assessment of recent agricultural land change over the entire Carpathians at 30m spatial detail. Our rates compare well to previous case studies in the region. For example, Kuemmerle et al. (2009c) detected 21% of abandoned cropland between 1990 and 2000. Our results suggest somewhat a higher abandonment rate of 24%. Likely reasons explaining these moderate differences are discrepancies in the abandonment definitions (the former study focused on cropland-grassland conversions while our study also considers cropland-forest conversions). Baumann et al. (2011) assessed 46% of post-socialist farmland abandonment in the Ukrainian Carpathians (but for a smaller area) between 1986 and 2008, which is about 12% below our estimate. Moreover, our abandonment rates are highest in the mountainous districts, while Baumann et al. (2011) found the highest rates to occur in the plains. The differences in spatial patterns likely result from different methodological approaches for change detection. Moreover, we used three observations per time step and therefore are more likely to capture land management (e.g. ploughing, harvesting) compared to Baumann et al. (2011) who used two images to characterize the 1980s. Regarding grassland conversion, a case study conducted in the Carpathians forelands in Hungary (Biró et al. 2013) based on military survey maps

assessed an annual conversion rate of 1.3% between 1988 and 1999 and a lower rate (0.35%) for the period from 1999 to 2010. While the first rate agrees very well with our current assessment of grassland conversion rates in the Hungarian part of the study region, our results suggest a similar conversion rate for recent years (table 3).

Our change map had a relatively high accuracy despite complex change classes. This underlines the value of the Landsat archive and of the compositing approach, which allow assessing unprecedented detail of change patterns with satellite data at regional scales. However, a few sources of uncertainty remain. Generally, our approach works very well as long as the landscape elements (e.g. agricultural fields) provide sufficient spectral contrast in the different seasonal composites. But many agricultural areas underwent substantial structural changes that led to the fragmentation of large collectively managed cropland plots, accompanied by a diversification of ownership and crop types within small areas. If a large cropland plot in 1985 experienced such fragmentation, the reflectance signal subsequently becomes a mixture of different components (e.g. soil, grass, crop), which compromises accurate detection (Ozdogan and Woodcock 2006). In these cases, our approach may have detected some of the decrease in spectral contrast as, for example, a change from cropland to grassland.

Overall though, our results corroborate the extensive land changes that occurred throughout the Carpathians between 1985 and 2010. Cropland abandonment was most widespread and 24% of the 1985 cropland and a further 11% of the 2000 cropland were no longer cultivated in 2000 and 2010, respectively. Interestingly, agro-ecological suitability showed strong linkages with agricultural abandonment and recultivation. The highest abandonment rates generally occurred on lands that are marginally suited for farming and in the years immediately following the collapse of socialism, as observed elsewhere in Eastern Europe (Müller and Munroe 2008; Mueller et al. 2009; Prishchepov et al. 2013). This suggests that post-socialist cropland abandonment in the Carpathians was strongly contingent on socialist farming strategies that subsidized substantial expansion of agricultural land use in order to increase outputs. As a result, most cultivable land was used for farming, including marginal areas. The collapse of socialism led to a massive drop in state support for agriculture as well as adjustments in input and output prices (Rozelle and Swinnen 2004). Moreover, land reforms led to the privatization and restitution of agricultural land resulting in a large number of small fragmented farms particularly in mountainous regions (Lerman et al. 2004). Combined, these changes grossly affected

agricultural production and caused significant amounts of cropland abandonment throughout the Carpathians.

Interestingly, the rates of cropland abandonment tend to be higher in countries of the former Soviet Union than in Eastern Europe, similar to results from other studies. For example, cropland abandonment rates of up to 50% were found in the Baltics and in the Russian enclave of Kaliningrad (Nikodemus et al. 2005), but abandonment was much lower in neighboring Poland (Prishchepov et al. 2012a) and in the non-Soviet countries in our study region (all except Ukraine). Arguably, more determined support for agriculture during socialism in the former Soviet Union, including the nationalization of land, contributed to the higher adaptation of land use after the collapse of socialism.

Recultivation rates were modest during the early phases of the post-socialist transition (totaling 4% of the 1985 grassland area). Compared to the extent of cropland that was abandoned during the transition period, about 18% were brought back into production during the EU accession period. Recultivation was pronounced since 2000 in all countries, and highest in Romania. It concentrated in areas favorable for farming (as forecasted by Lakes et al. (2009) for Southern Romania). Increasing profit opportunities in agriculture due to rising commodity prices since 2007 are likely the key underlying driver for the recultivation of cropland. Possibly, support through EU CAP contributed additional incentives for recent recultivation. In the coming years, expected further increases in agricultural commodity prices will likely provide additional incentives for recultivation of areas suitable for agricultural production. Furthermore, future biofuel production and the increasing demand for food, feed and fiber will compete with the requirement for nature protection in pristine landscapes like many parts of the Carpathian ecoregion. However, most future changes in land systems may not manifest in categorical changes of land use, as we have assessed, but in land use modifications (e.g. growing capital inputs in agriculture (Kuemmerle et al. accepted)), which still pose considerable challenges for remote sensing based monitoring approaches (Lambin and Linderman 2006). Because crop yields are still modest in many areas of the Carpathian ecoregion, increasing land use intensity may translate into considerable production gains on currently used lands (Kuemmerle et al. accepted).

**Acknowledgements**

This research was funded by the Belgian Science Policy Research Program for Earth Observation STEREO II, contract SR/00/133, as part of the FOMO project (Remote sensing of the forest transition and its ecosystem impacts in mountain environments). PH's contribution to this research is part of his activities in the Global Land Project and the Landsat Science Team. TK acknowledges support through the Einstein foundation and the European Union (VOLANTE, FP7-ENV-2010-265104).

# Chapter VI:
# Synthesis

## 1 Summary

Land use is central to human livelihoods but global land change and the conversion of natural ecosystems has a reached a critical degree and is threatening to undermine Earth's self-regulating abilities and thus human wellbeing (MEA 2005; Lenton et al. 2008). With a projected world population of 9 billion people during the 21st century, increasing affluent lifestyles, and ever growing resource consumption, accompanied by an increasing scarcity of arable land, it is a grand challenge for humanity to transition global land use towards sustainability (Lambin and Meyfroidt 2011; Tilman et al. 2011; Weinzettel et al. 2013). In order to mitigate the negative consequences of global land change on the environment, a better understanding of where and when land change occurs is required. Based on the patterns of change, a better understanding of the causal mechanisms that drive land change can be derived, especially regarding underlying drivers. This is important because increasing globalization, numerous competing interests for scarce land resources, and increasing influences of distant markets require a better understanding of what drives land change decisions. In this context, remote sensing is the most important tool to monitor land change in different geographical settings and the opening of the Landsat archive offers promising new opportunities, but also poses new challenges for remote sensing analyses.

This dissertation improves land change monitoring capabilities and investigates land change in the Carpathian ecoregion since the mid-1980s. The Carpathians are a unique study region for several reasons and during the last three decades, two drastic socio-economic transformations affected the regional land systems, but how these processes affected land use is not clear and the spatial patterns and temporal rates of recent land change remains largely unknown. A prerequisite to assess recent land changes in the Carpathians is to improve remote sensing analysis methodologies, especially regarding the sensitivity to non-linear and abrupt changes, as well expanding change mapping capabilities onto regional scales with appropriate spatial detail. The Landsat archive provides us with unique opportunities to do this.

My dissertation consisted of four core chapter, each mainly addressing one research question. In the following, each research questions is addressed and answered before the main conclusions are presented and future research requirements are discussed.

*Research Question I (Dissertation chapter II):* How can refined image analysis approaches better utilize the temporal depth of the Landsat archive in order to improve our

understanding of how rates and patterns of forest disturbance changed during massive ownership changes?

In Chapter II, a trajectory-based change detection approach was employed to derive annual forest disturbances along with forest growth and recovery dynamics in order to better understand how massive forest ownership changes in the Romanian Carpathians affected local harvesting patterns. Results showed that overall, each restitution phase was followed by increasing disturbance levels and that these levels continuously increased from the first to the third restitution phase. When the disturbance levels were considered on an annual interval, distinct temporal patterns were revealed: comparatively low disturbance levels during the late socialist years, followed by a drastic drop during the early transition period and then sharply increasing again following the first and second restitution phase, whereas disturbance levels exhibited a slightly decreasing tendency following the 2005 restitution law. Correspondingly, annual results also illustrated elevated disturbance levels in restituted forests (i.e. private forest districts) following the ownership transfer, and moreover that in some cases disturbance rates sharply increased right after forest management was taken over by non-state forest owners associations. My results additionally showed that peak disturbance levels following the restitution laws only occurred with considerable delay, especially following the first restitution phase. Such detailed, non-linear temporal dynamics would not have been understood using a temporal resolution of five or 10 years. Therefore, this study clearly exemplified the value of working with an increased temporal observation interval, and specifically working at an annual temporal resolution in the face of rapid socio-economic changes.

*Research Question II (Dissertation chapter III):* How can image datasets of regional extent be derived from the Landsat archive and how can these datasets be used for broad-scale land cover mapping and change detection?

In Chapter III, I described the development of a compositing algorithm for Landsat data. The algorithm produced cloud free image composites from data available from over 40 Landsat footprints and the achieved spatial extent was close to the coverage of a MODIS tile. Methodologically such an approach has become more practicable recently due to data with unprecedented geometric accuracy, automated atmospheric correction and cloud/shadow masking approaches, of which my algorithm takes full advantage of. Thus, my results prototype Landsat level-3 gridded image products which have so far not been produced operationally.

My composting algorithm achieved considerable annual, seasonal and radiometric consistency in the output image datasets. The results clearly showed that, the assumption of seasonal suitability trumping annual suitability is generally valid for many applications, and that this generally aids to the overall consistency and applicability of the resulting image composites. Incorporation of multi-year observations into composited datasets however is needed, especially in a mountainous environment with reduced image availability. Larger deviations from seasonal or annual targets were largely restricted to the composite boundaries or to areas with topographically caused quasi-permanent cloud cover. Results additionally showed that spectral correspondence to MODIS reflectance products was substantial and prevailed throughout the regional coverage but was highest when more spectrally stable land cover types such as forests were compared.

The overall consistency of the results was further underlined through land cover classifications, for which "global" models were trained using an interpreted random point sample for training, and classes were delineated successfully across the entire composited datasets. Additionally, these results demonstrated the usefulness of spectral-temporal variability metrics, which when included improved class delineations and prevented compositing artifacts to translate into classification results. However, certain land cover classes (e.g. grassland) were less well delineated and therefore require specific efforts regarding features and training data (for example, as those used in Chapter V).

The central feature of my compositing algorithm is the parametric evaluation and scoring of image and metadata characteristics for each available pixel observation. The presented approach can be easily extended to include additional parameters whereas established compositing approaches commonly relied on a single and often spectral criterion for compositing. My algorithm allows creating application-specific image datasets that are well suited for regional change analyses. For example, within Chapter IV, I created a series of mid-summer leaf-on image datasets that are allow capturing forest cover changes over time and over large regions. In Chapter V the algorithm was parameterized to approximate specific seasonal states (i.e. spring, summer, and fall) in the output composites, which capture the most crucial phenological characteristics of agricultural land use and changes therein.

Overall, the results presented in this study clearly demonstrate that automated algorithms can be designed to mine the Landsat archive for available cloud free pixel observations and to generate new regional image datasets. For this study the Landsat archive contained

several thousand scenes, but these featured considerably high levels of cloud cover. Simple land cover mapping with Landsat data as performed in Chapter III would have been very costly a few years or a decade ago, in terms of manual processing efforts, data costs and likely post-processing requirements in order to achieve consistency of results.

These results denote a paradigm shift in Landsat processing with the basic unit of operation becoming the individual pixel and no longer being the individual scene. This has several important methodological implications, as for example individual pixel observations can now be extracted from largely cloud obscured or erroneous imagery (e.g. SLC-off data) and the utilization of across-track overlaps between footprints potentially reduces the effective revisit times to 8 days (this does however not apply to equatorial latitudes).

*Research Question III (Dissertation chapter IV):* What were the rates and spatial patterns of forest cover changes in the Carpathians since 1985?

Chapter IV utilized a series of ecoregion wide, leaf-on image composites to map the distribution of broad forest types, as well as rates and patterns of forest disturbances and recovery from disturbance since 1985. Results indicated considerable differences regarding the forest composition in the individual countries, with some countries being dominated by deciduous forests (e.g. Hungary with roughly 80%), while coniferous forests accounted for a much greater share of the Carpathian forests in other countries (e.g. Poland, Czech Republic with more than 40%).

The results clearly showed that forest cover in the Carpathians changed substantially over the past 25 years. While Chapters IV and V both indicate that overall forest cover seems to have increased slightly, considerable changes in the composition of the forests in the Carpathians occurred. Overall, coniferous forests (and to a lesser degree mixed forests) decreased in favor of increasing deciduous forests and the strongest decrease in coniferous forests occurred in Romania and Ukraine, but was still substantial in other countries (compare Figure IV-3). Roughly a fifth of the forests in the Carpathians experienced stand replacing disturbances since 1985, but disturbance trends differed among and within countries. Overall, highest disturbance levels occurred between 1985/1990 and then dropped considerably during the early and especially later transition years.

The spatial-temporal disturbance patterns became very clear when disturbances were aggregated to administrative units (Figure IV-6). For example, the Czech, western Polish and Ukrainian Carpathians were major disturbance hotspots until 1995, but disturbance levels in these areas dropped drastically starting in 2000. The overall trend of highest

disturbance levels occurring during the late socialist years did not apply uniformly (Figure IV-5). In the Romanian Carpathians disturbance levels were comparably low during the late socialist years, then increased until 1995/2000 but decreased thereafter. In Ukraine, disturbance levels were already high for 1985/1990 and then increased markedly for 1990/1995, but decreased continuously afterwards. Within country differences were pronounced in the Polish Carpathians, where forest disturbances were widespread in the west but almost absent in the east (compare Figure IV-6).

Results moreover clearly showed that over time disturbances increasingly occurred in coniferous forests, and especially so in the Czech, Polish and Slovakian Carpathians. Post disturbance recovery was strong in Hungary, Romania and Ukraine but much less pronounced in other countries. Balancing forest increases, recovery and disturbances from the results of Chapter IV, net forest change showed unmistakably negative tendencies in the border region of Poland, Slovakia and the Czech Republic, while the northern parts of the Polish and Ukrainian Carpathians, north eastern Hungary and western central Romania clearly exhibited positive tendencies indicating forest cover increases (compare Figure IV-6C).

In Chapter V, I assessed the rates and spatial patterns of forests expanding on non-forest land, and the trends described above were largely reflected for the northern Polish and Ukrainian Carpathian forelands, suggesting that much of the forest cover increase in these areas rated to successional forest growth on abandoned agricultural land. On the other hand, positive net changes in forest cover assessed in Chapter IV for the western Romanian Carpathians seem to be rather related to forests recovering from disturbances that occurred prior to 1985.

*Research Question IV (Dissertation chapter V):* What were the rates and spatial patterns of agricultural land change in the Carpathians since 1985?

In Chapter V, I quantified agricultural land change processes in the Carpathians. Very different land change trajectories were relevant for specific areas while being virtually absent in other areas. Individual land change trajectories were then aggregated to broader agricultural land change processes, namely cropland abandonment, grassland conversion, recultivation and forest expansion on non-forest land (compare Table V-1).

Results showed that agricultural land change was overall widespread in the Carpathians. Cropland abandonment was the most abundant change process, and in 2000 about 24% of the 1985 cropland area was either no longer used or converted to other uses (e.g. grassland,

forest plantations). Between 2000 and 2010 cropland abandonment was less prevalent and only accounted for 9% of the 1985 cropland area. Results further suggested that socialist cropland in remote, marginal mountain areas was completely abandoned following the collapse of socialism. My results moreover clearly demonstrated that cropland abandonment predominantly occurred within areas that are less favorable for crop cultivation.

On the national level, Romania and Ukraine had the highest abandonment rates in the Carpathians. Grasslands were also frequently converted to other uses, accounting for 10% of the 1985 grassland area on the pan-Carpathian level. Most countries experienced more conversion of grasslands between 2000 and 2010, while in the Czech Republic conversions between 1985 and 2000 were twice as extensive as during the later period and occurred spatially highly clustered (compare frame 1 in Figure V-3). Recultivation became very prevalent throughout the 2000/2010 period accounting for 18% of the cropland that was abandoned after 1985. On the national level, the most extensive recultivation occurred in Romania and Ukraine, but recultivation rates were also high in the Hungarian part of the study region. Recultivation patterns within Romania indicated that while cropland abandonment was widespread in the Transylvanian Basin, recultivation was less prevalent in those areas and much stronger in the Carpathian forelands. A distinct hotspot of agricultural land change was north eastern Hungary where abundant grassland conversion, afforestation and recultivation processes occurred (compare Figures V-3 and V-4).

## 2 Main conclusions

Remote sensing offers unique capabilities to monitor land change and the Landsat archive now allows advancing analytical approaches in order to overcome commonly encountered limitations of existing methods. Assessing when and where land change occurred is a first step to better understand the causal mechanisms behind those changes. The overarching goal of this dissertation is to develop an appropriate toolset that allows to map and analyze rates and patterns of land change in the Carpathians since the mid-1980s and to discuss and interpret these changes in the context of recent socio-economic transformations.

How did the two grand socio-economic transformations of the last quarter century, i.e., the collapse of socialism and the accession to the EU affect land change in the Carpathians? The results presented in Chapters IV and V clearly showed that the most drastic and widespread land changes occurred during the main transition period following the collapse

of socialism. The level of forestry activities was strongly impacted, and overall disturbance levels decreased considerably after 1990 while certain areas continued to experience high disturbance levels during the early transition years. Spatial patterns of forest disturbances changed drastically between 1995/2000 which was also reflected in most country-wise disturbance rates. Likely causes for the overall decline in disturbance levels were the profound restructuring and reformation of the forest management and timber processing industries (Csóka 2005). Moreover, high disturbance levels in some regions during the earlier transition years (compare Figures IV-5 & 6) were likely affected by unauthorized and in some cases presumably illegal timber cutting activities that have been reported for several areas (Brandlmaier and Hirschberger 2005; Kuemmerle et al. 2009a). The substantial forest ownership changes that occurred in many parts of the Carpathians during the transition period likely affected the increased logging activities locally as was clearly demonstrated for the central Romanian Carpathians in Chapter II. Uncertainties regarding the persistency of tenure rights and other problems connected to the restitution process presumably led new owners to favor immediate economic returns over long term forest management.

The results of Chapter IV and also Chapter II clearly showed that coniferous forests generally experienced higher disturbance levels. One the one hand this may be due to the fact that coniferous forest and especially the spruce monoculture plantations are very susceptible to wind throw damages, insect infestations or pest outbreaks. The differentiation of logging and natural disturbance causes in remote sensing data requires specific analytical approaches and is not easily feasible. However, this also raised the question of how “natural” such disturbances are, if they occurred in highly vulnerable monocultures (often of foreign genetic origin) and were commonly followed by salvage logging. Thus, legacies of past land systems shape today’s disturbance regimes to a certain extent, as large scale spruce establishment was initiated under Austro-Hungarian rule (Turnock 2002). Similarly, legacies of the Soviet system affect disturbance levels today. This is exemplified through the disturbance hotspot in the Polish, Slovakian and Czech border region identified in Chapter IV (compare Figure IV-9(B)), where pollution legacies of the socialist heavy industries additionally decreased forests’ resilience (Main-Knorn et al. 2009).

The effect of the collapse on the agricultural system in the Carpathians became clear through results presented in Chapter V. On the pan Carpathian level, cropland abandonment was widespread (24% of former socialist cropland), but most abandonment

occurred in Ukraine and Poland, while it was rather limited to isolated localities in other parts of the Carpathians. Overall, abandonment occurred as the socialist approach to agricultural production was no longer profitable, but also because rural outmigration changed age structures of rural areas and thus the employment potential in agriculture. However, strong differences, as those between the Ukrainian and Romanian Carpathians compared to the other countries, are likely related to differences in land ownership and property reforms as well as population distributions (Kuemmerle et al. 2008). Moreover, my results strongly support the general assumption that abandonment predominantly occurs on marginal land. While most abandonment occurred through cropland-grassland conversions, cropland was also converted to forests, both actively (through afforestation) and passively (through natural succession). The formers process relates to the fact that in several Carpathian countries government incentives existed to afforest (degraded) agricultural lands and land managers were encouraged to activated convert cropland to forests (World Bank 2007; Biró et al. 2013).

The effects of the EU accession on land changes in the Carpathians are generally more difficult to discern than those of the collapse of socialism, because countries became EU members in different years and the accession involved policy reforms that were initiated several years before. Land change patterns were of a different direction and magnitude than those following the collapse of socialism. The decreasing levels of forest disturbances continued on the pan Carpathian level after 2000. On the individual country level, disturbance levels in Ukraine continued to decrease, while most countries showed increased levels compared to the early transition years, but far below those levels observed during the last years of socialism (compare Figure IV-5). Most Carpathian countries had by now restructured their forest management and timber processing industries which increased the level of their activities and they were now able to sell products within the integrated EU timber market. Ukraine is the only country of those considered that does not have such direct access to the European market which likely affected the observed trends. The fact that disturbance levels were overall considerably lower than during the late 1980s is likely related to a general shift from economically motivated forest management and timber processing (typical for the socialist period) towards more sustainable forest management and an increasing valuation of other forest related ecosystem services. Such a shift would match European policies and specifically the guiding principles of sustainable forestry in Europe (UNECE and FAO 2011), and is supported by the observed decrease in coniferous forests and an increasing prevalence of more natural forest compositions. One

of the most recent pieces of European forestry policy, the 2013 EU timber regulation, specifically targets the reduction of illegal timber markets through monitoring and certification schemes. While illegal timber harvesting generally declined in the Carpathians after 2000 compared to the transition period, it will be even more so in coming years.

Agricultural land change during the EU accession period took a different direction than those changes observed after the collapse of socialism. The most widespread processes were the recultivation of abandoned cropland and the conversion of permanent grasslands. While spatial patterns of abandonment during the 1985-2000 period strongly accentuated the Romanian and Ukrainian Carpathians, recultivation was prevalent throughout the Carpathians as abandoned cropland was brought back into production. Most likely European agricultural policies will have impacted land managers decisions to recultivate as the CAP enables farmers to receive subsidies that make production economically more attractive again. Interestingly, recultivation was also prevalent in the northern Ukrainian Carpathian forelands and thus other reasons than the CAP will have played a role here. The sharp increase in global agricultural commodity prices during recent years may have made crop production viable again, as has been shown recently for example in the mid-western U.S. (Wright and Wimberly 2013). Moreover, many areas in Eastern Europe where agricultural production is facing yield gaps have, despite protective legal mechanisms, become attractive for foreign investments in agriculture as well as for large scale foreign land acquisitions (Foley et al. 2011). Indeed, recent recultivation focused heavily on the most productive lands, which might suggest that market opportunities and increased revenues are more important than subsidy payments. Additionally, EU biofuel directives provided incentives for farmers to produce energy crops which led to widespread land changes throughout Europe (Borras and Franco 2012).

So what were the likely effects of the assessed land changes in the Carpathians on ecosystem services? First, regional carbon balances likely profited from the net forest cover increase that became evident from the results in Chapters IV and V. Based on carbon bookkeeping models, Ukrainian and Romanian forests changed from net carbon source to carbon sink over the past decades (Kuemmerle et al. 2011), but the effects of the restitution process could still result in net carbon emissions in Romania (Olofsson et al. 2011). Increased soil carbon sequestration occurred since the conversion of more than 30,000 km² of former socialist cropland into grassland or other land cover types. Potentially, this also affected different components of the regional hydrologic system positively (DLG 2005). While abandonment will eventually result in successional forests and thus create new

forest habitats throughout the region which will positively affect biodiversity in some ways, the loss of low intensity traditional farming landscapes will have negative effects on biodiversity (Fischer et al. 2012; Navarro and Pereira 2012). Prevailing excessive logging in certain areas and large scale wind throw disturbances will on the other hand increase the risk of flash flooding and landslides (Turnock 2002). Moreover, some logging activities are threatening remaining old growth forest and the integrity of protected areas and are calling for improved conservation efforts (Knorn et al. 2012a; Knorn et al. 2012b).

Results from this thesis clearly underline the value long term remote sensing archives in general and the Landsat archive specifically for reconstructing past land change. Open access to the extensive Landsat data record, the radiometric and geometric accuracy of Landsat data as well as new automated preprocessing algorithms have led to a paradigm change for Landsat data analysis where now the entire archive can be mined for the best observations on a per-pixel basis and new datasets specifically tailored for certain applications can be created. As my dissertation demonstrated, increased temporal observation frequency can allow for unprecedented process understanding during turbulent socio-economic circumstances. Compositing of the Landsat archive allows for the generation of consistent large area image datasets that can be used for cost effective land cover mapping and change detection. It would be ideal to have both - a high temporal detail and a large regional extent - but in reality this is not easily feasible as there are tradeoffs related to both approaches.

For example, while temporal segmentation and fitting of Landsat time series offers several key advantages (e.g. reduction of residual noise due to topographic shading) it simultaneously poses specific requirements on the imagery that is used. Moreover, the ability to describe subtle change processes through increased signal-to-noise ratio or the high disturbance detection without requirements for supervised training strongly depend on the quality of the time series, specifically the consistency of the provided anniversary dates. For analyses conducted in areas with strong seasonality, the incorporation of early or late acquisitions will considerably lower the quality of the fitted time series. In any event, data availability might not allow for an annual resolution without inclusion of such dates, especially in areas with scarce data availability or prevalent cloud coverage (Ju and Roy 2008; Huang et al. 2009).

Additionally, annual resolution is well suited to quantify many forest processes and moreover seems to be congruent with the annual interval of policy decisions. Nevertheless,

the Landsat archive provides even greater temporal depth than that. Yet, most algorithms for image classification, time series fitting or change detection require equidistant observations, and the Landsat archive is highly heterogeneous regarding the density and timing of observations, from the regional down to the pixel level. Thus, the full temporal record is not easily utilized in semi-operational approaches. Deriving new features from the full archive record, such as the spectral-temporal variability metrics that I utilized in this study can do that. Such metrics implicitly utilize the full temporal depth of the Landsat record. The developed compositing algorithms and the parametric decision scheme allow for the creation of radiometrically and seasonally consistent and application specific datasets and metrics which allow the quantification of complex land change trajectories over regional to continental scales. Thus in coming years, nested multi-scale approaches that utilize deep time series approaches alongside large area compositing approaches can be pursued.

This dissertation demonstrated the exceptional value of the Landsat archive for land change research and how improved temporal and extended spatial capabilities can improve pattern-process understanding. Landsat time series approaches provide unprecedented detail of land changes during turbulent socio-economic conditions when these processes often occur non-linearly. Compositing approaches on the other hand allow for cost effective wall-to-wall mapping of land cover and large area change detection regardless of administrative or ecological boundaries. By applying the developed toolset to the full Landsat record, land changes over the extended Carpathian ecoregion could be reconstructed with great detail. My results illustrate how forest cover and agricultural land changed in the Carpathians during major socio-economic restructuring. Land changes following the collapse of socialism were overall more drastic and widespread than those following the EU accession but were also of a different quality, i.e. strongly declining activities the forestry and agricultural sectors following the collapse and increasing levels of land use activities in both sectors following the EU accession. The results indicate the importance of underlying drivers of land change and an increasing importance of distant markets and transnational policies. The land change products created during this dissertation will allow for many interesting follow-up studies for which such datasets are a prerequisite. Enhanced land change monitoring capabilities as those developed in this dissertation will allow for a more thorough understanding of global land change and thus aid mitigating its negative consequences and help meeting the grand challenges that humanity faces today.

# References

Abrudan, I.V., Blujdea, S., Brown, V., Kostuhin, C., Pahontu, H., Phillips, H., & Voicu, M. (2003). Prototype Carbon Fund: Afforestation of degraded agricultural land in Romania. *Revista Padurilor, 118*, 5-17.

Abrudan, I.V., Marinescu, V., Ionescu, O., Ioras, F., Horodnic, S.A., & Sestras, R. (2009). Developments in the Romanian Forestry and its Linkages with other Sectors. *Notulae Botanicae Horti Agrobotanici Cluj-Napoca, 37*, 14-21.

Abrudan, I.V., Marinescu, V., Ignea, G., Codreanu, C. (2005). Present situation and trends in Romanian forestry. In Ioan Vasile Abrudan, F.S., Peter Herbst (Ed.) *Legal Aspects of European Forest Sustainable Development, Proceedings of the 6th International Symposium*, Poiana Brasov, Romania (pp. 157 - 171).

Anfodillo, T., Carrer, M., Valle, E.D., Giacoma, E., Lamedica, S., & Pettenella, D. (2008). *Current State of Forest Resources in the Carpathians*, Activity 2.7: Forestry and timber industry. Legnaro: Università Degli Studi Di Padova, Dipartimento Territorio e Sistemi Agro-Forestali.

Arino, O., Bicheron, P., Achard, F., Latham, J., Witt, R., & Weber, J.-L. (2008). GLOBCOVER The most detailed portrait of Earth. *Esa Bulletin-European Space Agency*, 24-31.

Arvidson, T., Goward, S., Gasch, J., & Williams, D. (2006). Landsat-7 long-term acquisition plan: Development and validation. *Photogrammetric Engineering and Remote Sensing, 72*, 1137-1146.

Aschbacher, J., & Milagro-Perez, M.P. (2012). The European Earth monitoring (GMES) programme: Status and perspectives. *Remote Sensing of Environment, 120*, 3-8. In English.

Atzberger, C., & Richter, K. (2012). Spatially constrained inversion of radiative transfer models for improved LAI mapping from future Sentinel-2 imagery. *Remote Sensing of Environment, 120*, 208-218. In English.

Badea, O., Anisoara, L., Georgeta, J., Peiov, A., Pajtik, J., Shparyk, Y., Tanase, M., Uhlirova, H., & Wawrzoniak, J. (2004). Forest health status in the Carpahian Mountains over the period 1997-2001. *Environmental Pollution, 130*, 93-98.

Banaduc, A., Feiler, J., Lelmen, A., Malbasic, I., Mititean, R., Petruta, M. (2002). *Comments on the Romanian Forestry Development Program (Loan No. RO-P067367, World Bank)*. World Bank.

Barona, E., Ramankutty, N., Hyman, G., & Coomes, O.T. (2010). The role of pasture and soybean in deforestation of the Brazilian Amazon. *Environmental Research Letters, 5*.

Bartholome, E., & Belward, A.S. (2005). GLC2000: a new approach to global land cover mapping from Earth observation data. *International Journal of Remote Sensing, 26*, 1959-1977.

Baumann, M., Kuemmerle, T., Elbakidze, M., Ozdogan, M., Radeloff, V.C., Keuler, N.S., Prishchepov, A.V., Kruhlov, I., & Hostert, P. (2011). Patterns and drivers of post-socialist farmland abandonment in Western Ukraine. *Land Use Policy, 28*, 552-562.

Baumann, M., Ozdogan, M., Kuemmerle, T., Wendland, K.J., Esipova, E., & Radeloff, V.C. (2012). Using the Landsat record to detect forest-cover changes during and after the collapse of the Soviet Union in the temperate zone of European Russia. *Remote Sensing of Environment, 124*, 174-184.

Bellard, C., Bertelsmeier, C., Leadley, P., Thuiller, W., & Courchamp, F. (2012). Impacts of climate change on the future of biodiversity. *Ecology Letters, 15*, 365-377.

Bennett, E.M., Carpenter, S.R., & Caraco, N.F. (2001). Human impact on erodable phosphorus and eutrophication: A global perspective. *Bioscience, 51*, 227-234.

Berger, M., & Aschbacher, J. (2012). Preface: The Sentinel missions—new opportunities for science. *Remote Sensing of Environment*.

Biró, M., Czúcz, B., Horváth, F., Révész, A., Csatári, B., & Molnár, Z. (2013). Drivers of grassland loss in Hungary during the post-socialist transformation (1987–1999). *Landscape Ecology, 28*, 789-803. In English.

Björnsen Gurung, A., Bokwa, A., Chełmicki, W., Elbakidze, M., Hirschmugl, M., Hostert, P., Ibisch, P., Kozak, J., Kuemmerle, T., Matei, E., Ostapowicz, K., Pociask-Karteczka, J., Schmidt, L., van der Linden, S., & Zebisch, M. (2009). Global Change Research in the Carpathian Mountain Region. *Mountain Research and Development, 29*, 282-288.

Bonan, G.B. (2008). Forests and climate change: Forcings, feedbacks, and the climate benefits of forests. *Science, 320*, 1444-1449.

Borras, S.M., Jr., & Franco, J.C. (2012). Global Land Grabbing and Trajectories of Agrarian Change: A Preliminary Analysis. *Journal of Agrarian Change, 12*, 34-59.

Bouriaud, L. (2005). Causes of illegal logging in Central and Eastern Europe. *Small-Scale Forestry, 4*, 269-291.

Brandlmaier, H., & Hirschberger, P. (2005). *Illegal logging in Romania*. Comissioned and published by WWF European Forest Programme and the Danube Carpathian Programme (DCP).

Breiman, L. (2001). Random forests. *Machine Learning, 45*, 5-32.

Broich, M., Hansen, M.C., Potapov, P., Adusei, B., Lindquist, E., & Stehman, S.V. (2011). Time-series analysis of multi-resolution optical imagery for quantifying forest cover loss in Sumatra and Kalimantan, Indonesia. *International Journal of Applied Earth Observation and Geoinformation, 13*, 277-291.

Caccetta, P., Furby, S., O'Connell, J., Wallace, J., & Wu, X. (2007). Continental monitoring : 34 years of land cover change using Landsat imagery. In, *Proceedings of 32nd International Symposium on Remote Sensing of Environment*. Costa Rica

Canty, M.J., & Nielsen, A.A. (2008). Automatic radiometric normalization of multitemporal satellite imagery with the iteratively re-weighted MAD transformation. *Remote Sensing of Environment, 112*, 1025-1036.

Card, D.H. (1982). Using known map category marginal frequencies to improve estimates of thematic map accuracy. *Photogrammetric Engineering and Remote Sensing, 48*, 431-439.

Cartwright, A. (2000). AGAINST 'DECOLLECTIVISATION': LAND REFORM IN ROMANIA, 1990-1992 PERSPECTIVE. In, *MAX PLANCK INSTITUTE FOR SOCIAL ANTHROPOLOGY WORKING PAPERS* (pp. 1-20). Halle / Saale: Max Planck Institute for Social Anthropology.

CERI (2001). *The status of the Carpathians*, WWF - Danube-Carpathian Programme. Vienna, Austria: Carpathian Ecoregion Initiative.

Chander, G., Markham, B.L., & Helder, D.L. (2009). Summary of current radiometric calibration coefficients for Landsat MSS, TM, ETM+, and EO-1 ALI sensors. *Remote Sensing of Environment, 113*, 893-903.

Chander, G., Xiong, X., Choi, T., & Angal, A. (2010). Monitoring on-orbit calibration stability of the Terra MODIS and Landsat 7 ETM+ sensors using pseudo-invariant test sites. *Remote Sensing of Environment, 114*, 925-939.

Chavez, P.S. (1996). Image-based atmospheric corrections revisited and improved. *Photogrammetric Engineering and Remote Sensing, 62*, 1025-1036.

Chazdon, R.L. (2008). Beyond deforestation: Restoring forests and ecosystem services on degraded lands. *Science, 320*, 1458-1460.

Choudhury, B.J., Digirolamo, N.E., & Dorman, T.J. (1994). A comparison of reflectances and vegetation indices from three methods of compositing the AVHRR-GAC data over Northern Africa. *Remote Sensing Reviews, 10*, 245-263.

Cihlar, J. (2000). Land cover mapping of large areas from satellites: status and research priorities. *International Journal of Remote Sensing, 21*, 1093-1114.

Cihlar, J., Manak, D., & Diorio, M. (1994). Evaluation of compositing algorithms for AVHRR data over land. *IEEE Transactions on Geoscience and Remote Sensing, 32*, 427-437.

Cioroianu, A. (2007). *Pe umerii lui Marx: o introducere în istoria comunismului românesc. [On Marxs Shoulders: an introduction to Romanian Communism]*.

Cochran, W.G. (1977). *Sampling Techniques*. New York, NY: Wiley.

Cohen, W.B., & Goward, S.N. (2004). Landsat's role in ecological applications of remote sensing. *Bioscience, 54*, 535-545.

Cohen, W.B., Yang, Z., & Kennedy, R. (2010). Detecting trends in forest disturbance and recovery using yearly Landsat time series: 2. TimeSync -- Tools for calibration and validation. *Remote Sensing of Environment, 114*, 2911-2924.

Coppin, P., Jonckheere, I., Nackaerts, K., Muys, B., & Lambin, E. (2004). Digital change detection methods in ecosystem monitoring: a review. *International Journal of Remote Sensing, 25*, 1565-1596.

Coppin, P.R., & Bauer, M.E. (1996). Digital change detection in forest ecosystems with remote sensing imagery. *Remote Sensing Reviews, 13*, 207 - 234.

Crist, E.P., & Cicone, R.C. (1984). A physically-based transformation of Thematic Mapper data - the TM Tasseled Cap. *IEEE Transactions on Geoscience and Remote Sensing, 22*, 256-263.

Csaki, C. (1990). Agricultural changes in Eastern-Europe at the beginning of the 1990s. *American Journal of Agricultural Economics, 72*, 1233-1242.

Csóka, P. (2005). Capital Management – the Forests in Countries in Transition – Welfare Impacts. In Innes, J.L., Hickey, G.M., Hoen; H.F. (Ed.) *Forestry and Environmental Change: Socio-economic and Political Dimensions*. Oxford: CABI Publishing.

Daily, G.C., Soderqvist, T., Aniyar, S., Arrow, K., Dasgupta, P., Ehrlich, P.R., Folke, C., Jansson, A., Jansson, B.O., Kautsky, N., Levin, S., Lubchenco, J., Maler, K.G., Simpson, D., Starrett, D., Tilman, D., & Walker, B. (2000). Ecology - The value of nature and the nature of value. *Science, 289*, 395-396.

Dearing, J.A., Braimoh, A.K., Reenberg, A., Turner, B.L., & van der Leeuw, S. (2010). Complex Land Systems: the Need for Long Time Perspectives to Assess their Future. *Ecology and Society, 15*.

DeFries, R.S., Foley, J.A., & Asner, G.P. (2004). Land-use choices: balancing human needs and ecosystem function. *Frontiers in Ecology and the Environment, 2*, 249-257.

Deininger, K. (2011). Challenges posed by the new wave of farmland investment. *Journal of Peasant Studies, 38*, 217-247.

Diaz, R.J., & Rosenberg, R. (2008). Spreading dead zones and consequences for marine ecosystems. *Science, 321*, 926-929.

DLG (2005). *Land abandonment, biodiversity, and the CAP. Land abandonment and biodiversity in relation to the 1st and 2nd pillars of the EU's Common Agricultural Policy; Outcome of an international seminar in Sigulda, Latvia, 7-8 October, 2004*. Utrecht, The Netherlands: The Netherlands, Government Service for Land and Water Management of the Netherlands (DLG).

Drusch, M., Del Bello, U., Carlier, S., Colin, O., Fernandez, V., Gascon, F., Hoersch, B., Isola, C., Laberinti, P., Martimort, P., Meygret, A., Spoto, F., Sy, O., Marchese, F., & Bargellini, P. (2012). Sentinel-2: ESA's Optical High-Resolution Mission for GMES Operational Services. *Remote Sensing of Environment, 120*, 25-36. In English.

Dudley, J.P., Ginsberg, J.R., Plumptre, A.J., Hart, J.A., & Campos, L.C. (2002). Effects of war and civil strife on wildlife and wildlife habitats. *Conservation Biology, 16*, 319-329.

FAO (2005). *Global Forest Resources Assessment 2005. Progress towards sustainable forest management.*, Forestry Papers. Rome, Italy: Food and Agriculture Organization of the United Nations.

FAO (2010). *Global Forest Resources Assessment 2010. Main Report.*, FAO Forestry Paper Rome, Italy: Food and Agriculture Organization of the United Nations.

Feranec, J., Hazeu, G., Christensen, S., & Jaffrain, G. (2007). Corine land cover change detection in Europe (case studies of the Netherlands and Slovakia). *Land Use Policy, 24*, 234-247.

Feranec, J., Jaffrain, G., Soukup, T., & Hazeu, G. (2010). Determining changes and flows in European landscapes 1990-2000 using CORINE land cover data. *Applied Geography, 30*, 19-35.

Fischer, J., Hartel, T., & Kuemmerle, T. (2012). Conservation policy in traditional farming landscapes. *Conservation Letters, 5*, 167-175.

Foley, J.A., Costa, M.H., Delire, C., Ramankutty, N., & Snyder, P. (2003). Green surprise? How terrestrial ecosystems could affect earth's climate. *Frontiers in Ecology and the Environment, 1*, 38-44.

Foley, J.A., DeFries, R., Asner, G.P., Barford, C., Bonan, G., Carpenter, S.R., Chapin, F.S., Coe, M.T., Daily, G.C., Gibbs, H.K., Helkowski, J.H., Holloway, T., Howard, E.A., Kucharik, C.J., Monfreda, C., Patz, J.A., Prentice, I.C., Ramankutty, N., & Snyder, P.K. (2005). Global consequences of land use. *Science, 309*, 570-574.

Foley, J.A., Ramankutty, N., Brauman, K.A., Cassidy, E.S., Gerber, J.S., Johnston, M., Mueller, N.D., O'Connell, C., Ray, D.K., West, P.C., Balzer, C., Bennett, E.M., Carpenter, S.R., Hill, J., Monfreda, C., Polasky, S., Rockstrom, J., Sheehan, J., Siebert, S., Tilman, D., & Zaks, D.P.M. (2011). Solutions for a cultivated planet. *Nature, 478*, 337-342.

Foody, G.M. (2002). Status of land cover classification accuracy assessment. *Remote Sensing of Environment, 80*, 185-201.

Friedl, M.A., Sulla-Menashe, D., Tan, B., Schneider, A., Ramankutty, N., Sibley, A., & Huang, X. (2010). MODIS Collection 5 global land cover: Algorithm refinements and characterization of new datasets. *Remote Sensing of Environment, 114*, 168-182.

Fritz, S., See, L., McCallum, I., Schill, C., Obersteiner, M., van der Velde, M., Boettcher, H., Havlik, P., & Achard, F. (2011). Highlighting continued uncertainty in global land cover maps for the user community. *Environmental Research Letters, 6*.

Furby, S., Caccetta, P.A., Wallace, J., Wu, X., O'Connell, J., Chia, J., Collings, S., Traylen, A., & Devereaux, D. (2008a). Continental scale land cover change monitoring in Australia using Landsat imagery. In, *Studying, Modelling and Sense Making of Planet Earth*. Mytilene, Lesvos, Greece

Furby, S.L., Caccetta, P., Wallace, J.F., Wu, X., O'Connell, J., Collings, S., Traylen, A., & Devereaux, D. (2008b). RECENT DEVELOPMENTS IN LANDSAT-BASED CONTINENTAL SCALE LAND COVER CHANGE MONITORING IN AUSTRALIA. *The XXI Congress of the International Society for Photogrammetry and Remote Sensing*, Beijing, China.

Gao, F., Masek, J.G., & Wolfe, R.E. (2009). Automated registration and orthorectification package for Landsat and Landsat-like data processing. *Journal of Applied Remote Sensing, 3*.

GLP (2005). *Science Plan and Implementation Strategy.*, IGBP Report No. 53/IHDP Report No. 19. Stockholm: IGBP Secretariat.

Godfray, H.C.J., Beddington, J.R., Crute, I.R., Haddad, L., Lawrence, D., Muir, J.F., Pretty, J., Robinson, S., Thomas, S.M., & Toulmin, C. (2010). Food Security: The Challenge of Feeding 9 Billion People. *Science, 327*, 812-818.

Google (2013). StreetView [online]. Available from: http://maps.google.com/help/maps/streetview/ [accessed 11.06.2013].

Goward, S.N., & Masek, J.G. (2001). Landsat - 30 years and counting. *Remote Sensing of Environment, 78*, 1-2.

Griffiths, P., Kuemmerle, T., Baumann, M., Radeloff, V.C., Abrudan, I.V., Lieskovský, J., Muntenau, C., Ostapowicz, K., & Hostert, P. (accepted). Forest disturbances, forest recovery, and changes in forest types across the Carpathian ecoregion from 1985 to 2010 based on Landsat image composites. *Remote Sensing of Environment*.

Griffiths, P., Kuemmerle, T., Kennedy, R.E., Abrudan, I.V., Knorn, J., & Hostert, P. (2012). Using annual time-series of Landsat images to assess the effects of forest restitution in post-socialist Romania. *Remote Sensing of Environment, 118*, 199-214.

Griffiths, P., Van der Linden, S., Kuemmerle, T., & Hostert, P. (2013). A pixel-based Landsat compositing algorithm for large area land cover mapping. *IEEE Journal of Selected Topics in Applied Earth Observations and Remote Sensing, PP*, 1-14.

Gutman, G., Byrnes, R., Masek, J., Covington, S., Justice, C., Franks, S., & Headley, R. (2008). Towards monitoring land-cover and land-use changes at a global scale: The Global Land Survey 2005. *Photogrammetric Engineering and Remote Sensing, 74*, 6-10.

Hansen, M.C., DeFries, R.S., Townshend, J.R.G., Carroll, M., Dimiceli, C., & Sohlberg, R.A. (2003). Global Percent Tree Cover at a Spatial Resolution of 500 Meters: First Results of the MODIS Vegetation Continuous Fields Algorithm. *Earth Interactions, 7*.

Hansen, M.C., DeFries, R.S., Townshend, J.R.G., Sohlberg, R., Dimiceli, C., & Carroll, M. (2002). Towards an operational MODIS continuous field of percent tree cover algorithm: examples using AVHRR and MODIS data. *Remote Sensing of Environment, 83*, 303-319.

Hansen, M.C., & Loveland, T.R. (2012). A review of large area monitoring of land cover change using Landsat data. *Remote Sensing of Environment, 122*, 66-74. In English.

Hansen, M.C., Roy, D.P., Lindquist, E., Adusei, B., Justice, C.O., & Altstatt, A. (2008). A method for integrating MODIS and Landsat data for systematic monitoring of forest cover and change in the Congo Basin. *Remote Sensing of Environment, 112*, 2495-2513.

Healey, S.P., Cohen, W.B., Yang, Z.Q., & Krankina, O.N. (2005). Comparison of Tasseled Cap-based Landsat data structures for use in forest disturbance detection. *Remote Sensing of Environment, 97*, 301-310.

Held, M., Jakimow, B., Rabe, A., van der Linden, S., Wirth, F., & Hostert, P. (2012). EnMAP-Box Manual, Version 1.4 [online]. Available from: http://indus.caf.dlr.de/forum/ [accessed 10.10.2012].

Henebry, G.M. (2009). Global change - Carbon in idle croplands. *Nature, 457*, 1089-1090.

Herold, M., Hubald, R., & Di Gregorio, A. (2009). *Translating and evaluating land cover legends using the UN land cover classification system (LCCS)*, GOFC-GOLD. Jena, Germany:

Heymann, Y., Steenmans, C., Croisille, G., & Bossard, M. (1994). *CORINE land cover. Technical Guide*. Luxembourg, Luxembourg: Office for Official Publications of the European Union.

Holben, B.N. (1986). Characteristics of maximum-value composite images from temporal AVHRR data. *International Journal of Remote Sensing, 7*, 1417-1434.

Homer, C., Dewitz, J., Fry, J., Coan, M., Hossain, N., Larson, C., Herold, N., McKerrow, A., VanDriel, J.N., & Wickham, J. (2007). Completion of the 2001 National Land Cover Database for the conterminous United States. *Photogrammetric Engineering and Remote Sensing, 73*, 337-341.

Hostert, P., Kuemmerle, T., Prishchepov, A., Sieber, A., Lambin, E.F., & Radeloff, V.C. (2011a). Rapid land use change after socio-economic disturbances: the collapse of the Soviet Union versus Chernobyl. *Environmental Research Letters, 6*.

Hostert, P., Kuemmerle, T., Prishchepov, A., Sieber, A., Lambin, E.F., & Radeloff, V.C. (2011b). Rapid land use change after socio-economic disturbances: the collapse of the Soviet Union versus Chernobyl. *Environmental Research Letters, 6*, 045201.

Hostert, P., Roder, A., & Hill, J. (2003). Coupling spectral unmixing and trend analysis for monitoring of long-term vegetation dynamics in Mediterranean rangelands. *Remote Sensing of Environment, 87*, 183-197.

Houghton, R.A. (2003). Revised estimates of the annual net flux of carbon to the atmosphere from changes in land use and land management 1850-2000. *Tellus Series B-Chemical and Physical Meteorology, 55*, 378-390.

Huang, C., Coward, S.N., Masek, J.G., Thomas, N., Zhu, Z., & Vogelmann, J.E. (2010a). An automated approach for reconstructing recent forest disturbance history using dense Landsat time series stacks. *Remote Sensing of Environment, 114*, 183-198.

Huang, C., Goward, S.N., Masek, J.G., Thomas, N., Zhu, Z., & Vogelmann, J.E. (2010b). An automated approach for reconstructing recent forest disturbance history using dense Landsat time series stacks. *Remote Sensing of Environment, 114*, 183-198.

Huang, C., Song, K., Kim, S., Townshend, J.R.G., Davis, P., Masek, J.G., & Goward, S.N. (2008). Use of a dark object concept and support vector machines to automate forest cover change analysis. *Remote Sensing of Environment, 112*, 970-985.

Huang, C.Q., Goward, S.N., Masek, J.G., Gao, F., Vermote, E.F., Thomas, N., Schleeweis, K., Kennedy, R.E., Zhu, Z.L., Eidenshink, J.C., & Townshend, J.R.G. (2009).

Development of time series stacks of Landsat images for reconstructing forest disturbance history. *International Journal of Digital Earth, 2*, 195-218.

Huang, C.Q., Townshend, J.R.G., Liang, S.L., Kalluri, S.N.V., & DeFries, R.S. (2002). Impact of sensor's point spread function on land cover characterization: assessment and deconvolution. *Remote Sensing of Environment, 80*, 203-212.

Hwang, T., Song, C., Bolstad, P.V., & Band, L.E. (2011). Downscaling real-time vegetation dynamics by fusing multi-temporal MODIS and Landsat NDVI in topographically complex terrain. *Remote Sensing of Environment, 115*, 2499-2512.

IIASA, & FAO (2012). Global Agro-ecological Zones (GAEZ v3.0). In IIASA (Ed.). Laxenburg, AustriaRome, Italy: International Institute for Applied Systems Analysis.

Ioffe, G., Nefedova, T., & Kirsten, D.B. (2012). Land Abandonment in Russia. *Eurasian Geography and Economics, 53*, 527-549.

Ioras, F., & Abrudan, I.V. (2006). The Romanian forestry sector: privatisation facts. *International Forestry Review, 8*, 361-367.

IPCC (2000). *Land Use, Land-Use Change, and Forestry*, IPCC Special Report - Summary for Policymakers. IPCC.

IPCC (2007). *Climate Change 2007: The Physical Science Basis*, Contribution of Working Group I to the Fourth Assessment Report of the Intergovernmental Panel on Climate Change. Cambridge, United Kingdom and New York, NY, USA: Intergovernmental Panel on Climate Change.

Irimie, D.L., & Essmann, H.F. (2009). Forest property rights in the frame of public policies and societal change. *Forest Policy and Economics, 11*, 95-101.

Irish, R.R., Barker, J.L., Goward, S.N., & Arvidson, T. (2006). Characterization of the Landsat-7 ETM+ automated cloud-cover assessment (ACCA) algorithm. *Photogrammetric Engineering and Remote Sensing, 72*, 1179-1188.

Irland, L.C. (2008). State Failure, Corruption, and Warfare: Challenges for Forest Policy. *Journal of Sustainable Forestry, 27*, 189 - 223.

Irons, J.R., Dwyer, J.L., & Barsi, J.A. (2012). The next Landsat satellite: The Landsat Data Continuity Mission. *Remote Sensing of Environment, 122*, 11-21. In English.

Ju, J., & Roy, D.P. (2008). The availability of cloud-free Landsat ETM plus data over the conterminous United States and globally. *Remote Sensing of Environment, 112*, 1196-1211.

Kareiva, P., Watts, S., McDonald, R., & Boucher, T. (2007). Domesticated nature: Shaping landscapes and ecosystems for human welfare. *Science, 316*, 1866-1869.

Keeton, W.S., & Crow, S.M. (2009). Ecological Economics and Sustainable Forest Management: Developing a Trans-disciplinary Approach for the Carpathian Mountains. In Soloviy, I. & Keeton, W.S. (Eds.), *Sustainable forest management alternatives for the Carpathian Mountain region: providing a broad array of ecosystem service.* Lviv, Ukraine: Ukrainian National Forestry University Press.

Kennedy, R.E., Cohen, W.B., & Schroeder, T.A. (2007). Trajectory-based change detection for automated characterization of forest disturbance dynamics. *Remote Sensing of Environment, 110*, 370-386.

Kennedy, R.E., Yang, Z., & Cohen, W.B. (2010). Detecting trends in forest disturbance and recovery using yearly Landsat time series: 1. LandTrendr -- Temporal segmentation algorithms. *Remote Sensing of Environment, 114*, 2897-2910.

Knorn, J., Kuemmerle, T., Radeloff, V.C., Szabo, A., Mindrescu, M., Keeton, W.S., Abrudan, I., Griffiths, P., Gancz, V., & Hostert, P. (2012a). Forest restitution and protected area effectiveness in post-socialist Romania. *Biological Conservation, 146*, 204-212.

Knorn, J., Rabe, A., Radeloff, V.C., Kuemmerle, T., Kozak, J., & Hostert, P. (2009). Land cover mapping of large areas using chain classification of neighboring Landsat satellite images. *Remote Sensing of Environment, 113*, 957-964.

Knorn, J.A.N., Kuemmerle, T., Radeloff, V.C., Keeton, W.S., Gancz, V., BiriŞ, I.-A., Svoboda, M., Griffiths, P., Hagatis, A., & Hostert, P. (2012b). Continued loss of temperate old-growth forests in the Romanian Carpathians despite an increasing protected area network. *Environmental Conservation, FirstView*, 1-12

Kohavi, R. (1995). A study of cross-validation and bootstrap for accuracy estimation and model selection. In, *Proceedings of the 14th international joint conference on Artificial intelligence - Volume 2* (pp. 1137-1143). Montreal, Quebec, Canada: Morgan Kaufmann Publishers Inc.

Kovalčík, M., Sarvašová, Z., Schwarz, M., Moravčík, M., Oravec, M., Lásková, J., & Tutka, J. (2012). Financial and socio-economic impacts of nature conservation on forestry in Slovakia. *Journal of Forest Science, 58*, 425-435.

Kozak, J. (2010). Forest Cover Changes and Their Drivers in the Polish Carpathian Mountains Since 1800. In Nagendra, H. & Southworth, J. (Eds.), *Reforesting Landscapes Linking Pattern and Process* (pp. 253-273). Springer.

Kozak, J., Björnsen Gurung, A., & Ostapowicz, K. (2011). *Science for the Carpathians - Research Agenda for the Carpathians: 2010-2015*. Krakow:

Kozak, J., Estreguil, C., & Troll, M. (2007). Forest cover changes in the northern Carpathians in the 20th century: a slow transition. *Journal of Land Use Science, 2*, 127 - 146.

Kozak, J., Ostapowicz, K., Szablowska-Midor, A., & Widacki, W. (2004). Land abandonment in the Western Beskidy MTS and its environmental background. *Ekologia-Bratislava, 23*, 116-126.

Kuemmerle, T., Chaskovskyy, O., Knorn, J., Radeloff, V.C., Kruhlov, I., Keeton, W.S., & Hostert, P. (2009a). Forest cover change and illegal logging in the Ukrainian Carpathians in the transition period from 1988 to 2007. *Remote Sensing of Environment, 113*, 1194-1207.

Kuemmerle, T., Erb, K., Meyfroidt, P., Müller, D., Verburg, P.H., Estel, S., Haberl, H., Hostert, P., Jepsen, M.R., Kastner, T., Levers, C., Lindner, M., Plutzar, C., Verkerk,

P.J., van der Zanden, E.H., & Reenberg, A. (2013). Challenges and opportunities in mapping land use intensity globally. *Current Opinion in Environmental Sustainability*.

Kuemmerle, T., Erb, K.H., Meyfroidt, P., Müller, D., Verburg, P.H., Estel, S., Haberl, H., Hostert, P., Kastner, T., Levers, C., Lindner, M., Rudbeck, J., Plutzar, C., Verkerk, P.J., van der Zanden, E.H., & Reenberg, A. (accepted). Mapping land use intensity globally. *Current Opinion on Environmental Sustainability*.

Kuemmerle, T., Hostert, P., Radeloff, V.C., Perzanowski, K., & Kruhlov, I. (2007). Post-socialist forest disturbance in the Carpathian border region of Poland, Slovakia, and Ukraine. *Ecological Applications, 17*, 1279-1295.

Kuemmerle, T., Hostert, P., Radeloff, V.C., van der Linden, S., Perzanowski, K., & Kruhlov, I. (2008). Cross-border comparison of post-socialist farmland abandonment in the Carpathians. *Ecosystems, 11*, 614-628.

Kuemmerle, T., Kozak, J., Radeloff, V.C., & Hostert, P. (2009b). Differences in forest disturbance among land ownership types in Poland during and after socialism. *Journal of Land Use Science, 4*, 73 - 83.

Kuemmerle, T., Muller, D., Griffiths, P., & Rusu, M. (2009c). Land use change in Southern Romania after the collapse of socialism. *Regional Environmental Change, 9*, 1-12.

Kuemmerle, T., Olofsson, P., Chaskovskyy, O., Baumann, M., Ostapowicz, K., Woodcock, C., Houghton, R.A., Hostert, P., Keeton, W.S., & Radeloff, V. (2011). Post-Soviet farmland abandonment, forest recovery, and carbon sequestration in western Ukraine. *Global Change Biology, 17*, 1335-1349.

Lakes, T., Mueller, D., & Krueger, C. (2009). Cropland change in southern Romania: a comparison of logistic regressions and artificial neural networks. *Landscape Ecology, 24*, 1195-1206.

Lambin, E.F., & Geist, H.J. (Eds.) (2006a). *Land Use and Land Cover Change. Local Processes and Global Impacts*. Berlin, Heidelberg, New York: Springer Verlag.

Lambin, E.F., & Geist, H.J. (2006b). *Land Use and Land Cover Change. Local Processes and Global Impacts*. Berlin, Heidelberg, New York: Springer Verlag.

Lambin, E.F., & Linderman, M. (2006). Time series of remote sensing data for land change science. *Geoscience and Remote Sensing, IEEE Transactions on, 44*, 1926-1928.

Lambin, E.F., & Meyfroidt, P. (2010). Land use transitions: Socio-ecological feedback versus socio-economic change. *Land Use Policy, 27*, 108-118.

Lambin, E.F., & Meyfroidt, P. (2011). Global land use change, economic globalization, and the looming land scarcity. *Proceedings of the National Academy of Sciences of the United States of America, 108*, 3465-3472.

Lawrence, A. (2009). Forestry in transition: Imperial legacy and negotiated expertise in Romania and Poland. *Forest Policy and Economics, 11*, 429-436.

Lawrence, A., Szabo, A. (2005). Forest restitution in Romania: Challenging the value system of foresters and farmers. In, *European forests in ethical discourse*. Berlin, Germany

Lee, C.A., Gasster, S.D., Plaza, A., Chang, C.-I., & Huang, B. (2011). Recent Developments in High Performance Computing for Remote Sensing: A Review. *Ieee Journal of Selected Topics in Applied Earth Observations and Remote Sensing, 4*, 508-527.

Lenton, T.M., Held, H., Kriegler, E., Hall, J.W., Lucht, W., Rahmstorf, S., & Schellnhuber, H.J. (2008). Tipping elements in the Earth's climate system. *Proceedings of the National Academy of Sciences of the United States of America, 105*, 1786-1793.

Lerman, Z. (1999). Land reform and farm restructuring: What has been accomplished to date? *American Economic Review, 89*, 271-275.

Lerman, Z. (2001). Agriculture in transition economies: from common heritage to divergence. *Agricultural Economics, 26*, 95-114.

Lerman, Z., Csaki, C., & Feder, G. (2002). *Land Policies and Evolving Farm Structures in Transition Countries*, Policy Research Working Paper, 2794. Washington: World Bank Development Research Group.

Lerman, Z., Csaki, C., & Feder, G. (2004). Evolving farm structures and land-use patterns in former socialist countries. *Quarterly Journal of International Agriculture, 43*, 309-335.

Lerman, Z., Csaki, C., Feder, G. (2004). Evolving farm structures and land-use patterns in former socialist countries. *Quarterly Journal of International Agriculture, 43*, 309-335.

Lillesand, T.M., & Kiefer, R.W. (2000). *Remote Sensing and Image Interpretation*. New York, USA: John Wiley & Sons.

Loveland, T.R., & Dwyer, J.L. (2012). Landsat: Building a strong future. *Remote Sensing of Environment, 122*, 22-29.

Lu, D., Mausel, P., Brondizio, E., & Moran, E. (2004). Change detection techniques. *International Journal of Remote Sensing, 25*, 2365-2407.

Lucht, W., Schaaf, C.B., & Strahler, A.H. (2000). An algorithm for the retrieval of albedo from space using semiempirical BRDF models. *Ieee Transactions on Geoscience and Remote Sensing, 38*, 977-998.

MacDonald, D., Crabtree, J.R., Wiesinger, G., Dax, T., Stamou, N., Fleury, P., Lazpita, J.G., & Gibon, A. (2000). Agricultural abandonment in mountain areas of Europe: Environmental consequences and policy response. *Journal of Environmental Management, 59*, 47-69.

Machlis, G.E., & Hanson, T. (2008). Warfare ecology. *Bioscience, 58*, 729-736.

Main-Knorn, M., Hostert, P., Kozak, J., & Kuemmerle, T. (2009). How pollution legacies and land use histories shape post-communist forest cover trends in the Western Carpathians. *Forest Ecology and Management, 258*, 60-70.

Malenovský, Z., Rott, H., Cihlar, J., Schaepman, M.E., García-Santos, G., Fernandes, R., & Berger, M. (2012). Sentinels for science: Potential of Sentinel-1, -2, and -3 missions for scientific observations of ocean, cryosphere, and land. *Remote Sensing of Environment*.

Markham, B.L., Storey, J.C., Williams, D.L., & Irons, J.R. (2004). Landsat sensor performance: History and current status. *Ieee Transactions on Geoscience and Remote Sensing, 42*, 2691-2694.

Masek, J.G., Huang, C.Q., Wolfe, R., Cohen, W., Hall, F., Kutler, J., & Nelson, P. (2008). North American forest disturbance mapped from a decadal Landsat record. *Remote Sensing of Environment, 112*, 2914-2926.

Masek, J.G., Vermote, E.F., Saleous, N.E., Wolfe, R., Hall, F.G., Huemmrich, K.F., Gao, F., Kutler, J., & Lim, T.K. (2006). A Landsat surface reflectance dataset for North America, 1990-2000. *IEEE Geoscience and Remote Sensing Letters, 3*, 68-72.

Mather, A.S., Fairbairn, J., & Needle, C.L. (1999). The course and drivers of the forest transition: the case of France. *Journal of Rural Studies, 15*, 65-90.

MEA (2005). *Ecosystems and Human Well-being: Synthesis*, Millennium Ecosystem Assessment. World Resources Institute.

Meyfroidt, P., & Lambin, E.F. (2011). Global Forest Transition: Prospects for an End to Deforestation. In Gadgil, A. & Liverman, D.M. (Eds.), *Annual Review of Environment and Resources, Vol 36* (pp. 343-371).

Meyfroidt, P., Lambin, E.F., Erb, K.-H., & Hertel, T.W. (2013). Globalization of land use: distant drivers of land change and geographic displacement of land use. *Current Opinion in Environmental Sustainability*.

Meyfroidt, P., Rudel, T.K., & Lambin, E.F. (2010). Forest transitions, trade, and the global displacement of land use. *Proceedings of the National Academy of Sciences of the United States of America, 107*, 20917-20922.

Mihai, B., Savulescu, I., & Sandric, I. (2007). Change detection analysis (1986-2002) of vegetation cover in Romania: A study of alpine, subalpine, and forest landscapes in the Lezer mountains, Southern Carpathians. *Mountain Research and Development, 27*, 250-258.

Mihai, B., Savulescu, I., Sandric, I., & Oprea, R. (2006). Application of change detection to the study of vegetation dynamics in the Bucegi Mountains (Southern Carpathians, Romania). *Télédétection, 6*, 215 - 231.

Mihalciuc, V., Simionescu, A., & Mircioiu, L. (1999). Sanitary state of coniferous stands calamited by wind and snow on 5./6. November 1995 in Eastern carpathians from Romania. In Forster, B., Knízek, M. & Grodzki, W. (Eds.), *Methodology of Forest Insect and Disease Survey in Central Europe. Second Workshop of the IUFRO WP*

*7.03.10.* (pp. 238-241). Sion-Châteauneuf, Switzerland: Swiss Federal Institute for Forest, Snow and Landscape Research (WSL).

Mueller, D., Kuemmerle, T., Rusu, M., & Griffiths, P. (2009). Lost in transition: determinants of post-socialist cropland abandonment in Romania. *Journal of Land Use Science, 4*, 109 - 129.

Müller, D., & Munroe, D.K. (2008). Changing Rural Landscapes in Albania: Cropland Abandonment and Forest Clearing in the Postsocialist Transition. *Annals of the Association of American Geographers, 98*, 855-876.

Munteanu, C., Kuemmerle, T., Boltiziar, M., Butsic, V., Gimmi, U., Halada, L., Kaim, D., Király, G., Konkoly-Gyuró, E., Kozak, J., Lieskovsky, J., Mojses, M., Müller, M., Ostafin, K., Ostapowicz, K., Shandra, O., Štych, P., Walker, S., & Radeloff, V.C. (Submitted). Forest and agricultural land change in the Carpathian region – a meta-analysis of long-term patterns and drivers of change. *Land Use Policy*.

Nagendra, H., Reyers, B., & Lavorel, S. (2013). Impacts of land change on biodiversity: making the link to ecosystem services. *Current Opinion in Environmental Sustainability, 5*, 1-6.

NASA (2009). Landsat 7 - Science Data Users Handbook [online]. Available from: http://landsathandbook.gsfc.nasa.gov/pdfs/Landsat7_Handbook.pdf [accessed 19.07.2013].

Navarro, L.M., & Pereira, H.M. (2012). Rewilding Abandoned Landscapes in Europe. *Ecosystems, 15*, 900-912.

Nijnik, M. (2004). To an Economist's Perception on Sustainability in Forestry-in-Transition. *Forest Policy and Economics, 6*, 403-413.

Nijnik, M., & van Kooten, G.C. (2000). Forestry in the Ukraine: the road ahead? *Forest Policy and Economics, 1*, 139-151.

Nikodemus, O., Bell, S., Grine, I., & Liepins, I. (2005). The impact of economic, social and political factors on the landscape structure of the Vidzeme Uplands in Latvia. *Landscape and Urban Planning, 70*, 57-67.

Olofsson, P., Foody, G.M., Stehman, S.V., & Woodcock, C. (2013). Making better use of accuracy data in land change studies: Estimating accuracy and area and quantifying uncertainty using stratified estimation. *Remote Sensing of Environment, 129*, 122 - 131.

Olofsson, P., Kuemmerle, T., Griffiths, P., Knorn, J., Baccini, A., Ganz, V., Houghton, R.A., Abrudan, I.V., & Woodcock, C.E. (2011). Carbon implications of the forest restitution in post-socialist Romania. *Evironmental Research Letters, 6*.

Olthof, I., Butson, C., & Fraser, R. (2005). Signature extension through space for northern landcover classification: A comparison of radiometric correction methods. *Remote Sensing of Environment, 95*, 290-302.

Olthof, I., Latifovic, R., & Pouliot, D. (2009). Development of a circa 2000 land cover map of northern Canada at 30 m resolution from Landsat. *Canadian Journal of Remote Sensing, 35*, 152-165.

Oszlanyi, J. (1997). Forest health and environmental pollution in Slovakia. *Environmental Pollution, 98*, 389-392.

Ozdogan, M., & Woodcock, C.E. (2006). Resolution dependent errors in remote sensing of cultivated areas. *Remote Sensing of Environment, 103*, 203-217.

Pal, M., & Mather, P.M. (2005). Support vector machines for classification in remote sensing. *International Journal of Remote Sensing, 26*, 1007-1011.

Palmieri, A., Dominici, P., Kasanko, A., & Martino, L. (2011). *Diversified landscape structure in the EU Member States - Landscape indicators from the LUCAS 2009 survey*, Statistics in focus. EUROSTAT - European Comission.

Pan, Y., Birdsey, R.A., Fang, J., Houghton, R., Kauppi, P.E., Kurz, W.A., Phillips, O.L., Shvidenko, A., Lewis, S.L., Canadell, J.G., Ciais, P., Jackson, R.B., Pacala, S.W., McGuire, A.D., Piao, S., Rautiainen, A., Sitch, S., & Hayes, D. (2011). A Large and Persistent Carbon Sink in the World's Forests. *Science, 333*, 988-993.

Paquette, A., & Messier, C. (2010). The role of plantations in managing the world's forests in the Anthropocene. *Frontiers in Ecology and the Environment, 8*, 27-34.

Pax-Lenney, M., Woodcock, C.E., Macomber, S.A., Gopal, S., & Song, C. (2001). Forest mapping with a generalized classifier and Landsat TM data. *Remote Sensing of Environment, 77*, 241-250.

Pekkarinen, A., Reithmaier, L., & Strobl, P. (2009). Pan-European forest/non-forest mapping with Landsat ETM+ and CORINE Land Cover 2000 data. *ISPRS Journal of Photogrammetry and Remote Sensing, 64*, 171-183.

Pfaff, A.S.P. (1999). What drives deforestation in the Brazilian Amazon? Evidence from satellite and socioeconomic data. *Journal of Environmental Economics and Management, 37*, 26-43.

Plaza, A., Du, Q., Chang, Y.-L., & King, R.L. (2011). High Performance Computing for Hyperspectral Remote Sensing. *Ieee Journal of Selected Topics in Applied Earth Observations and Remote Sensing, 4*, 528-544.

Popa, I. (2008). Windthrow risk management. Results from Romanian forests. *Forest Disturbances and Effects on Carbon Stock: The Non-Permanence Issue*, San Vito di Cadore.

Potapov, P., Hansen, M.C., Stehman, S.V., Pittman, K., & Turubanova, S. (2009). Gross forest cover loss in temperate forests: biome-wide monitoring results using MODIS and Landsat data. *Journal of Applied Remote Sensing, 3*.

Potapov, P., Turubanova, S., & Hansen, M.C. (2011). Regional-scale boreal forest cover and change mapping using Landsat data composites for European Russia. *Remote Sensing of Environment, 115*, 548-561.

Potapov, P.V., Turubanova, S.A., Hansen, M.C., Adusei, B., Broich, M., Altstatt, A., Mane, L., & Justice, C.O. (2012). Quantifying forest cover loss in Democratic Republic of the Congo, 2000–2010, with Landsat ETM+ data. *Remote Sensing of Environment*.

Powell, S.L., Cohen, W.B., Healey, S.P., Kennedy, R.E., Moisen, G.G., Pierce, K.B., & Ohmann, J.L. (2010). Quantification of live aboveground forest biomass dynamics with Landsat time-series and field inventory data: A comparison of empirical modeling approaches. *Remote Sensing of Environment, 114*, 1053-1068.

Prishchepov, A.V., Mueller, D., Dubinin, M., Baumann, M., & Radeloff, V.C. (2013). Determinants of agricultural land abandonment in post-Soviet European Russia. *Land Use Policy, 30*, 873-884.

Prishchepov, A.V., Radeloff, V.C., Baumann, M., Kuemmerle, T., & Mueller, D. (2012a). Effects of institutional changes on land use: agricultural land abandonment during the transition from state-command to market-driven economies in post-Soviet Eastern Europe. *Environmental Research Letters, 7*.

Prishchepov, A.V., Radeloff, V.C., Dubinin, M., & Alcantara, C. (2012b). The effect of Landsat ETM/ETM plus image acquisition dates on the detection of agricultural land abandonment in Eastern Europe. *Remote Sensing of Environment, 126*, 195-209.

Ptacek, P., Letal, A., Ruffini, F.V., & Renner, K. (2009). Atlas of the Carpathian Macroregion. *Europa Regional, 17*, 108 - 122.

Ramankutty, N., Heller, E., & Rhemtulla, J. (2010). Prevailing Myths About Agricultural Abandonment and Forest Regrowth in the United States. *Annals of the Association of American Geographers, 100*, 502-512.

Richards, J.A. (2005). Analysis of remotely sensed data: The formative decades and the future. *Ieee Transactions on Geoscience and Remote Sensing, 43*, 422-432.

Richards, J.A., & Jia, X. (2005). *Remote Sensing Digital Image Analysis*. Berlin, Germany: Springer.

Rockstrom, J., Steffen, W., Noone, K., Persson, A., Chapin, F.S., III, Lambin, E.F., Lenton, T.M., Scheffer, M., Folke, C., Schellnhuber, H.J., Nykvist, B., de Wit, C.A., Hughes, T., van der Leeuw, S., Rodhe, H., Sorlin, S., Snyder, P.K., Costanza, R., Svedin, U., Falkenmark, M., Karlberg, L., Corell, R.W., Fabry, V.J., Hansen, J., Walker, B., Liverman, D., Richardson, K., Crutzen, P., & Foley, J.A. (2009). A safe operating space for humanity. *Nature, 461*, 472-475.

Roder, A., Hill, J., Duguy, B., Alloza, J.A., & Vallejo, R. (2008a). Using long time series of Landsat data to monitor fire events and post-fire dynamics and identify driving factors. A case study in the Ayora region (eastern Spain). *Remote Sensing of Environment, 112*, 259-273.

Roder, A., Udelhoven, T., Hill, J., del Barrio, G., & Tsiourlis, G. (2008b). Trend analysis of Landsat-TM and -ETM+ imagery to monitor grazing impact in a rangeland ecosystem in Northern Greece. *Remote Sensing of Environment, 112*, 2863-2875.

Rotzer, T., & Chmielewski, F.M. (2001). Phenological maps of Europe. *Climate Research, 18*, 249-257.

Roy, D.P., Ju, J., Kline, K., Scaramuzza, P.L., Kovalskyy, V., Hansen, M., Loveland, T.R., Vermote, E., & Zhang, C. (2010). Web-enabled Landsat Data (WELD): Landsat ETM plus composited mosaics of the conterminous United States. *Remote Sensing of Environment, 114*, 35-49.

Rozelle, S., & Swinnen, J.F.M. (2004). Success and failure of reform: Insights from the transition of agriculture. *Journal of Economic Literature, 42*, 404-456.

Rozylowicz, L., Popescu, V.D., Patroescu, M., & Chisamera, G. (2011). The potential of large carnivores as conservation surrogates in the Romanian Carpathians. *Biodiversity and Conservation, 20*, 561-579.

Rudel, T.K., Coomes, O.T., Moran, E., Achard, F., Angelsen, A., Xu, J.C., & Lambin, E. (2005). Forest transitions: towards a global understanding of land use change. *Global Environmental Change-Human and Policy Dimensions, 15*, 23-31.

Rudel, T.K., Schneider, L., & Uriarte, M. (2010). Forest transitions: An introduction. *Land Use Policy, 27*, 95-97.

Ruffini, V., Hoffmann, C., Streifeneder, T., & Renner, K. (2008). *SARD-M Report for the Carpathian Convention Member States. Assessment of Policies, Institutions and Processes, Regional Synthesis for Czech Republic, Hungary, Poland, Romania, Republic of Serbia, Slovak Republic and Ukraine.* Bozen: EURAC.

Rulli, M.C., Saviori, A., & D'Odorico, P. (2013). Global land and water grabbing. *Proceedings of the National Academy of Sciences of the United States of America, 110*, 892-897.

Sala, O.E., Chapin, F.S., Armesto, J.J., Berlow, E., Bloomfield, J., Dirzo, R., Huber-Sanwald, E., Huenneke, L.F., Jackson, R.B., Kinzig, A., Leemans, R., Lodge, D.M., Mooney, H.A., Oesterheld, M., Poff, N.L., Sykes, M.T., Walker, B.H., Walker, M., & Wall, D.H. (2000). Biodiversity - Global biodiversity scenarios for the year 2100. *Science, 287*, 1770-1774.

Salvatori, V., Okarma, H., Ionescu, O., Dovhanych, Y., Find'o, S., & Boitani, L. (2002). Hunting legislation in the Carpathian Mountains: implications for the conservation and management of large carnivores. *Wildlife Biology, 8*, 3-10.

Sarris, A.H., Doucha, T., & Mathijs, E. (1999). Agricultural restructuring in central and eastern Europe: implications for competitiveness and rural development. *European Review of Agricultural Economics, 26*, 305-329.

Sarvasova, Z., Salka, J., & Dobsinska, Z. (2012). Mechanism of cross-sectoral coordination between nature protection and forestry in the Natura 2000 formulation process in Slovakia. *J Environ Manage*. In Eng.

Scheffer, M., Carpenter, S., Foley, J.A., Folke, C., & Walker, B. (2001). Catastrophic shifts in ecosystems. *Nature, 413*, 591-596.

Schelhaas, M.J., Nabuurs, G.J., & Schuck, A. (2003). Natural disturbances in the European forests in the 19th and 20th centuries. *Global Change Biology, 9*, 1620-1633.

Schierhorn, F., Müller, D., Prishchepov, A., & Balmann, A. (2012). Grain potentials on abandoned cropland in European Russia. In, *Annual World Bank Conference on Land and Poverty*. Washington, D.C.: World Bank.

Schmidt, M., Udelhoven, T., Gill, T., & Roder, A. (2012). Long term data fusion for a dense time series analysis with MODIS and Landsat imagery in an Australian Savanna. *Journal of Applied Remote Sensing, 6*, 063512-063518.

Singh, A. (1989). Digital change detection techniques using remotely-sensed data. *International Journal of Remote Sensing, 10*, 989-1003.

Skole, D., & Tucker, C. (1993). Tropical deforestation and habitat fragmentation in the Amazon - satellite data from 1978 to 1988. *Science, 260*, 1905-1910.

Soltes, R., Skolek, J., Homolova, Z., & Kyselova, Z. (2010). Early successional pathways in the Tatra Mountains (Slovakia) forest ecosystems following natural disturbances. *Biologia, 65*, 958-964.

Sonnenschein, R., Kuemmerle, T., Udelhoven, T., Stellmes, M., & Hostert, P. (2011). Differences in Landsat-based trend analyses in drylands due to the choice of vegetation estimate. *Remote Sensing of Environment, 115*, 1408-1420.

Spulerova, J., Dobrovodska, M., Lieskovsky, J., Baca, A., Halabuk, A., Kohut, F., Mojses, M., Kenderessy, P., Piscova, V., Barancok, P., Gerhatova, K., Krajci, J., & Boltiziar, M. (2011). Inventory and classification of historical structures of the agricultural landscape in Slovakia. *Ekologia (Bratislava), 30*, 157-170.

Stancioiu, P.T., Abrudan, I.V., & Dutca, I. (2010). The Natura 2000 ecological network and forests in Romania: implications on management and administration. *International Forestry Review, 12*, 106-113.

Steffen, W., Andreae, M.O., Bolin, B., Cox, P.M., Crutzen, P.J., Cubasch, U., Held, H., Nakicenovic, N., Scholes, R.J., Talaue-McManus, L., & Turner, B.L. (2004). Abrupt changes: The Achilles' heels of the Earth System. *Environment, 46*, 8-20.

Steffen, W., Crutzen, P.J., & McNeill, J.R. (2007). The Anthropocene: Are humans now overwhelming the great forces of nature. *Ambio, 36*, 614-621.

Suchomel, J., Gejdos, M., Tucek, J., & Jurica, J. (2011). *Analýza náhodných ťažieb dreva na Slovensku*. Zvolen, Slovakia: Technická univerzita vo Zvolene.

Sunderlin, W.D., Angelsen, A., Resosudarmo, D.P., Dermawan, A., & Rianto, E. (2001). Economic crisis, small farmer well-being, and forest cover change in Indonesia. *World Development, 29*, 767-782.

Svajda, J., Solar, J., Janiga, M., & Buliak, M. (2011). Dwarf Pine (Pinus mugo) and Selected Abiotic Habitat Conditions in the Western Tatra Mountains. *Mountain Research and Development, 31*, 220-228.

Swinnen, J.F.M. (1999). The political economy of land reform choices in Central and Eastern Europe. *Economics of Transition, 7*, 637-664.

Taff, G.N., Mueller, D., Kuemmerle, T., Ozdeneral, E., & Walsh, S.J. (2010). Reforestation in Central and Eastern Europe After the Breakdown of Socialism. In Nagendra, H. & Southworth, J. (Eds.), *Reforesting Landscapes: Linking Pattern and Process* (pp. 121-147).

Tan, B., Woodcock, C.E., Hu, J., Zhang, P., Ozdogan, M., Huang, D., Yang, W., Knyazikhin, Y., & Myneni, R.B. (2006). The impact of gridding artifacts on the local spatial properties of MODIS data: Implications for validation, compositing, and band-to-band registration across resolutions. *Remote Sensing of Environment, 105*, 98-114.

Tilman, D., Balzer, C., Hill, J., & Befort, B.L. (2011). Global food demand and the sustainable intensification of agriculture. *Proceedings of the National Academy of Sciences of the United States of America, 108*, 20260-20264.

Tilman, D., Cassman, K.G., Matson, P.A., Naylor, R., & Polasky, S. (2002). Agricultural sustainability and intensive production practices. *Nature, 418*, 671-677.

Toader, T., & Dumitru, I. (2005). *Romanian forest - national parks and natural parks*. Bucharest: National Forest Administration ROMSILVA.

Townshend, J.R., Masek, J.G., Huang, C., Vermote, E.F., Gao, F., Channan, S., Sexton, J.O., Feng, M., Narasimhan, R., Kim, D., Song, K., Song, D., Song, X., Noojipady, P., Tan, B., Hansen, M.C., Li, M., & Wolfe, R. (2012). Global characterization and monitoring of forest cover using Landsat data: opportunities and challenges. *International Journal of Digital Earth*.

Turner, W.R., Brandon, K., Brooks, T.M., Costanza, R., da Fonseca, G.A.B., & Portela, R. (2007). Global conservation of biodiversity and ecosystem services. *Bioscience, 57*, 868-873.

Turnock, D. (2002). Ecoregion-based conservation in the Carpathians and the land-use implications. *Land Use Policy, 19*, PII S0264-8377(0201)00039-00034.

UNECE, & FAO (2011). *State of Europe's Forests 2011. Status &Trends in Sustainable Forest Management in Europe.*, Forest Europe. Oslo, Norway: Ministerial Conference on the Protection of Forests in Europe, 2011

UNEP (2007). *Carpathians Environment Outlook*. Geneva: United Nations Environment Programme.

van der Werf, G.R., Morton, D.C., DeFries, R.S., Olivier, J.G.J., Kasibhatla, P.S., Jackson, R.B., Collatz, G.J., & Randerson, J.T. (2009). CO2 emissions from forest loss. *Nature Geoscience, 2*, 737-738.

Vasile, M., Mantescu, L. (2009). Property reforms in rural Romania and community-based forests. *Romanian Sociology (Sociologie Românească), 7*, 96 - 113.

Veen, P., Fanta, J., Raev, I., Biris, I.A., de Smidt, J., & Maes, B. (2010). Virgin forests in Romania and Bulgaria: results of two national inventory projects and their implications for protection. *Biodiversity and Conservation, 19*, 1805-1819.

Vermote, E., Tanré, E., Deuzé, J.L., Herman, M., & Morcrette, J.J. (1997). Second Simulation of the Satellite Signal in the Solar Spectrum. An Overview. *IEEE Transactions Geosci. Remote Sens., 35*, 675-686.

Visser, O., & Spoor, M. (2011). Land grabbing in post-Soviet Eurasia: the world's largest agricultural land reserves at stake. *Journal of Peasant Studies, 38*, 299-323.

Vitousek, P.M. (1997). Human domination of Earth's ecosystems. *Science, 277*, 494 - 499.

Vuichard, N., Ciais, P., Belelli, L., Smith, P., & Valentini, R. (2008). Carbon sequestration due to the abandonment of agriculture in the former USSR since 1990. *Global Biogeochemical Cycles, 22*.

Waske, B., van der Linden, S., Benediktsson, J.A., Rabe, A., & Hostert, P. (2010). Sensitivity of Support Vector Machines to Random Feature Selection in Classification of Hyperspectral Data. *Ieee Transactions on Geoscience and Remote Sensing, 48*, 2880-2889.

Waske, B., van der Linden, S., Oldenburg, C., Jakimow, B., Rabe, A., & Hostert, P. (2012). imageRF – A user-oriented implementation for remote sensing image analysis with Random Forests. *Environmental Modelling & Software, 35*, 192-193.

Weinzettel, J., Hertwich, E.G., Peters, G.P., Steen-Olsen, K., & Galli, A. (2013). Affluence drives the global displacement of land use. *Global Environmental Change-Human and Policy Dimensions, 23*, 433-438.

Weiss, G., Guduric, I., & Wolfslehner, B. (2012). *Review of forest owners' organizations in selected Eastern European countries.*, Forestry Policy and Institutions Working Paper. Rome: FAO.

Williams, D.L., Goward, S., & Arvidson, T. (2006). Landsat: Yesterday, today, and tomorrow. *Photogrammetric Engineering and Remote Sensing, 72*, 1171-1178.

Wolfe, R.E., Roy, D.P., & Vermote, E. (1998). MODIS land data storage, gridding, and compositing methodology: Level 2 grid. *Ieee Transactions on Geoscience and Remote Sensing, 36*, 1324-1338.

Woodcock, C.E., Allen, R., Anderson, M., Belward, A., Bindschadler, R., Cohen, W., Gao, F., Goward, S.N., Helder, D., Helmer, E., Nemani, R., Oreopoulos, L., Schott, J., Thenkabail, P.S., Vermote, E.F., Vogelmann, J., Wulder, M.A., Wynne, R., & Landsat Sci, T. (2008). Free access to Landsat imagery. *Science, 320*, 1011-1011.

Woodcock, C.E., Macomber, S.A., Pax-Lenney, M., & Cohen, W.B. (2001). Monitoring large areas for forest change using Landsat: Generalization across space, time and Landsat sensors. *Remote Sensing of Environment, 78*, 194-203.

World Bank, W. (2007). *Integrating Environment into Agriculture and Forestry Progress and Prospects in Eastern Europe and Central Asia - Romania Country Review*.

World Bank, W.B. (2005). *Romania. Country assistance evaluation.* , World Bank Report No. 32452. Washington D.C.:

Wright, C.K., & Wimberly, M.C. (2013). Recent land use change in the Western Corn Belt threatens grasslands and wetlands. *Proceedings of the National Academy of Sciences*.

Wulder, M.A., & Masek, J.G. (2012). Preface to Landsat Legacy Special Issue: Continuing the Landsat Legacy. *Remote Sensing of Environment, 122*, 1-1. In English.

Wulder, M.A., Masek, J.G., Cohen, W.B., Loveland, T.R., & Woodcock, C.E. (2012). Opening the archive: How free data has enabled the science and monitoring promise of Landsat. *Remote Sensing of Environment, 122*, 2-10. In English.

Xie, Y., Sha, Z., & Yu, M. (2008). Remote sensing imagery in vegetation mapping: a review. *Journal of Plant Ecology, 1*, 9-23.

Zak, M.R., Cabido, M., Caceres, D., & Diaz, S. (2008). What drives accelerated land cover change in central Argentina? Synergistic consequences of climatic, socioeconomic, and technological factors. *Environmental Management, 42*, 181-189.

Zhu, Z., & Woodcock, C.E. (2012). Object-based cloud and cloud shadow detection in Landsat imagery. *Remote Sensing of Environment, 118*, 83-94.

# Publikationen

**PEER REVIEWED ARTICLES**


Griffiths, P., Mueller, D., Kuemmerle, T., & Hostert, P. (in review). Agricultural land change in the Carpathian ecoregion after the breakdown of socialism and expansion of the European Union. *Environmental Research Letters*.

Griffiths, P., Kuemmerle, T., Baumann, M., Radeloff, V., Abrudan, I.V., Lieskovský, J., Muntenau, C., Ostapowicz, K., & Hostert, P. (accepted). Forest disturbances, forest recovery, and changes in forest types across the Carpathian ecoregion from 1985 to 2010 based on Landsat image composites. *Remote Sensing of Environment*.

Griffiths, P., van der Linden, S., Kuemmerle, T., & Hostert, P. (2013). A Pixel-Based Landsat Compositing Algorithm for Large Area Land Cover Mapping. *IEEE Journal of Selected Topics in Applied Earth Observations and Remote Sensing*, PP, 1-14.

Griffiths, P., Kuemmerle, T., Kennedy, R.E., Abrudan, I.V., Knorn, J., & Hostert, P. (2012). Using annual time-series of Landsat images to assess the effects of forest restitution in post-socialist Romania. *Remote Sensing of Environment*, 118, 199-214.

Griffiths, P., Hostert, P., Gruebner, O., & der Linden, S.v. (2010). Mapping megacity growth with multi-sensor data. *Remote Sensing of Environment*, 114, 426-439.

Kennedy, R.E., Andréfouët, S., Cohen, W., Gómez, C., Griffiths, P., Hais, M., Healey, S.P., Helmer, E., Hostert, P., Lyons, M., Meigs, G., Pflugmacher, D., Phinn, S.R., Powell, S., Scarth, P., Sen, S., Schroeder, T.A., Schneider, A., Sonnenschein, R., Vogelmann, J., Wulder, M., & Zhu, Z. (in review). Bringing an ecological view of change to Landsat-based remote sensing. *Frontiers in Ecology and the Environment*.

Alcantara, C., Kuemmerle, T., Baumann, M., Bragina, E.V., Griffiths, P., Hostert, P., Knorn, J., Mueller, D., Prishchepov, A., Schierhorn, F., Sieber, A., & Radeloff, V.C. (in review). Mapping the extent of abandoned farmland in Central and Eastern Europe using MODIS time series satellite data. *Environmental Research Letters*.

Knorn, J., Kuemmerle, T., Radeloff, V., Keeton, W.S., Gancz, V., Biris, I.A., Svoboda, M., Griffiths, P., Hahatis, A., & Hostert, P. (2013). Continued loss of temperate old-

growth forests in the Romanian Carpathians despite an increasing protected area network. *Environmental Conservation*.

Knorn, J., Kuemmerle, T., Radeloff, V.C., Szabo, A., Mindrescu, M., Keeton, W.S., Abrudan, I., Griffiths, P., Gancz, V., & Hostert, P. (2012). Forest restitution and protected area effectiveness in post-socialist Romania. *Biological Conservation*, 146, 204-212.

Olofsson, P., Kuemmerle, T., Griffiths, P., Knorn, J., Baccini, A., Ganz, V., Houghton, R.A., Abrudan, I.V., & Woodcock, C.E. (2011). Carbon implications of the forest restitution in post-socialist Romania. *Evironmental Research Letters*, 6.

Kuemmerle, T., Muller, D., Griffiths, P., & Rusu, M. (2009). Land use change in Southern Romania after the collapse of socialism. *Regional Environmental Change*, 9, 1-12.

Mueller, D., Kuemmerle, T., Rusu, M., & Griffiths, P. (2009). Lost in transition: determinants of post-socialist cropland abandonment in Romania. *Journal of Land Use Science*, 4, 109 - 129.

**CONFERENCE PROCEEDINGS**

Griffiths, P., Hostert, P., & van der Linden, S. (2012). Beyond Landsat - pixel-based large area composites for added value Sentinel-2 products. Sentinel-2 Preparatory Symposium, ESA-ESRIN, Frascati, Italy.

Griffiths, P., van der Linden, S., Waske, B., Gruebner, O., Hostert, P. (2008). Multi-sensoral analysis of urban trajectories in the megacity of Dhaka, Bangladesh. In Jürgens, C. (Ed.) 2nd Workshop EARSeL Special Interest Group on Urban Remote Sensing, Bochum, Germany.

Müller, D., Kuemmerle, T., Griffiths, P. (2007). Drivers of postsocialist cropland abandonment in Romania. In, Science and Education of Land Use: A transatlantic, multidisciplinary and comparative approach. Washington, DC, USA

Müller, D., Kuemmerle, T., Griffiths, P., Hostert, P. (2007). Postsocialist land cover dynamics in Romania. In, Framing Land Use Dynamics II. Utrecht University, The Netherlands

Müller, D., Kuemmerle, T., Rusu, M., Griffiths, P. (2007). Drivers of post-socialist cropland abandonment in Romania. Conference on the Science and Education of Land Use: A transatlantic, multidisciplinary and comparative approach. , Washington D.C., USA.

**CONFERENCE PRESENTATIONS**

Griffiths, P., Hostert, P., & van der Linden, S. (2012). Beyond Landsat - pixel-based large area composites for added value Sentinel-2 products. Sentinel-2 Preparatory Symposium, ESA-ESRIN, Frascati, Italy.

Griffiths, P., Kuemmerle, T., Knorn, J., & Hostert, P. (2012). Pixel-based compositing approaches for fine-scale land cover change mapping across the entire Carpathian ecoregion – first results. Forum Carpaticum 2012, Stara Lesna, Slovakia.

Griffiths, P. (2012). New approaches to large area mapping at high resolutions – harmonizing land change estimates beyond national statistics. IAMO Forum 2012 - Land Use in Transition: Potentials and Solutions - Between Abandonment and Land Grabbing, Halle, Saale.

Griffiths, P., Kuemmerle, T., & Hostert, P. (2012). Large area change detection using pixel based compositing of Landsat data – 25 years of forest change in the Carpathian Mountains. ForestSAT 2012, Corvallis, Oregon, USA.

van der Linden, S., , Waske, B., , Rabe, A., , Gollnow, F., , Griffiths, P., , Kuemmerle, T., , & Hostert, P., [oral]. (2009). On the use of support vector machines and decision trees in land cover mapping - a review from the user perspective. In: 3rd Workshop EARSeL SIG Land Use and Land Cover. Bonn

Hostert, P., Griffiths, P., van der Linden, S., Gruebner, O., Mueller, D., Lakes, T. (2009). Understanding urban growth and local livelihoods in megacity regions. In: 7th International Scientific Conference on the Human Dimensions of Global Environmental Change. Bonn

Griffiths, P., , Hostert, P., , van der Linden, S., , & Gruebner, O., [Poster]. (2009). Monitoring urban growth in a complex megacity region - the example of Dhaka, Bangladesh. In: 3rd Workshop EARSeL SIG Land Use and Land Cover. Bonn

# Eidesstattliche Erklärung

Hiermit erkläre ich, die vorliegende Dissertation selbstständig und ohne Verwendung unerlaubter Hilfe angefertigt zu haben. Die aus fremden Quellen direkt oder indirekt übernommenen Inhalte sind als solche kenntlich gemacht. Die Dissertation wird erstmalig und nur an der Humboldt Universität zu Berlin eingereicht. Weiterhin erkläre ich, nicht bereits einen Doktortitel im Fach Geographie zu besitzen. Die dem Verfahren zu Grunde liegende Promotionsordnung ist mir bekannt.

Patrick Griffiths

Berlin, den 31.07.2013